INVESTIGATION OF THE LOSS MODES INDUCED IN OPTICAL FIBRES DURING THE CABLING PROCESS.

P. Sutton, B. Eng (Tech), AM I. Mech. E.

A dissertation submitted to the Council for National Academic Awards for the degree of Master of Philosophy.

The Polytechnic of Wales,
Department of Electrical and Electronic Engineering,
and
Pirelli Cables, Communication Cables Division.

November 1991

DECLARATION

This dissertation has not been, nor is being currently submitted for the award of any other degree or similar qualification.

P. Sutton.

ACKNOWLEDGEMENTS

I would like to extend my thanks for the help, cooperation and support given by Mr. Alan Phoenix and Dr. David Rees of the Polytechnic of Wales throughout and after this project.

My thanks are also extended to Mr. Llyr Roberts and to Mr. Andy Summers of Pirelli Cables, for their donation of knowledge and experience to this project.

Finally, I would like to thank the SERC/DTI teaching company scheme, through whom the collaboration between the Polytechnic of Wales and Pirelli Cables came about and created the project which culminated in this dissertation.

SYNOPSIS

The process of fibre optic telecommunication cable production is hampered by a number of cable induced sources of attenuation which act upon the fibres. The majority of fibres receive a "normal" or average set of attenuation inducements. Despite this, observations of process attenuation increments show that some fibres show a greater increase in attenuation than others. The same levels of inducements therefore lead to varying levels of attenuation. These observations suggest that fibres have varying inherent levels of resistance to the loss modes of the cable and that the degree of resistance could be related to the fundamental parameters of the fibres. This work is aimed at evaluating this possible link, firstly between the fibre parameters and a specific mode of loss known as "microbending", and subsequently upon the fibre parameters and the general "cable induced loss mode".

As part of this research programme, a highly repeatable test was developed capable of inducing very pure microbends in fibre and a strong correlation was established between the parameters of fibres and their performance on the test. The test method was investigated by British Telecom., and the cabling industry and adopted as a reference test method for the measurement of fibre susceptibility to the microbend effect.

The work was extended to the cabled fibre product and using the same regression techniques as in the first part of the work, a possible link between cabled fibre performance, microbend test results and fibre parameters was explored. While it is shown that there is some correlation, it became evident at this stage of the investigation, that other variables apart from fibre parameters were affecting cable performance.

The overall project resulted in an increased level of awareness and understanding of cable induced loss modes in general and microbending in particular.

CONTENTS

CHAPTER 1.0.

INTRODUCTION.

1.1 Optical Fibre-Prognosis and Economic Impact.

Optical fibre is an excellent transmission medium. It has many advantages over the other media including low signal attenuation, high bandwidth, small size, strength, flexibility, low cost, electromagnetic noise immunity and safe and quiet operation. This unique combination of features make fibre by far the most useful of all transmission media.

Optical fibre was originally intended to do little more than act as a light guide. However, twenty years of development have transformed it into the most promising of all transmission media. Alongside the dramatic development of the fibres themselves, optical transmitters and detectors have so improved the transmission and reception of optical signals that optical fibres are now approaching their full potential.

The prognosis for optical fibre is excellent. Society and industry is advancing towards an information intensive society, where optical fibre is an essential component, providing arterial highways for the information traffic of the future. As fibre performance continues to improve, and the infra structure of related technology continues to build up, the range of applications of optical fibre will continue to broaden.

The attenuation of current silica fibres is close to its theoretical (asymptotic) minimum value of approximately 0.14 dB/Km at the 1550 nm wavelength. The fine tuning of this loss is aimed at achieving a practical single mode fibre with low dispersion over the usable spectral region which can be manufactured at low cost. More basic work on an exact electromagnetic solution for waveguides

with frequency dependent and profiled index distribution, [1.1], will improve fibre design. The basic work on glass-material-formation mechanisms and its relationship to scattering, radiation hardness[1], refractive index and non-linear coefficients will substantially increase our ability to tailor fibres to specific applications. Continuing work on new fibre fabrication methods promises to reduce the basic cost further, so that the cost of a single mode fibre will eventually be less than the cost of a pair of copper wires.

In the future silica fibre, with its advantageous mechanical properties and abundance of the necessary raw materials, will constitute the majority of transmission fibres. Except where repeater spacing must be as great as possible, (eg. trans Atlantic optical links with spacings greater than 200 km.), silica fibre is adequate for most applications. Where repeater spacing must be minimised, fluoride glasses, chalco genide glasses and infra red transmitting crystals appear to yield the low losses required, if material structure can be controlled and impurities differentiated and removed, [1.2].

Special single mode fibres can be used for sensor application, (where grids are used and matched to the beat length of the light within the fibre), where maintenance of polarisation is crucial; and for component application.

For applications in hostile environments and in some sensor applications, silica fibre requires a coating of non glassy material. Silicon Nitride, (SiN_2), and metals have been used to successfully coat the fibre to form a hermetic shield. However, some coating methods reduce the strength of fibres, possibly due to surface crack formation. Coating uniformity can also cause excessive temperature dependent bending losses. Research in this area involves controlling the deposition of material on the glass surface by better regulation of the chemical reactions involved. The objective is to improve

---

1 radiation hardness-the ability of a fibre to resist opacity following the electromagnetic shock wave from a nuclear blast

deposition uniformity and adhesion, as well as broadening the range of materials usable for the fibre coating.

Advances in fibre technology have led to increases in information carrying capacity, (bandwidth), and decreases in signal attenuation over the length of the fibre. Advances have now brought fibres to the point where their full potential is only limited by the terminal equipment. Significant technological advances in signal processing capabilities at the terminals are required if the full potential of existing fibres is to be achieved.

Fibres currently available can handle 1000 GHz bandwidth. Current fibre systems have been designed to handle signals up to 2.24 Gb/s. Highest bit rate signal transmission demonstrated is below 10 Gb/s. Two pertinent questions are:

(i) Is 10^{12} b/s, (tera bit rate), possible for future optoelectronic components?

(ii) If 10^{12} b/s can be attained, how should the design of signal handling systems be changed to take advantage of such high signal processing speeds?

These questions are timely since the transmission capabilities of the fibre are adequate to cater for these signalling rates. Indeed, several applications indicate that the demand on information capacity, transmission and processing rate can make use of such high signalling rates.

For example, if video phones at 70 Mb/s per channel are as densely installed as telephones at 64 kb/s per channel today, the transmission requirement would be 1000 times the current trunk system transmission rates of 560 Mb/s; hence 560 Gb/s would be required [1.3].

The lag of the capabilities of the "end" technologies behind the optical fibres has led to a shift of emphasis in the areas of principle research of the fibre optic producers and users since the gradient of the improvement curve has now decreased. The research can now broadly be split into two areas:

(i) Improvement of fibre and telecommunication cable production methods for improved yields,

(ii) Modifications to fibre and applied protective layers to produce specialised performance characteristics or enhance performance of fibres exposed to specific or extreme conditions, (eg. radiation hardened fibre does not become opaque in the electromagnetic shock wave which follows a nuclear blast.

Area (ii), is concerned primarily with the leading edge of fibre and cable development, and is very dependent upon customer requirements. A production company is approached by a customer with specific requirements; or a market, (geographical or technological), is addressed and suitable products are developed. This means that this is a shifting set of criteria defined by various customers, which are specifically targeted and researched on an interactive basis with the customer to develop products fully compliant with requirements. For the purposes of this project, area (ii), was not addressed as no single research area existed. Projects connected with this area of research were primarily of a short-term nature and were therefore unsuitable as a teaching company project.

Area (i) was concerned with the concept of quality within the workplace and with the integrity of a product throughout the production cycle. The area of study sought to make changes to production methods to improve the final product by "fine tuning" the input materials and processes. Area (i) did not cater for the needs of any one customer, but sought to improve the standard of product and improve cost effectiveness for all customer products.

1.2 Optical Fibres, a Description

An optical fibre is essentially a dielectric waveguide. It has been known for some time that high-frequency electromagnetic energy can be transmitted along a glass or plastic rod and, indeed, simple observation shows that short rods are translucent to light. Unfortunately, two factors prevented that knowledge from being used to produce useful light guides:

(i) energy carried near the periphery of the dielectric was radiated out to the surrounding air,

(ii) the dielectric production techniques were primitive and could achieve only product where attenuation was so large that worthwhile transmission distances could not be achieved.

The first difficulty, though almost insurmountable at microwave frequencies, was overcome in the optical and infrared parts of the electromagnetic spectrum by enclosing the guide in a cladding of similar material, but which has a slightly smaller refractive index. The boundary between the cladding and the core acts as a reflecting surface to the transmitted light using the property of total internal reflection. The second problem, that of high attenuation, could only be reduced by refining the methods of producing and drawing the glass so that the impurities and irregularities were reduced to a minimum. The attenuation now achievable in the laboratory is almost as low as possible, at about 0.2 dB/km.

Fibres of varying quality are used for communications, but when distances are significant, care is taken to ensure that the lowest attenuation possible is achieved. This involves choosing the best operating frequency for the particular fibre material, and ensuring that any contaminating elements are removed from the glass during manufacture. Before considering the loss mechanisms inherent in

any fibre, we will look at the different fibres used, and examine, with the help of ray theory, the way in which light propagates along the optical waveguide.

A practical fibre must have a light guiding core enclosed in a coaxial cladding of a second transparent material whose index is lower than the core. The larger the index difference, the larger the angle of acceptance. For optical fibres, the criteria for efficient and large light carrying capacity are:

(i) large core diameter,

(ii) high core refractive index,

(iii) low cladding refractive index,

(iv) sufficient cladding thickness,

(v) good flexibility,

(vi) good transmission efficiency.

These criteria are qualitative and served initially as engineering design yardsticks.

The journey of all light waves through an optical fibre starts at a source: usually a laser or a light-emitting diode. The source is placed close to one end of the fibre. Light from the source illuminates the core. Some of this light will pass straight along the axis of the core, while the remainder will enter at an angle and will eventually hit the core-cladding interface. Light striking the interface at steep angles will breach the interface and cladding, and will then be absorbed typically

by a plastic coating meant to protect the fibre from mechanical damage. Light striking the interface at shallow angles will be totally reflected back into the core. This total reflection process occurs repeatedly, guiding light rays along the length of the fibre.

The total reflection is the result of the fact that light and all other electromagnetic waves travel at different speeds in different materials. The speed with which light travels through a material is represented by the index of refraction: the ratio of the speed of light in a vacuum (which is the fastest) to the speed of light in the material. Since light travels slower in the core than in the cladding, the core has a higher index of refraction. Whenever light travels from a material of high refractive index to one of low refractive index, some is reflected and some is transmitted. The fraction of light reflected depends on both the angle at which light strikes and the refractive index difference between the two substances.

Fine tuning the difference in refractive index between the core and the cladding and controlling the diameter of the core, can enhance the guiding effect so that light signals stay focused and all signal components arrive at the receiver simultaneously. If all goes well, some of the light from the source emerges at the far end of the fibre core and illuminates a receiver, which is usually a photosensitive detector on a circuit wafer.

1.3 The Problem

Based on the above description of light transmission in a fibre, it might be supposed that the attenuation of a fibre would be fixed after the fibre had been made. In practice however, a curious effect is observed in that the attenuation of fibres increase during the cable production process, this amount being known as the attenuation increment. The area chosen for this research was to investigate the attenuation increments observed in fibres as they progress through the production process when

they are put into cables. Samples of fibres observed throughout production of telecommunications cables can be seen to behave in a characteristic way. The performance and final signal loss in most fibres is closely related to the level of attenuation measured in the fibre before the start of cabling. These fibres, which we may regard as having standard performance, constitute by far the largest percentage of all fibres produced. Although initial attenuations of some fibres are not noteworthy, they can subsequently behave in a non standard way. It would appear that for these fibres the increment in attenuation at each stage of production, and more importantly the attenuation observed in the completed cable, does not follow the pattern which is attributed to normal fibres. These fibres can be called "rogues" and can often be the cause of costly reworking or even scrapping of a cable. With 96 fibre cables in regular production, one rogue fibre can be a very costly event.

Many modes of loss are active in telecommunications cable and all cause attenuation in fibres to varying degrees. When inserted in cables, fibres in the main produce a basically standard set of "cable induced losses", which in normal fibres cause an attenuation increment of a certain amount. The rogue fibres discussed above however, show a raised level of susceptibility to the cable production induced losses modes and tend therefore to produce unacceptable levels of attenuation in finished cable. It was therefore decided that the research would be based in two areas:

(i) Investigation of the nature of fibres which showed higher than normal levels of susceptibility to the set of cable induced loss modes.

(ii) Investigation of one of the more dominant modes of loss active in cables, namely microbending.

Without doubt, the most significant loss mechanism active in the cabling process is that of microbending, [1.4] . Despite this, microbending remains one of the least understood loss

mechanisms. There are no entirely satisfactory methods tests in existence to test the effect or the susceptibility of fibres to it; neither are there measures incorporated in cable designs specifically to eliminate it.

The purpose of the study was therefore to carry out an investigation into the nature of microbending and the susceptibility of fibres to it; and to examine the general set of cable induced losses in order to minimise their effects and maximise cable acceptance rates. By improving the quality of knowledge in both of these areas, it was judged that a greater understanding of the cable production process and of the requirements for optimum fibre and cable designs could be attained. The achievement of these objectives would directly improve the quality and the cost competitiveness of the products produced. A variable would be removed from the production process, and the process of producing cables would become more scientific and therefore more controlled.

This dissertation will present methods of fibre and cable production and investigate the related theories governing optical fibres and cables, which will then lead on to identify the problem being addressed, and the approach adopted to resolve the issues raised.

The project targets the area of test research to establish modes of microbending and to examine the validity of mathematical modelling. Following the successful development of a repeatable, pure microbending test and the successful modelling of results obtained on the test using fibre parameters- proving the inherent susceptibility of fibres to the microbending mode of loss, the direction of the study was altered to address the situation of cabled fibres. Three bodies of data arose: the fibre parameters, the test results of the fibres and the cabled fibre performance. The first part of the work was presented at the 1989 International Wire and Cable Symposium in Atlanta, Georgia as a technical paper, while the second area of research indicated the shortcomings of the work carried out thus far, the potential for future resolution of the cabled fibre attenuation increment problem and finally the

establishment of the innate susceptibility of individual fibres to the loss modes imposed on it by the cabling process.

The dissertation will end with a report, firstly of the pilot study undertaken to verify the validity of the work, secondly of the method of research chosen and finally a discussion of the main project.

References.

[1.1] Stern et al., "Short Wavelength Transmission on 1300 nm optimised single mode fibre", Optical Engineering-October 1988 Vol. 27 No. 10.

[1.2] Dreschage and Moynihan, "Infrared Optical Fibres", Scientific American, November 1988.

[1.3] C. K. Kao, "Optical Fibre", pp 149-150, Peter Peregrinus, 1988, on behalf of the Institute of Electrical Engineers.

[1.4] Grasso and Meli, "Microbending Losses of Cabled Single mode Fibres", Societa Cavi Pirelli SpA. Viale Sarca, 222-20126 Milano (Italy).

CHAPTER 2.0.

Characteristics and Classes of Optical Fibre.

2.1 Introduction

In the constant search for increased information capacity and decreased attenuation, the chemical composition and the geometric characteristics of fibres are under constant scrutiny and manipulation. Chapter 4 deals with the improving standards of glass clarity whereas the purpose of this chapter is to define the mode of operation of fibres and the various designs in existence to improve their performance.

There are two basic theories which explain fibre optic performance. The first, in existence before light was understood to be an electro magnetic wave, is ray optics. While later electromagnetic wave theories offer an in-depth and accurate description of a fibre's characteristics; physical and particularly geometrical optics provide a readily understood description which is helpful in developing a physical understanding of the performance of the fibre. Ray optics, provide design guidelines, as well as suggesting how electromagnetic solution can be constructed by suitable approximations.

The second descriptive theory alluded to already, uses electromagnetic wave theory developed by Maxwell, and in particular is explained using Maxwell's equations. The equations treat the fibre as a dielectric waveguide, and yield results which are "precise solutions".

By the time light was identified as electromagnetic energy, Maxwell's equations governing electromagnetic wave behaviour were already well known. Specific solutions have been obtained for many important practical problems in the fields of waveguides and antennae. However, analytic solutions are obtained only when the geometry and boundary conditions are favourable. The dielectric

waveguide or fibre problem had been solved for some ideal cases namely, the planar waveguide cases early in the 20th century. The classical approach starts with the set of Maxwell's equations for a linear, isotropic, loss less dielectric material having no current or charges, [2.1]. These are used to deduce the progression of light along the dielectric guide.

A plane wave in free space is also one solution of Maxwell's equations. Its physical characteristics can be verified in practice as electromagnetic energy in the form of radio or optical waves. The laws of optics can be derived formally in ray formalism. Polarisation of the optical plane wave is seen to be associated with the direction of the E, electric field vector, or H the magnetic field vector. The E and H vectors in a plane wave are transverse and perpendicular to each other. Power is expressible in the form of a Poynting vector. The dielectric-waveguide problem was solved early in the 1900's, both for planar infinite slab guides and for the circular rod surrounded by a second infinite medium. Whilst the solution is valid only for ideal dielectric material, it does provide a means to determine the field distribution of propagating and radiative modes, as well as propagation constants. It shows that a finite number of modes can propagate in a dielectric structure corresponding to specific geometric ray directions. The radiative modes form a continuum and correspond to unguided refracted rays. The wave description provides an exact description of the characteristics of the fibre as a waveguide, and allows the fibre design to be improved.

The earlier of the two theories, the ray optics approach as previously discussed, is less precise than the electromagnetic system described above. However its usefulness as a means of approximating the exact solution of the electromagnetic theory results is apparent. This is demonstrated by considering the concept of an optical beam or a ray in relation to the infinite plane wave. If a plane wave front is infinite in extent, it satisfies Maxwell's equations and can be exactly characterised by a direction of propagation normal to the wave front and a polarisation direction of the transverse E vector. When a cylindrical optical beam has a cross-section measured in many wavelengths across its diameter, the

beam spread is small, especially over short distances. It is reasonable to expect that the beam front behaves as a localised plane wave of infinite extent. Although this approximation is theoretically difficult to manage, and has not been satisfactorily quantified in a general and useful way, a slender beam of light 0.1 mm in diameter at a wavelength of 1 μm, only diverges at approximately 1/100 radian, so that when propagating to a point 100 wavelengths away, the diameter increases by only 1 %. Its behaviour can therefore be said to closely resemble that of a plane wave.

In a straight fibre, the ray approximation appears to have good validity. This can be explained readily in a planar waveguide. The propagating modes of a planar waveguide can be shown to be equivalent to the intersection of two plane waves. Hence, a ray analysis is exact. In the fibre, the propagating of modes can be shown to be able to be constructed from a spectrum of plane waves, indicating again that ray representation should be exact.

2.2 Fibre Types

2.2.1 Introduction

Glass is an obvious candidate material for optical fibre light guides. It is transparent and can be pulled into a thread of uniform cross section. From early times, a flexible means of guiding light was theoretically possible. The steps towards developing a light guide with prescribed performance meeting practical application requirements are many and involve a series of scientific and technological breakthroughs.

The optical fibre can serve as a light pipe for visible light. A practical fibre may be produced with two glasses, of differing refractive indices. The glass with the higher refractive index serves as the light guiding core; the other with lower refractive index serves as cladding which allows the fibre to

be handled without disturbing the light propagation. A practical fibre is therefore made up of a light guiding core enclosed in a coaxial cladding of a second transparent material who's refractive index is lower than that of the core. The larger the index difference, the greater the angle of light acceptance into the fibre, (the numerical aperture-see chapter 3).

Were the only design criteria the volume of light power transmitted, conformance to these criteria would be all that was required from fibres. However, information is transmitted along the fibres by modulation of the light signal, and it is found that the requirements of signal capacity (bandwidth), are opposed to those of light power, (see later chapters). In specifying physical dimensions and refractive index profiles of fibres, therefore, a compromise has to be established between these two opposing requirements.

Three types of fibre are shown in Fig 2.1, and discussed in 2.2.2, which demonstrates the progression in understanding of light:

(i) from the flexible light pipe where, because of low glass purity light power had to be maximised;

(ii) designs where glass purity had been improved to a point where light power could be so limited that only one mode propagated in order to increase the fibre bandwidth;

(iii) a design where the principal causes of bandwidth limitation-dispersion, (see chapter 6), are minimised, while large core diameter is maintained for large numerical aperture and therefore high light power insertion.

It is found that this last design, graded index fibre, has the highest production cost of the three types.

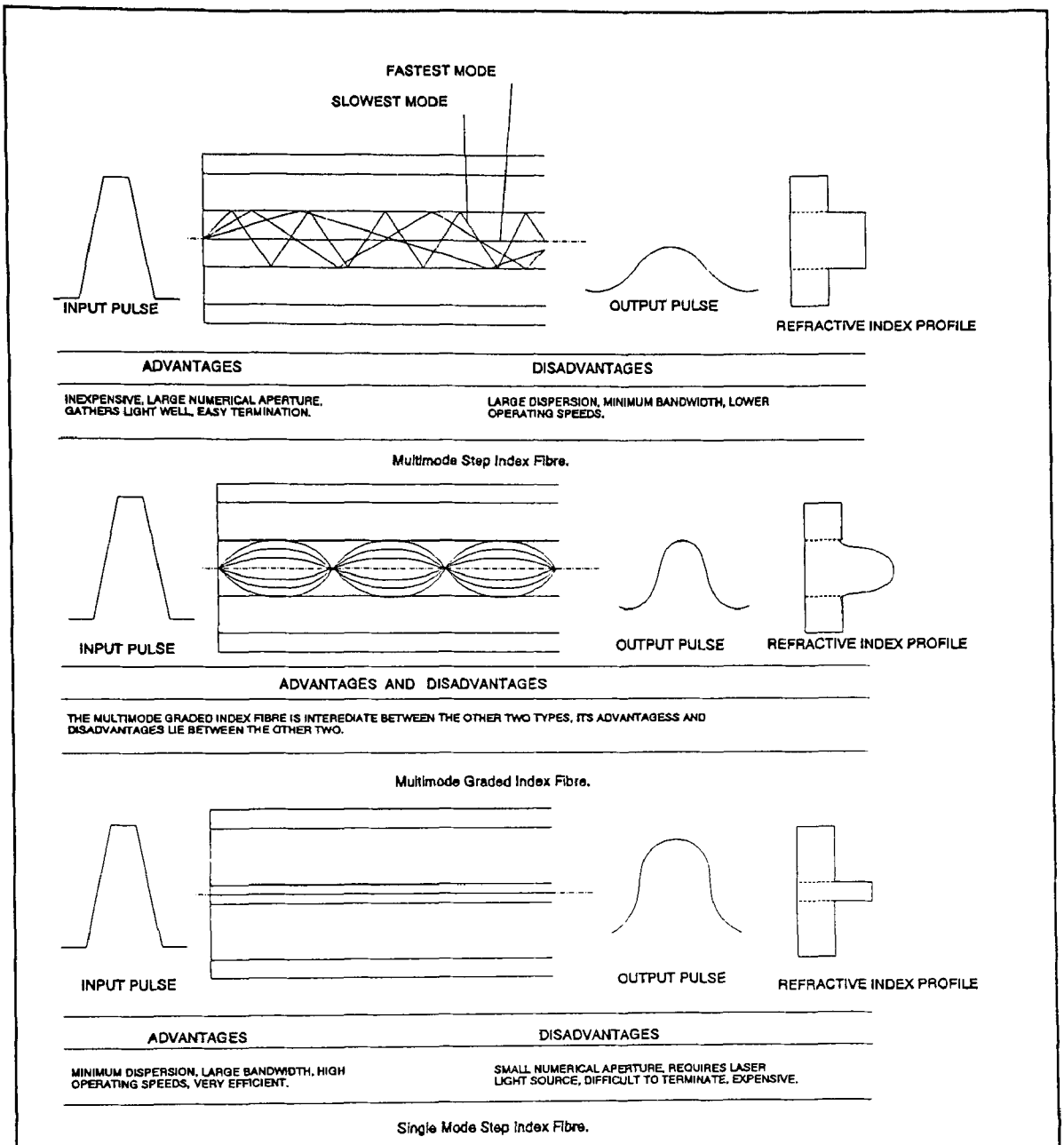

Figure 2.1 Types of Light Propdagation in Different Fibre Designs.

2.2.2 Fibre Designs

Wide variations exist between fibre designs. Differences exist principally between the cores and their refractive index profiles. Fig 2.1 shows three of the most popular designs, their effect on signal pulses

and the mode of propagation of light along these fibres. The following sections discuss the merits of these and other fibre types.

2.2.2.1 Multimode Fibre

The multimode fibre is the most basic of the fibre designs which will be discussed here. It is a step index fibre which is made up of a high index core surrounded by a cladding of a lower index. The diameter of the core can vary and examples of multimode fibres contain cores with diameters of, for example 50 and 62.5 μm. The diameter of the cladding is normally 125 μm.

Multimode step index fibres may be fabricated from either multi-component glass compounds or doped silica. These fibres can have reasonably large core diameters and large numerical apertures to facilitate efficient coupling to incoherent light sources such as light emitting diodes, (LED's). The performance characteristics of this fibre type may vary considerably depending on the materials used and the method of preparation; the doped silica fibres exhibit the best performance.

Structure:

Core diameter	50-400 μm
Cladding diameter	125-500 μm
Buffer jacket diameter	250-1000 μm
Numerical aperture	0.16-0.5[1]

1 See chapter 3 for definition of numerical aperture.

Performance Characteristics:

Attenuation: 4-50 dB/km limited by absorption or scattering. The wide variation in attenuation is due to the large differences both within and between the two overall preparation methods.

Bandwidth: 6-25 MHz.km

Applications: These fibres are best suited for short haul, limited bandwidth and relatively low cost applications.

2.2.2.2 Single Mode Fibres

Single mode fibres can have either a step index or graded index profile. However, the benefits of using a graded index profile are less significant than in the case of multimode fibres[2]. Therefore at present commercially available single mode fibres are almost exclusively step index. They are high quality fibres for wide band, long haul transmission and are generally fabricated from doped silica, (silica clad silica), for minimum attenuation. Although single mode fibres have small core diameters to allow single mode propagation, the cladding diameter must be at least ten times the core diameter to avoid losses from the evanescent field[3]. Hence with a buffer jacket to provide protection and strength, single mode fibres have similar overall diameters to multimode fibres.

---

2 Graded index fibres are intended to speed up the high order light modes, hence there is no advantage with monomode, which transmits no higher order modes.

3 The evanescent field is the portion of transmitted light power carried outside the fibre core.

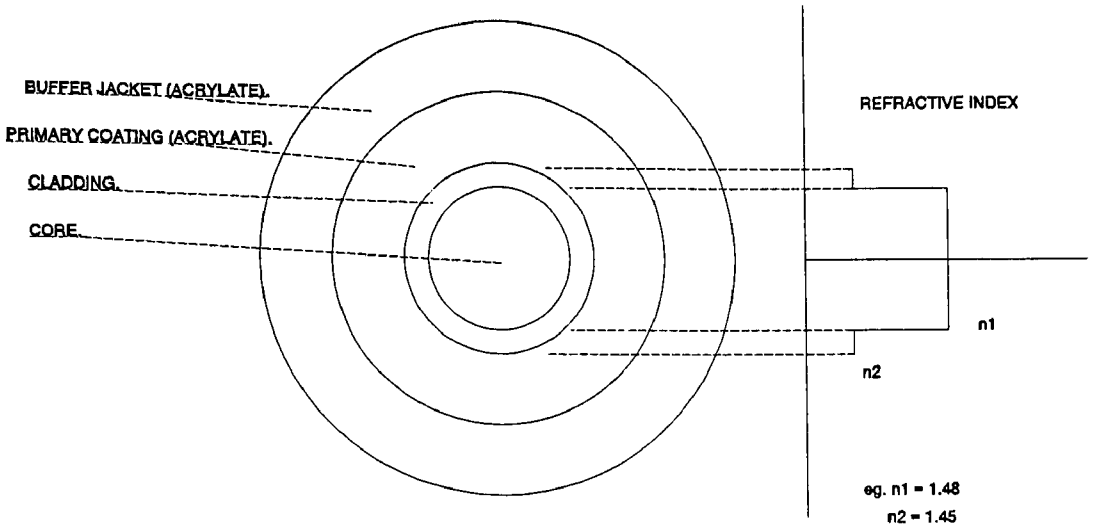

Fig 2.2 Typical Structure for a Glass Multimode Double Coated Step Index Fibre.

Structure:

Core diameter	3-10 μm
Cladding diameter	50-125 μm
Buffer jacket diameter	250-1000 μm
Numerical aperture	0.08-0.15, usually around 0.10

2.2.2.3 Multimode Graded Index Fibres

Multimode fibres which have a graded index profile may be fabricated using multi-component glasses or doped silica. However, they tend to be manufactured from materials with higher purity than the majority of multimode step index fibres in order to reduce fibre attenuation.

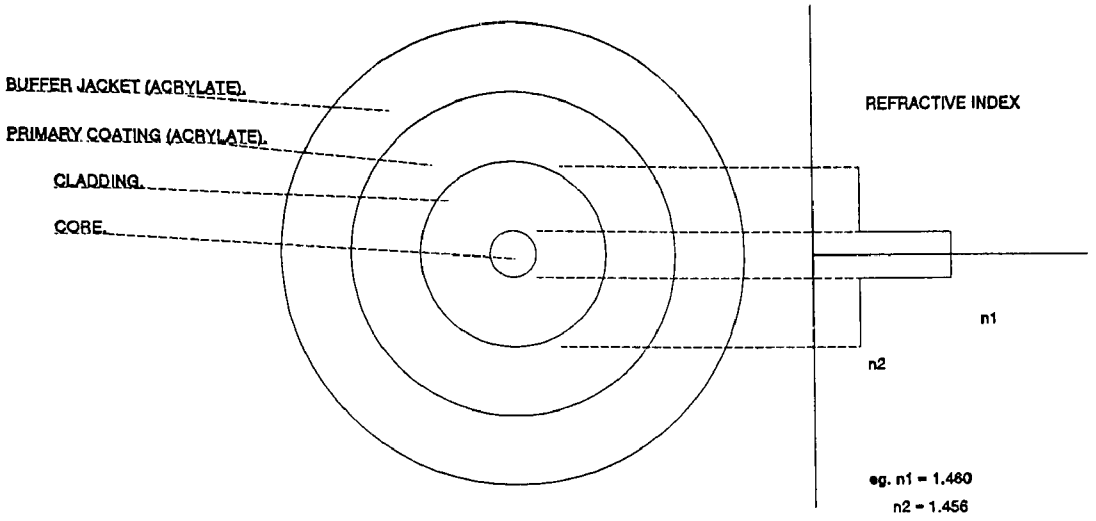

Fig 2.3 Typical Structure for a Single Mode Step Index Fibre.

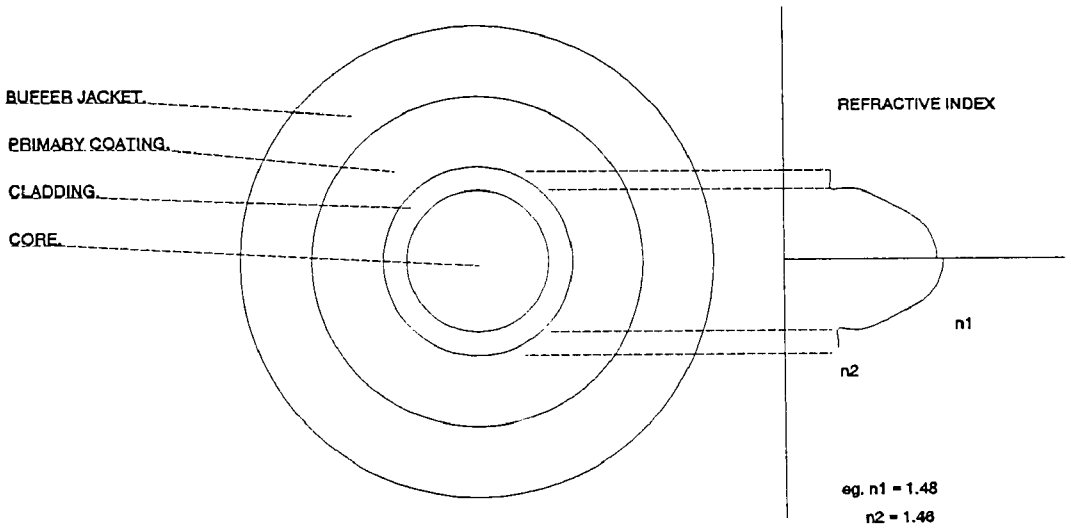

Fig 2.4 Typical Structure for a Glass Multimode Double Coated Graded Index Fibre.

Structure:

Core diameter — 30-60 μm, (a standard of 50 μm has been established for telecommunications applications).

Cladding diameter	100-150 μm, (a standard of 125 μm has been established for telecommunications applications).
Buffer jacket diameter	250-1000 μm
Numerical aperture	0.2-0.3

Performance Characteristics:

Attenuation: 2-10 dB/km, generally limited by scattering.

Bandwidth: 150 Mhz.km to 2 GHz.km

Applications: These fibres are best suited for medium haul, medium to high bandwidth applications using incoherent and coherent multi mode sources, (ie. LED's and injection lasers respectively).

It is useful to note that there are a number of partially graded index fibres commercially available. These fibres generally exhibit slightly better performance characteristics than corresponding multimode step index fibres but are somewhat inferior to the fully graded index fibres described above.

2.2.2.4 Plastic Clad Fibres

Plastic clad fibres have high levels of attenuation and are therefore normally multimode with either a step index or a graded index profile. They have a plastic cladding, (often a silicone rubber), and a glass core which is frequently silica, (ie. plastic clad silica-PCS fibres). The PCS fibres exhibit lower radiation induced losses than silica clad silica fibres and therefore, have an improved performance in certain environments. Plastic clad fibres are generally slightly cheaper than the

corresponding glass fibres, but usually have more limited performance characteristics. A typical structure for a step index plastic clad fibre, (which is more common), is shown in Fig 2.5.

Structure:

Core diameter	Step index	100-500 μm.
	Graded index	50-100 μm.
Cladding diameter	Step index	100-500 μm.
	Graded index	50-100 μm.
Buffer jacket diameter	Step index	500-1000 μm
	Graded index	250-1000 μm.
Numerical aperture	Step index	0.2-0.5
	Graded index	0.2-0.3

Performance Characteristics:

Attenuation:	Step index	5-50 dB/km
	Graded index	4-15 dB/km

2.2.2.5 All Plastic Fibre

All plastic fibres are exclusively of the multimode step index type with large core and cladding diameters because of the additional ruggedness of this design. There is therefore a reduced requirement for a buffer jacket for fibre protection and strengthening. These fibres are cheap to produce and are easier to handle than the corresponding glass variety. However, their performance, (especially for optical transmission in the infrared), is severely restricted, giving them very limited

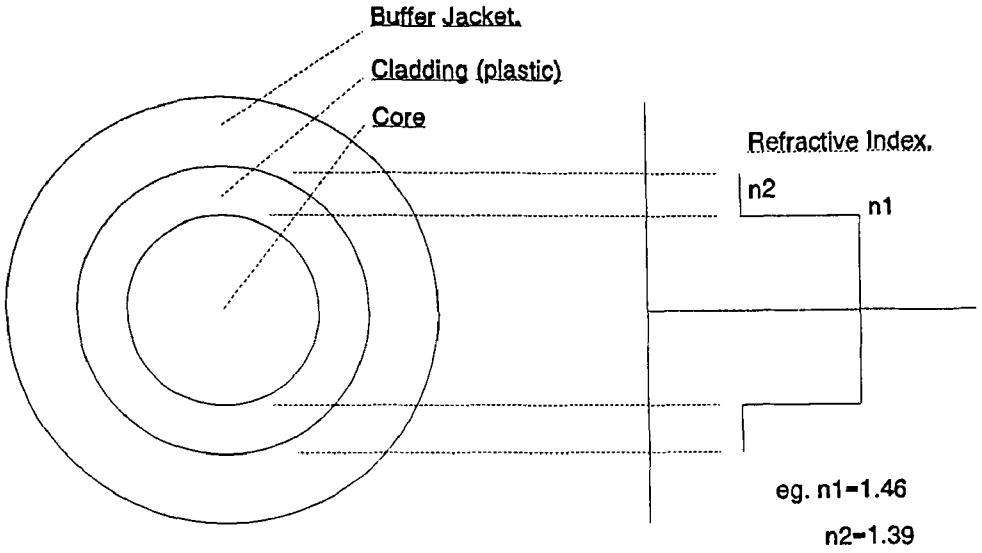

Fig 2.5 Typical Structure for a Plastic Clad Silica Multimode Step Index Fibre.

use in communication applications. All plastic fibres generally have large numerical apertures which allow easier coupling of light into the fibre from a multimode source.

Structure:

Core diameter	200-600 μm.
Cladding diameter	450-1000 μm.
Numerical aperture	0.5-0.6

Performance Characteristics:

Attenuation: 350-1000 Db/km, at a wavelength of 0.65 μm.

Bandwidth: This is not usually specified as transmission is generally limited to tens of metres.

Applications: These fibres can only be used for very short haul, (ie. in house), low cost links. However, fibre coupling and termination are relatively easy and do not require sophisticated techniques.

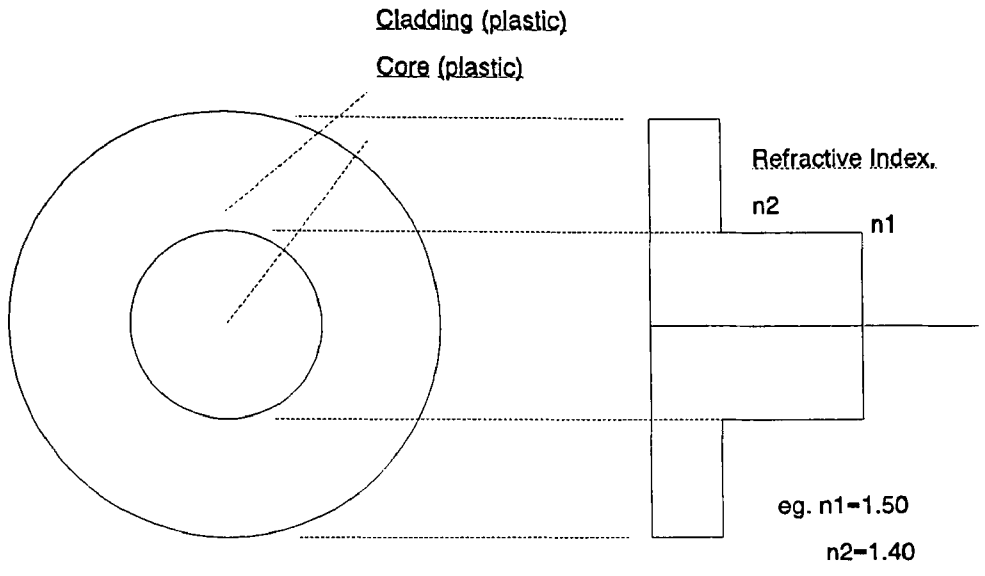

Fig 2.6 Typical Structure for an All Plastic Multimode Step Index Fibre.

2.3 Characteristics of Optical Fibres.

The fibre optic telecommunication market's continuing growth, has led to increasingly complex and specialised fibres being produced. Traditional parametric definitions often require re-specification, and new parameters defined in an attempt to adequately describe the fibres. The importance of measurements and hence the ability to completely classify a fibre, is demonstrated by the conservative estimate that 20% of the cost of fibre optic production, is taken up with measurements.

The need to classify fibre, has led to the development of a set of parameters which describe factors such as the quality of the fibre and its ability to transmit light. Mechanical parameters, such as those

describing the physical strength and hardness of a fibre exist, but these have been disregarded since they do not, in general directly affect a fibre's transmission capabilities, and so are outside the scope of this text. Parameters which are listed below, assist in describing the means by which light travels down a fibre, and the modes of light the fibre is capable of supporting at different wavelengths.

2.3.1 Physical Characteristics

The following section deals with the parameters describing the characteristics of the fibre. While these parameters were not developed to describe the light within a fibre, their variation affects both the level of the signal and the characteristics of the transmitted mode. It will be shown that the individual parameters listed below will have a direct relationship, in varying degrees, with the transmission characteristics listed under section 2.3.2. For the purposes of this work, the physical characteristics have therefore been described as "primary" parameters, while the transmission characteristics have been termed "secondary" parameters. The possibility that a particular combination of primary characteristics lead to a good or bad set of secondary characteristics and the ability of the researcher to predict the latter from the former will be discussed in later chapters.

2.3.1.1 Cross Sectional Dimensions

The methods employed in the production of optical fibres and in the subsequent application of protective acrylate layers, lead to significant stress and surface tension forces. The effect of the combination of forces on the completed fibre package is to render its various layers both concentric and circular in cross section. Fig 2.7 shows the normal cross section of a single mode, step index, single coated fibre. (The MCVD, (Modified Chemical Vapour Deposition), process mentioned in the figure title is discussed in Chapter 3.

The outside diameter of the fibre, or reference surface diameter (RSD), is so called because it is often used as a reference when geometric measurements are carried out. On all telecommunications fibres, the RSD is 125 μm. Fibre manufactures add a substrate tube to a fibre preform to allow the RSD requirement to be met, while still maintaining preform length yield, a typical preform yielding up to 40 km of usable fibre.

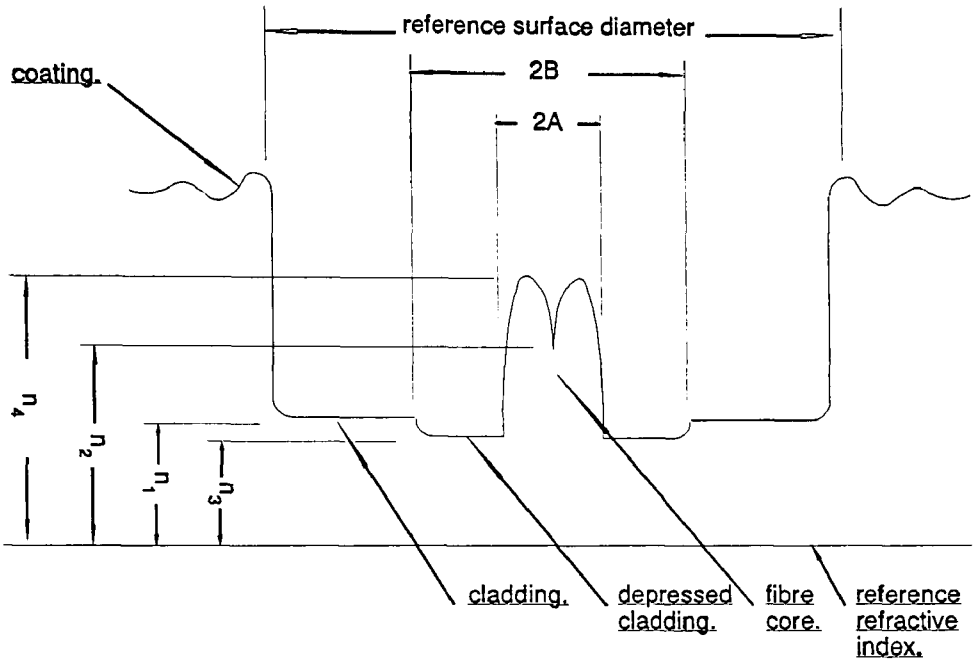

Figure 2.7 Refractive Index Profile of a Step Index, Singlemode Fibre with Depressed Cladding Produced by the MCVD Process.

The fibre core in Fig 2.7 is 8 μm. in diameter, which is standard for singlemode fibres. Multimode fibres have a core whose diameter is much larger, to allow propagation of light along the fibre by many differing "paths". Graded index fibres use a core whose refractive index profile is a parabolic curve. As explained in Chapter 2, this allows multi mode fibres to be used with higher bit rates by reducing dispersion, and effectively means that no clear boundary to the core exists.

In all cases, core diameter and the longitudinal consistency of that dimension, are tightly specified in order to ensure that the light path is not obstructed by any irregularities. As discussed above,

several acrylic coating options exist. Most fibres are either singly or doubly coated. The implications of the coating options are discussed above, but for the purposes of this chapter and regardless of coating design, the outside diameter of the completed package is normally 250 μm, as a general industry standard.

A third coating option is also available, although this cannot strictly be classified as a coating in the same way as the primary and secondary coats are. The option is to add a tertiary coat to the fibre. This third coat is added on top of the 250 μm. layers of acrylic material, and increases the outside diameter of the fibre by an order of millimetres. This design differs from those of single or double coat in that when triple coated, a fibre requires no further protection and may be stranded as part of a cable: see "Cable Production".

2.3.1.2 Core/Reference Surface Concentricity Error.

The various cross sectional components of a fibre as described above, should automatically achieve concentricity due to the nature of the production process.

The concentricity error of these components is defined as "the distance y, between the core centre and the centre of the reference surface, divided by the core diameter and expressed as a percentage."[2.2]

2.3.1.3 Ovality or Non Circularity.

Ovality of the fibre core.

The core non circularity is defined as the difference in length between two chords each passing through the fibre core centre, one chord being the longest line connecting points on the core/cladding interface, divided by the core diameter.

Ovality of the reference surface.

The reference surface non circularity is defined as the difference in length between two chords each passing through the reference surface centre, one chord being the longest line connecting points on the reference surface and the other chord being the shortest line connecting points on the reference surface, divided by the reference surface diameter.

2.3.1.4 Refractive Index Profiles.

Earlier sections dealt with refractive index options for multi- and mono-mode fibre, characteristics of each fibre type and the effect each type had upon the signal travelling within it. Later sections will attempt to describe the fine tuning of the basic refractive index profiles which have taken place to further optimise fibre performance in recent years. It falls to this section therefore, to define the various refractive index measurements carried out on fibres-both relative and absolute, which assist in the task of classifying fibres.

In order to assist with the definitions of refractive index measurement, Fig 3.1 shows a refractive index profile of a mono-mode, step index fibre with a depressed cladding, produced by the MCVD[4] production process.

2.3.1.5 Absolute Refractive Index Measurements.

Cladding refractive index

In a depressed cladding fibre such as that shown in Fig 3.1, the cladding refractive index is the refractive index of that portion of the cladding which has the higher refractive index. In MCVD

---

4 The MCVD, (modified chemical vapour deposition), method of fibre production is discussed in Chapter 3.

processes, (see Chapter 3), this is the substrate tube section of fibre outside the deposited layers. In Fig 3.1, the index is shown as the index n_1, above the datum line n_0-which is the refractive index for air.

Depressed cladding refractive index.

The refractive index of the section of cladding closest to the fibre core, can be intentionally depressed with respect to the index of the outer cladding layers as a means of modifying fibre performance, (see Chapter 3). Fig 2.7 shows the depressed cladding index as the dimension n_3. In the MCVD process, this is done merely by reducing the refractive index of the deposited layers of cladding.

Core refractive index.

The refractive index of the highest part of the fibre core, (ignoring the dip at the core's centre which is a feature of fibres produced by the MCVD production process-see Chapter 4), is shown in Fig 3.1, as being n_4.

Dip refractive index.

The refractive index of the dip at the centre of the core can only be measured in fibres whose production process produce the dip such as the MCVD process, (see Chapter 4). The dip refractive index in Fig 3.1, is shown as being n_2.

2.3.1.6 Relative Refractive Index Measurements.

Cladding depression.

The reasons for depressing a section of the inner cladding are described in Chapter 6. The numerical value for cladding depression is taken to be:

$n_3 - n_4$

so that if a depression in the cladding exists, its descriptive value is always negative.

Relative height of core, or ΔN.

Two definitions of relative core refractive index are in existence although of the two shown below, the latter is more commonly used.

Definition 1:

$$\Delta N = n_1 - n_3 \qquad 2.1$$

Definition 2:

$$\Delta N = \frac{n_1^2 - n_3^2}{2n_1^2} \qquad 2.2$$

Dip size.

The dip size is given as a difference:

$$\delta n = n_1 - n_2 \qquad 2.3$$

2.3.1.6 B/A Ratio.

The B/A ratio is the ratio of deposited core radius to deposited cladding radius. Chapter 4 describes how the MCVD process deposits layers of glass inside a substrate tube, starting with inner cladding layers and ending with the fibre core. The change from cladding to core glass is made simply by

changing the relative levels of the reactant chemicals entering the production process to affect a change in refractive index level. By delaying or advancing the moment at which the change in the chemical ratio is made, the position of the core/cladding interface within the fibre can be made closer or more distant to the fibre centre. The ratio of thickness of core to deposited cladding glass may therefore be controlled.

The B/A ratio can be used to closely control the level of cut off wavelength. The advantages of such control are described in Section 3.3.1 below. Because the deposited layers of glass are much more pure than the substrate tube, light travelling in the tube is attenuated much more quickly than that within the deposited layers. The LP_{11} light mode, [2.6] will be greatly effected by this ratio. If the B/A ratio is raised, the amount of deposited cladding will be increased and so the LP_{11} mode will move through very pure deposited layers which will tend to reduce its attenuation per Km. thus raising the cut off wavelength. Lowering the B/A ratio, will reduce the amount of deposited cladding and thus force more of the LP_{11} mode to travel in the substrate tube. This has the effect of raising the attenuation of the mode, in effect lowering the cut off wavelength.

The importance of close control of the cut off wavelength is discussed below. The importance of the B/A ratio as a control parameter is apparent.

2.3.2 Transmission Based Parameter Definitions.

As discussed above, "secondary" characteristics are most often a measure of the effects on transmission properties of the levels and variations of the primary characteristics. Primary characteristics can be viewed as having been set at levels to produce certain performances in fibres: the secondary parameters measure the success of the primary set in meeting this objective, and of the consistency with which the objective is met.

While other "secondary" parameters exist, those described here were seen to be most important in the classification of fibres, and in the work of the associate.

2.3.2.1 Cut-Off Wavelength (λ_c).

All fibres are capable of transmitting light via multiple modes. Modal "leakage" from fibres increases with light wavelength, reducing its capacity to transmit power. One definition of cut-off wavelength, is that it is the wavelength of transmitted light, above which single mode fibre is capable of transmitting only the fundamental transverse mode (HE_{11} or LP_{01}), which has no cut-off wavelength. The fundamental mode theoretically travels coaxially with the core of the fibre. All modes of higher order than this are cut off, or have attenuations high enough to prevent them form becoming guided modes for $\lambda > \lambda_c$.

This simple definition is not sufficient to describe cut off wavelength. Higher order modes can have large attenuations at wavelengths much below the theoretical value of cut of. It is therefore taken that the "effective" cut off wavelength is defined as the wavelength at which second order modal power is below a given level compared to the fundamental LP_{01} mode power. The cut off wavelength therefore depends upon fibre length and curvature: a fact borne out by the problems of the fibre industry in defining the test conditions.

Generally, λ_c in a cabled fibre is less than that in a bare fibre, which in turn is less than the theoretical λ_c. The standard test condition is currently specified as being 2m; and the standard curvature is a 28 cm radius loop placed in the 2m length of fibre.

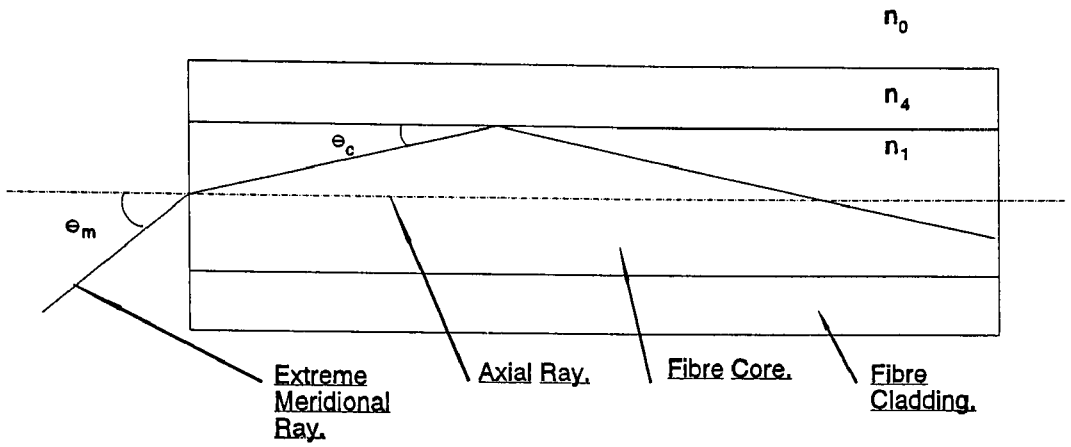

Figure 2.8 Sectional View of Meridional Rays Travelling Along a Multimode Fibre with No Cladding Depression.

2.3.2.2 Numerical Aperture.

For a step index fibre, all rays of light incident on the core at angles less than the acceptance angle, Θ_m, are trapped within the core. Two possible paths for the light being transmitted by the fibre are shown in Fig 2.8.

The law of refraction suggests that the largest possible mode angle is Θ_c, where:

$$\cos \Theta_c = \frac{n_4}{n_1} \qquad 2.4$$

but,

$$\frac{\cos (90-\Theta_m)}{\cos (90-\Theta_c)} = \frac{n_1}{n_0} = n_1 \qquad 2.5$$

therefore,

$$\sin \Theta_m = n_1 \sin \Theta_c = n_1\sqrt{(1-\cos^2\Theta_c)} \qquad 2.6$$

$$\sin \Theta_m = n_1\sqrt{(n_1^2-n_4^2)} \qquad 2.7$$

Numerical aperture, the maximum acceptance angle for light entering a multimode fibre, is:

$$NA = \sin\Theta_m = \sqrt{(n_1^2-n_4^2)} \qquad 2.8$$

but,

$$\Delta N = \frac{(n_1^2-n_4^2)}{2n_1^2} \qquad \text{(see 2.3.1.5.)} \qquad 2.9$$

therefore,

$$NA = n_1\sqrt{(2\Delta N)} \qquad 2.10$$

For a given system, a trade-off must be made between short and long length losses. For very short cables, the end losses make the dominant contribution to the total insertion loss, whereas for very long cables, attenuation losses dominate. Thus, for some short-distance applications with large area sources, it is advantageous to use large numerical aperture, large core fibres (or even a number of such fibres in parallel as is the case for endoscopes), for long cables, small core, lower numerical aperture fibres are best (see 2.2.1., mono-mode fibres).

The following is an example of a numerical aperture calculation-for use in 2.3.2.3. below.

$$\Delta N = \frac{(n_1-n_4)(n_1+n_4)}{n_1^2} \approx \frac{(n_1-n_4)}{n_1} \qquad (\text{if } n_1 \approx n_2) \qquad 2.11$$

Typically, $\Delta N = 0.01$, $n_1 \approx 1.5$. Therefore,

NA (numerical aperture) = 0.2[5]

2.3.2.3 "V" Number or Normalised Waveguide Width.

The V number is defined as the percentage of energy contained within the core of a fibre, compared to the total energy within the fibre.

$$V = \frac{2\pi a\sqrt{(n_1^2-n_2^2)}}{\lambda} = \frac{2\pi a(NA)}{\lambda} \qquad [2.3]$$

2.12

(a = radius of core)
(λ = wavelength of signal light)

It may be shown [2.3], that the number of possible modes which a fibre is capable of transmitting, N, is given by:

$$N = \frac{V^2}{2}$$

2.13

When λ is not very much greater than a, the ray theory is no longer valid. An exact analysis using Maxwell's equations shows that if:

$$V = \frac{2\pi a(NA)}{\lambda} < 2.405$$

2.14

then only one mode, the LP_{01}, can exist. That is the fibre begins acting as a single mode fibre, when the V number drops below 2.405.

---

5 Equates to Θ_m, or a cone of acceptance with included angle $2\Theta_m = 23.07°$.

2.3.2.4 Mode Field Diameter.

Mode field diameter is the width of the fundamental mode, guided by a single mode fibre above its cut off wavelength. It is commonly taken to be the diameter of the $2/\sqrt{e}$ point of the optical power. MFD is, in principle a very useful parameter, as it allows the prediction of splicing losses, and has an effect on microbend sensitivity. The wavelength dependence of the MFD, allows prediction of bending losses, and of waveguide dispersion (see 6.2.2.).

It has been said "MFD appears to be a parameter in turmoil. Its importance is well understood, but no consensus on its fundamental definition, or measurement method has yet emerged. Several measurement techniques and definitions have been proposed during the past few years. None of these methods is universally accepted as a reference test method, nor is any method more or less fundamentally correct than the others".

The degree of consistency between the different techniques is a direct result of the choice of a definition for the MFD.

Gaussian definition of MFD.

The Gaussian approximation, as produced by Marcuse [2.4],[2.5], and illustrated in Fig 2.9, so widely used for the first generation of single mode fibres, is now severely questioned. Small systematic errors result for even quasistep index fibres when the Gaussian approximation is used, especially at longer wavelengths. Also, the second generation fibres with non-step refractive indices, for dispersion shifting and dispersion flattening, do not exhibit Gaussian fields at any wavelength.

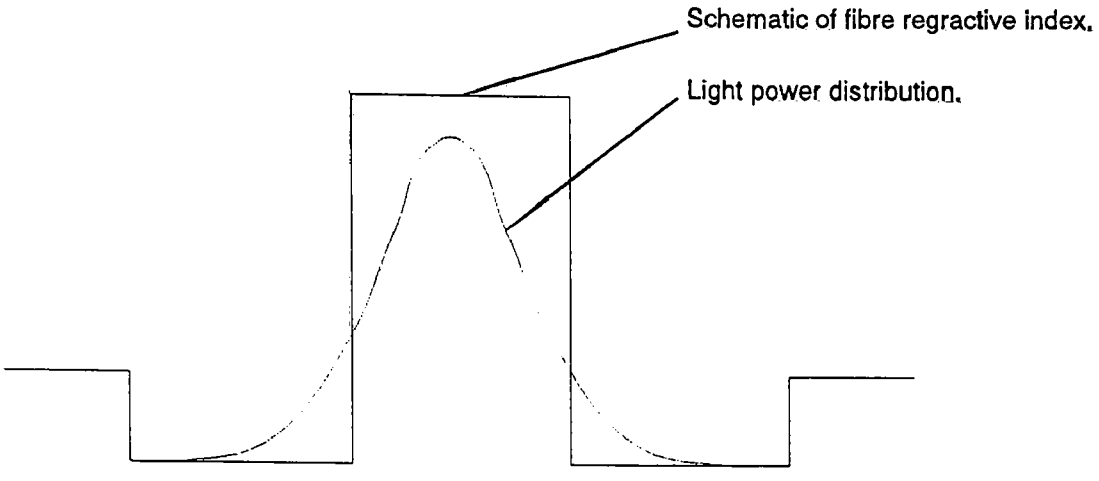

Figure 2.9 Gaussian Approximation to the Mode Power Distribution.

Petermann definition of MFD.

An alternative definition of MFD, based on the moments of the near field, which is called the Petermann 2 definition. This approximation can, in theory, solve problems of consistency, and reduce the systematic errors [2.7]. The primary difference with respect to the Gaussian definition, is that the Petermann definition uses the measured field directly, making no assumption about the shape of the field. This distinction, has caused the Petermann 2 definition to become more widely accepted.

2.3.2.5 Bandwidth.

Bandwidth is a measure of the information carrying capacity of a transmission medium. Bandwidth gives the threshold of bit rate, that is the number of data pulses per second, at which the transmitted power drops byu half. Bandwidth is expressed in MHz, but is often quoted in MBit/sec., using an approximation that 1 MHz=2 MBit/sec.

Bandwidth is length dependent, because of the length dependent nature of the mechanisms which limit it. Therefore when a specific length of transmission media is not being addressed and generalisations have to be made, the units of bandwidth normally used are:

$$\text{Bandwidth} = \frac{\text{Mbit}}{\text{sec.Km.}} \qquad 2.15$$

References.

[2.1] Hecht, "Optics-Second Edition", Addison-Wesley Publishing Co. Inc. copyright 1987,1984.

[2.2] British Telecommunications Specification CW 1500 part 1, Controlled document.

[2.3] Barnoski M. K., "Fundamentals of Optical Fibre Communication" second edition, Academic Press Inc. copyright 1981.

[2.4] Marcuse.D.,"Loss analysis of single mode fibre splices",Bell Syst. Tech. J., 1977, 56, pp 703-718.

[2.5] Marcuse.D.,"Gaussian approximation for single-mode fibres", J. Opt. Soc. Am., 1978, 68, pp 103-109.

[2.6] C. K. Koa, "Optical Fibre", pp 40-42, IEE materials and devices series 6. Peter Peregrinus Ltd., London, UK, 1988.

[2.7] Anderson.W.T.,"Status of Singlemode Fibre Measurements", Technical digest symposium on optical fibre measurements, National Bureau of Standards, US department of commerce, 1986, pp 77-90.

CHAPTER 3.0.

Methods of Fibre Production.

3.1 Introduction

The advantages of optical fibres over other signal transmission media, lie in two areas: the first is that fibres attenuate signals passing through them only very slightly; the second is that compared to alternative transmission systems, they exhibit an extremely wide bandwidth.

The requirements of high quality optical fibres are:

i) near perfect cross-sectional geometry, both for circularity and concentricity and consistency of the cross-sectional dimensions along the fibre length;

ii) high strength, durability and good flexibility;

iii) lowest possible cost;

iv) long, continuous lengths of fibre,

v) high dielectric purity.

The last point is particularly important, since if it were not possible, the task of processing fibres would become much more difficult. In order to make the fibre industry more profitable, flow methods of production and economies of scale are used to minimise costs. Should the production lengths of fibre drop, the cost and difficulty in selling and producing fibres increases.

3.2 Fibre Production Processes

Two methods are available for producing optical fibres. Optical fibre can be drawn from molten glass. Surface tensions active in the material induce in it a near perfect cylindrical geometry which on hardening, is retained. Cross sectional consistency, along the length of the fibre can be assured by maintaining a constant ratio of rate of drawing to mass flow rate.

A second alternative for producing fibre is to stretch a glass rod of large dimension until it has attained a pre-defined geometry. Production is in two stages, the first is to produce the glass rod, the second is to stretch it to the required dimensions. The two areas of production involved in this method are dealt with in detail separately below. This method is most frequently used where a fibre has a core/cladding arrangement within it, although fibres with geometries other than circular can also be produced. In the latter case, the degree of heating is critical. The more softening of a glass rod which takes place, (the less viscous the glass melt), the more significant the forces of surface tension become. A less viscous softened glass produces a fibre more circular than a more viscous one-regardless of preform shape. As stated above, consistent drawing maintains the cross-sectional consistency of the fibre and in the same way, maintains the dimensional ratios of core to cladding from the preform.

Fibre may therefore be produced by drawing molten glass from crucibles or by stretching rods known as preforms down to the required sizes. While the former method is theoretically capable of producing fibres able to meet all of the requirements listed above, the latter method based on the chemical vapour deposition process, provides the better solution. The advantage of the chemical vapour deposition method is that it allows the in-situ purification of the constituent glass materials. By continually purifying the glass as it is produced, a high purity product is possible without contamination. This is unfortunately not the case with the former molten glass based system.

3.2.1 Molten Glass Methods.

These involve pulling a thin strand of glass from a molten pool. It can be carried out in one of two ways: either it is drawn upwards from the top of a crucible full of the molten liquid, or it is allowed to flow out through a nozzle located at the crucible bottom. The two processes are known as upward and downward drawing respectively.

Requirements to ensure product quality are difficult to achieve with this method. Requirements are:

i) glasses used must be produced in bulk with a high degree of purity, and must remain contamination-free throughout the pulling process;

ii) the transition temperatures of the core and cladding glasses, (if both are to be present), are compatible in order to minimise stresses and unbalanced shrinkage on solidification;

iii) the viscosities of the two glasses must be compatible;

iv) a uniform fibre drawing rate is necessary, as discussed above.

The last point can be especially difficult to achieve with this method, as the levels of glass contained in the crucibles are constantly changing and hence effecting the pressure within the crucibles.

The first two of these points require constituent materials for the glass which are of high purity. The materials then have to be handled, mixed and processed without contamination. This can prove almost impossible since contamination can come from the crucible insulating material, the heating element used, the stirrer for the fluid, or even from the crucible walls themselves. The nature of the process means that no self purification action is present and because of this, contamination can occur at almost every stage of production.

The silica based materials from which the glass handling equipment is made, mean that if the glass melt temperature approaches the softening point of fused silica, the problem of contamination will become severe. It is therefore essential that not only are the materials for handling the glass chosen carefully but also that the type of glass produced by this process is carefully selected. Even with optimum choices of handling materials, the only glasses which the process can produce are borosilicate glasses which have low melting points and can be made with reasonable purity.

The main advantages of this method are:

i) the high quality of the core/cladding interface within the finished fibre, (the liquid to liquid contact during processing produces a perfect inter-surface, even though diffusion of high mobility ions (such as OH^-) will take place (the result is only that a graded refractive index interface is produced));

ii) fibre can be produced continuously in large quantities. This obviously matches the requirement stated in 3.1, and will mean that economies of scale can be applied to the process.

The best attenuation figure for a fibre produced in this way is 5 dB/km at 850 nm.

3.2.2 Preform Based Methods.

3.2.2.1 Rod and Tube Technique.

This method is used where a step index fibre is to be produced. A glass rod which will become the fibre core is inserted into a tube which becomes the cladding of the fibre. The pressure in the gap between rod and tube is then reduced and by applying heat to the assembly, and the tube is collapsed onto the rod. The solid rod produced in this manner is then heated and drawn as described in section 3.3.

This method is an alternative to the one in section 3.2.1, but was developed in the same fashion and so has all of the same pit-falls. Like the molten glass method, pure glass has to be produced in large quantities and kept pure throughout handling and processing. The rod and tube method introduces additional difficulties because the collapsed gap between the core and the cladding records all imperfections and contaminations of the rod surface and the inside wall of the tube.

The rod and tube method was used in early fibre production. Today it is used to increase the thickness of the cladding on the outside of fibres. The imperfections introduced by the method in this case are not as critical as before, since the extra level of cladding is less important than the main core/cladding interface region. Adopting this method increases the yield from preforms produced by other processes.

3.2.2.2 Chemical Vapour Deposition.

The techniques discussed above cannot produce the very pure high silica fibres because of purification problems and the high processing temperatures required. A silica fibre requires temperatures of 1500-2000 °C which is far too high for the crucibles used for containing the molten glass.

The development of the optical based telecommunications industry was hampered because of the inability to process silica, hence preventing production of glass of superior purity. The inability of the high attenuation glass to transmit signals efficiently slowed the development of the optical end technologies. Eventually, the technique of Chemical Vapour Deposition was adapted for use by the fibre optic industry. Prior to its adoption by the fibre optic industry, the method had been used for coating semi-conductor devices with SiO_2.

The technique of chemical vapour deposition, uses a system of graduated temperature processing to produce the required high silica fibre. That is:

i)	Glass forming	800 °C.
ii)	Fusing	1500 °C.
iii)	Collapsing	1900 °C.
iv)	Drawing	2100 °C.

The key to the production system lies in the fact that vaporisable $SiCl_4$ can be decomposed in O_2 to form $SiCl_2$ in a plasma[1]. The reaction contains no water and so does not introduce migratory OH^- ions to the fibre.

The reaction is:

$$SiCl_4 + O_2 \rightarrow SiCl_2 + 2Cl_2 \qquad 3.1$$

an oxidation process, which is highly exothermic occurs at approximately 800 °C.

The CVD process deposits SiO_2 in a vitreous state, onto the outside surface of a rotating pedestal and fused in place by the plasma. As the process proceeds, the SiO_2 grows to form a cylindrical boule as the pedestal slowly retreats. Boules can easily be produced which are tens of centimetres long and several centimetres in diameter.

---

[1] A plasma is a gas containing approximately equal quantities of positive ions and free electrons.

The CVD technique eventually evolved into three successful techniques for producing silica low loss fibre capable of fulfilling all prerequisites listed in 4.1. These techniques are now addressed separately below.

Modified chemical vapour deposition (MCVD).

The process of oxidising halides in quartz or SiO_2 tubes is known as "inside" processing or modified chemical vapour deposition (MCVD). As is normal with chemical vapour deposition processes, the constituent materials used to produce the required glass are liquid halides. The principle halides used are: $SiCl_4$ (the main glass constituent material); phosphorous in the form of $POCl_3$; and Bromide in the form of BBr_3.

Storage of the materials is in all glass, or all stainless steel containers. When stainless steel containers are used, all water has to be removed in order to avoid contamination of the process.

Oxygen is blown through the halides to provide a carrier, and the saturated vapour produced delivered to the reaction chamber. Mass flow controllers regulate the constituent flow: they monitor the quantity of material entering the reaction chamber, rather than the flow rate of the oxygen carrier gas so that a change in oxygen volume flow rate will not necessarily corrupt the process.

Saturation of the oxygen by the constituent materials is essential: this makes the method of bubbling the oxygen through the halide and conveyance of gases critical. The containment vessels are designed to hold large volumes of liquid, and the oxygen is bubbled through from near the bottom. The container vessel is kept at a constant temperature and the exit pipes are kept free of condensate.

The whole material delivery system on an inside deposition process, is programmed to deliver the necessary materials in gaseous form to the reaction zone. The quartz tube containing the reaction zone is heated externally by flame, or internally by plasma. If external heating is used, it is essential that the quartz tube be of uniform cross-section, and longitudinal straightness. If either of these conditions do not apply, the temperature across the reaction zone may not be constant. Variation of these factors, will have a direct effect the geometry of the finished fibre. A significant variation in the reaction zone temperature or the tube geometry, may lead to the fibre being incapable of meeting the performance requirements.

During processing, the tube is mounted on a lathe bed and rotated. A Rotatable sealed joint fixed at the end of the tube, allows the reactants to be introduced to the inside of the tube. Fig 3.1 shows a schematic representation of the process.

For the external heat process, an oxohydrogen flame is used to increase the zone temperature to a constant value of 1800 °C. The lathe traverses the flame along the tube from input to exhaust end gradually moving the reaction zone. During production, many passes of the flame over the tube are made.

In the hot zone, halides oxidise to SiO_2 and GeO_2. The final glass composition is therefore a function of the relative percentages of constituent gasses and the temperature applied by the flame. The material resulting from the reaction forms a soot which is carried downstream past the hot zone. Thermo-phoretic forces cause the soot to be deposited to the inner surface of the tube. A percentage of the soot is not deposited and passes out of the quartz tube as part of the process exhaust. As the flame moves along the tube towards the exit end, it vitrifies the deposited soot into a layer of glass.

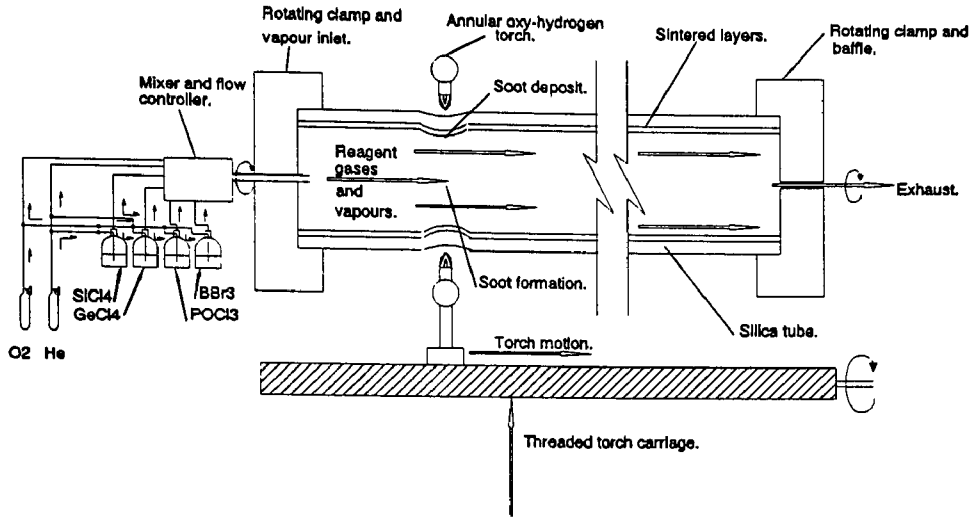

Figure 3.1 A Schemtic Diagram of Preform Manufacture using Internal Chemical Vapour Deposition.

The process effectively reduces the inside diameter of the quartz tube. The decreasing inside radius progressively hampers the flow of reactant gasses before finally stopping it completely.

When gasses finally stop, a small void is always left at the centre of the core of the preform. The last stage of the MCVD process is therefore to heat the tube and the deposited cladding to a high temperature. Under these conditions, the surface tension forces acting in the semi-molten tube cause it to collapse and close up the centre void. The deposited material is therefore the core and cladding of a preform tube which is supported within the quartz tube. The process never completely collapses the central void and all MCVD fibres have a region at the centre of the core with low refractive index caused by the lower density glass at that point. The characteristic shape of the MCVD fibre refractive index profile is shown in Fig 3.2. An alternative MCVD produced profile with depressed cladding refractive index is shown in Fig 3.3.

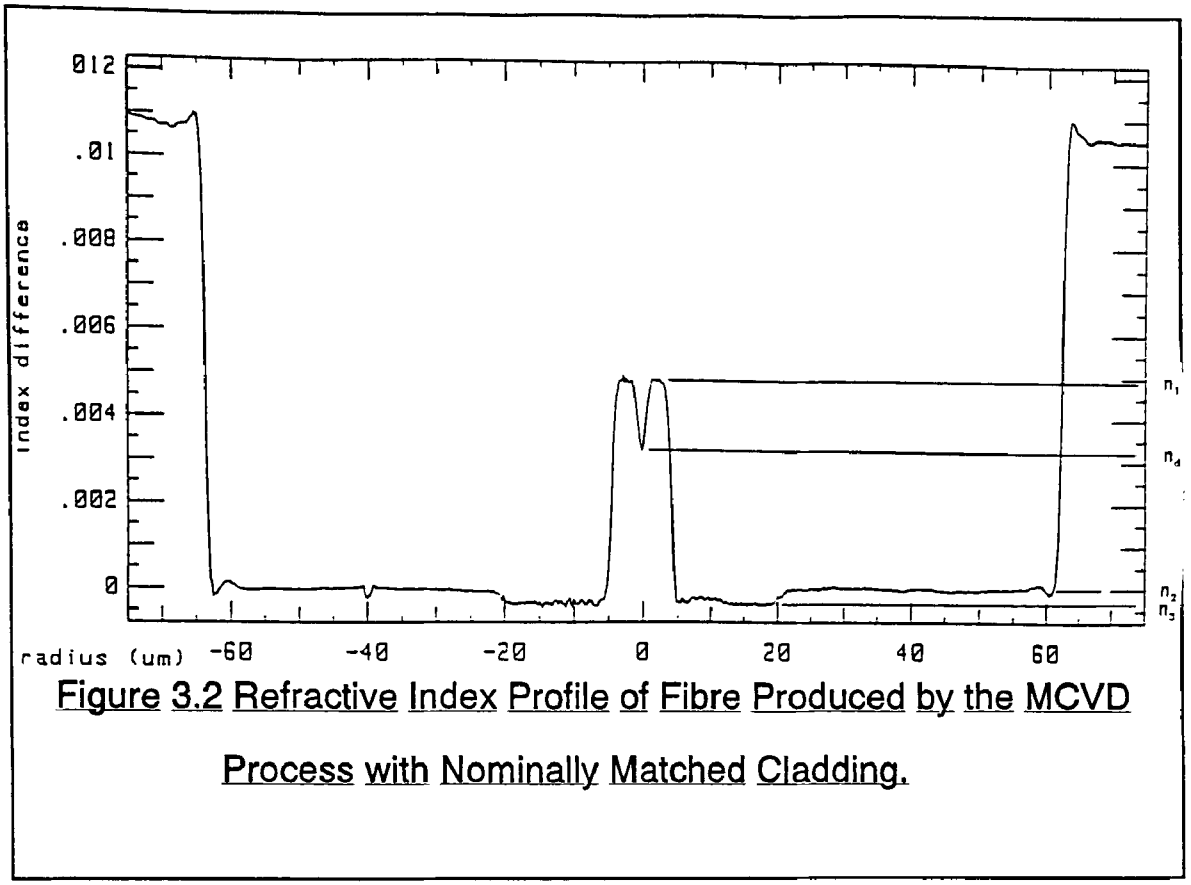

Figure 3.2 Refractive Index Profile of Fibre Produced by the MCVD Process with Nominally Matched Cladding.

Outside vapour deposition (OVD).

Outside deposition processes function by depositing soot particles over mandrels of quartz or graphite. The glass constituent materials (in a vapour form), are produced using processing equipment the same as that described for MCVD processes. The difference between the two methods of producing preforms is in the manner of applying the heat to the process.

In OVD processes, glass constituent materials are fed through a tube concentric to an oxohydrogen coaxial torch (see Fig 3.4). The arrangement allows the reagents to be fed to the hot zone where oxidation takes place and soot of desirable particle size is produced. The soot is sprayed onto the mandrel and after many passes of the burner, a soot preform is produced. In addition to producing the soot, the burner also causes the soot to coalesce.

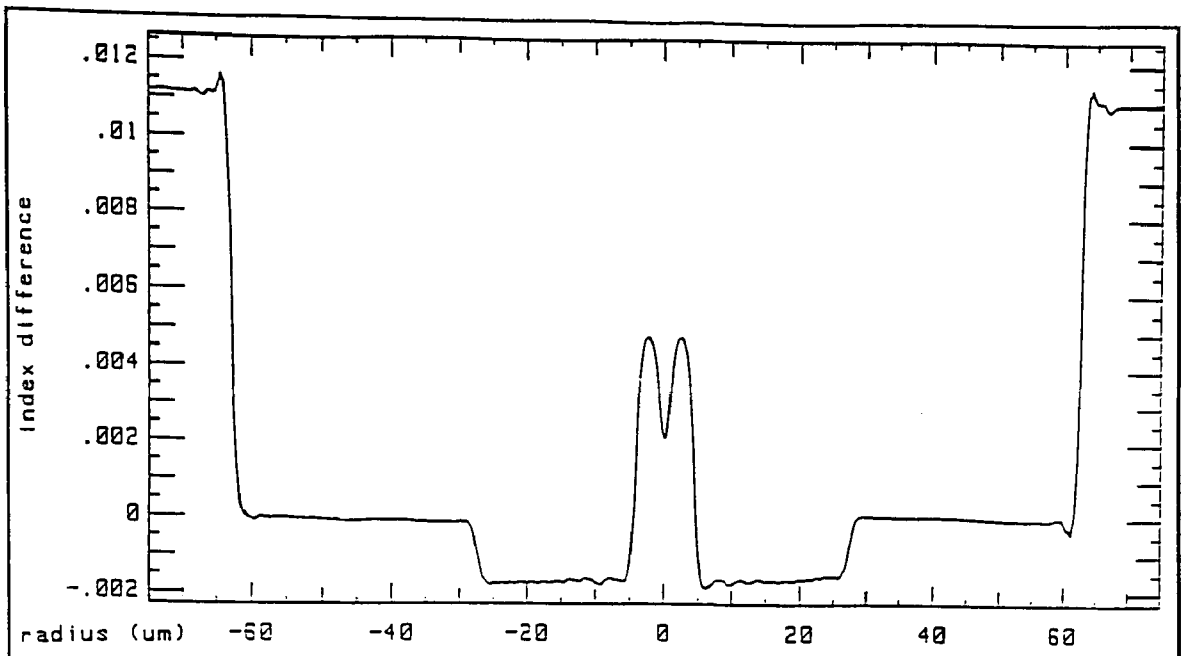

Figure 3.3 Refractive Index Profile of Fibre Produced by the MCVD Process with Depressed Cladding.

On completion of the forming part of the operation, the mandrel is withdrawn. The soot preform is dehydrated, sintered and collapsed into a preform rod. Dehydration of the preform is necessary, since the process of SiO_2 formation is one of hydrolysis. Because the soot is porous, dehydration can be simply carried out by heating it in Cl_2 gas. The reaction which takes place is:

$$Cl_2 + H_2O \rightarrow 2HCl + O_2 \qquad 3.2$$

The HCl gas produced is carried away in vapour form leaving the soot preform dehydrated.

The next operation to be carried out on the preform is sintering. During the sinter, the soot particles consolidate to form clear glass. The density of the porous solid means that during the sintering operation, the linear dimensions shrink by a factor of 2. This effect is taken into account when

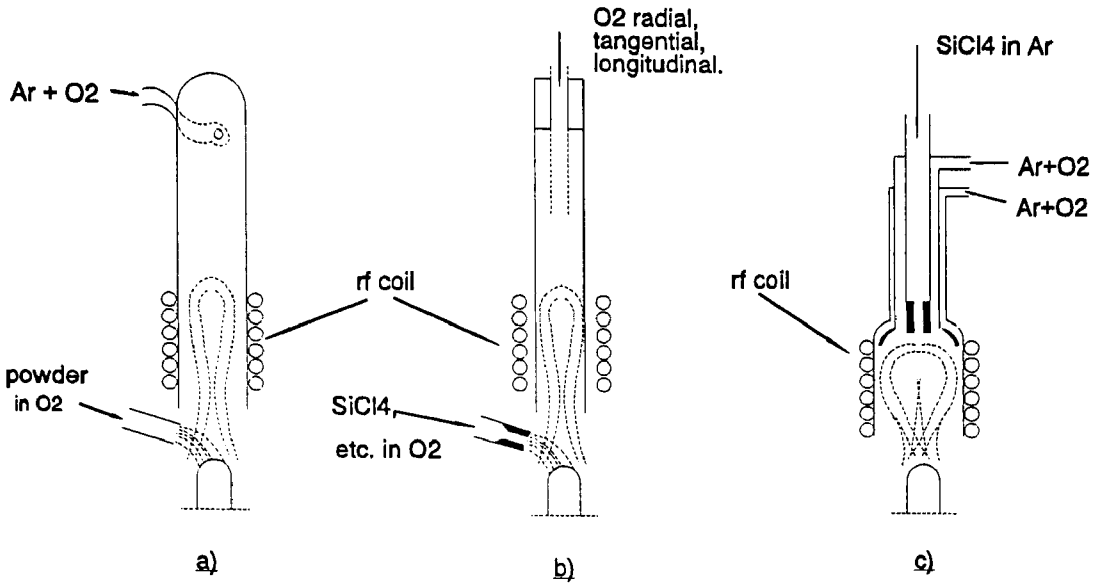

Figure 3.4 Schematic of Outside Vapour Deposition Production Process.

The Plasma Torch as Used for the Preparation of Vitreous Silica or High Silica Glasses.

designing the preform to produce fibre of a certain dimension.

The advantage of the outside process is that it can be scaled up easily. Multiple torches and larger mandrels allow very high deposition rates to be achieved.

Residual stress in the material must be carefully controlled so that its residual stress can be evenly distributed so that successful sintering without preform rupture can be completed. Fig 3.5 shows the characteristic refractive index profile of a fibre produced by the OVD process.

Vapour axial deposition (VAD).

A process which uses no mandrel is referred to as a vapour axial deposition process. Deposition takes place on a withdrawing platform and the deposited material forms a lengthening boule. By arranging the torch position in relation to the boule centre, a graded index fibre core can be made. The soot

boule is dehydrated and sintered as in the previous case. One difference is that the VAD process has no mandrel to be withdrawn. Another difference is in the control of the material deposited. The thermal profile of the soot boule and the flow of the incoming soot control the composition of the deposited material, even though the incoming soot formed by homogeneous reaction, would have a uniform composition. The advantage of the VAD technique is the possibility of making long preforms that can even be in a continuous form if dehydration and sintering can be carried out in tandem.

The resultant preforms produced by the outside deposition processes can be a complete composite fibre preform or a core rod with a relatively thin cladding. By sleeving the core with a quartz tube, a much larger preform is achieved. This application of sleeving is a development of the rod in tube fibre making technique discussed in 4.2.2. The techniques for high silica fibre fabrication all result in the formation of a preform which must be reduced to a suitable size for final fibre drawing. This can be done by re-drawing of the preform. Tailoring of a final preform dimension to the required final fibre outer diameter and core diameter can be performed at this stage.

The characteristic refractive index profile of fibre produced by this method is shown in Fig 3.5.

3.3 Fibre Drawing.

The sections above discuss the methodology developed for producing fibre preforms. The final stage of production which converts the preform into a fibre complete with single or multiple layers of protective coating is that of drawing. Fig 3.6 is a schematic diagram of a pulling tower on which fibre preforms are drawn down to final size and primary layer(s) of coating are applied.

Preforms are drawn into fibres by a pulling process. Fibres are orientated vertically and sections starting at its bottom and moving progressively towards its top are heated and allowed to be

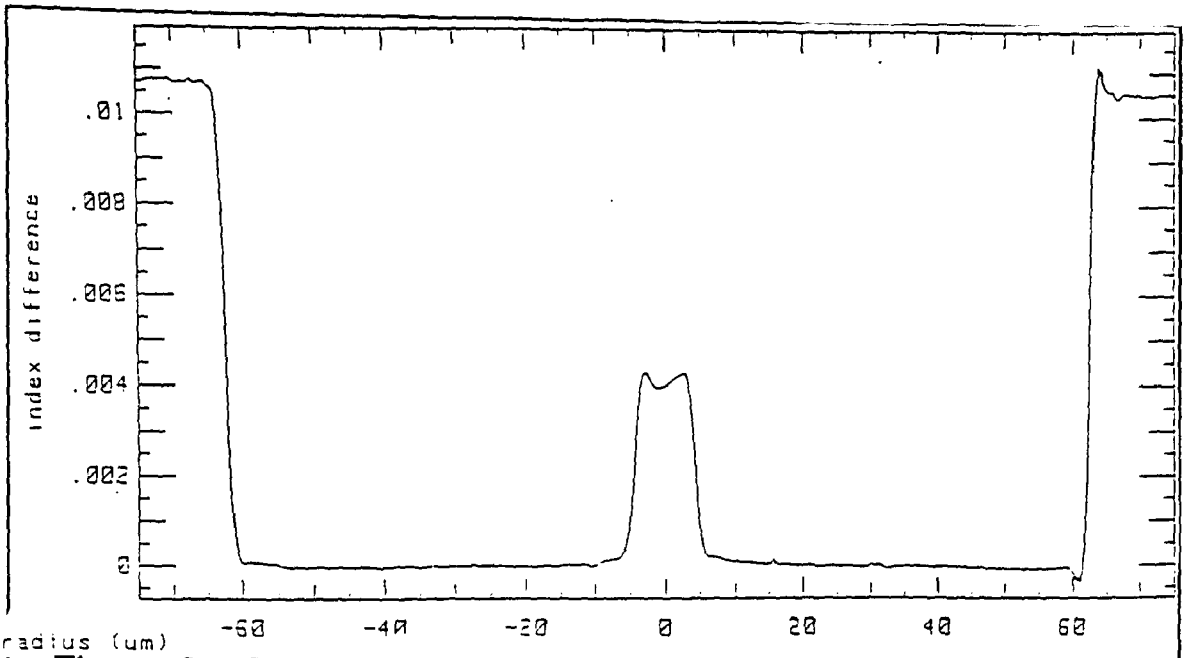

Figure 3.5 Refractive Index Profile of Fibre Produced by the OVD Process.

"stretched" away from the preform down to the final fibre diameter. A fibre drawing apparatus consists of a furnace, rod feed mechanism and fibre pulling mechanism.

Draw down ratio[2] dictates the feed and pulling rates. The furnace heating zone is profiled to provide a neck down region for the fibre. The furnace is suitable for balancing the viscous and surface tension forces until uniform size reduction is achieved without instabilities. Fig 3.8 shows a schematic sectional representation of a zirconium induction furnace. A direct heating graphite furnace is also available.

The mechanical stability of the system and the gas flow, effects the stability of fibre drawing. This is particularly true in the neck down region where viscosity can change rapidly. Mechanical damage caused by particles from the furnace hitting the fibre in the hot zone is prevented by passing gas in

---

[2] Draw down ratio is the ratio of the diameter of the fluid fibre before and after drawing, during which time, its diameter reduces.

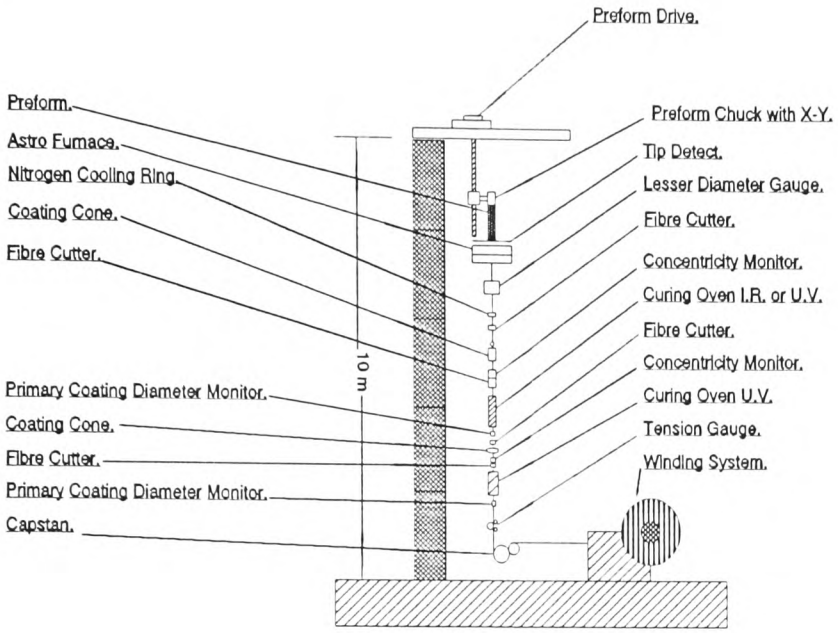

Figure 3.6 Schematic Representation of an Optical Fibre Pulling Tower.

a steady flow through the hot zone; this preventative design also results in good dimensional stability.

In fibre drawing equipment, the freshly drawn fibre is uniformly protected by a coating which offers mechanical protection. The characteristics of the material are chosen so that it may be readily cured without appreciable changes in dimension, with good abrasion resistance with the desired hardness, and the ability to retain flexibility over a wide temperature range.

The coater must be properly designed for high velocity coating to avoid cavitation and turbulence. Coating at over 10 m/s can be achieved with some coating materials. In general, the fibre tends to self centre. The restoration forces however, are small so that mechanical alignment of preform and coater nozzle is essential and must be controlled.

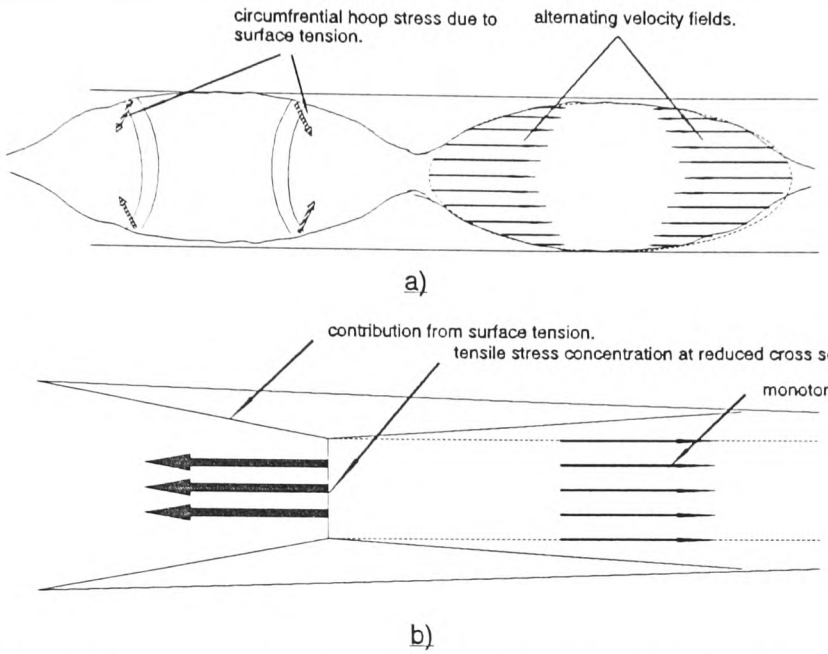

Figure 3.7 Comparison of Capillary and Tensile Instabilities in Hot Fibres during Draw Down.

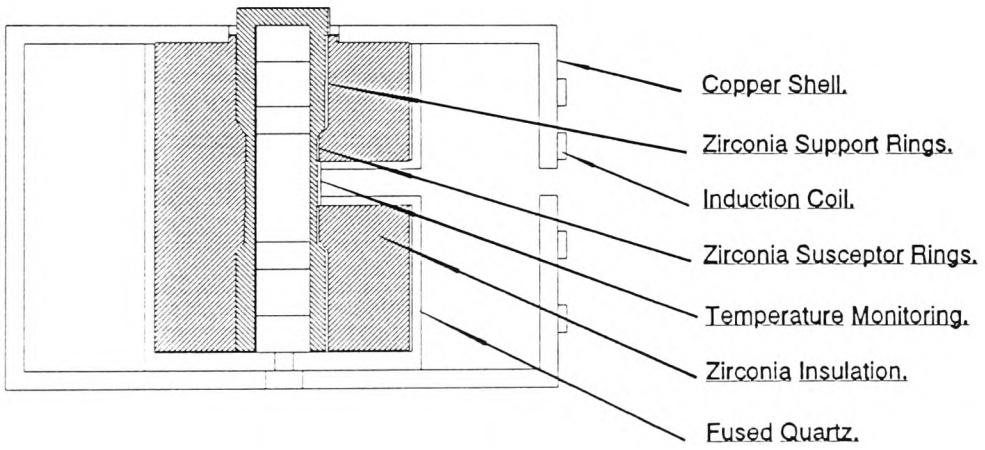

Figure 3.8 Schematic Section through a ¦irconium \induction Furnace.

For high speed draw, the fibre must be force cooled so that it can enter the coater at a low enough temperature. Line fibre diameter and concentricity measurements are needed and can be provided by illuminating the fibre transversely and observing the refracted and diffracted rays. The technique allows a feedback control loop to be established, which allows coating concentricity and fibre outside diameter to be kept within a tight tolerance of 1-3 %.

3.4 Technical Improvements in Fibre Production.

Since the 1960's the transparency of glass has been increased 10,000 fold by the refinement technique for producing pure silicon dioxide. It was this technique that made long haul optical fibres possible. Silica based glasses are now standard in fibre optic telecommunications, reaching their limit of transparency by 1979.

A second generation is now emerging, consisting of materials that transmit infrared light at longer wavelengths. Such fibres belong to three classes of materials: the halide-containing crystals, the chalco-genide glasses and the heavy-metal fluoride glasses. These infrared optical materials promise greater transparencies than those feasible with silica fibres, and they are being tested for many new applications.

To attain this goal and to develop new short-distance fibre technologies, examinations of numerous glasses and crystals that are transparent in the infrared range have been carried out. Consideration of the basic structure and inter-atomic forces that guide and attenuate light through a fibre have shown the halide containing crystals, the chalco-genide glasses and the heavy-metal fluoride glasses to be the most practical candidates.

Technology has advanced to the point where fibres can be produced which are resistant to the intrinsic losses of scattering and absorption, (discussed in later chapters). There is difficulty however, producing these fibres so that they are resistant to extrinsic modes of loss such as microbending. The fibres will tend to be excellent in the theoretical case, but of limited application in practical cabling. Until these problems can be overcome, the cabling industry will be unable to utilize these high performance fibres, although the possibilities in this field remain enticing.

A problem which requires constant attention in cabling design is that of water penetration or hydroxide ion migration to the fibre. The first can lead to flooding of cables and eventually cable junctions, (see Chapter 4), the latter will cause high signal attenuations in cabled fibres as the migration of hydroxide to the silica of the fibre leads to increased opacity.

In order to make the optical fibre more resistant to the effects of water contamination, various fibre coatings have been developed. A coating which currently excites much interest is that of coating the fibre hermetically for increased water resistance.

The potential in this area allows development fibres for use in more harsh environments such as under water. In environments such as these, mechanical as well as hermetic strength is required. The design concept is to protect the optical fibre with a metal tube. The tube is intended to protect the fibre from moisture, hydrogen, lateral pressure and tensile force.

Much work has been carried out on thin hermetic coatings [3.1], (both metallic and non-metallic). A problem exists in that thick metal coatings are difficult to apply on top of buffered optical fibre in a single process, and the buffering layer cannot be removed because the mechanical and transmission characteristics of silica fibre depend upon it. The buffer material provides a "last defence" against damage and must also be protected from harsh environments.

Techniques have been developed which allow both the application of a metal jacket to a fibre's buffer surface and of a fibre reinforced metal jacket. The jackets induce no attenuation increment due to microbending from jacket shrinkage or from temperature induced stresses and offer exceptional resistance to mechanical damage.

3.5 The Cabling Process.

The improving performance of fibres in the telecommunications network, while being primarily due to the technological advances in fibres, should also be acknowledged as having been due to advances in cabling technologies.

Improvements have been made in the areas of materials, design and machinery, and it is to this important area of fibre telecommunications technology that the next chapter is directed.

References.

[3.1] Yoshizawa et al, "Low loss Hermetic Optical fibre continuously metal casted over the buffer layer". NTT Transmission Systems Laboratories, Tokai, Ibraki Ken, 319-11, Japan.

CHAPTER 4.0.

The Cable Production Process.

4.1 Introduction

Installation of cables in ducts, directly into the ground and on telephone poles is carried out routinely. In addition, cables are under development capable of withstanding the rigours of battlefield use and installation from helicopters. This level of mechanical performance in fibre handling and installation is possible because of the success of a concerted effort by industry to overcome problems with cabling induced attenuation and fibre damage.

In relation to their size and mass, optical fibres have a potential strength which is proportionally very high. In the real situation however, abrasion and water attack can seriously reduce the strength of unprotected fibres and improper cabling can cause bends in the fibre which significantly increase attenuation. Plastic coating techniques have been developed to preserve fibre strength and to inhibit cabling induced attenuation, and cabling designs and methods are in existence which allow plastic coated fibres to be incorporated into foldable cables with little or no cabling induced attenuation.

It is therefore the aim of Chapter 4, to describe the various layers of protection developed for application to a fibre which enhance its resilience and therefore prolong its life. It is intended that in addition to the alternatives for protecting fibre, the problems with cabling and installing fibre will be addressed, and solution of these problems described.

4.2 Primary Coatings.

During production of a fibre, great care is taken to ensure that contaminants are kept away from both the fibre and the drawing "hot zone". If the process is successful, it produces a fibre whose surface is perfect. After cooling and hardening, the surface of a fibre remains vulnerable to the action of contaminants and so as soon as is possible, (immediately the fibre is solid, and before it has been wound onto a take up drum), it is protected using plastic or resin coatings. One or a number of "primary" coats are applied to a fibre, their total outside diameter never exceeding 250μm.

The surface protection of a fibre, and fibre strength are closely linked. The mechanical characteristics of fibres have been the subject of intensive studies, as tough practical requirements for fibre strength and durability are needed for different applications. Glass is a special solid with a linear stress-strain relationship holding theoretically up to 20% elongation. The malleability is zero and an uncorrupted glass surface, where imperfections and defects have not weakened it, allows high strain breaks where the glass fractures as a brittle solid: the break traceable to the rupture of the Si-O-Si bond. For glass with flaws in the form of cracks due to contaminants, the mechanical characteristics are very different. In this case, the failure of the fibre is governed by the stress at the crack tip. If the environment is corrosive, ie. it can react with glass, the crack will propagate even if the tip stress is well below the bend fracture stress. This increase in crack size and corresponding decrease in remaining intact fibre area, leads the crack tip stress to increase and hence accelerate the crack propagation speed. When the tip stress reaches fracture stress, catastrophic failure takes place and the fibre undergoes "fast" failure. The strain based fatigue described here and originating due to contaminating particles, can be prevented by "clean" practices and the prompt application of primary coatings immediately after drawing.

In addition to fibre mechanical failure, the presence of contaminants can also lead to absorption based fibre attenuation losses. As discussed in section 4.6.2, the prevention of hydroxyl ion based absorption losses are the main attenuation problem facing fibre technologists. Application of the primary coats go some way to alleviating the problem, ions which would otherwise mean the diffusion into the fibre of the OH^- ions and an increase in attenuation. Problems can arise when badly selected coatings actually generate OH^- during their cure augmenting rather than solving the problem.

In addition to providing the barrier layer(s) necessary for prolonged fibre performance maintenance, the primary coat has a second function: it provides a "last defence" for the fibre against mechanical effects such as sharp objects or microbending it might encounter when installed. It makes the fibre more robust, which is an essential factor if the fibre is to negotiate the rigours of the production process successfully.

Thus, it can be seen that the successful application of primary coats to the fibre are essential for its performance. The application of primary coats also, unfortunately constitutes a significant engineering task. The requirements for the coating material can be deduced from the above,. They are that the coating should be:

i) reasonably hard,

ii) abrasion resistant,

iii) strippable, (for jointing and terminating purposes),

iv) contain no abrasive material,

v) sometimes be of higher refractive index than the cladding[1].

---

[1] Design specifications require that in fibres, any cladding modes be "stripped" out of a fibre within the first few metres of its length. In single mode fibre, this is done to prevent interference due to the bonding of the cladding modes to the core modes within the fibre. The most simple way to strip off cladding modes is to raise the refractive index of the coat. In this situation, on coming into contact with the fibre coating interface, light is refracted away from the core and out of the fibre. Cladding designed to carry out this function is known

Processibility of the fibre is another significant aspect in the primary coating technology. The primary coating process is part of the drawing process and as such, must be closely controlled because of the flow nature of the latter. Requirements for a primary coating material are that its viscosity should be reasonable so that a suitable applicator can be designed; the material should be heat or ultra-violet curable, and contain no solvent; and the rate of cure should be great enough to ensure that between application and being wound onto a take-up bobbin with a fibre, complete cure has taken place. Obviously the choice of material is not arbitrary.

The largest degree of freedom available to design engineers with regard to primary coats, is the number of layers which are applied. STC currently apply a single coat to their fibres intended for use in loose tube and open channel applications, (discussed below). The dimensions of a single mode singly primary acrylate coated fibre are as follows:

i) diameter of fibre core- 8μm,

ii) fibre cladding- 125μm,

iii) acrylate coating- 250μm.

The fibre coating is drawn onto a cooled fibre as discussed above and cured as required before the completed package is wound onto the first take-up drum. The dimensions of this type of fibre are shown in Fig 4.1.

A second option is to doubly coat fibres. The differences between single and double primary coatings are discussed below.

---

as "mode stripping cladding".

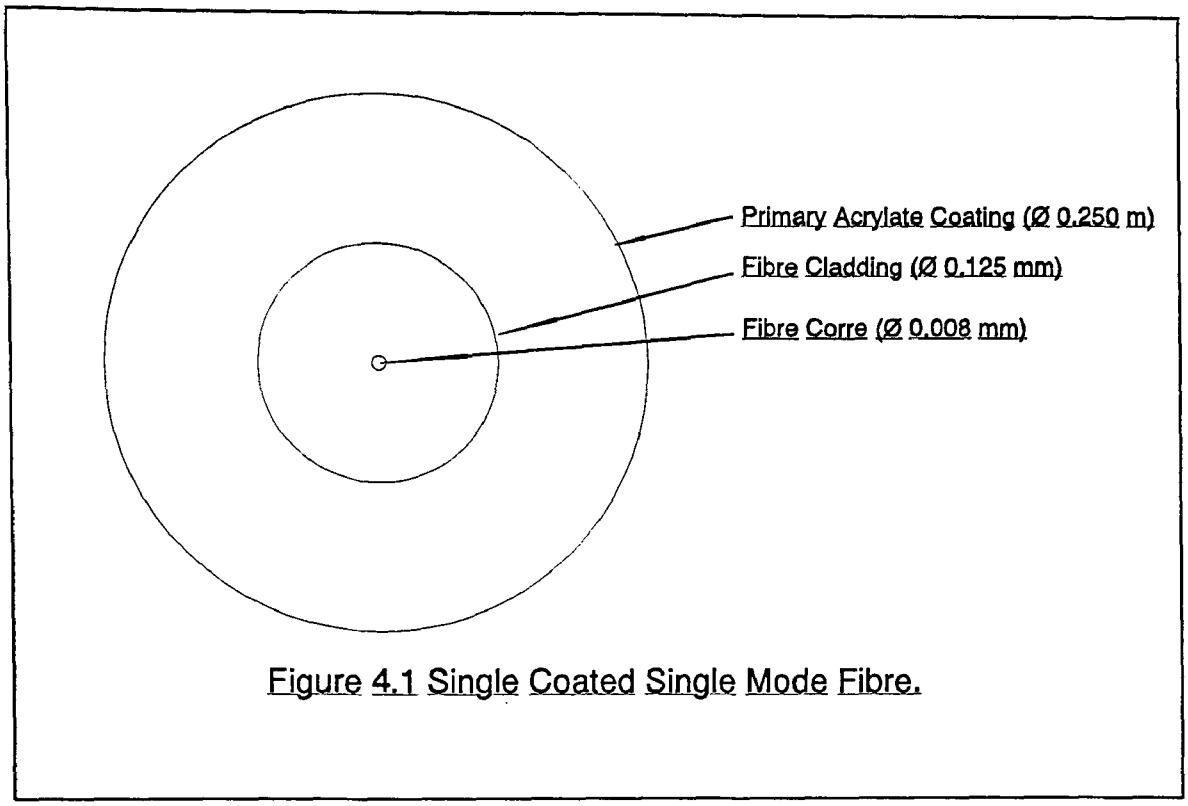

Figure 4.1 Single Coated Single Mode Fibre.

4.2.1 Doubly Coated Fibres.

Double coated fibres are used by fibre producing companies such as Corning of America. Two layers of coating material are applied to the fibre rather than one before the fibre is first wound onto the take-up drum. When two thin layers of coating are applied rather than one thick one, the ratios of the coating thicknesses and relative hardness of the layers can vary depending upon the design objectives. The outer diameter of the package however is always maintained at 250μm. The implication of the situation where all parameters are varied except total diameter, is that additional protection for the mechanical and optical performance of a fibre are not obtained from a greater thickness of coating, but from the combination of the layers in the coating package. The contention is that a "combination package" of this sort can be finely tuned to meet a fibre's protection needs.

Claimed advantages for dual coated fibres include:

i) superior microbend resistance,

ii) improved yield, both in fibre and cabling plants,

iii) easier processibility-hard outer coating has more favourable surface properties and the superior microbend resistance makes the package more forgiving,

iv) coloured secondary coatings-dye can be added to the outer coating as it does not come into contact with the fibre, (this removes the inking process-a necessity with single coated fibres).

Disadvantages of the double coat system of primary fibre protection are:

i) more complex production equipment-expensive and harder to run,

ii) lower tower utilisation,

iii) lower tower yield,

iv) more complex resin inventory-particularly if adopting the self coloured options.

While manufacturers contend the merits of the double coat systems, it is certain that more production alternatives are offered by the dual coats. Not only can geometric ratios be altered for the coats, but the ratio of coating hardness and the method of cure can also be varied. Diameters commonly used for first and second coats include: 170/250μm, 185/250μm, and 200/250μm.

It is generally accepted that the inner layer of coating is softer than the outside one. In this way, it is supposed that the inner layer cushions the fibre, while the outer layer repels any mechanical effects. Singly coated fibre takes the middle path between these two extremes so that the single layer is not so hard that it damages the fibre, while not being so soft that it allows damage of the fibre from the outside.

Cure methods vary between coating combinations and are determined mainly by the convenience of the methods and the equipment to be used to apply and cure them. The two most significant applications are wet on dry and wet on wet coatings. The first method, wet on dry, as its name infers, applies the first layer of coating and then cures it, then applies the second layer of coating and cures that. The method has the advantage that it is simple, but requires the space necessary to separate the coating applicators for the curing lamps. The second method, as its name suggests has both coats applied to the fibre before curing commences. It has the advantage that sets of equipment are kept close together, but it requires careful selection of materials because in order to cure the inner layer, radiation has to pass through the outer layer without effecting it. This is done by selecting wavelengths of curing radiation and materials so that the outer layer is transparent to the light intended to cure the inner layer. If the calculations are wrong, then over-cure of either layer, or under cure of the inner layer can easily take place.

4.3 Buffer Layers.

The production of optical fibre telecommunications cables can be viewed, as discussed above, as the application of successive levels of protection to fibres.

If primary coating is the first level of protection, and sheathing of a completed cable the last, then the application of buffer layers constitute the intermediate steps. Buffer layers have become very specialised and vary between cable designs. Characteristically, they make fibre easier to handle by collecting it together in groups, or by making it very much more robust, and add a final protection against the demanding final cable production operations.Any cables referred to as receptacles for the buffer layers discussed here, are described in detail in 4.4.

4.3.1 Secondary Coated Fibre.

Tight construction cable designs use secondary coated fibre, since there are no guides for the fibres as in loose tube cable designs. The secondary coat involves a coat of Nylon 12, as the outer jacket, Fig 4.2.

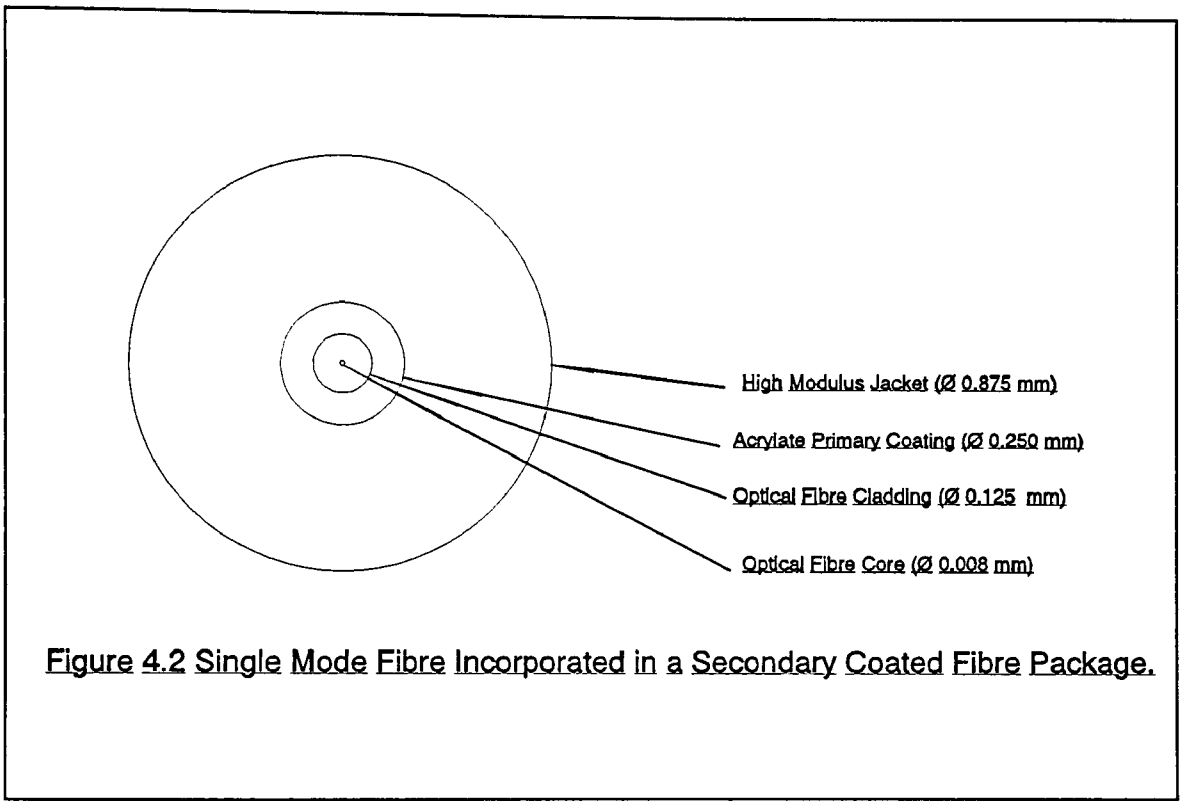

Figure 4.2 Single Mode Fibre Incorporated in a Secondary Coated Fibre Package.

The dimensions of a singlemode secondary coated fibre are as follows:

i) fibre core- 8μm,

ii) fibre cladding- 125μm,

iii) fibre primary coating- 250μm,

iv) Nylon 12- 850μm.

Secondary coated fibres are also used in single fibre cables. Those cables are bound in Kevlar yarn and then sheathed in PVC. Their main use is as terminating cables since they are physically flexible. They are always used internally to either link an external cable to terminal equipment, or to link equipment within a building, (ie. intra office).

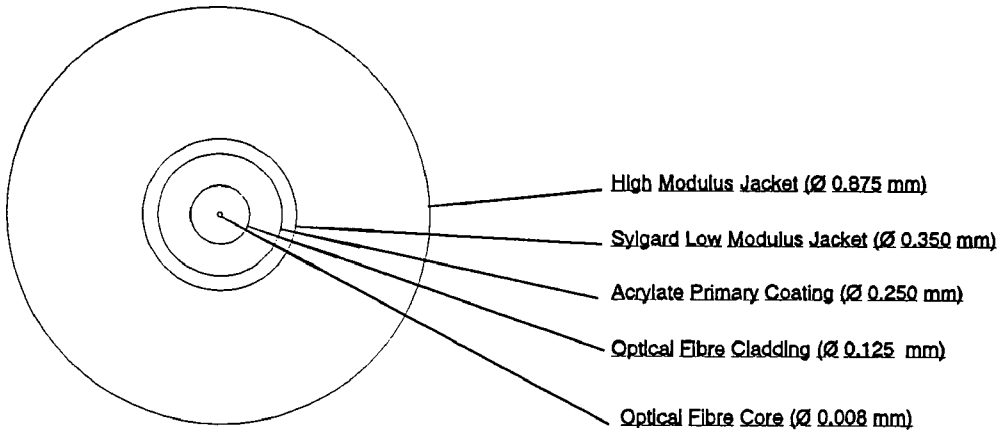

Figure 4.3 Single Mode Fibre Incorporated in a Triple Coated Fibre Package.

4.3.2 Triple Coated Fibre.

Triple coated fibre developed by STC, is a basic acrylate fibre (see primary coated fibres), coated with a thin layer of Sylgard and an outer jacket of Nylon 12, Fig 4.3.

The advantage of this process is that the fibre is drawn and the primary coat is applied by one process, and the two outer coats (Sylgard and Nylon), subsequently applied by a separate process at a later date. This has the effect of simplifying the process considerably.

The performance parameters of triple coated fibre is comparable with that of secondary coated fibre and both products have the same applications. Fig 4.4 shows a single fibre cable incorporating a triple coated fibre at its centre. Cost savings in manufacture therefore make it a viable alternative to the more costly secondary coating option.

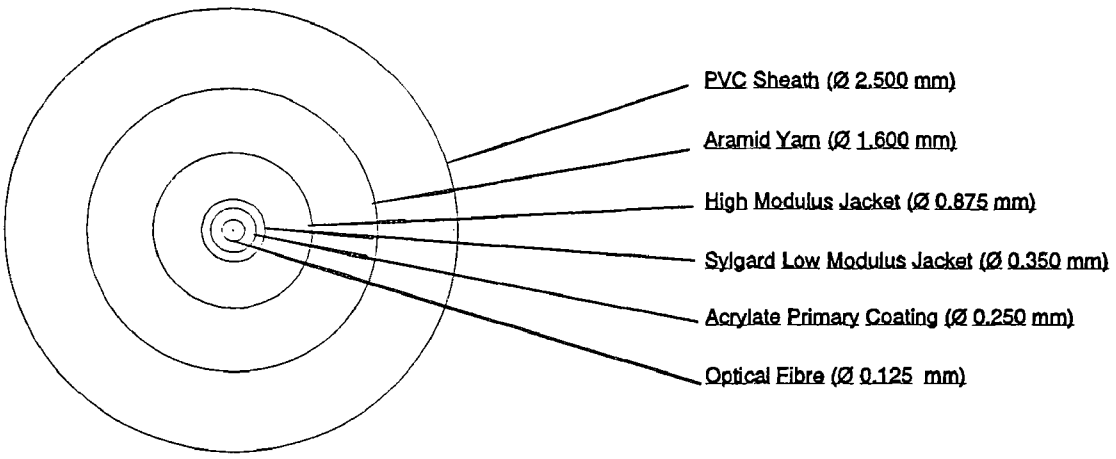

Figure 4.4 Single Fibre Cable Incorporating a Triple Coated Fibre at its Centre.

The dimensions of a singlemode triple coated fibre are as follows:

i)	fibre core-	8μm,
ii)	fibre cladding-	125μm,
iii)	Silicon Elastomer- (Sylgard)	350μm,
iv)	Nylon 12-	850μm.

4.3.3 Hermetic Coating.

Hermetic fibre is the logical answer to the need to seal fibre against the mechanical and chemical forces which would otherwise degrade its performance. The study of the durability of fibre and how to improve durability, leads to the study of how to make the fibre hermetic. The passivation of a fibre surface can be achieved by coating a fibre surface with a hermetic material such as SiN_2, or metal. While the mechanical and chemical effects of this process are still under study, there is no doubt that hermeticity is a way to prevent hydrogen diffusion into the fibre causing attenuation increase.

In order to make optical fibre more usable in harsh environments such as under the sea, not only hermeticity, but also mechanical strength is required. Hermetically sealing a fibre, has come to mean protecting it with a metal tube of about 1 mm, outside diameter. The metal tube is able to protect an optical fibre from moisture, hydrogen and lateral pressure, as well as tensile force.

These fibres have the potential to increase productivity, by making fibres more robust, increasing the field life of fibres and reducing the cost of fibres by allowing the removal of some of the currently essential layers of protection.

4.3.4 Ribbon Fibre.

Ribbon fibre is a number of acrylate coated fibres joined together by a resin to form a ribbon. STC would use a ribbon such as this within a fibrespan aerial cable, although cables using multi-two fibre ribbons have been designed by other manufacturers. The main advantages of ribbons are their neatness and compactness, and the easy manner in which they can be applied within the cable core without the fibres twisting and crossing. Fig 4.5, shows layers of ribbon inserted into a completed fibrespan cable.

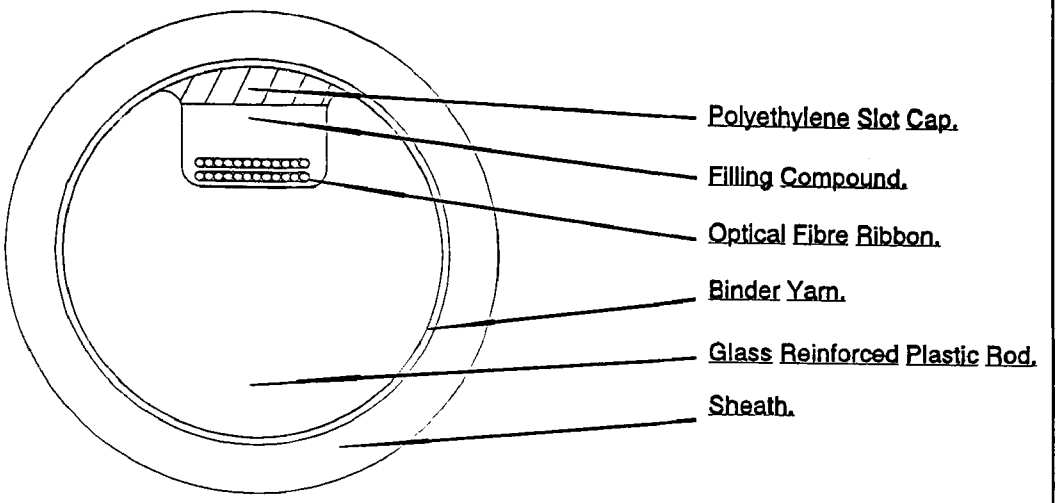

Figure 4.5 24 Fibre Ribbon Design Non Metallic "Fibrespan" Aerial Cable.

Ribbons are based on ultra violet coating technologies similar to those used for fibres. Up to twelve coated fibres are coloured in line, coated with a UV curable bonding matrix, and bonded into an array of twelve continuous fibres.

Many options for ribbon geometry are available as shown in Fig 4.6. These options are obtainable by varying the method of ribbon application. It has been found [4.1], that the symmetrical structure of ribbon such as that shown in Fig 4.6,b, with relatively flat ribbon surfaces gives the optimal performance. The ribbon shown in Fig 4.6,a, is found to be thicker than necessary, making single fibre access difficult and packing efficiency smaller. The pronounced asymmetrical meniscus structure of the ribbon in Fig 4.6,d, can induce preferential bending strains during cure and temperature changes, while a design such as that shown in Fig 4.6,c, was found although symmetrical, can restrict freedom of ribbons to move transversely and relieve cabling and environmentally induced strains.

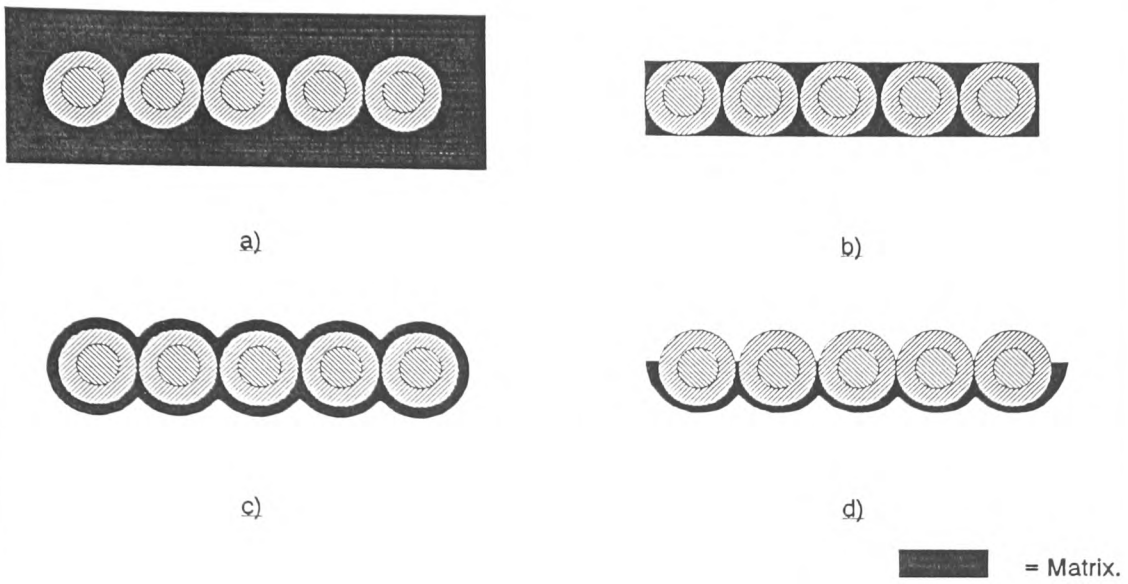

Figure 4.6 Various Ribbon Matrix Designs.

4.3.5 Loose Tubes.

Loose tubes are hollow cylinders extruded from Polybutyltetraphthelate, (PBTP), to carry between one and eight acrylate coated fibres. Examples of tube sizes are 1.5, 2.2 and 3.0 mm diameters with fibre counts ranging between one in a 1.5 mm the to a maximum of eight in a 3.0 mm tube. Loose tubes are designed specifically for insertion into a "loose tube cable", the design of which is discussed in 4.4.

The loose tube theory is that the fibres contained within tubes, lie in sinusoidal or helical paths, immersed in high viscosity filling compound inside hollow tubes. The paths of the fibres mean that the length of fibre is greater than the length of tube which contains it, and so a percentage excess is generated. Currently, excess is nominally set between 0.15 and 0.20% and is intended to give a degree of strain relief. If the tube is stretched, its elongation can be as great as 0.20%, before the fibres within it experience strain.

In addition, a well tuned production process will generate loose tubes in which fibres come into contact with neither tube wall or other fibres and should this occur, they are free to move apart. The system is designed to reduce microbend effects and both protect and cushion fibres by a similar theory to that which was seen double primary coating (with a soft/hard design).

4.4 Optical Fibre Cables.

Within STC cable products division at Newport, several variations of fibre optic cables are manufactured. The three major cable construction types are namely Loose Tubes, Tight Construction, and Open Channel (slotted core). Other types not used as extensively or which are still under development are Fibrespan, Mini Open Channel, Figure of 8, and FOTS-LH (Fibre Optic Transmission System-Long Haul).

4.4.1 Loose Tube Cables.

These cables are suitable for trunk, inter exchange junction and subscriber local loop applications. Various types of multimode and singlemode optical fibres and a wide selection of cable constructions are available for duct and direct buried applications.

Cable variants to suit customers' specifications include steel or dielectric central strain members, steel tape or wire armouring, polyethylene, PVC or low fire risk sheathing compounds. Copper pairs may also be incorporated.

The cable consists of either single or multiple fibres loosely contained within loose tubes. Tubes are laid around a central strength member, wrapped with tape and then sheathed to form a cable. The cable interstices may also be filled with special compound to provide a genuinely fully filled cable.

Longitudinal freedom and cushioning with the tubes ensures the fibres are protected against stresses applied to the cables during handling and installation operations. Fibres and tubes may be colour coded to enable easy identification.

Loose tubes are laid helically around the central strength member to enhance strain relief performance afforded already by the excess built into the tubes. Care must be taken when setting the pitch of the loose tube helices that the macrobend critical radius is not attained.

Fig 4.7, shows an unarmored cable as used in the trunk network and installed in ducts. The design incorporates twelve optical fibres and two copper pairs. The cable consists of a strength member of compacted steel strand, coated with paper tape. The tubes are of extruded polybutyltetraphthelate, and each tube contains four acrylate coated optical fibres. The fillers are of extruded polyethylene. An aluminium/plastic laminated moisture barrier is applied over the core and the cable is sheathed with low density polyethylene.

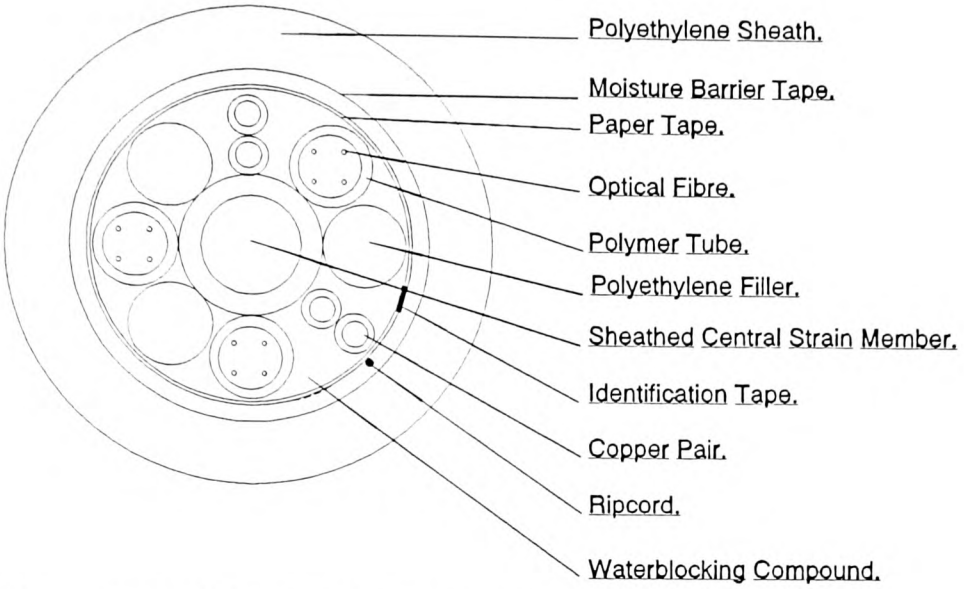

Figure 4.7 12 Fibre, 2 Copper Pair Unarmoured Trunk Cable for Duct Use.

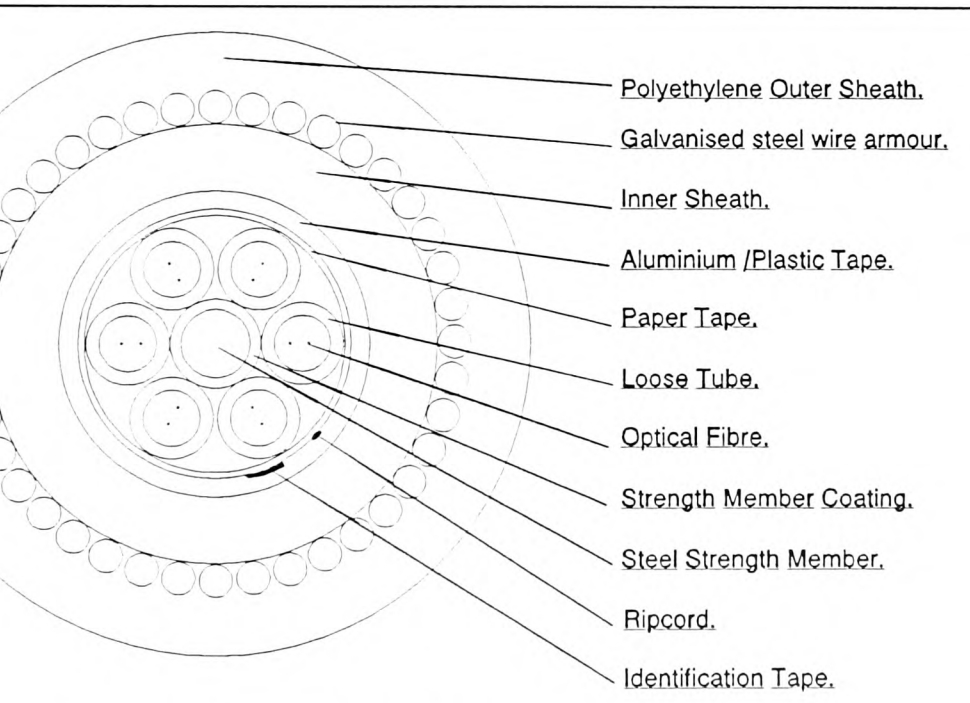

Figure 4.8 Armoured 12 Fibre Loose Tube Cable.

Fig 4.8, is also a twelve fibre loose tube cable, but has six tubes (two fibres per tube), and four fillers. There are no copper pairs. Also present in this design is a galvanised steel wire armouring.

4.4.2 Tight Construction.

This type of tightly buffered cable is suitable for installation into ducts. Cables are designed with space for up to ten elements, each of which may be either an optical fibre (secondary or triple coated), filler or insulated copper wire. The cables are small, flexible, lightweight and optimise the use of existing duct space.

The cable construction as seen in Fig 4.9 which has ten secondary coated fibres, has a polyethylene coated steel central strain member over which the fibres, copper conductors or filler elements are stranded. The interstices are filled with a water blocking compound, except when used in pressurised systems. The unit is wrapped with a paper tape and ripcord included, over which are applied an aluminium/plastic laminate and an outer sheath of polyethylene.

4.4.3 Fibrespan Aerial Optical Cable.

Fibrespan optical cable meets the requirements of electric power utilities as an efficient telecommunications medium for the transmission of data for supervisory, maintenance, control and telephony purposes. Fibrespan cable may be installed on existing overhead power lines without the need for power cut-off and provides a simple and cost effective means of establishing a telecommunications data network.

Fibrespan is a low-loss, wide bandwidth, non-inductive, non-metallic, lightweight, self-supporting aerial cable, suitable for span widths up to 1 Km.

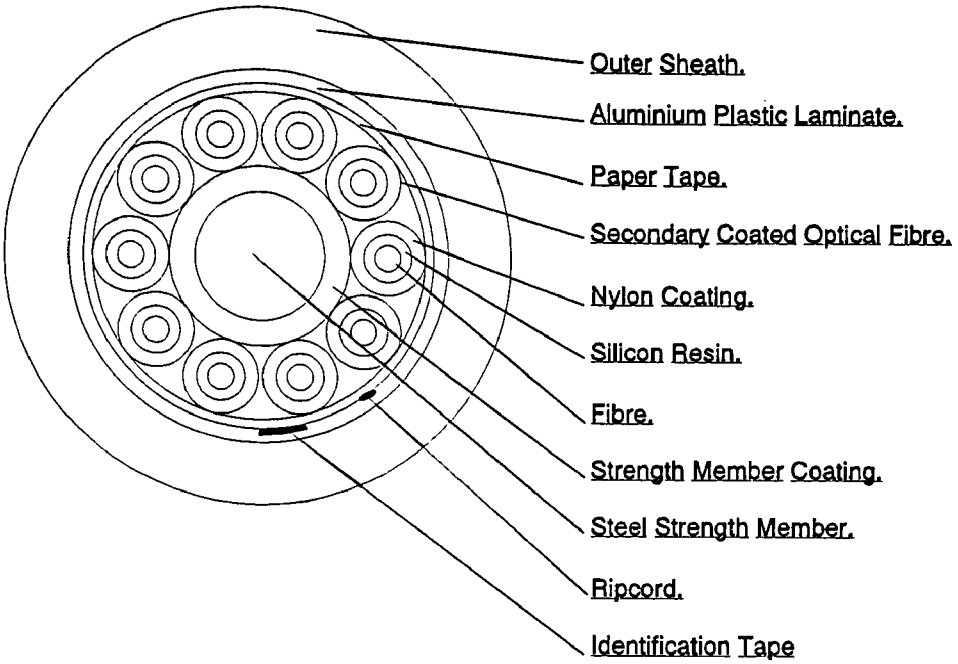

Figure 4.9 10 Tight Construction Fibre Cable

Fibrespan cable, has very high strength and withstands the combined effects of icing, wind loads and the high electric fields generated by adjacent power cables. The smooth circular profile of Fibrespan inhibits galloping, with spiral preformed dampers installed on each span to minimise aeolian vibration[2].

A prime feature of the design is the easy access to the fibres for terminating and splicing. Rapid installation is possible using lightweight equipment due to the low cable weight and tensions. The cable does not kink and preformed spiral clamps and dampers are easily fitted.

The design enables exceptionally high excess fibre lengths to be incorporated by snaking the fibres in the slot which is then filled with soft gel to cushion the fibres against vibration. It also prevents ingress of moisture whilst retaining freedom of movement. The cable design minimises the application

[2] Aeolian vibrations, are the wind induced high frequency vibrations experienced in small diameter overhead cables.

of strain of the fibres, thus ensuring optimum and stable optical performance even at maximum working tension.

Fig 4.5, shows a Fibrespan cable with 24 optical fibres. The fibres are bound together to form a ribbon.

4.4.4 Open Channel (Slotted Core).

These cables may be used as an alternative to loose tube designs in similar application areas.

Cable variants to suit customer's specifications include steel or dielectric central strain members, steel tape or steel wire armouring, polyethylene, PVC or low fire risk sheathing compounds. Copper conductors may also be included.

The cable core is a six slot, reversing helix polyethylene former with an integral central strength member. Acrylate coated fibres are laid into the slotted former which protects them from the stresses applied during handling and installation. Fibres may be colour coded to enable easy identification.

The diagram in Fig 4.10, shows a slotted core cable. For particular duct installations, it may consist of 16 optical fibres and one copper pair, assembled in the slots with a water blocking compound. A binding yarn secures these elements in place and a paper tape helically applied followed by a longitudinal covering of aluminium/plastic laminate completes the central section. The cable is sheathed with low density polyethylene.

A hybrid cable designed for the subscriber network has recently been developed by Fujikura Ltd. of Japan. The design combines the mechanical fibre protection offered by the open channel design, with

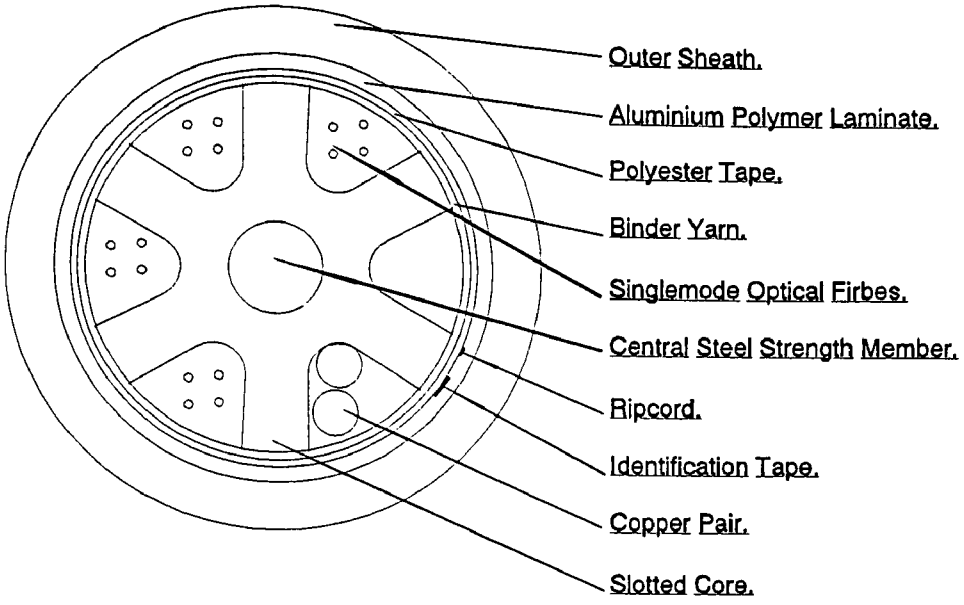

Figure 4.10 Open Channel Slotted Core, 16 Fibre, One Copper Pair Cable

the accessibility and space economy of fibre ribbons. The cable uses a reverse helix (the helix direction of the core periodically reverses), so that when the sheath is cut away from the cable, excess fibre can easily be produced for splicing-even if the splice is to be in the middle of the cable (Fig 4.11). In order to carry out a splicing operation on a mid-span cable section, 15cm. of free fibre is required. By stripping back 500 mm of sheath, this amount of fibre can be made available. Fig 4.12 shows the process of mid span jointing.

The outer protective layers of the cable are the same as for standard slotted core design. A full description is available from [4.2].

4.4.5 Air Blown Fibre (ABF).

One of the most damaging periods in the life of an optical fibre is during the installation of the cable containing it. ABF designs allow (for relatively short distances), cables containing tubes similar to

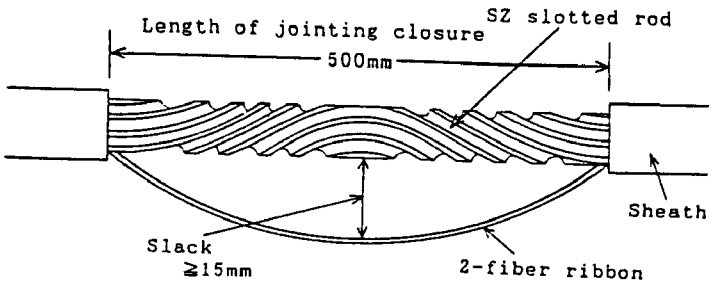

Figure 4.11 Cut Away Section of an SZ Slotted Core Cable.

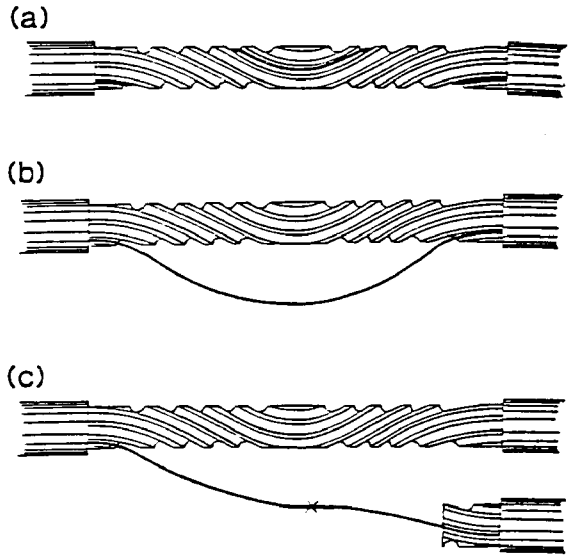

Figure 4.12 The Process of a Mid Span Joint Carried Out on an SZ Cable.

the loose tube design but completely hollow, to be installed in their ducts or on their aerial stations. After successful installation of the cable in the field, fibres are blown along the hollow tubes thus

reducing the risk of damage. The design removes the need for a degree of armouring, since part is normally added to protect the fibre during its installation.

The ABF system, was proposed by British Telecom. Research Labs. [4.3], in 1983, and details of the latest advances in this technology can be found in [4.4].

4.5 Merits of Various Cabling Approaches.

Table 4.1 is a comparison of the performance of the cable design alternatives. It indicates the merits and deficiencies of the design options available.

Table 4.1 Comparison of cable design approaches.

Factor.	Circularly symmetric unit.	Flat ribbon unit.
Microbending loss.	Easier to control.	Harder to control.
Low temperature stability.	Easier to control.	Harder to control.
Space efficiency. (fibres/area)	More complex.	Simpler.
Ease of fibre handling and identification.	Poorer.	Superior.
Suitability for mass splicing.	Poorer.	Superior.
Suitability for repair splicing.	Good.	More difficult.
Ease of manufacture.	Good.	Poor.
Compatibility with conventional cable manufacturers.	Good.	Poor.

4.6 Common Cable Faults

The fibre faults discussed in this chapter can be divided broadly into two areas: those which actively attenuate a signal passing through the fibre; and those which distort the signal and hence effectively limit the bandwidth of the fibre.

Solutions of the fibre optic industry to the problems experienced in fibres are listed, as well as an attempt to quantify the improvement in performance which has resulted.

4.6.1 Dispersion.

Dispersion can be defined as the process by which a fibre distorts a signal passing through it. The standard classifications of dispersion and their interrelation, are shown in Fig 4.13

4.6.1.1 Multimode or Intermodal Dispersion (τ_m).

This type of dispersion is peculiar to multimode fibres, of both step and graded index types. It is caused, basically by optical power travelling along a fibre via different waveguide modes. Each optical mode has a differing path length and group velocity. Pulse width will therefore be distance dependent.

The two modes displayed in Fig 2.8, show the maximum difference possible for meridional modes with $\Theta = \Theta_c$ and $\Theta = 0°$. That is, the angles of the two light beams are respectively, as great as possible without the light escaping; and directly along the fibre axis.

The difference in time between the arrival of the fastest and slowest signals at the receive end of the fibre due to multimode dispersion, τ_m, after a length of fibre L, can be derived thus:

$$V = \frac{c}{n} \qquad 4.1$$

therefore the time between the fastest and slowest light modes arriving:

$$\tau_m = \frac{1}{v} \text{ (length of longest path - length of shortest path)} \qquad 4.2$$

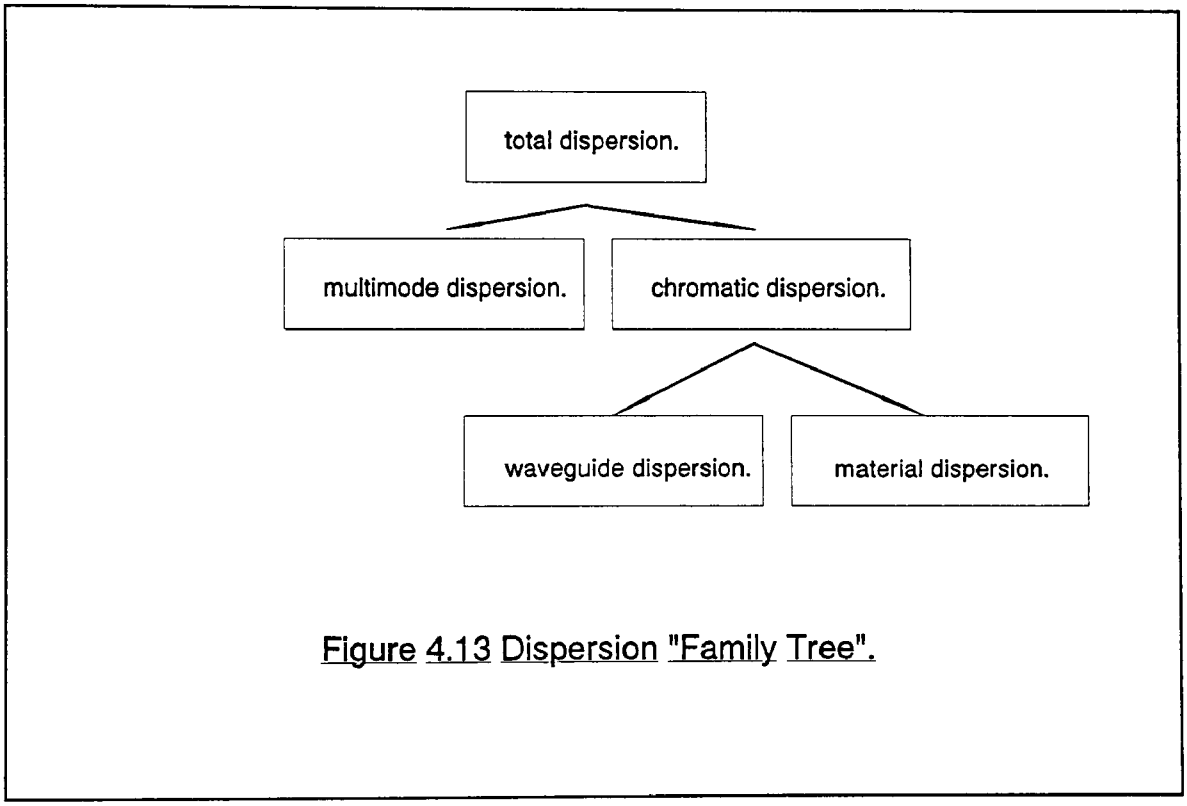

Figure 4.13 Dispersion "Family Tree".

$$\tau_m = \frac{1}{v}\left[\frac{L}{\cos\theta_c} - L\right] \qquad 4.3$$

$$= \frac{Ln_1}{c}\left[\frac{1}{\cos\theta_c} - 1\right] \qquad 4.4$$

but,

$$\cos \Theta_c = \frac{n_2}{n_1} \qquad 4.5$$

therefore,

$$\tau_m = \frac{Ln_1}{c}\left[\frac{n_1 - 1}{n_2}\right] \qquad 4.6$$

but, (from Chapter 2),

if $n_1 \approx n_2$

$$\Delta N \approx \frac{n_1 - n_2}{n_1} \approx \frac{n_1 - n_2}{n_2} \qquad 4.7$$

therefore,

$$\tau_m = Ln_1\Delta N \qquad 4.8$$

4.6.1.2 Chromatic Dispersion

A second class of dispersion is known as chromatic dispersion. The effect occurs because the group velocity of light is a function of wavelength. The effect is very much smaller than the multi mode dispersion, but becomes relevant in singlemode fibres, where multi mode dispersion does not occur.

Two factors contribute to the chromatic dispersion effect: material and waveguide dispersion.

4.6.1.2.1 Material Dispersion (τ_n).

Material dispersion is a result of the effect that apparent refractive index of a medium varies with the wavelength of light passing through it. The effect is a consequence of the fact that monochromatic rays of light are not truly monochromatic. All light rays have, however small, a finite bandwidth. The varying wavelengths therefore result in varying refractive indices which, over a length of fibre cause a signal impulse to broaden.

For this effect, the group delay can be calculated thus:

$$V = \frac{c}{n} \qquad 4.9$$

therefore,

τ = group delay.
= (time for arrival of slowest - time for arrival of fastest)
$= (V_s - V_f)L$ 4.10

$$= \frac{1}{c}\left[n - \lambda_0 \frac{dn}{d\lambda_0} \right] L \qquad 4.11$$

note: group refractive index.

$$n_{gr} = n - \lambda_0 \frac{dn}{d\lambda_0} \qquad 4.12$$

The change in group delay τ_n for a change in wavelength $\delta\lambda_0$, is given by:

$$\tau_n = \frac{d\tau}{d\lambda_0}.\delta\lambda_0 \qquad 4.13$$

$$= \frac{1}{c}\left[\frac{dn}{d\lambda_0} - \lambda_0\frac{d^2n}{d\lambda_0^2} - \frac{dn}{d\lambda_0}\right]\delta\lambda_0.L$$

4.14

$$= \frac{-\lambda_0}{c} \cdot \frac{d^2n}{d\lambda_0^2}.\delta\lambda_0.L$$

4.15

$$= D_n.\delta\lambda_0.L$$

4.16

4.6.1.2.2 Waveguide Dispersion (τ_w).

The waveguide dispersion is always negative. It is defined by:

$$\tau_w = \frac{n_1.\Delta N}{\lambda_0.c}.D_w(V).\delta\lambda_0.L$$

4.17

$$= \frac{(NA)^2}{2n_1.\lambda_0.c}.D_w(V).\delta\lambda_0.L$$

4.18

Where $D_w(V)$ is a function of the normalised wavelength and is negative for single mode fibres.

Waveguide dispersion is caused by the variation in speed between the proportion of light carried within, and that travelling outside the fibre's core.

4.6.1.3 Solutions.

The dispersion effect is dealt with in three ways. The first accepts the existence of the effect, but attempts to suppress it; the second attempts to move the effect to an area of spectrum where it can do no harm; while the third approach is to remove the effect from the fibre by altering the fibre's composition.

4.6.1.3.1 Minimising Chromatic Dispersion.

Dispersion in single mode fibre arises due to the spread of the signal frequency. In other words, in an ideal singlemode fibre, the group velocity of the signal is fully characterised when the optical carrier is a truly single frequency coherent wave. The dispersion can be expressed as a pulse spread in a convenient unit such as ps/Km.nm. The dispersion is a function of the operating V value of the waveguide, see Fig 4.14.

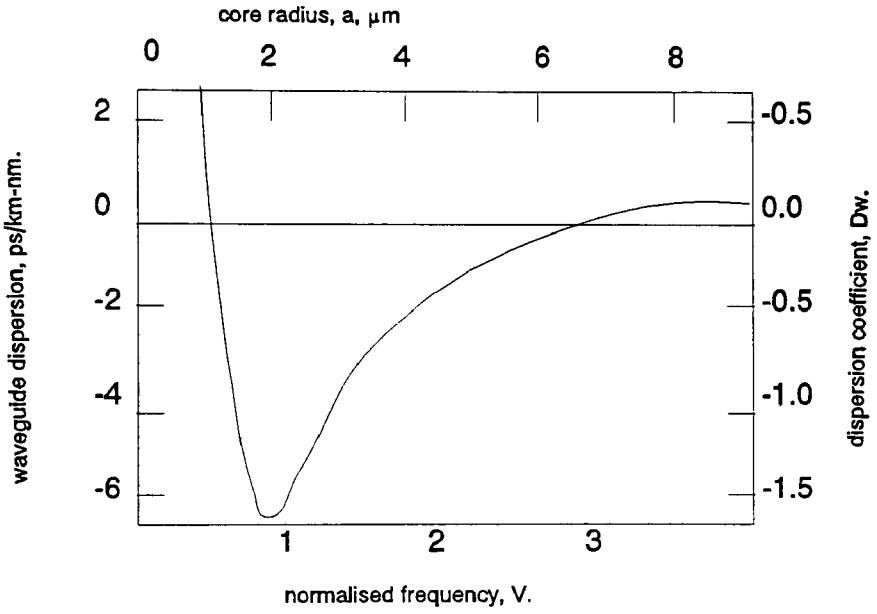

Figure 4.14 Waveguide Dispersion versus V value for Single Mode Fibre

Signal bandwidth corresponding to a 1nm wavelength spread at the 1μm carrier wavelength is approximately $3*10^{11}$Hz., corresponding to an RMS pulse width of ~2ps. Fig 6.14, shows that a single mode fibre can handle a signal bandwidth over 1Km. of $3*10^{11}$Hz., provided it operates near the cut off point of the second mode of V = 2.4.

4.6.1.3.2 W Index Fibre.

The W fibre, or depressed cladding fibre was an attempt to modify the cut off wavelength and the group velocity vs V number curve. It is possible to design the waveguide to tailor a near zero dispersion region.

Modified fibres impose three optional conditions. The first is an increase in fibre manufacturing tolerance requirement, and the second is an increase in scattering loss. The third is a more stringent splicing or jointing tolerance requirement. Since the information-bandwidth-distance product is of the order of 10^{11}Hz.Km, an uncompensated fibre operating with a narrow width optical source offers a good solution for most long distance trunking and inter-city transmission applications. For special applications, where the longest repeater spacings are mandatory; for example in repeaterless submarine systems and trans-continental links, the special fibre optimised for maximum bandwidth -distance product could be justified.

4.6.1.3.3 Graded Index Fibre.

The effect of mode dispersion can be minimised, and in theory eliminated, by using a graded index profile, as explained above. The difference between theory and practice, is that it is very difficult to produce the exact profile required, and the effect of a slight deviation from it is marked. Not only is it difficult to produce the fibre to conform with theory, but there is an inevitable variation of profile with length, and this will allow dispersion to occur, with a consequent reduction in bandwidth. The ideal profile is discussed in Chapter 2.

The graded index changes paths followed by the waves travelling down the fibre. In terms of the ray theory, the light will travel faster at the outer reaches of the core than at its centre.

Skew rays will still follow a helical path with their velocity increasing with distance from the fibre's centre.

The effectiveness of a particular profile on reducing the multimode dispersion, is also a function of wavelength. It is therefore possible to reduce the dispersion of a fibre be operating at its most favourable wavelength. The effect of varying the profile of the index can be seen from Fig 4.15. The sharp minimum shows why great importance is attached to producing fibre with the optimal value of α, (index gradient).

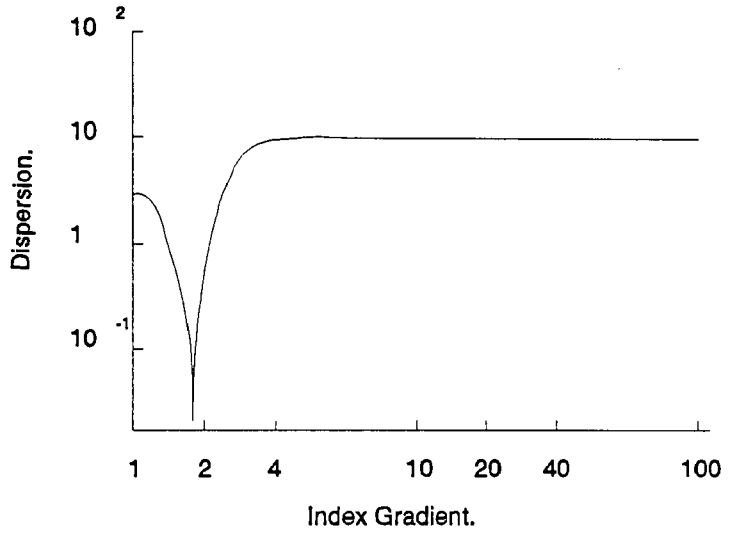

Figure 4.15 The Effect of Varying the Profile of the Fibre Core Refractive Index Upon the Mode Dispersion.

4.6.1.3.4 Dispersion Shifted Fibres (DS fibres).

For shifting the zero dispersion wavelength and maintaining low-loss propagation, a triangular refractive index profiled fibre was developed. The triangular designs shifted the cut-off wavelength, as well as changing the magnitude of the waveguide dispersion, so that for a fibre construction, the

zero dispersion point could be shifted to 1550nm., where the fibre loss was a minimum. For this type of fibre, low loss of 0.23dB/Km., has been achieved, which compares reasonably well with a low loss figure of <0.2 dB/Km., for an uncompensated fibre.

4.6.1.3.5 Dispersion Flattened Single Mode Fibres (DFSM fibres).

Standard singlemode fibres have a zero dispersion point, as discussed above at around 1300nm., but a high dispersion value in the third, 1550nm., transmission window (about 20ps/Km.nm.). For DSSM fibres, the refractive index profiles have been designed so as to yield zero dispersion at 1550nm. These fibres however, have high values of dispersion in the second, 1300nm., transmission window. The dispersion flattened fibre offers the best of both worlds by giving low dispersion in both the second and the third transmission window.

So far, DFSM fibres have a slightly higher attenuation than standard single mode fibres. This still proves to be a limiting factor in long haul projects.

The advantages of DFSM fibres are that they offer the possibility of wavelength division multiplexing at several wavelengths within the 1300 and 1550nm. windows for high bit rate transmissions using LED's and other low cost components.

Fig 4.16, shows the refractive index profile of a DFSM fibre. The outermost index step is light guiding and as such, reduces the Macrobend loss, characteristic of the fibre.

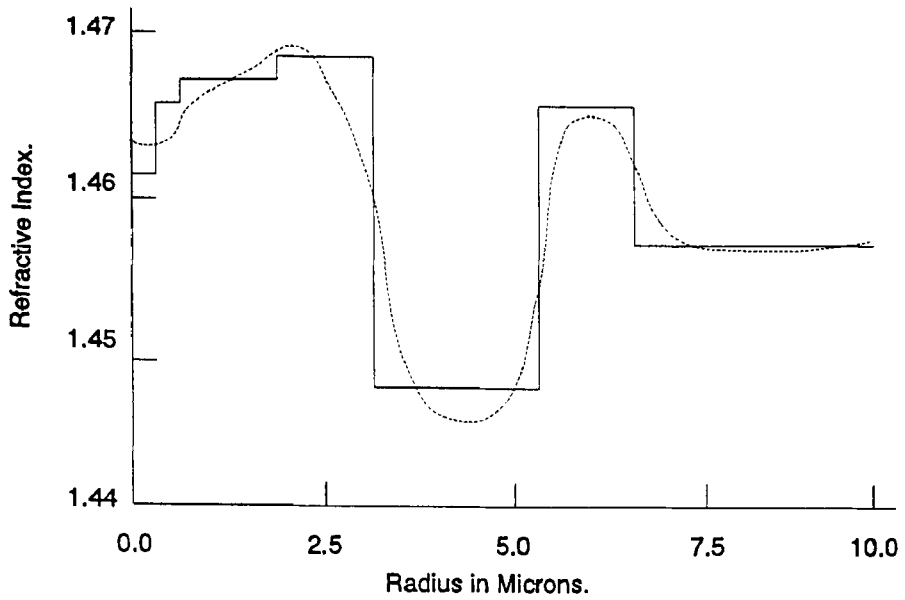

Figure 4.16 Refractive Infex Profile of the Designed DFSM-Fibre with Typical Dip (solid line) and Measured Profile of a Fabricated Fibre, Solid Line).

4.6.2 Mechanisms of Loss.

Loss mechanisms in fibre, are the methods by which a fibre attenuates the signals passing through it. Fig 4.17 shows the interrelation and hierarchy of loss mechanisms which can be active in fibres. The figure illustrates the position within the hierarchy of the focus of the project: microbending.

Attenuation of a signal as it travels along the guide is caused by several factors. The main ones are absorption, scatter and radiation. Each is important, but as fibre production methods have improved, and the limits on the operating conditions of the fibre have been optimised, the attenuation is eventually determined by the scattering loss.

Fig 4.18, shows the positions of the various attenuation modes and the total loss which they contribute to.

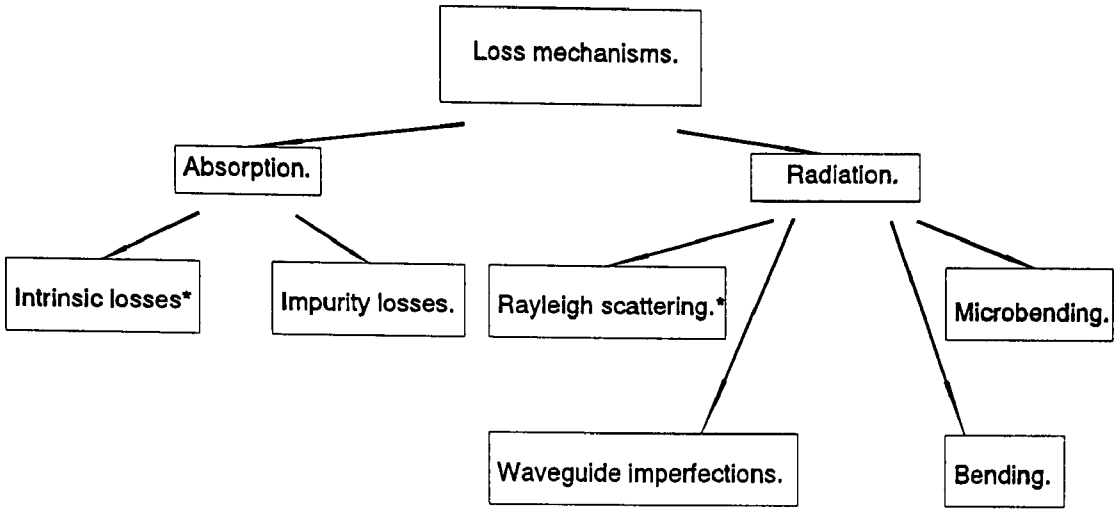

Figure 4.17 The Heirarchy of Modes of Loss active within Optical Fibres.

* unavoidable losses of the fibre material (silica).

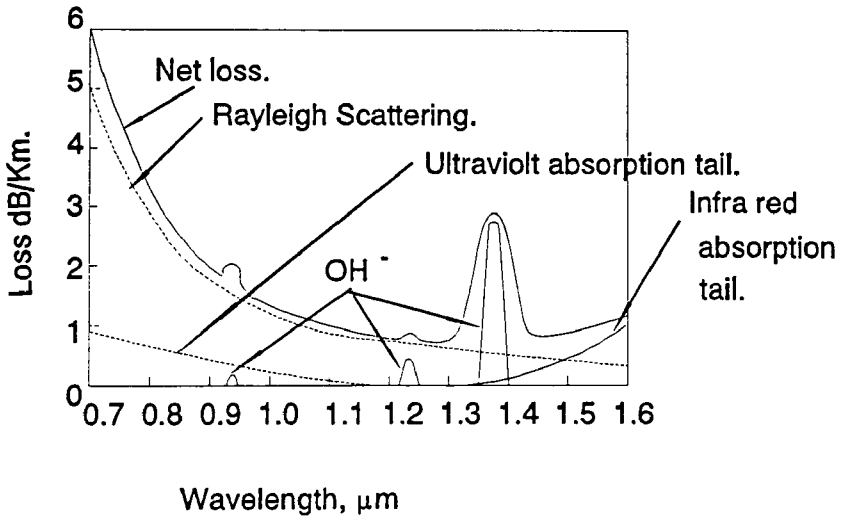

Figure 4.18 The Sources of Attenuation and their Significance across the Transmission Windows.

4.6.2.1 Absorption.

From Fig 4.18, it can be seen that two mechanisms of absorption exist, and that one of these is an unavoidable mode of loss.

4.6.2.1.1 Intrinsic Absorption Loss.

The light which constitutes the signal passing through an optical fibre, has an effect on the silica material from which the fibre is made. It is for this reason that intrinsic absorption loss cannot be reduced, leaving wavelength selection as the only possible means of negating its effect.

Intrinsic absorption is made up of two absorption effects:

i) Ultra violet absorption-where the U.V> light is capable of exiting the outer electrons of the silica to take up higher energy levels, (In this way, the light passing through the fibre's energy is depleted by electron transitions, which effectively attenuate the signal),

ii) Infra red absorption-the infra red electromagnetic wavelengths are attenuated because the silica lattice of the fibre uses their energy to vibrate as a whole, (the energy absorption for lattice vibrations peaks at 9000nm).

It can be seen that intrinsic loss, therefore cannot be reduced, but inspection of Fig 4.18, shows that by choosing 1300 and 1550nm., transmission windows, its effect will be minimised.

4.6.2.1.2 Impurity Absorption.

Contaminating elements in glass, particularly the transition elements, (V, Cr, Mn, Fe, Co, Ni), have electron energy levels that will absorb energy from incident light. The amount of energy absorbed, depends upon the proportion of impurity atoms present. With care in the manufacture of glass, and in the drawing of the fibre, these impurities can be reduced to about one part per billion and at this level, the loss is negligible.

The absorption produced by the transition metals is not very dependent on the wavelength of the signal, and so is not easily avoided by choosing a suitable wavelength for the light source.

The other main absorption mechanism is that due to the presence of water: the hydroxyl ion, OH^-. The water ion absorbs readily at 2.8μm., and there are less strong, but still pronounced absorption peaks at wavelengths which are almost direct harmonics: 1.4μm., 0.97μm., and 0.75μm., (see Fig 4.18).

Some reduction in this absorption -frequency characteristic can be obtained by pre-drying the powders used to form the glass. The strong frequency dependence of this mode of loss, allows signal wavelengths to be chosen which will minimise the effect. A deeper discussion of this subject will be found in [4.5].

4.6.2.2 Radiation.

Radiation is a mode of attenuation where, rather than light energy being taken up by the dielectric medium, it is re-directed by one or more of the several mechanisms out of the fibre. The term "light

leakage" has often been applied to this mode of loss. The following sections detail some of the more common means of leakage.

4.6.2.2.1 Rayleigh Scattering.

This mode of loss, like the intrinsic absorption above, is unavoidable and as such is compensated for rather than being solved.

Rayleigh scattering is caused by fibre variations in atomic shape, occurring over very small distances compared with wavelength. The scattering comes about because of small variations within the glass of refractive index profile and the loss coefficient is proportional to λ^{-4}.

The unavoidable nature of the loss mode means that it provides a lower limit to the attenuation levels which can be achieved. Fig 4.18, shows the Rayleigh loss curve. Equation (4.20) is an approximate calculation showing the value of the loss is a function of the fibre and its constituent glass:

$$ls = \frac{8\pi^3}{3\lambda^4} (n^2 - 1) K.T.\beta \qquad 4.20$$

where:
ls = scattering induced loss,
n = refractive index
β = isothermal compressibility,
k = Boltzmann's constant,
T = absolute temperature,
λ = wavelength of light.

Other types of scatter can occur. In particular, Mie scatter, which is due to variations in the structure of the glass which occur at about one wavelength intervals, and waveguide scatter, which is caused

by fluctuations in the geometry of the core along its length. These last types of loss con be made insignificant by tightening production tolerances on fibres.

4.6.2.2.2 Radiation from Bends.

Energy is radiated at a bend in a fibre. The amount of radiation is usually small, but proportional to the bend radius. As the radius is decreased, there is a very rapid change at a critical radius, R_c. As the radius decreases past R_c, the amount of loss changes from low to high. The value of R_c depends on the numerical aperture of the guide, and the radius of its core. Increasing NA (ie. reducing the MFD thus causing a grater percentage of light power to be carried within the core), and reducing the core size, will help to decrease the minimum bending radius.

The mechanism that causes radiation, results from the fact that the field pattern of the guided wave penetrates into the cladding. At a bend, the field at the outside of the bend has to travel faster than that at the inside, in order to maintain the phase relationship in the mode. At some distance from the fibre, the velocity of the wave will attain the velocity of light; therefore the energy at a larger radius must be radiated. As the bend radius decreases, the radiation radius moves closer to the fibre. At the critical radius, half of the light into the bend is lost. For many materials, the critical bend will be very small, and sometimes less than the limit imposed by the mechanical stress due to bending.

[4.6] deals more fully with the bending effect in fibres.

4.6.2.2.3 Microbending.

Microbending, discussed extensively below is a form of radiation loss from bends. It is the small axial perturbations of a fibre axis, which lead a shift in the mode power such that enough light is travelling outside the core for radiation to occur.

The microbend effect is a function of several primary and secondary fibre parameters, and is very much harder to diagnose due to its multi dependent nature than its pure, macrobending relation.

4.6.2.2.4 Waveguide Imperfections.

Waveguide imperfections include variations in fibre cross sectional dimension and refractive index profiles; and microbubbles within a fibre. All of these effects lead to attenuation of a fibre signal, and improved production methods have gone a long way to making their effect negligible.

References.

[4.1] Jackson, Patel, et. al., "An enhanced ribbon structure for high fibre count cables in the loop", pp 569-574, AT&T. Bell laboratories, Norcross, Georgia, 1989 International Wire and Cable Symposium minutes.

[4.2] Okada, Mogi, et. al., "A SZ slot ribbon fiber cable for subscriber network", Fujikura Ltd., Tokyo, Japan, pp 155-161, 1989 International Wire and Cable Symposium minutes.

[4.3] Cassidy, Reave. "A radically new approach to the installation of optical fibre using the viscous flow of air", Tohoku Electric Powqer Co. Inc, pp 250-253, November 1983, International Wire and Cable Symposium minutes.

[4.4] Sano, Hayashi, et. al., "Development of optical fibre units for air blown fibre (ABF) cabling systems.", Sumitomo Electric Industries Ltd., pp 69-75, November 1989, International Wire and Cable Symposium minutes.

[4.5] Midwinter. T. E., "Optical fibres for transmission", Wiley, Chichester 1979.

[4.6] Roberts, Summers, Barnes, "Bend Characteristics of Fibres Manufactured by CVD, OVD and VAD Techniques", STC Telecommunications, November 1987, Proc. EFOC/LAN, Amsterdam, 1988.

CHAPTER 5.0.

Issues Relating to Microbending.

5.1 Introduction

Microbending is a problem which permeates every level of the fibre optic industry. It is taken into account when fibres are drawn and has to be included in the final calculations used in cable design.

Chapter 4 defines microbending as the microscopic perturbations of a fibre's axis and classes it as a form of bend radiation along with macrobending. While the latter of these two effects has been thoroughly defined, researched and resolved, the former remains an unknown area. It has been proven [5.1][5.2], that macrobending occurs when a fibre attains a critical bend diameter and that certain parameters such as cut-off and mode field diameter, (spot size), define this critical diameter.

Given these two facts, macrobending can be counteracted in two ways. These are:

i) manipulation of certain fibre parameters can be used to adjust the critical diameter sufficiently so that it becomes small enough to make the effect insignificant,

ii) or taken account of during cable design, as described in Chapter 4, (in this case, adjustments are affected to the fibre helix angles around the central core of a cable so that the critical bend diameter is never attained).

Obviously macrobending is a problem which, given a closely controlled fibre production process and cable design, can be overcome.

Microbending is unfortunately not as well defined as this. While all agree that microbending is the microscopic perturbation of a fibre along its axis, no agreement can be reached as to the parameters of the fibre which define its susceptibility to the microbend effect; or the mechanisms active in cables which induce it. For these reasons, microbending has been neither minimised by manipulation of fibre parameters, nor specifically taken into account during cable design in the same way as macrobending. The lack of understanding of the problem has led it to become a kind of scape goat to which all unexplained cabled fibre attenuations are attributed.

There are two main approaches to microbending research:

i) the effects on transmission of a pattern of perturbations along the fibre axis: a theoretical perturbation pattern is generated and the theoretical performance of a theoretical fibre calculated,

ii) the effect of a chosen parameter on the microbend susceptibility of a fibre: a parameter is chosen and the effect upon the signal attenuation measured or calculated.

Neither of these approaches has a great deal of credibility or use in practical applications. The reason is that the approaches do not address the real microbend problem. They deal either in the first case with perturbations which were the result of a set of simplifying assumptions; or in the second case with a parameter or set of parameters which were chosen arbitrarily and which therefore might not be those with significant effect upon microbend performance in cables. The overall effect is to cause these theories to lack a base in reality, which would afford them the credibility they require. They take no account of real perturbation patterns or the relative significance of fibre parameters on fibre performance in their calculations.

The definition of microbending therefore, while being sufficient as an abstract concept is of little use to the cable production industry attempting to find solutions to the problems presented by

microbending. In order to come to terms or solve the problems posed by microbending, it is necessary to either find a way to accurately quantify the perturbations experienced by a cabled fibre, or discover all significant fibre parameters in the determination of microbend susceptibility.

5.2 Statement of the Problem.

The problem to which this piece of work was initially addressed, was simply to investigate the microbend effect on various fibres. From 5.1, it becomes obvious however, that the microbend problem splits easily into two areas of research:

i) what causes the varying levels of susceptibility to the microbending effect in fibre samples,

ii) and what induces microbending in cabled fibres.

Results arising from research in either of these areas would constitute a step forward in levels of understanding.

The method of research was to be founded in experimentation, and would set about finding links between fibre microbend performance and fibre parameters. In this way, it was hoped that all relevant factors in the determination of microbend susceptibility would be taken into account, and that any theories developed would have enhanced accuracy.

The policy of delaying the introduction of theory, meant that in order to comprehend experimental results, a system would have to be adopted which related information about fibres and processes to the results. It would introduce data to explain fibre performance only if that data became relevant. In this way, no assumptions at all were made about results, which gave conclusions attained much more credibility. The technique therefore, started with a pure method of research. It involved

measuring and collecting data, linking data and relevant factors about fibres and processes, and finally introducing theory to explain the nature of the descriptive relationship which had been developed.

Solution to the problem, like the problem itself was split into two areas. The first involved investigation of the susceptibility of fibres to the microbend effect, the second was the reasons for the perturbations when fibre is cabled. Once in the process of cable production, the attenuation of a signal passing through a fibre can be attributed to many causes, only one of which could be described as microbending. In real situations therefore, quantifying the microbend effect becomes very difficult since any results obtained are obscured by many spurious modes of loss. The additional complexity of the microbend problem when viewed "in situ", lead the researcher to start the investigation by examining fibre susceptibility to the microbend effect away from the cables. In this way, it was hoped that a "feel" for the effect could be obtained before embarking on the investigation of causes of the effect in cables.

In order to examine the microbend effect in isolation and therefore the susceptibility of fibres to it, a test which induced almost pure microbending in fibres had to be constructed. In cables, the axial perturbations of microbending could be due to effects as diverse as fibre strain due to an insufficient amount of excess in a loose tube, an amount of excess so large that fibre is forced into contact with the tube wall, a bad mixture of tube filling compound or even the fibres crossing and coming into contact in a disadvantageous manner. In order to build a rig which would simulate these effects, the possibility was first examined of artificially inducing them in fibre. The method was quickly abandoned as the test required to induce the required number of cumulative effects would prove impossible to duplicate with any accuracy for repeated tests. The method which was instead adopted, was to reduce microbending to its most basic form and have the test induce that. The obvious development method for the test was to have it induce-in a highly controlled and repeatable

manner-the axial perturbations which are the basis of microbending. In the study, this was the first occasion on which previous microbending work was actively used to assist in development.

5.3 Requirements for an Efficient Microbend Test.

In order to clearly define the microbend test and to be sure when an end point had been achieved, the requirements of the test were positively defined before the commencement of the work.

Four features were identified which, if taken into account during the design of the microbend test would yield a satisfactory result. The features required in the microbending test were:

i) the microbend test should be highly repeatable,

ii) the spatial frequency of the perturbations induced by the test should cover a broad range,

iii) the test should induce only microbending as a mode of signal attenuation in test fibres and minimise any spurious modes of loss,

iv) the test should be completely non destructive to any fibres under test.

The failings of existing tests are addressed in subsequent sections. The reasons for requiring the above features in the final test are discussed below.

Repeatability is necessary in the test for two reasons: it is essential that the experiences of successive fibre test samples are as similar as possible and that if a fibre were tested on the test, removed and then tested again, the two sets of results would be very similar. The former of these two conditions would mean that direct comparisons between fibre results could be made with no fear of inconsistency. This would lead to a higher degree of integrity for the results of the test, and would make the setting of standards for specifications more easy. The latter condition would again add a

degree of integrity to the results which, because of a normally high results scatter for microbend tests is characteristically low.

In the past, the absence of these factors has led to a low degree of acceptance within the fibre optic industry for microbend tests. They have been viewed with scepticism which has prevented their widespread adoption by the whole industry. Any test which lacks repeatability in the two areas described above would be both low in credibility from the point of view of individual fibre results; and would produce results which were of little use for specification or comparison use.

Microbends induced in cabled fibre will be of a variety of frequencies. The different frequency perturbations will have varying effects upon fibre attenuation depending on their amplitude. Any simulation of the microbending effect should take into account the wide variety of perturbation frequencies a fibre might experience in a cable. For this reason the microbending test must induce perturbations in the fibre, which have spatial frequencies covering as wide a spectrum as possible. A test which was capable of inducing perturbations of this kind, would fully test the fibre and would be more likely to show up any electro magnetic wavelengths at which a fibre was particularly sensitive to the microbending mode of loss.

The third condition states that the fibre under test should experience only the microbending mode of loss when on the microbending test. While this condition seems to be a prerequisite rather than a named condition of the microbending test, it is essential that it is highlighted. A problem with the existing tests as described in 8.2, is that they do not induce pure microbending. Characteristically, they induce a number of modes of loss, relegating the microbending to a position of relative insignificance when compared to the total loss system they develop. Any test which could prove that it induced very small amounts of spurious signal attenuation when compared to the amount of microbending based attenuation would gain much credibility.

The fourth condition can now be seen to be evolved from the previous three. If a test is in any way degrading to a sample fibre, not only will it be highly unrepeatable, but it will also not be inducing pure microbends. Loss modes induced by a destructive test will include fibre kinks, and in some cases fibre violation and even breaking. Clearly, any test which is destructive in any way to the test fibres will be unsuitable.

5.4 The Real Situation.

After addressing the susceptibility of fibres to the microbend effect, the cable orientated half of the problem was investigated. The object was to investigate the causes of microbending. It quickly became clear that the pure approach described above, was opposed to the stated policy of withholding the introduction of theory for as long as possible. Microbending is one of a number of mechanical effects experienced by fibre in cables. If pure measurement techniques are used, it is impossible to discern between microbending and other forms of attenuation inducement. For the same reasons, it is therefore impossible to isolate the causes of microbending in cables.[1]

The real situation gave no possibility of isolating the microbend effect. For this reason, it became necessary to regard attenuation exhibited by cabled fibre as being the result of a total effect termed "process induced attenuation". The effects leading to attenuation when viewed as a whole could be easily quantified and measured for the real cabled situation without the need for assumptions of any kind to be made.

Therefore before the cabled fibre situation could be examined, it became necessary firstly to gain experience of the microbend effect in a pure environment. It was important to investigate the

[1] Optical time domain reflectometer, (OTDR), readings of cabled fibres are said to show microbending in fibres as a series of small "kinks" along the attenuation trace they produce. This theory is unsubstantiated and even if correct, would not be useful since there would be no way of quantifying it.

microbend effect away from other modes of cable loss. For this reason, a microbend test was developed. The objective was to gain a "feel" for the microbend effect on a test which produced highly repeatable, pure microbends. The causes of fibre susceptibility to the effect was examined by attempting to model and predict fibre performance on the test using fibre parameters.

Should it prove possible to accurately predict how fibres would resist microbending and possible other modes of loss, a major variable would have been removed form the cabling process.

References.

[5.1] Roberts, Summers, Barnes, "Bend Characteristics of Fibres Manufactured by CVD, OVD and VAD Techniques", STC Telecommunications, November 1987, Proc. EFOC/LAN, Amsterdam, 1988.

[5.2] E. Suhir, "Effect of Initial Curvature in Low Temperature Microbending in Optical Fibres", Journal of Lightwave Technology, Vol. 6., No. 8., August 1988.

CHAPTER 6.0.

Development of the Microbend Test.

6.1 Introduction.

The microbend test was developed in order to examine the microbend effect in isolation. In addition to giving a "feel" for the effect, it was envisioned that the test would give an insight into the susceptibility of fibres to the effect.

As has already been discussed, the microbend effect could not be isolated in a cabled fibre and investigated thoroughly. The test was therefore required to induce pure microbending, which became its design priority. A discussion in Chapter 5 listed the requirements of the test required and in designing the test, these were taken into account.

Before commencement of the design procedure, existing test methods used by the cabling industry and research establishments were examined. This was the only point at which existing techniques were referred to. Shortcomings of existing tests were assessed and attempts made, on the design of the new test to counteract them.

6.2 Review of Existing Microbend Tests.

This section attempts to isolate the failings of microbend tests in existence, and seeks to identify possible reasons for their shortcomings. Most of the criticisms of the tests discussed, were based upon measured results and comparisons with the definition of microbending from Chapter 5.

Microbend tests currently in existence fall into two basic categories, they are compression tests and winding tests.

The test alternatives will be dealt with separately.

6.2.1 Compression Tests.

6.2.1.1 Design.

Here, a length of fibre is forced against a roughened surface in an attempt to induce microbends. Fig 6.1, is a schematic diagram of a compression microbend test. The diagram displays every possible layer the method of test might contain. It should be noted that most compression tests do not contain all of these layers. The microbend inducement can be placed above or below the test fibre as can the holding material/soft former (where present), the variation in applied force due to the weight shift involved being insignificant.

The base plate provides a rigid base for the test and holds the microbend inducement and holding material, which are normally not rigid. In some cases the base plate is machined flat in order to ensure that the only perturbations in the fibre are from the microbend inducement.

The microbend inducement, as its name implies is intended to cause the axial perturbations in the fibre which are described as microbending. Inducements are always rough and fall into two categories, random and regular inducements. Random inducements tend to be glass or sand paper, the various grades of each providing differing levels of severity of axial perturbation in a test fibre. Regular inducements are normally metal meshes which will induce a regular perturbation pattern in test fibres. In the case of mesh, the intensity of the perturbation is dependent upon the mesh size.

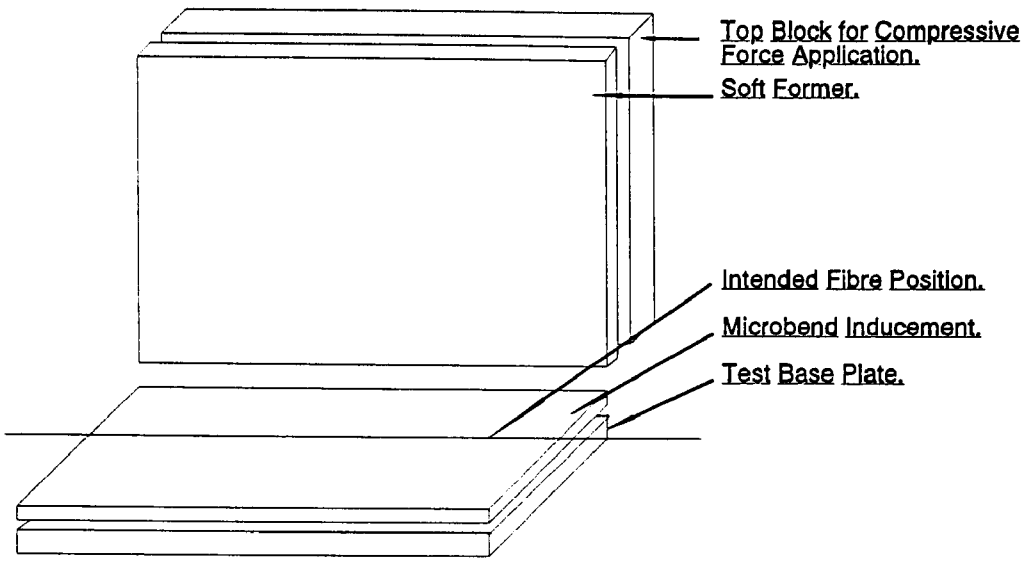

Figure 6.1 Schematic Diagram of a Compression Microbend Test Incorporating a Soft Former and Designed for use on a Straight Sample.

Both of these methods are popular and induce, to a certain extent, microbends.

The fibre under test is normally laid straight across the microbend inducement, the direction of the force causing inducing axial perturbation. The soft former is a feature of only a small number of microbend tests. Most rely on the top block (discussed below), forcing the fibre down onto the microbend inducement. These more simple tests will not be considered, since they cause signal attenuation by constricting the fibre and damaging it rather than inducing microbends. Obviously because of the spurious loss modes they induce, these tests do not actually qualify as "microbend tests", they are however in use in many establishments. The soft former should be of a material soft enough to prevent constriction of the fibre between it and the inducement; and hard enough to ensure that the fibre is forced into the shape of the mesh and not allowed to sink into the former away from the mesh.

The top block provides a strengthening member for the soft former and is normally made of metal. It provides the initial force pushing the test fibre onto the inducement. It is normally of a known size and weight and if so, provides better control of the microbend test.

6.2.1.2 Shortcomings.

Selection of the microbend inducement material was found to be critical. In the case of mesh inducements, one too fine was found to subject the test fibre to a loss mode based on compression. This was discovered by examination of results which showed that below a certain roughness, attenuation induced dropped significantly. This was because the mode of loss had shifted from axial perturbation to cross sectional strain related loss[1]. If a mesh too harsh were selected, macrobending would become a possibility and differential strains between the inside and outside radii of the bent fibre would again result in polarisation based attenuation.

Sand paper as a microbend inducement offered at best a poor source of the microbends sought. A grit paper too fine would result in a compression test unsuitable for the reasons listed above; while a grit paper too rough would damage the fibre. As stated in Chapter 5, one of the requirements of a microbend test is that its repeatability extends to it being totally non-destructive of fibres under test. The danger with grit paper is that it can cause modes of loss as various as constrictions in fibres, mechanical damage, fibre strain, coating puncture, etc. Despite this, grit paper remains a popular method of inducing microbends.

The reason for the apparent preference of the fibre optic industry for grit paper based tests, is due to the realisation that the perturbations induced on any test have to be of a wide range of frequencies.

---

[1] Strain induced loss is a significant, if separate are of research which requires high amounts of normal loading to induce attenuation through polarisation of significant magnitude. It is outside the scope of this research.

Two reasons are commonly given for this preference. The first as discussed in 7.3, is that a range of spatial frequencies of perturbations are necessary in order to fully simulate the cabled fibre situation. It is felt that the random nature of the grit paper is most likely to achieve all of the spatial frequencies necessary. The second reason for the preference of the industry is that microbending in cables is a random effect and so an essentially random set of perturbations is the most suitable answer.

Both of these arguments are fundamentally flawed. Because of the random nature of the perturbations, it is wrong to assume a complete spectrum of spatial frequencies will be automatically attained. There is a chance that it will, but to assume this, adds a degree of uncertainty to the test. In addition, the assumption that because the microbending in a cabled fibre is of a random nature, the nature of the test perturbations should also be random is false. There is a greater possibility of the fibre experiencing the required conditions if the test induces microbends in a very controlled manner. The less random elements which are allowed to occur in a test, the more control and therefore the more understanding the researcher will have of the work and results.

Members of the optical fibre industry who favour compression tests, must choose a microbend inducement which while being rough enough to ensure that microbend and not compression tests are carried out; is smooth enough to prevent spurious modes of loss and in the case of grit paper, damage to the fibre itself. In the course of the investigation, it was concluded that while some ideal grade of mesh might exist, there was no "optimum" grit paper available. Either it was too smooth to induce any loss modes except strain related ones, or it began introducing spurious loss modes by damaging the fibre. For this reason, grit paper was discarded as being unsuitable. The option remaining was wire mesh which appeared, from initial work to be capable of achieving an optimum value of percentage microbending amongst the loss modes induced, providing a novel approach were adopted.

Compression tests tend to be based around a straight piece of fibre laid across the test. This approach has a number of drawbacks. The first of these is that there is a danger of spurious loss modes from edge effects. Microbend inducements, particularly meshes, are often cut so that they finish flush with the edges of the top and bottom blocks. Where a more rigid mesh is used, this will mean that the fibre will not be experiencing what was intended as part of the test and may be subjected to spurious loss mechanisms. It is often assumed in placing the fibre onto the inducement, that because the perturbation pattern will be random, (as in the case of grit paper), its actual positioning will not matter. This is obviously not true for grit papers, as a finite paper size is used which means that for each placement, a different set of perturbations will be induced. It is particularly untrue for the wire mesh. If laid straight across the mesh, a fibre will experience either a set of high points, or a set of troughs. This will fail to induce any but a single frequency of spatial perturbation and will make the mesh unsuitable for microbend inducement. Both forms of inducement will also be hindered by the fact that each time the fibre is laid across them at slightly varying angles, a different length of fibre is tested. This effectively alters the loading values and falsifies results obtained.

Compression tests used without a soft former will break a fibre tested on them: grit paper based tests will puncture, constrict, strain and degrade them more readily. The former-less test will be disregarded as being unsuitable to test any quality of a fibre except the resilience of its coating. Where soft formers are used, they have to be chosen taking the microbend inducement material into account. The former is critical as described above and, as one of its numerous requirements must be resilient to fatigue.

With compression tests, the positioning of the weight with respect to the fibre under test, the inducement and the former, is critical. Many tests rely on arbitrary placement of the top block and take the resulting unrepeatable results to be normal for microbend tests. It is essential that the position of all elements of the microbend test should at best be fixed relative to each other, or at worst have

a location point marked. The latter is not entirely suitable even if account is taken of the orientation of the various components.

The final fault of compression tests is the lack of knowledge with respect to the amount of force applied to the fibre under test. There is a requirement to make the microbend inducement considerably larger than the fibre in a direction perpendicular to the fibre axis. This cuts down the possibility of edge effects along the length of the test fibre. The inducement is not perfectly flat, and this fact, coupled with the yielding of the soft former means that the whole area of contact between the former and the inducement is loaded. The implication of this is that a fibre only carries a percentage of the total load applied and the actual load carried by the fibre cannot be calculated. This problem can be reduced in two ways: either the whole area of contact between former and inducement can be covered with fibres, or for a particular rig, the area and placement of the fibre could be kept constant. The latter method is the only solution to the problem, although it means that all rigs would have to be calibrated in terms of attenuation due to effective applied force; and that any change in equipment on a rig would force the recalibration of the whole rig.

6.2.2 Winding Tests.

These tests are based around the winding of a fibre onto a cylinder of a sufficiently large radius to prevent the macrobending mode of loss from becoming active. Winding tests use drums which are either smooth or covered in some abrasive material such as grit paper. Tests using smooth drums have fibre precision wound onto them in multiple passes. The theory is that each successive layer of winding passes over the previous set in the opposite direction. The cross over pattern generated is designed to cause fibres to experience perturbations due to previous and subsequent layers as they are added. The advantage of this method is that a wide spectrum of perturbation spatial frequencies can be generated on a cheap smooth drum, providing good winding equipment is available. The second

alternative, using a roughened or "ruggedised" drum uses a single winding pass and again requires precision equipment if large volumes of fibre are to be applied. Strain in the fibre pulls it down onto the grit paper which, in the same way as in compression tests is designed to generate the required axial perturbations of microbending. Winding tests, particularly those which use grit paper often require a "settling time", after the fibre has been wound onto them before readings may be taken of attenuation.

Winding tests use strain to pull the fibres tight onto the ruggedised drum, or previous layers of fibre. Strain can be applied to the fibre in one of two ways. Fig 6.2, shows end elevations of two drums fitted to induce each type of strain. The first design, shown in Fig 6.2,a, is a drum used as part of a Mandrel test. This type of drum has a fixed radius and does not alter during a test. Fibre is wound onto the drum with a certain back tension. Equipment required to do this includes pay-offs with

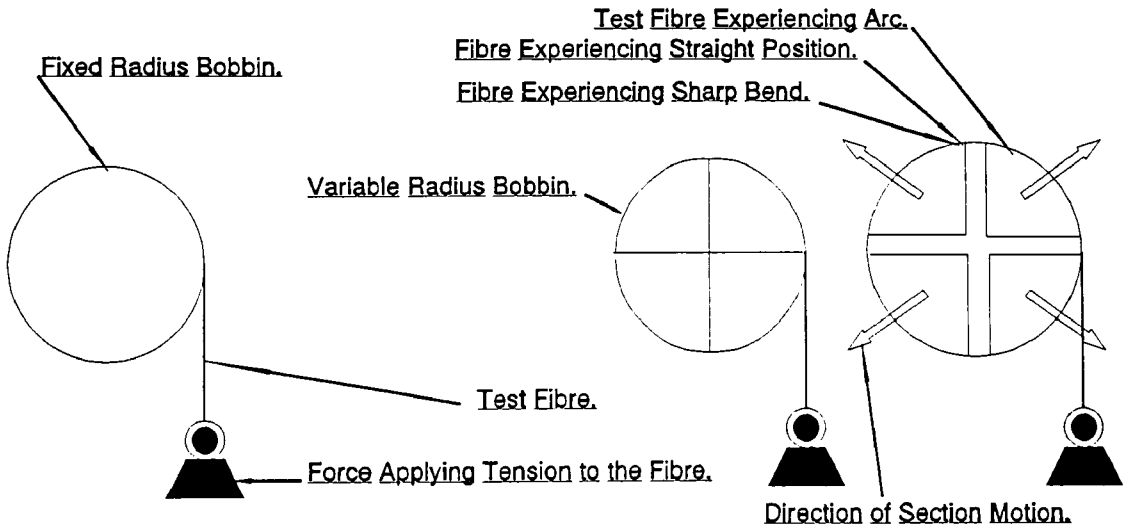

a) Fixed radius bobbin based test. b) Expanding bobbin basket weave test.

Figure 6.2 Schematic Diagram demonstrating Alternative Methods of Inducing Strain in Fibres Wound onto Microbend Test Drums.

varying back tensions and take ups with precision drives and traversing fibre guides. The alternative, which is no less costly, is to use the drum design shown in Fig 6.2,b. The test which incorporates this type of drum is known as a "basket weave test". The fibre is loaded onto the drum at a minimum back tension and then when winding is complete, the drum is expanded to apply strain to the test fibre and pull it down onto the grit paper or lower layers of fibre. The basket weave design allows the tension in the fibres to be varied during a test, which allows a set of data for attenuation versus strain to be generated without the need for time consuming rewinds.

6.2.2.1 Discussion of Winding Tests.

The winding based microbend tests have the advantage of testing long lengths of fibre. The advantage of this is that if grit paper is used, the random pattern generated will probably generate a full spectrum of spatial interference frequencies. Thus, a fibre tested on a winding test can be expected to attenuate equally across the whole transmission spectrum. This fact means that the need for precise placement so important in compression tests where shorter fibre lengths are used, is removed.

The disadvantage of using such long lengths of fibre, particularly from the point of view of the destructiveness of the test, (as discussed below), is that tests on lengths of fibre, which are normally in 2 km. lengths, make them unusable for production. Thus, having tested a fibre using a winding test, that 2 Km. length is rendered unusable. Apart from being costly, this means that results obtained would be wasted. The work covered in this thesis, is based on the fact that fibres have an inherent susceptibility to microbending, which is a function of a number of the fibre parameters. Given variations in these parameters, susceptibilities will vary not only between fibres of different preforms, but even between fibres from different sections of the same preform. If this is the case, there is no advantage to be gained by testing a long length of fibre destructively, since the results would be of no use. The only reason for testing fibres would be to attempt to establish the fibre susceptibility, or

link between susceptibility and parameters. The testing of fibres would be a costly exercise if the remainder of the fibres could not be used for some production application.

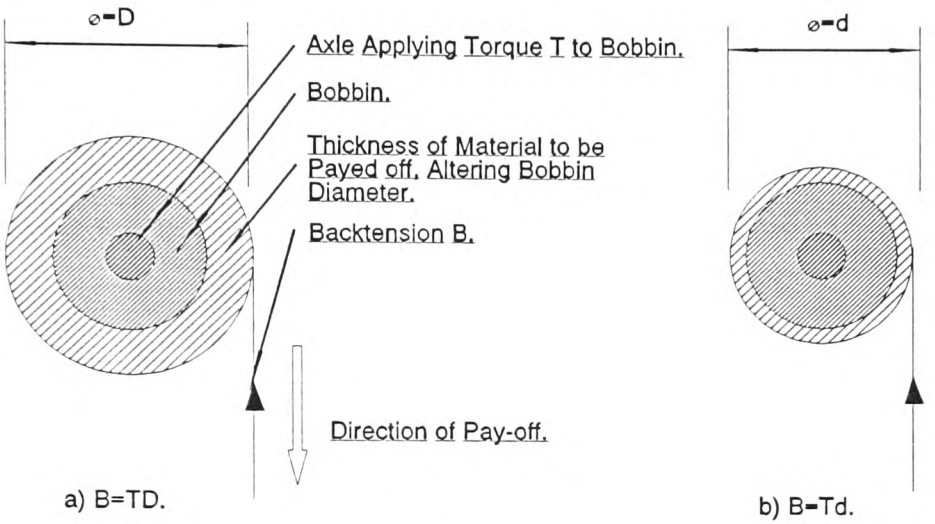

Figure 6.3 Demonstration of the Effect upon Tension in Fibre Issuing from a Drum whose Apparent Radius is Decreasing.

Additional high costs induced by this form of test are: the high cost of winding equipment and the time penalty for the preparation of the test. Not only does precision take up equipment have to be designed to allow high quality winding onto the test drum, (particularly important in multiple pass tests where spacing is essential); but pay offs for passing fibre from storage to test drums have to be carefully designed. As has already been stated, long lengths of fibre are often used with winding tests. The fibre, as it pays of the drum reduces its effective diameter, (Fig 6.3). The pay offs therefore have to apply a constant back tension, rather than constant drag, since the reducing effective diameter of the pay off drum would vary the back tension of the fibre as it was fed onto the take up test drum. These considerations lead to costly, time consuming and complex equipment which at best will only come close to the requirement for a suitable test.

The largest failing of the winding test design is in the uncertainty of the modes of loss they induce. As stated above, strain, induced by various methods, is used to pull fibres down onto the interference surface of the drum. This practice produces a number of loss modes, none of which can be clearly identified as microbending. Active modes induced by the winding tests were:

i) polarisation losses, (the strain used to pull test fibres down onto the interference pattern would cause polarisation based loss modes which would have the potential to attenuate signals by up to 50%).

ii) constriction losses, (particularly in multiple pass winding tests, successive layers of fibre would "pinch" one another constricting fibre and effectively inducing further strain related polarisation losses),

iii) sharp bend losses, (losses induced in fibres by forcing them to suddenly change direction is a thoroughly researched area of work [6.1]. This type of loss has nothing however to do with microbending),

iv) punctures, (many winding tests use a "settle time" for fibres on the test before readings may be taken, giving weight to the argument that the strain, rather than encouraging the test fibre to follow the contours of the grit paper, is at best pulling it tight between adjacent high points, and at worst pulling the fibre so hard that the coating is punctured, and the fibre damaged).

The last of these problems is accentuated in basket weave tests, where the expanding drum would cause fibre to move over the surface of the grit paper and tear, as well as puncture coatings.

The degradation of test fibres in winding tests is well known and most winding tests recommend not using the same test length of fibre more than once. As described in Chapter 5, any deterioration in the performance of a fibre suggests that modes of loss other than microbending have been induced.

Fig 6.2, shows the closed and open format of a basket weave test winding drum. It is clear that while strain can be controlled and varied easily, the fibre does not experience a circle on the test. The experience of the fibre around the drum is alternately arcs and straight sections. This pattern leads to errors as the transition between straight and bent sections, (and visa versa), are a form of attenuation in their own right, again which have no relation to microbending.

6.3 The Microbend Test.

During commencement of the work, it became clear that the way to construct a microbend test was not to find the causes of microbending in cabled fibres and then attempt to simulate them. As described in Chapter 5, this approach would be impractical and ineffective. The solution to the problem was to find a way to induce microbends which were as pure as possible, away from the cable situation by any means available.

The discussion in 6.2, is the reasoning which lead to conclusions as to the design of the proposed microbend test, or its objectives. The winding tests were discarded on the basis of cost of equipment, amount of fibre used and loss modes induced.

Cost of equipment and manpower, (as stated in 5.2), would be high to produce windings whose quality would be below the required standards. The amount of fibre used would be prohibitive from a production perspective. There is little point in testing a fibre, (to the point where it can no longer be used for production purposes), if it will never be used. The reason for testing fibres is to assess their individual resilience to a certain effect, in this case microbending. Devotees of the winding tests would say that extra lengths of fibre are required for a proper microbend test, since in cabled fibres, microbends occur along their whole length. This is a fallacy in the same way as it is assumed often that a test should contain sharp bends, edge contact and fibre cross overs to induce the microbend

effect correctly. It can be proven[2], that microbending is length independent. The implication of this is that the attenuation/m., in a test fibre, for example on a compression test caused by 2 N/m. will be the same regardless of the test fibre length. For this reason, the length of the test fibre is of no significance. All that is important is that a representative amount of microbending should be induced by the test regardless of length of test fibre, or method used. Finally, the loss modes induced by the winding test, as stated in 6.2, would be wide ranging. It is doubtful that any of the induced modes are microbending as described in this dissertation, and it was for this reason above all of the others, that winding tests were rejected as a feasible base design for the microbend test to be produced.

These reasons left only compression based tests as being feasible for the pure microbending inducement sought. For the reasons listed in 6.2, grit paper based microbend tests had to be disregarded, particularly with the short lengths used on compression tests. These deductions led to the conclusion that the best possible design for a microbend test would be a compression based test which incorporated mesh and a soft former as an integral part of the design.

The test described, would have several favourable design features which are discussed in 6.4. There were however, drawbacks to the design concept. These were:

---

[2] The common unit of attenuation is dB/Km. For the purposes of tests which often do not use fibre lengths which are multiples of Km.'s long, the normal unit is dB/m.

In a compression test for example, an amount of force is applied laterally to a length of fibre under test. The units used are N/m.

The attenuation induced on a test due to a certain applied force will therefore have the units:

$$\frac{\text{dB/m.}}{\text{N/m.}} = \frac{\text{dB}}{\text{N}}$$

That is, regardless of the length of fibre under test, attenuation due to an applied force will be the same.

i) edge effects: a piece of fibre laid straight across a piece of mesh, would encounter the edges of the test in two places. This would lead to the generation of spurious loss modes owing to a variation in test conditions at these points).

ii) limited perturbation spectrum: a piece of fibre laid straight across a piece of mesh experiences only one frequency of spatial perturbations. As discussed in 6.1, a full spatial spectrum is required to fully simulate the conditions experienced by fibres in cables.

iii) position errors: positioning on mesh tests is essential. The fibre must be accurately positioned with respect to mesh and applied force positions if the lateral position of a fibre on a mesh alters, the fibre's experience will be altered. If the fibre angle changes, more fibre will be loaded, a greater number of perturbations will be induced and the frequency of the perturbations, (which will be of single frequency), will change. Any alteration of the fibre with respect to the load position, will cause unequal and inconsistent loading, the implications of which could be harmful to the quality and credibility of the results.

iv) incorrect choice of mesh: the mesh must be chosen and matched with the forming material, the combination of which, while being coarse enough to perturb rather than compress the test fibre, will be smooth enough to prevent spurious loss modes being accidentally generated.

v) compressive force uncertainty: the actual amount of force being applied to the test fibre as discussed in 6.2, will remain an unknown quantity. The soft former and mesh will be pushed together and will carry some of the force intended to push the fibre into the contours of the mesh.

6.4 Design of the Preferred Microbend Test.

The discussion in 6.3, highlighted the mesh branch of compression microbend tests as being the most suitable test option to develop on. Fig 6.1, shows a standard mesh test, (incorporating a soft former). Fibre is laid straight across the mesh and force gradually applied to push the fibre down so that it

follows the contours of the mesh and microbending is induced. In the preferred test the novel approach of using a circle of fibre was adopted.

Advantages of this design, highlighted in 6.3, were:

i) a small amount of fibre is required for testing,

ii) the method was likely to lead to the most pure microbending of all available options,

iii) it induced no mechanical damage in the fibre under test. This meant that the criteria for repeatability, described in 5.3, was met,

Modifications to the design had to be made in order to overcome the problems listed in 6.3, and to allow the test to meet all of the design criteria from 5.3. The final test design is shown in Fig 6.4.

The test finally used, consisted of:

i) a base plate:

The base plate forms a flat bed on which the test is based. Two posts were fixed into the base plate. The posts were designed to act as reference points for all successive layers so that everything above the plate was either located on the posts, or was fixed to something which was. The base plate therefore took on a much more significant role than in the more traditional microbend mesh tests.

ii) a microbend inducement,

The mesh which was intended to induce the required microbend effect, is shown on top of the base plate and located on the reference posts in Fig 6.4. The mesh is holed so that an

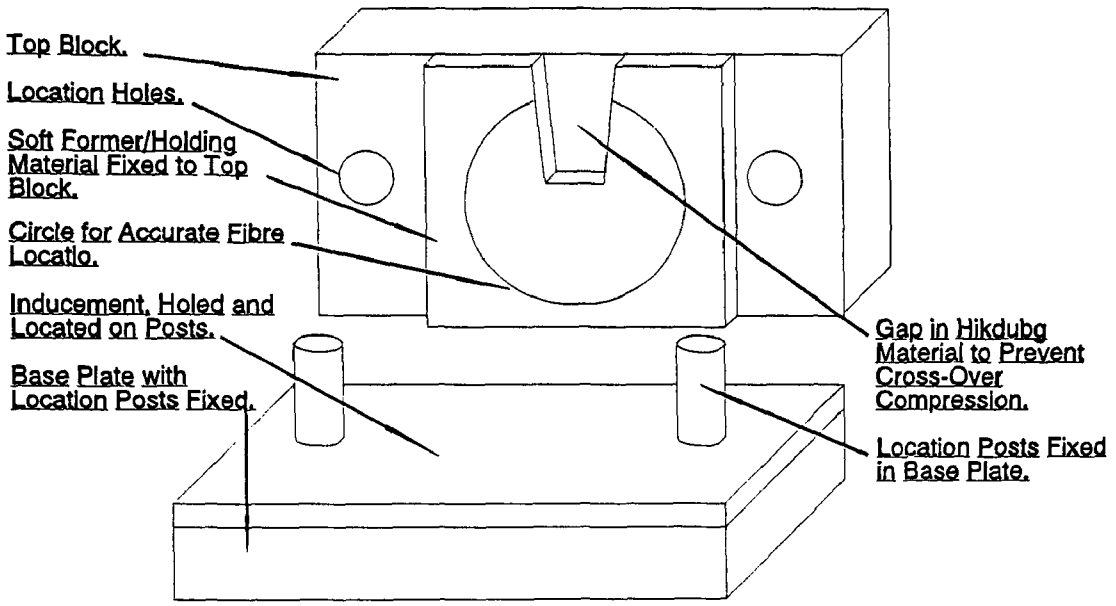

Figure 6.4 Final Microbend Test Design for use with a Fibre Circle.

accurate fit on the reference posts is achieved, without inducing undesirable friction which would Otherwise hold the mesh off the test fibre. The mesh is marked, so that the same orientation on the reference posts is achieved during every test. The grade of mesh is critical and the nature of the loss modes induced are a function of the interaction between it and the holding material. The selection of the type of mesh is discussed in Chapter 7.

The loop of fibre fixed onto the soft former, (discussed below), is presented with a set of perturbations as consistent as could be achieved with the equipment. The loop, as described below allowed a wide spectrum of perturbation frequencies which was intended to yield equal attenuation across the whole spectrum of interest.

iii) the soft former,

The soft former is fixed to the top block. As stated above, its purpose is to induce the fibre to follow the perturbation pattern of the wire mesh. The material of the former was a compromise between hardness, which would prevent the fibre from retreating into it rather

than following the contours of the mesh; and softness which would push the fibre into the contours of the mesh rather than simply crushing it against the high points of the mesh. Fig 6.4, shows a circle drawn on to the surface of the former. The circle is marked in pencil and gives the location of the fibre to be tested. Because the former is fixed to the top bock which locates on the reference posts of the base plate, any fibre lying around the circle, will have an identical position relative to all other layers of the test. This will serve to improve the repeatability of the microbend test, and enhance the test's credibility.

It was essential that the former was perfectly flat so that the fibre could not retreat from the mesh into it. The pencil circle provided a way of marking the former which would not damage its flat surface or alter its mechanical properties in any way. The flat, undamaged surface requirement of the former, meant that any test fibre had to be fixed to it, rather than using locating points on the surface. The method selected to hold the fibre under test in position around the circumference of the circle was tape. It was found that if a maximum of three pieces of tape, not more than 3 mm. wide were used, the attenuation measured in the test fibre during testing was not affected. The method was therefore to place the fibre on the drawn pencil loop and then fix it in place with a maximum of three pieces of tape.

The reason for using a loop of fibre, was primarily to overcome the problem of perturbation frequencies. As described in 6.3, a full spectrum of spatial perturbation frequencies is required if attenuation is to occur equally across the whole electromagnetic transmission spectrum. Mesh tests have traditionally been rejected on the basis of only being able to induce a single perturbation frequency when a fibre was laid straight across them. The circle of fibre has several advantages. The circle ensures that rather than only one spatial perturbation frequency, the fibre will experience a wide range of frequencies because it encounters the mesh at all possible angles of intercept. The result is to cause the mesh to constantly alter its perturbation frequency, ensuring the fibre experiences as broad a range of frequencies as possible.

The circle ensures that the directional inconsistencies normally associated with mesh test, (and discussed in 6.3), are eliminated, because the circle obviously has no dominant direction. From Fig 6.4, it can be seen that a section of the former has been cut away. The purpose of this is to prevent the test fibre cross over point, (which must occur when a loop of fibre is used), from being compressed by the test. Were the cut out not included, a spurious mode of loss would be induced, thus reducing the integrity of the results. The width of the cut away was chosen with consideration for two criteria. The first was that were it too large, the compression pattern of the mesh on the rest of the fibre under test would be altered. The second was that were it too small, when the fibre was bent back to bring it out of the test along the channel created by the cut out, the macrobend effect would be induced, again affecting the results.

The cut out, apart from preventing spurious loss modes from being induced in the region of the fibre cross over, held a number of advantages. The first was that it allowed the fibre to be placed at the centre of the test with no apparent alteration in results. This fact meant that the edge effects normally associated with a fibre at the edges of a compression microbend test where conditions are different to those experienced at the centre were avoided.

iv) a top block:

The top block as shown in Fig 6.4., has two holes drilled in it. These allow repeatable placement of the compressive force with respect to the rest of the test, and in particular to the fibre under test. The hole size was chosen so that good repeatability is achieved with minimum levels of friction being induced. It was essential that the holes be large enough to allow the block to move freely without the need for external lubrication. A lubricant would constitute an unwanted variable in the test which, as its level changed, would cause the effective compressive force applied by the top block to alter. The orientation of the mass was always the same on the test to further enhance the repeatability of the test.

The top block constituted the first force to be applied to the test with additional masses subsequently being added to the centre of the top of the block. The centre of the block was marked and each additional mass, like the top block itself was lowered as gently as possible onto the test to prevent spurious loss modes or damage to the fibre under test being induced. While, as was stated in 6.3, the actual amount of force applied to the fibre itself due to the spreading ability of the mesh and holding material, this was not a problem. With a fibre repeatably positioned with respect to the test, it is reasonable to expect that an amount of force applied through the top block will always induce a certain amount of compression in a fibre. For this reason, the amount of force applied to a fibre becomes academic and the investigation focuses upon finding the force which must be applied to the top block to induce the correct amount of microbending attenuation.

Examination of the requirements for the microbend test as detailed in 7.3, reflect well upon the solution presented here. the repeatability of the microbend test from the perspective of both the consistency of results, (due to the highly accurate positioning of components), and eliminating damage of fibres under test has been attained. The loop of fibre ensures that a broad spectrum of perturbation spatial frequencies will be attained, that all fibres will see the same spectrum, and that no spurious loss modes will be induced.

A pilot study, which is the subject of Chapter 7, was carried out to measure the performance of the microbend test against its objectives, before embarking on a full scale study of the performance of fibres within cables.

CHAPTER 7.0.

Pilot Study.

7.1 Introduction

On completion of the design and construction of the microbend test equipment, (as described in Chapter 6), a pilot study was carried out to assess the success with which the stated criteria and objectives had been met. Chapter 7 details the methodology of the pilot study and the results obtained. The objectives of the pilot study were to:

i) validate the microbend test which had been developed,

ii) give an indication of the performance and resilience of various fibre and coating types using the test,

iii) assess the feasibility of modelling fibre test performances mathematically,

At the conclusion of the pilot study, the results and methods used to validate the test were presented in the form of a technical paper at the 1989 International Wire and Cable Symposium, (IWCS), in Atlanta, Georgia, (Appendix A).

7.2 Initial Evaluation

Preliminary trials using the newly constructed microbend test, showed that the results obtained from test fibres varied greatly depending upon the wire mesh and holding material chosen. It was therefore decided that in order to optimise the results the microbend test was capable of producing, careful selection of mesh and holding material would have to be made. To this end, various wire meshes and

holding materials were made available, with the intention of selecting the optimum combination during the pilot study.

Two meshes known to be non-destructive to test fibres, which produced differing test results were chosen. One was chosen because it was considered a "safe" mesh in as much that it was unlikely to induce spurious loss modes. This mesh came to be known as the "smooth mesh". The second mesh chosen was more rough to provide a comparison for the results produced using the smooth mesh. This mesh came to be known as the "rough mesh". It produced results which lay closer to the boundary of the microbend/macrobend dividing line.

The specifications of the meshes chosen were:

i) smooth mesh: 70 mesh; smooth drawn wire; $\varnothing_{wire} = 0.18$ mm,

ii) rough mesh: 20 mesh; smooth drawn wire; $\varnothing_{wire} = 0.44$ mm.

The holding materials, (soft formers), were chosen specifically for use with the meshes described above and were intended, given the meshes in use, to ensure that no spurious modes of loss were induced during testing. The holding materials were also chosen, as described in 6.4, for their ability to force the fibres onto the meshes and induce microbending without causing any mechanical damage.

The two choices for holding material finally made were:

i) vulcanised rubber: thickness = 4 mm; Shore A Hardness = 73-75,

ii) paper card: thickness = 0.75 mm.

Each test variation therefore contained a mesh and a holding material, and each test was carried out at both 1550 and 1300 nm. Each individual fibre was thus tested on four test variations, with each test being carried out at two wavelengths.

The final design chosen for the circle drawn on the holding material is shown in Fig 6.4. The diameter of the circle used was:

$\varnothing = 98.50$ mm.

the circumference of the circle used was therefore:

$c_c = 306.30$ mm.

thus, with the cut away, the length of fibre tested was:

$l = 225.00$ mm.

The circumference was chosen so that macrobending was not induced in the plane perpendicular to the circle axis, and it was ensured that the circle was placed centrally on the test to prevent edge effects producing any spurious loss modes.

Having defined the mechanical characteristics of the test, the remaining factors to be determined were the forces to be applied to induce microbending, and the method of data handling.

The force applied by the top block was 30 N. This was taken as the first level of applied force and was followed by incremental increases in force of 10 N. up to a total of 70 N. One set of readings

would therefore be made up of the attenuations produced by forces of 30, 40, 50, 60, and 70 N. Five sets of readings were collected for each holding material/mesh combination giving a total of twenty five data values. The test was carried out at 1300 and 1550 nm. giving the total number of data points for all four combinations of holding material and mesh including both wavelengths as 200. The concept of the data system and the method of collecting data is explained fully in Appendix B.

Spreadsheets were used to store the data collected, and an excerpt from the spreadsheet relating to the 1550 nm. results from fibres on the rough mesh and rubber test is shown in Appendix C, along with the manipulative programming involved. Eight spreadsheets were used to store the data by test variation and light wavelength. It was necessary to split the results up to this degree because of the volume of data involved.

Once in spreadsheet format, it became a simple matter utilising the organisational power of the spreadsheets, to retrieve any number of fibre records as required, total the results as detailed in Appendix B[1], find average values and plot results such as those shown in Appendix C and Figs. 7.1-7.4.

7.3 Validation of the Microbend Test.

The validation of the test involved comparing the capabilities of the new microbend test with the criteria which had been defined at the start of the work. Three criteria were applied to the test, which was required to fulfil all of them. The criteria were:

i) the microbend test must be highly repeatable,

---

[1] Appendix B gives full details of the handling of test data and shows how it was used to produce performance graphs.

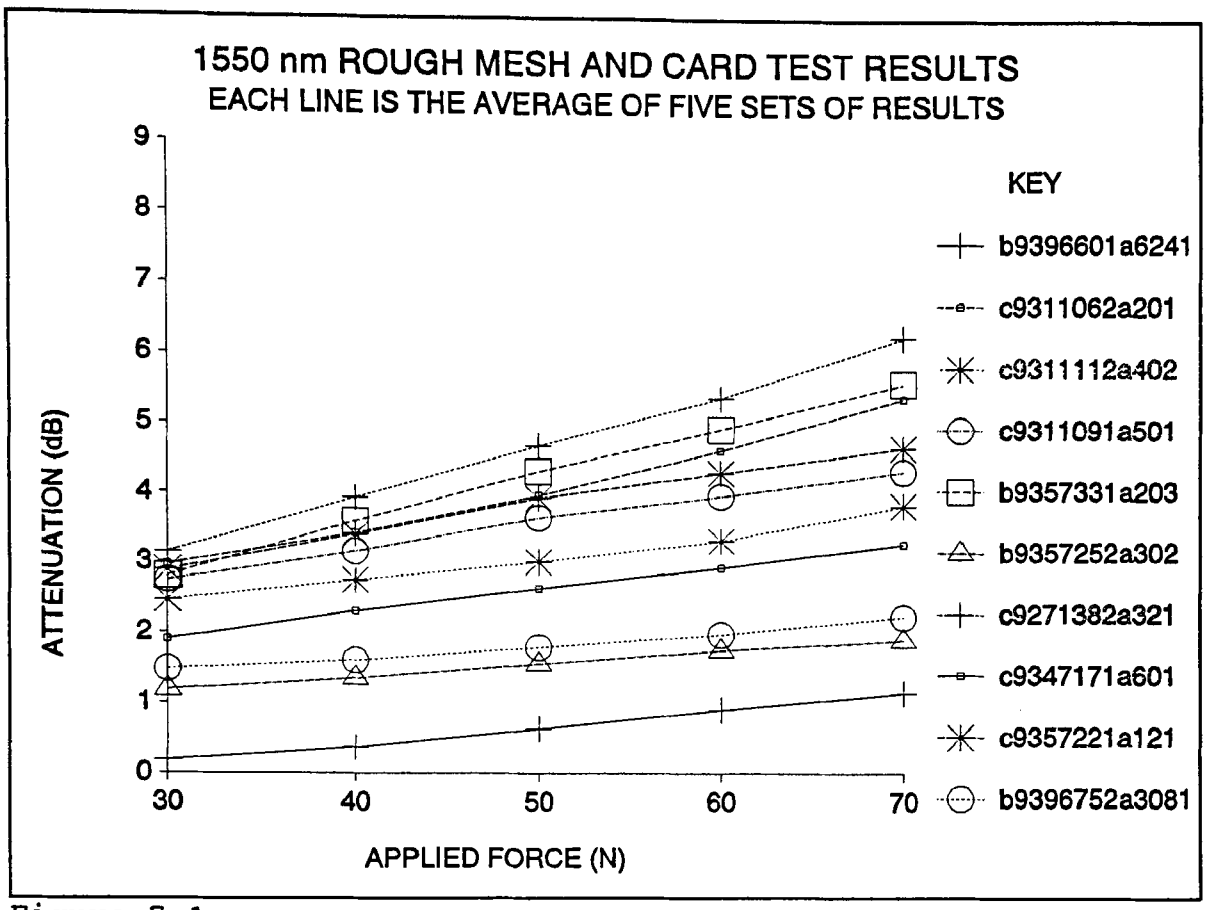

Figure 7.1

ii) the spatial frequencies of axial perturbations induced must cover a broad spectrum,

iii) the test must induce microbending as the sole mode of signal attenuation.

These criteria were discussed in detail in section 5.3. In 5.3 however, four criteria were given; the fourth being that the test should be completely non-destructive. This is now taken to be included in the criteria for high repeatability. Clearly, were the test causing mechanical damage to the fibres under test, the results produced would not be repeatable.

The repeatability, (and also non-destructiveness), of the four available test variations was assessed using standard fibre test procedure. As discussed in Appendix B, a normal fibre test involves taking five sets of measurements, ie. five individual measurements at each of the five applied forces, and taking each mean value to be the performance at that value of applied force. In order to assess

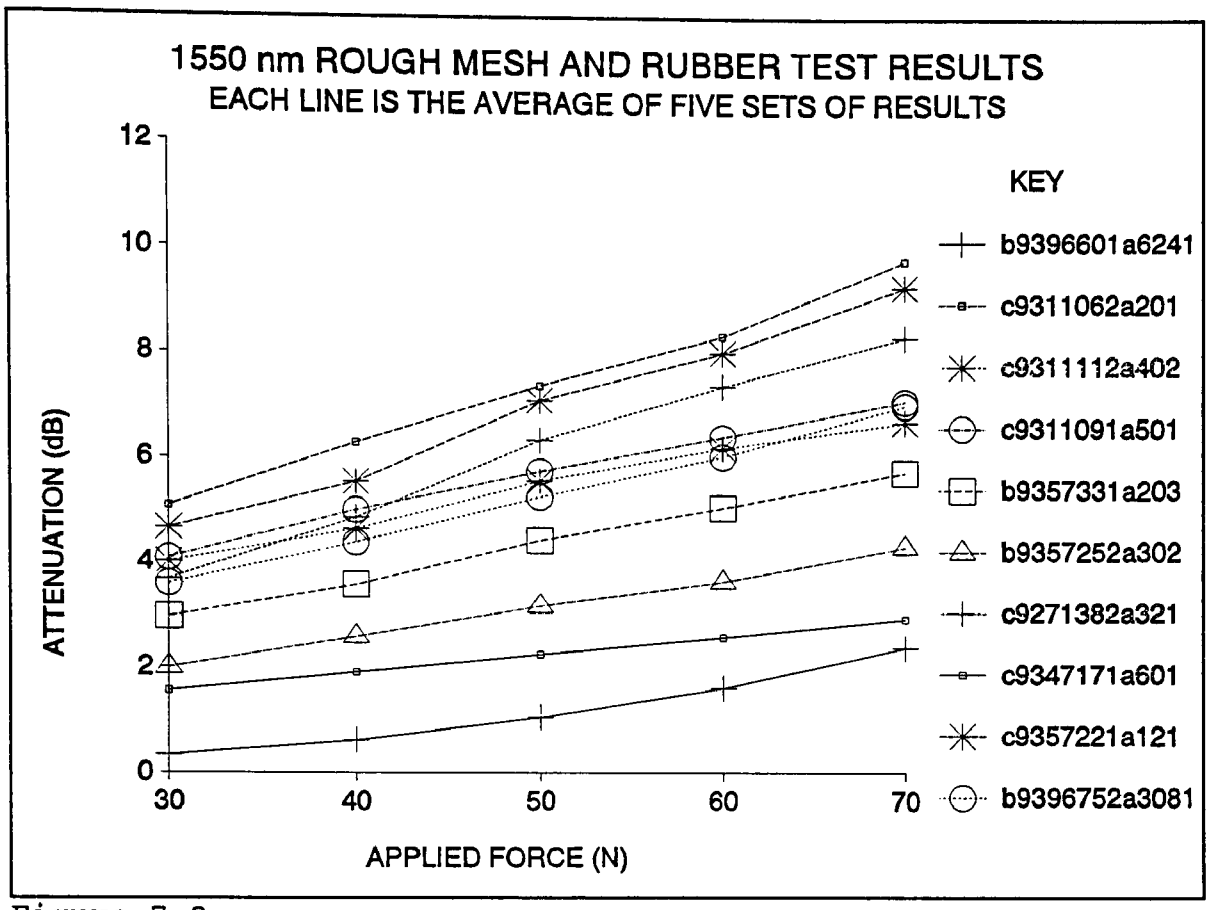

Figure 7.2

repeatability and non destructiveness of the test, a tolerance was placed around the mean value at each applied force and the scatter of measurements throughout the tolerance range observed. Graphs displaying scatter of measurement throughout the tolerance range were produced for several fibres on each test variation, (Fig 7.5 is an example of one such graph displaying the five performance lines produced by a fibre of the rough mesh and card test at the 1550 nm wavelength). Examination of these graphs revealed the "normal" repeatability performance of each variation, and the merits of each variation's performance was then assessed from these representative graphs. Each of the graphs was examined to ensure that no trends in results existed between successive measurement sets. A gradually increasing set of attenuations would suggest for example, that mechanical damage or deterioration of the test fibre had occurred and that the test was therefore unacceptable. In this way therefore, both the repeatability and non-destructiveness of the microbend test variations were assessed using the same sets of performance graphs.

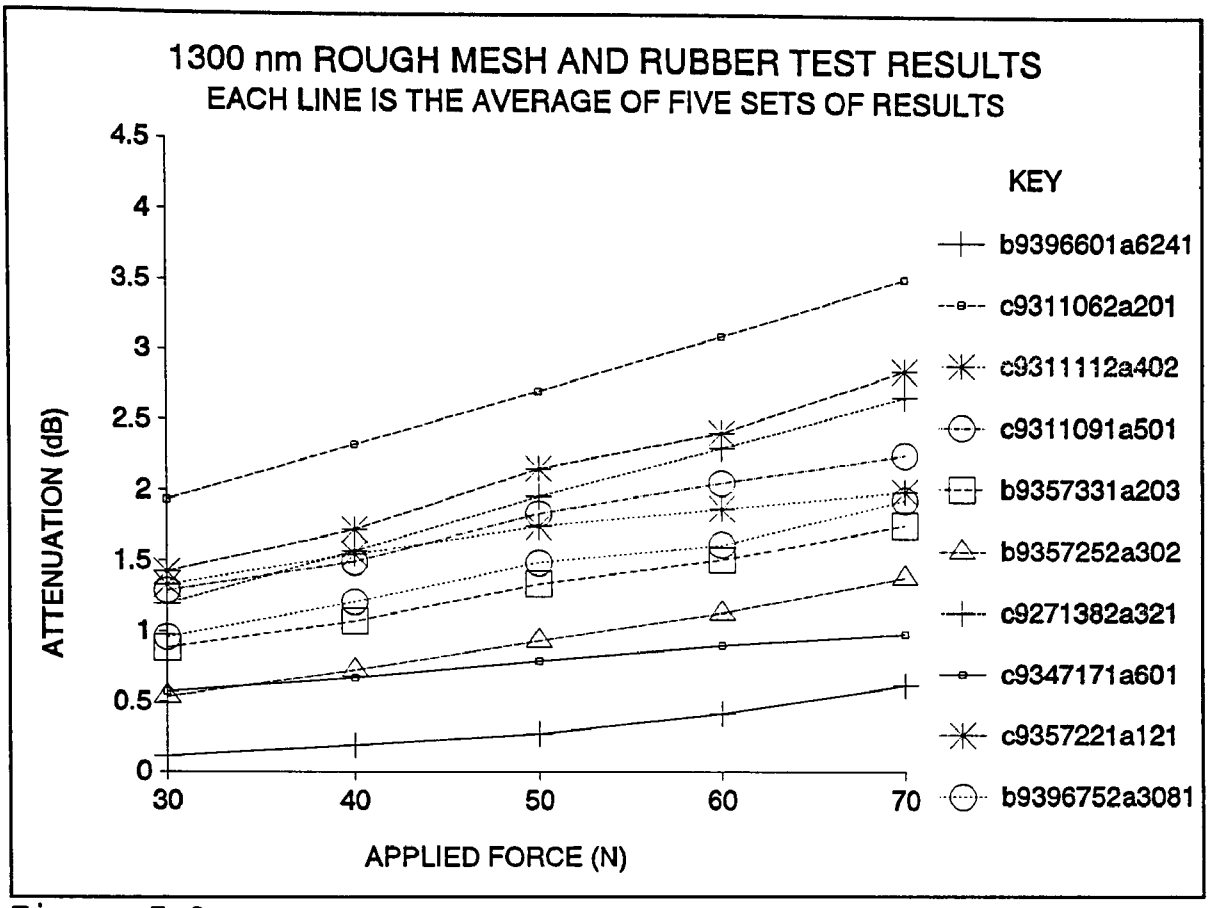

Figure 7.3

The distribution of the perturbation spatial frequencies was assessed using the spectral analysis approach. As discussed above, if the spatial frequencies of the perturbations induced by the microbend test favoured any particular value, then where the wavelength of the light caused co-incidence with the beat length of the signal within the fibre, excessive loss would result at the corresponding wavelength. By examining the spectral traces produced by the test variations, it would become clear whether the perturbations were scattered over a wide or narrow spectrum. A smooth trace would indicate an "optimal"result where perfect distribution of perturbations had been achieved, while a single peak in attenuation would indicate only one frequency of perturbation would be expected for microbend tests which favoured straight pieces of fibre. It would be expected that the actual results would fall between these two extremes, with periodic emphasis on particular wavelengths. If the oscillations produced by the test in sample fibre's attenuation traces were judged to be acceptable, they would be taken as normal for a "real" system where compromises between theory and reality

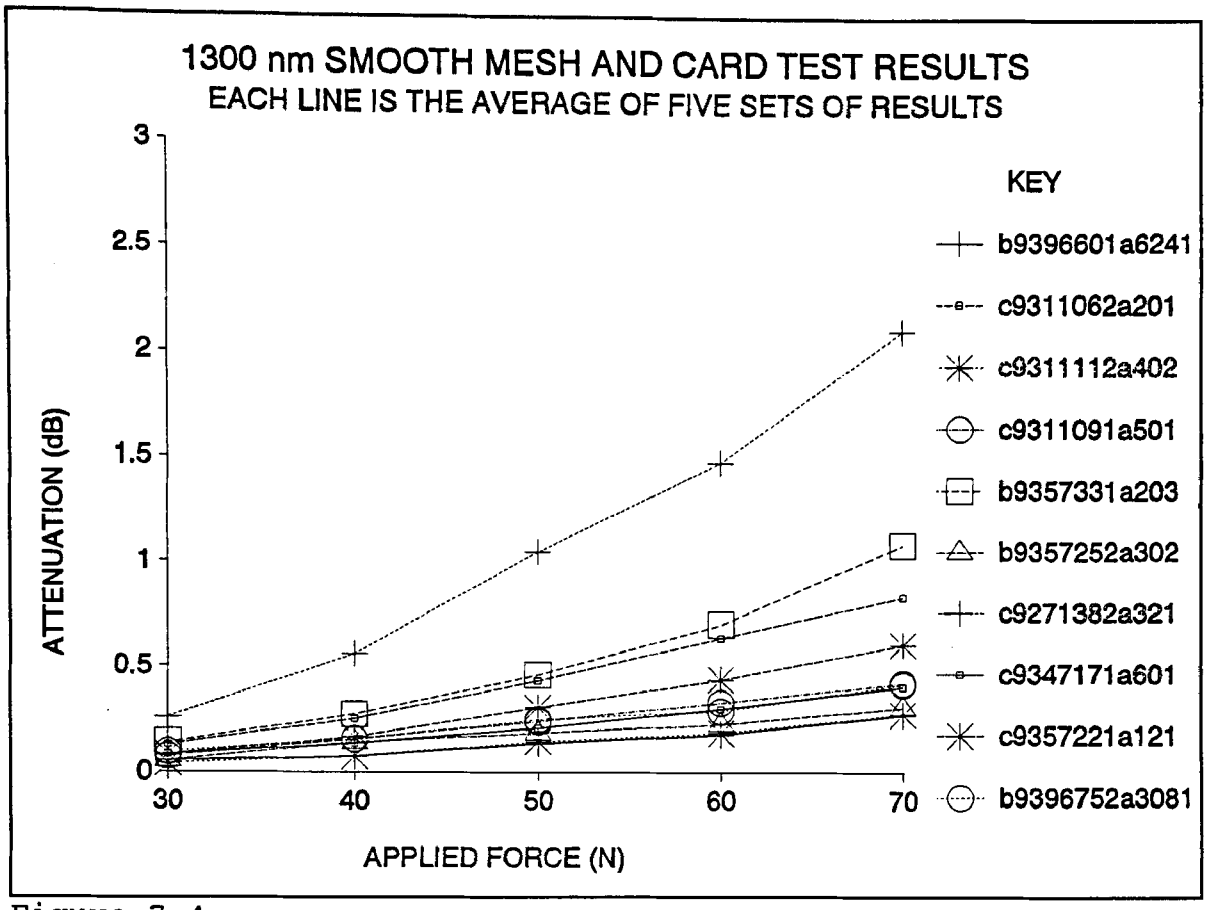

Figure 7.4

have to be made.

The purity of the modes of loss induced by the microbend test were assessed according to the various incorrect types of modes the test was also capable of inducing. It was found that if a mesh which was too smooth was selected, that is one which would produce the least drastic perturbations in the test fibre, the test would produce a compression rather than a microbend effect. This was easily detected because the loads required in a compression test to induce significant attenuation are much greater than those required on a microbend test. Therefore, if the mesh were too smooth for the purpose of microbend induction, the attenuation observed on the test would drop dramatically.

If a mesh were too rough, the effect on the test fibres would vary from macrobend modes of loss in less severe cases to actual mechanical damage of the fibre in more severe ones. While the implications

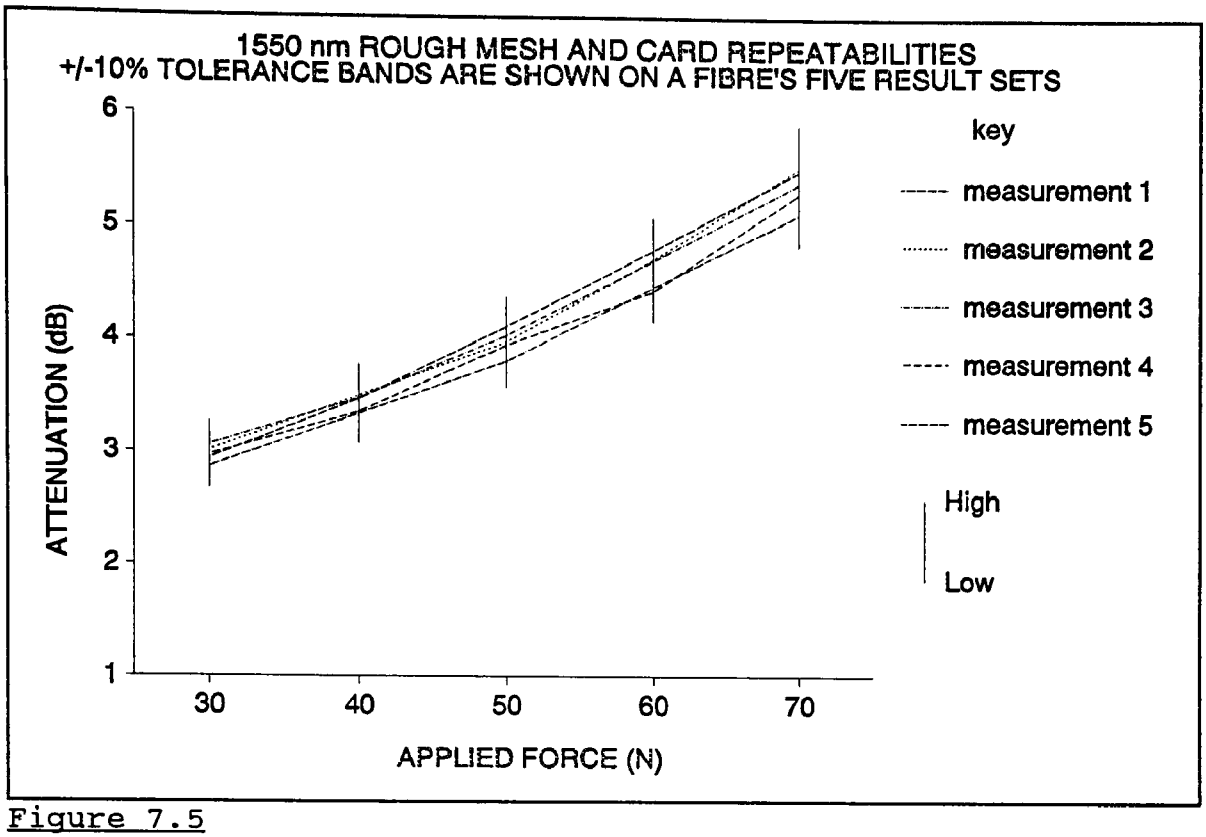

Figure 7.5

of choosing a mesh which was at the more severe end of the spectrum were significant, a bad choice could be easily detected and therefore the problem could be avoided. Meshes which were so rough that they physically damaged a fibre could be identified from a gradually deteriorating, or highly non repeatable set of results on the microbend test. In the worst cases, the fibre would fail and no signal would be received at all from the test.

Meshes which were too smooth, or too rough that they damaged the fibre could therefore be easily detected. The only remaining incorrect mode of loss which the microbending test was capable of inducing was macrobending. The method chosen to identify meshes coarse enough to induce macrobending but still not so severe as to induce damage in the fibre, relied on spectral attenuations. A general and coarse approximation for bend induced loss modes, is that in a system where the loss mechanism is either macro or microbending, if a spectral scan of attenuation were carried out, one of two conditions could apply:

i) if the incremental change in attenuation observed at 1550 nm was greater than twice that at 1300 nm, then the dominant mode of loss would be macrobending,

ii) if attenuation at 1550 nm was less than or equal to the attenuation at 1300 nm, then the dominant mode of loss would be microbending.

Given the criteria and the methods of assessing the test, validation trials were carried out. These are described in the following sections.

7.3.1 Repeatability of the Microbend Test.

As described above, repeatability was tested by examining the scatter of individual results about their mean value and tolerance limits applied about the mean. Repeatability was first examined using graphs such as that shown in Fig 7.5. Here, the average produced by the five sets of data was used to produce tolerances, (shown in the graphs), and the position within these tolerance limits of the five sets of data was then displayed. A "perfect", performance by the microbend test would mean that at each of the five applied forces, one point from each of the samples, five points in all, would appear superimposed on their mean value.

Examples of repeatability graphs for all test variations, at both the 1550 and 1300 nm transmission wavelengths are shown below, along with a full analysis of the repeatability results.

Figs 7.5 and 7.6, show typical results from the rough mesh and card test at the 1300 and 1550 nm wavelengths. It was found that repeatability on this test was consistently high, with all five readings at each applied force falling well within the $\pm 10\%$ limits imposed by the figures shown. Clearly the average attenuations given at all applied forces were equally representative of fibre performance. 1300 nm wavelength results on the rough mesh and card test were often more highly correlated about the

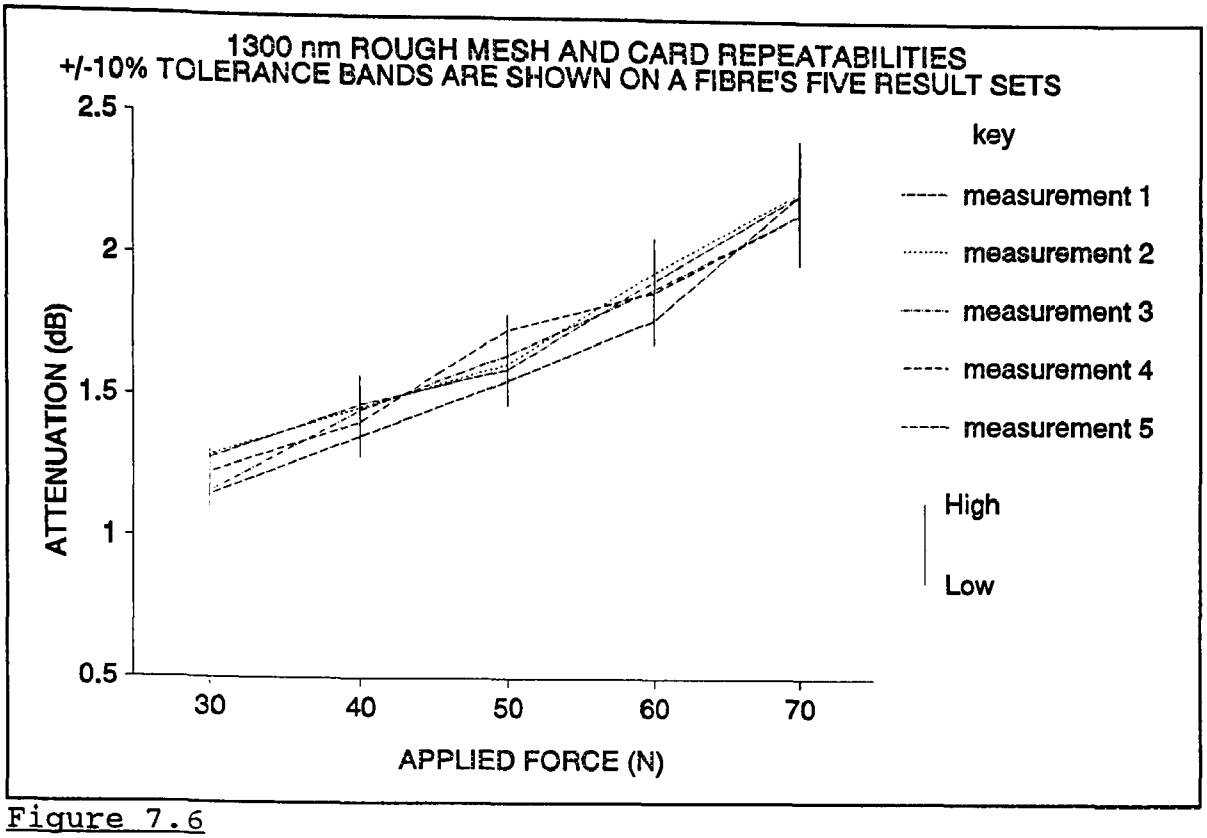

Figure 7.6

mean value than the 1550 nm ones, suggesting that at 1550 nm, slight variations in test conditions became more significant than at 1300 nm. The 1300 nm results were therefore more likely to give consistent results, while 1550 nm results would give a greater spread while indicating more precisely the microbend susceptibility performance of fibres.

The greater susceptibility of fibres to minor variations in test conditions at 1550 nm was to be expected. The mode field diameter of the light in the fibre at the higher wavelength was much greater than at 1300 nm. A larger mode field diameter increases the percentage of the light signal carried outside the fibre core. A greater percentage of light outside the core, allows the critical point at which light begins to escape from the fibre is more easily attained. A less severe perturbation will be capable of causing light to escape, thus rendering a fibre carrying 1550 nm light more susceptible to microbending than one carrying 1300 nm light.

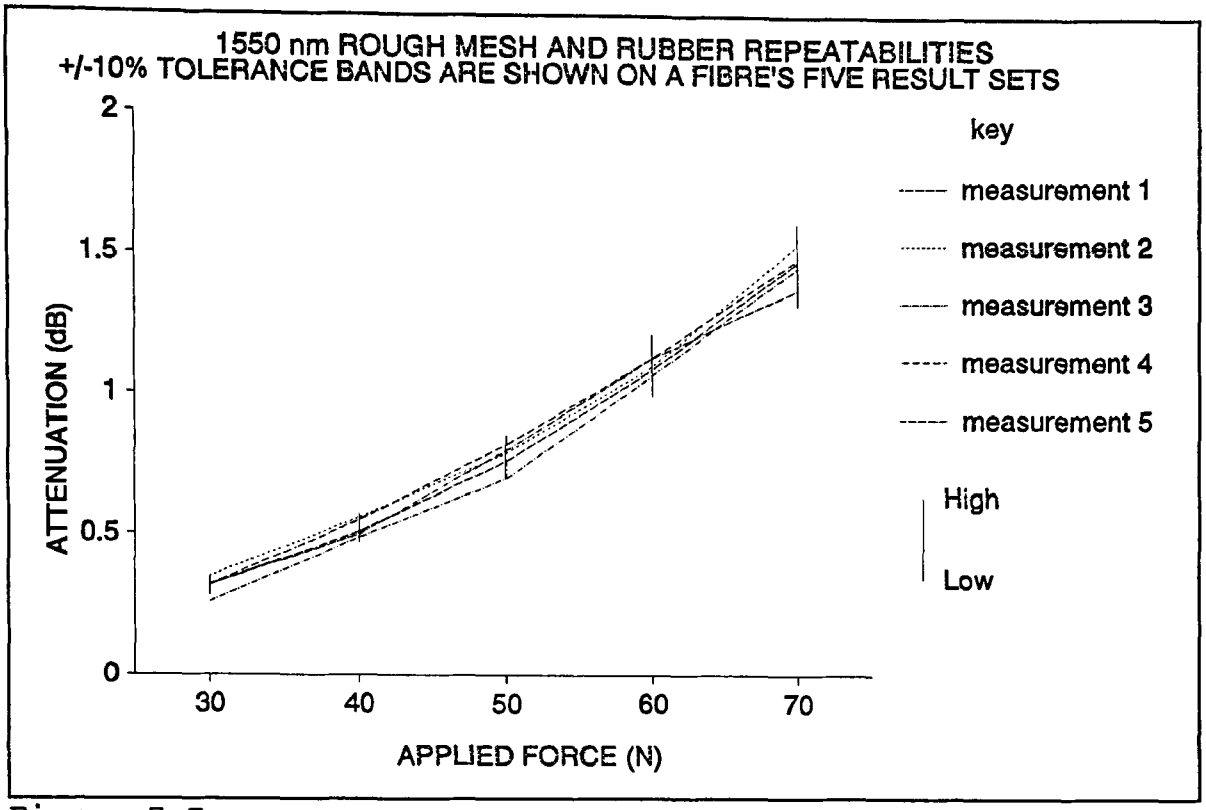

Figure 7.7

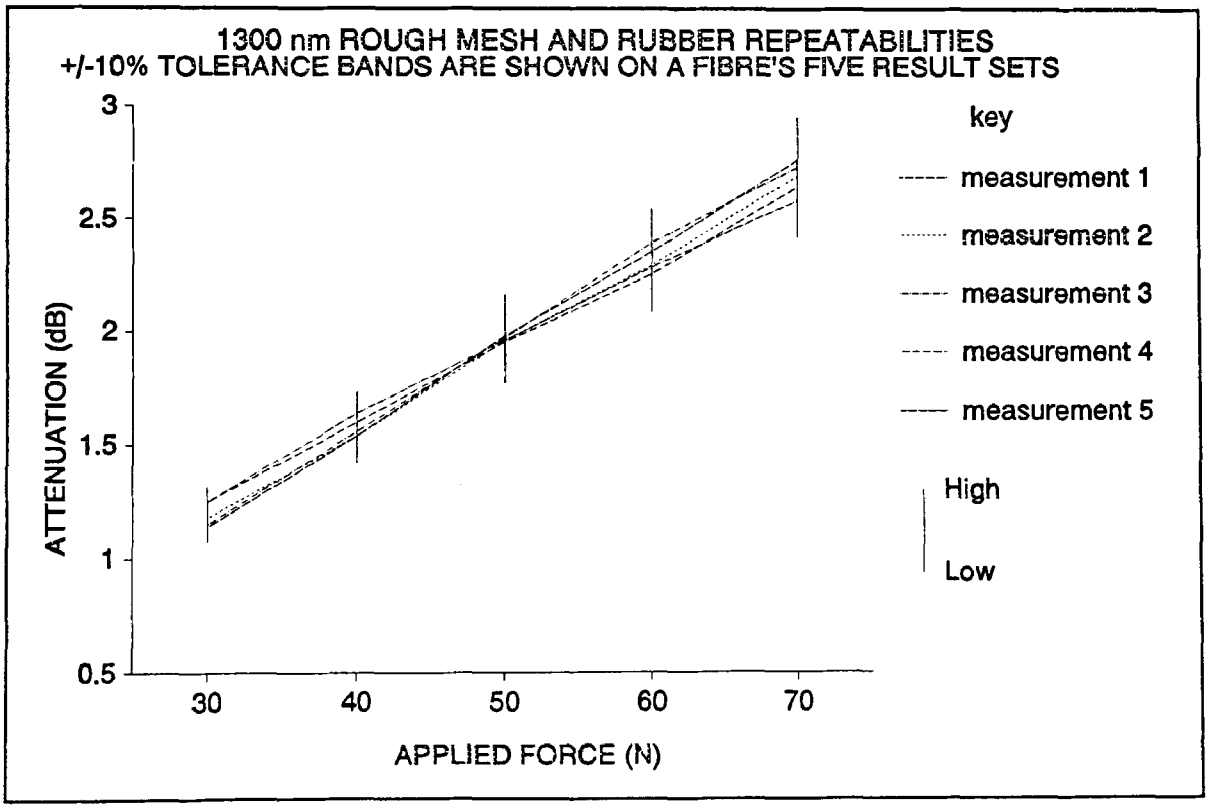

Figure 7.8

Figs 7.7 and 7.8, show the repeatability performance of the rough mesh and rubber test on a representative sample of test fibres at 1550 and 1300 nm. It is clear that the spread of the data is less consistent than had previously been observed with the rough mesh and card test. This suggested that the test was showing more susceptibility to minor variations in conditions which again might have pointed towards microbend modes of loss. On the rough mesh and rubber test, it was more common than on the rough mesh and card test to observe a reading which fell outside of the $\pm 10\%$ tolerances. This effect was most common amongst fibres with low attenuation values and the lower levels of applied force. This suggested that while the qualities of the mesh and holding material used affected the repeatability of measurements, another important factor was the level of attenuation induced. The noise induced by the measurement equipment must have been of a level which hampered accurate measurement of induced attenuation levels. A constant level of noise would be proportionally more significant with respect to lower signal levels than to high level ones. Higher level signals would therefore have proportionally wider tolerances with respect to noise levels reducing the significance and effects of the noise; while at low signal levels, noise would induce wide variations in measurement or even no measurements at all.

The smooth mesh and rubber test repeatability graphs, (Figs 7.9 and 7.10), show the greater scatter common amongst test variations inducing lower values of attenuation. The smooth mesh and rubber variation shows a change from test behaviour as observed above: the 1550 nm wavelength results appear to give a higher repeatability than their 1300 nm counterparts. In order to show the greater spread of results produced by a lower attenuation inducing test, it was necessary to increase the tolerance limits of the figures to $\pm 25\%$. Examination of the results within the wider tolerance bands show the effect of noise on the signal levels measured. The 25% tolerance limits appear to contain most of the measurement points at the 1550 nm wavelength. At the 1300 nm wavelength however, particularly the results at the lower applied force end, readings fall inside the base noise levels and are effectively lost. The severity of the problem is demonstrated by the fact that the higher applied

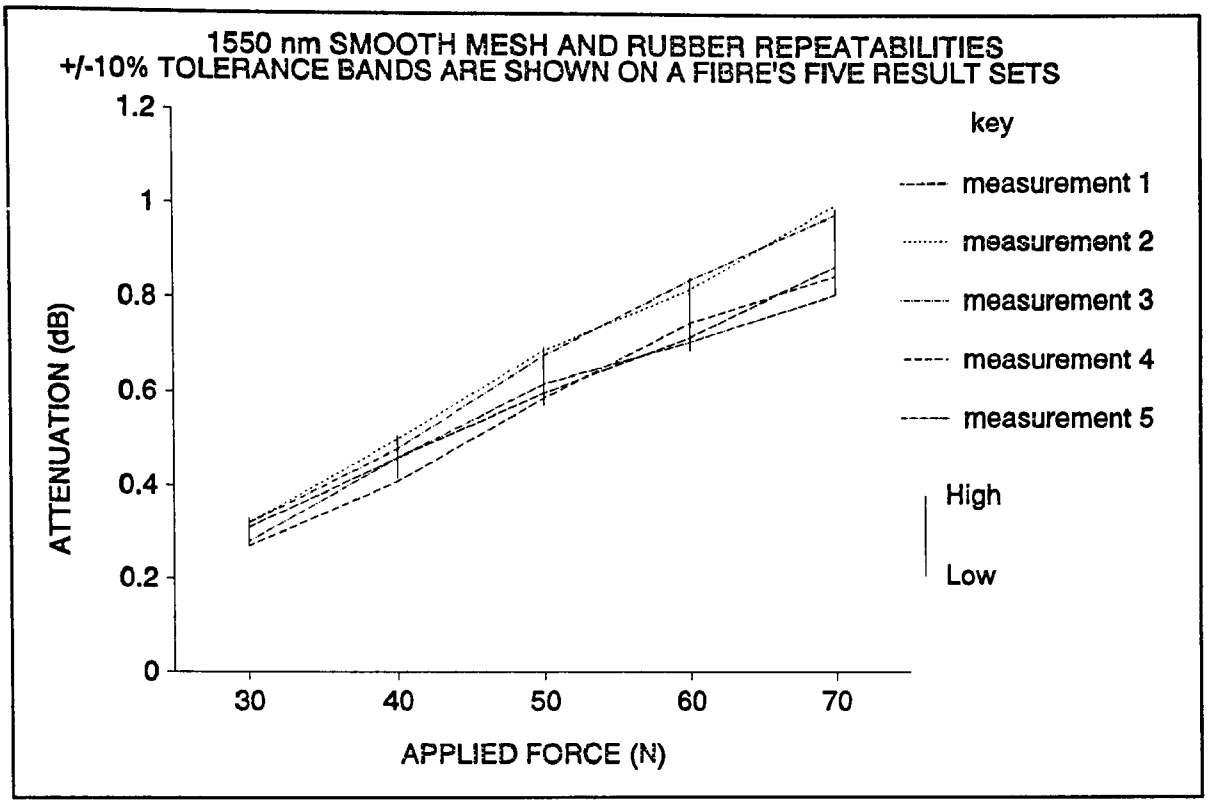

Figure 7.9

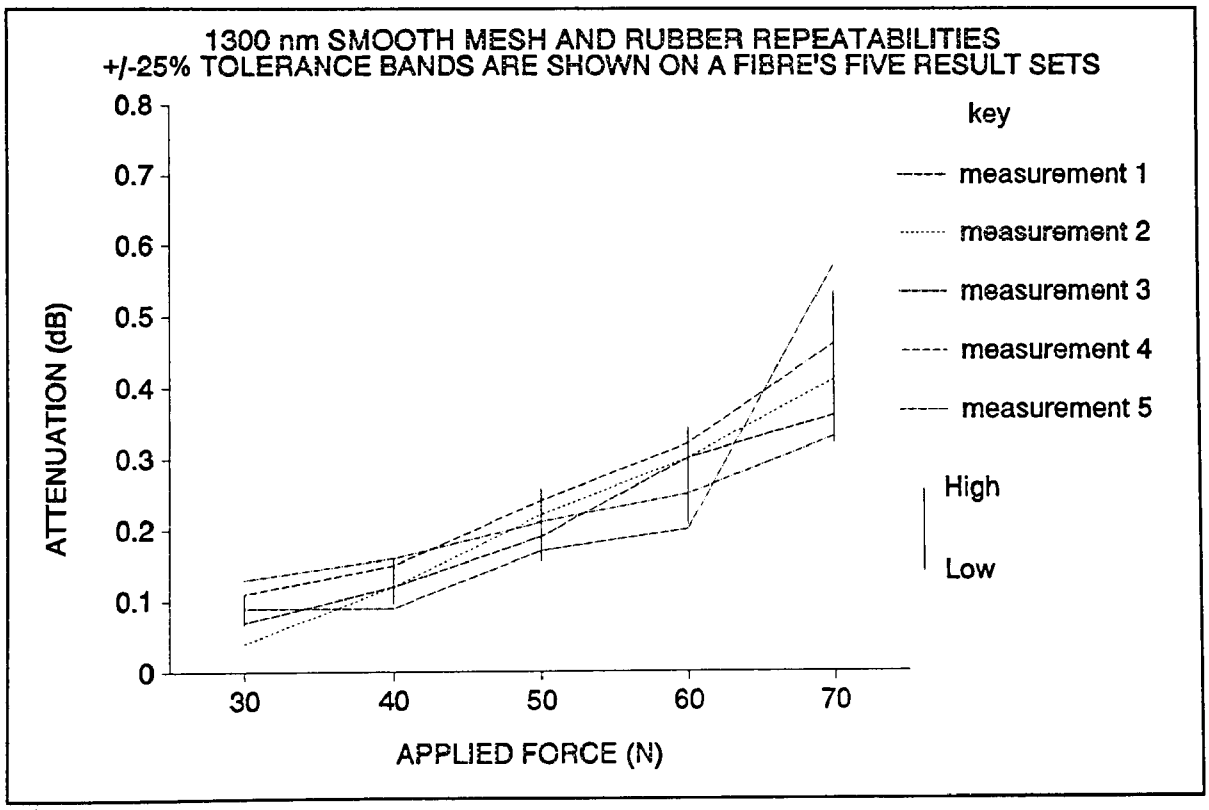

Figure 7.10

forces should include a considerably larger accumulated measurement error due to the method of data handling, (explained in Appendix B), than the smaller applied forces. (The lower force results, unlike the larger ones are not the sum of several results and therefore should have a smaller accumulated error.) The smaller force results show a greater degree of scatter than the larger applied force attenuations. It can therefore be deduced that the potential repeatability of the microbend test produced is hampered by the measurement equipment used. Were equipment of a better quality available, repeatability results could be greatly enhanced.

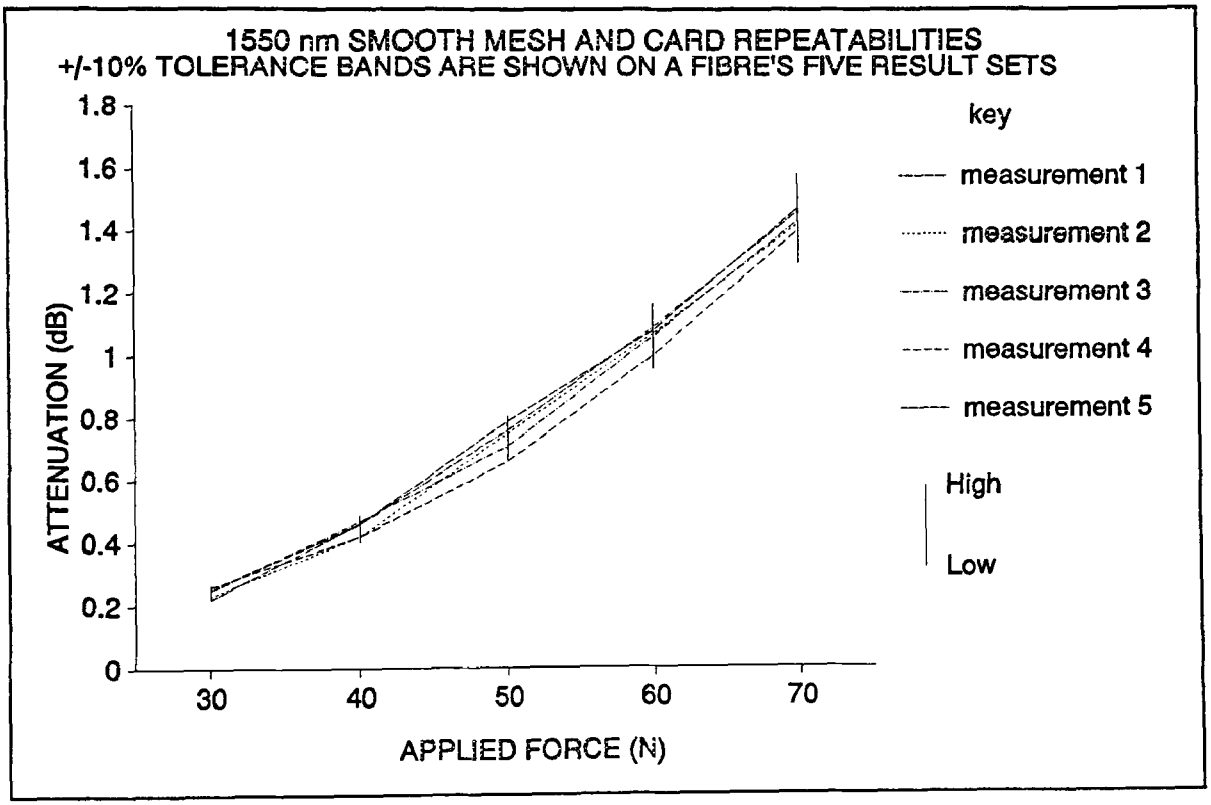

Figure 7.11

Figs 7.11 and 7.12, show the repeatability results from the smooth mesh and card test variation. The repeatability of the 1550 nm wavelength results, except at the 30 and 40 N applied force levels, was high enough to allow tolerances of $\pm 10\%$ to be imposed. Clearly the card based tests yielded a high repeatability figure, which deteriorated when the level of induced attenuation dropped below the level of background noise. The graphs produced from readings taken at the 1300 nm wavelength were

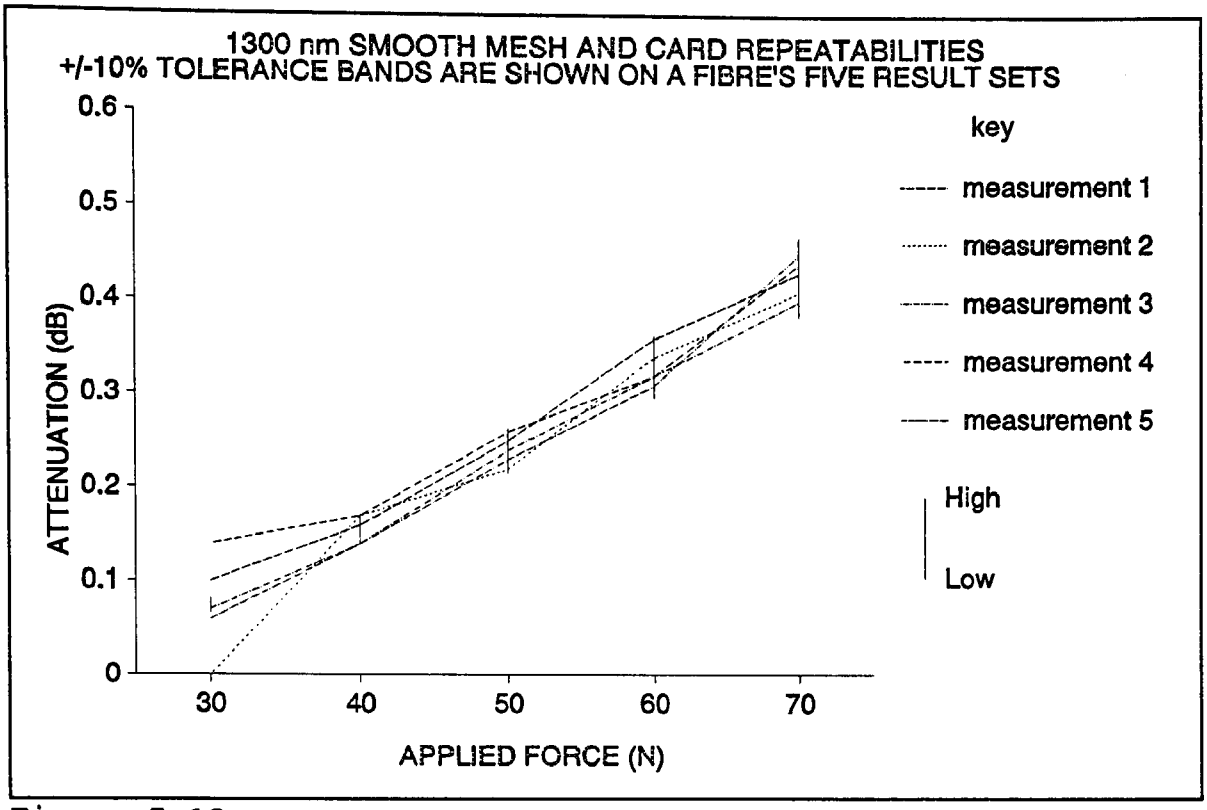

Figure 7.12

small enough to force widening of the tolerances to ±25%.

It had become clear that the level of background noise introduced by the measurement equipment was of the order of 0.1-0.2 dB. Thus any result which had an increment between adjacent readings or an absolute value of 0.2 dB or less should be discarded or examined closely on the grounds that measurement noise could have induced it. This conclusion is borne out by Figs 7.1-7.4. The lines in each of these graphs is a plot of results taken from a single sample fibre. The lines are the average of five individual sets of results.It can be seen that the rough mesh and card results show mainly steady increases in attenuation with only occasional slight variations in line gradient. The 1300 nm wavelength average results lines showed less stability and more gradient changes than their 1550 nm rough mesh and card equivalents. The absolute attenuations involved as well as the increments, were smaller than at 1550 nm, and while the results could be expected to all fall within ±10% of the average values represented as lines here, it was clear that the 1550 nm results were more stable.

While the 1300 nm results were known to be less susceptible to test variations than the 1550 nm results, the background noise was more significant with the lower level attenuations. It can be deduced that background noise is a more significant cause of result inaccuracy and that the quality of the results produced by the test could be greatly improved with a better measurement system.

The smooth mesh and rubber test average results lines' attenuations were much lower than those see with the rough mesh and card test. Results below the 0.1 dB mark show a greater tendency towards reduced stability. It is not unusual to observe *reductions* in average attenuation levels with increasing applied force at these levels. It is very unlikely that negative increments would result from increasing applied force, which suggests strongly that these results are incorrect and are adversely affected by measurement noise. If the errors induced are due to measurement equipment shortcomings, the cut-off point below which measurements have to be discounted due to excessive background noise levels would be the same for all test variations. For this reason, it has been possible to set a minimum base and incremental induced attenuation level and thus at this stage to highlight tests most likely to be rejected because their readings consistently fall short of the criteria.

The conclusions drawn in this section are summarised in section 7.3.4.

7.3.2 The Spectral Distribution of Induced Perturbation Spatial Frequencies.

Much was made of the loop of fibre design which, in addition to improving repeatability and purity of loss modes, was incorporated into the test to ensure that induced microbend perturbation spatial frequencies covered a wide spectrum. This section seeks to assess the success with which the design achieved this goal. The success of the loop design was tested using spectral plots such as those shown in Figs 7.13 and 7.14.

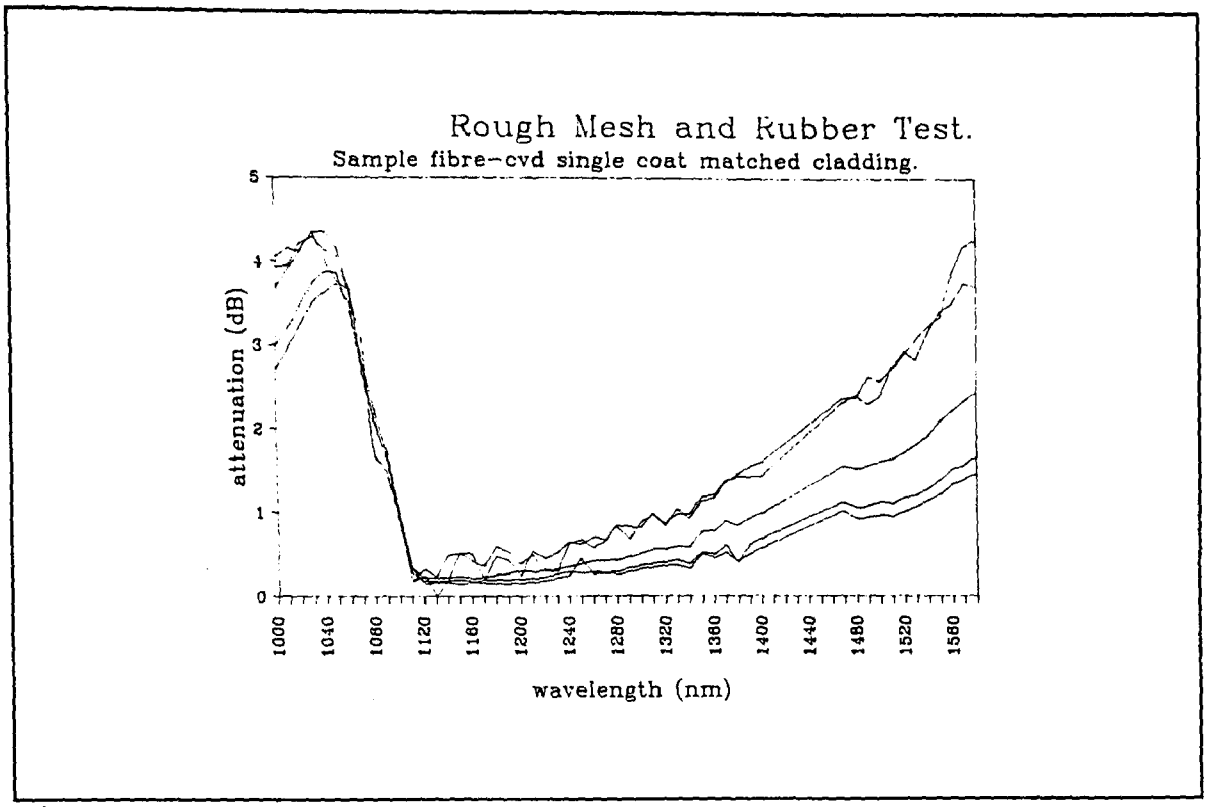

Figure 7.13

Figs 7.13 and 7.14, show the spectral attenuations induced by two of the microbending test variations. Each figure shows the results obtained from a single representative sample fibre with each line indicating the attenuation observed at one applied force. The line representing the lowest levels of attenuation, relates to attenuation induced by an applied force of 30 N, (the lowest level of force), and the line showing the highest levels of attenuation, the greatest value of applied force, (70 N). The results lines between these two extremes, represent the attenuations induced by the remaining applied forces of 40, 50 and 60 N each force representing a higher level of attenuation across the light spectrum.

In the ideal theoretical case, the design would induce all possible frequencies of perturbation thus simulating more accurately the cabled situation. This situation would produce a completely accurate spectral trace line. The practical case could not be expected to achieve this perfect level of

performance, and so each test variation was judged on its ability to perform as close to the ideal case as possible.

Because the mesh has a finite size and therefore the number of interactions between fibre and mesh is limited, all light wavelengths cannot be attenuated equally. It would be assumed that as the fibre's angle to the mesh gradually changed, the perturbation spatial frequency would increment at each interaction. Were a more rough mesh used, the increment between adjacent perturbation spatial frequencies would be larger. Results reflecting this, would show highly attenuated light wavelengths interspersed with large gaps of wavelengths which had been less severely attenuated. A smoother mesh would have a smaller incremental change between adjacent perturbation spatial frequencies and more interactions, effectively yielding a higher resolution when the spectral attenuation traces were measured. The effect would be to reduce the width of the lower attenuated bands of light, theoretically giving an attenuation curve which had a much higher percentage of higher attenuated wavelength bands. Before actual examination of the figures, theory would therefore seem to suggest that a smoother mesh would give a higher density of highly attenuated wavelengths leading to a smoother spectral attenuation curve.

Examination of Figs 7.13 and 7.14, shows that the fibre loop theory is correct. By placing a loop of fibre onto the wire mesh, the fibre interacts with the wire mesh at constantly varying wavelengths inducing perturbations covering a wide spectrum of spatial frequencies. The curves are as expected, with equal attenuation across the whole transmission window. Thus the range of spatial perturbation frequencies is of sufficient breadth to test telecommunication fibres. The large peak at the left hand side of both Figs 7.13 and 7.14, is a water absorption peak which is a feature of silica optical fibres, and which was not removed from the traces by the software of the measuring device.

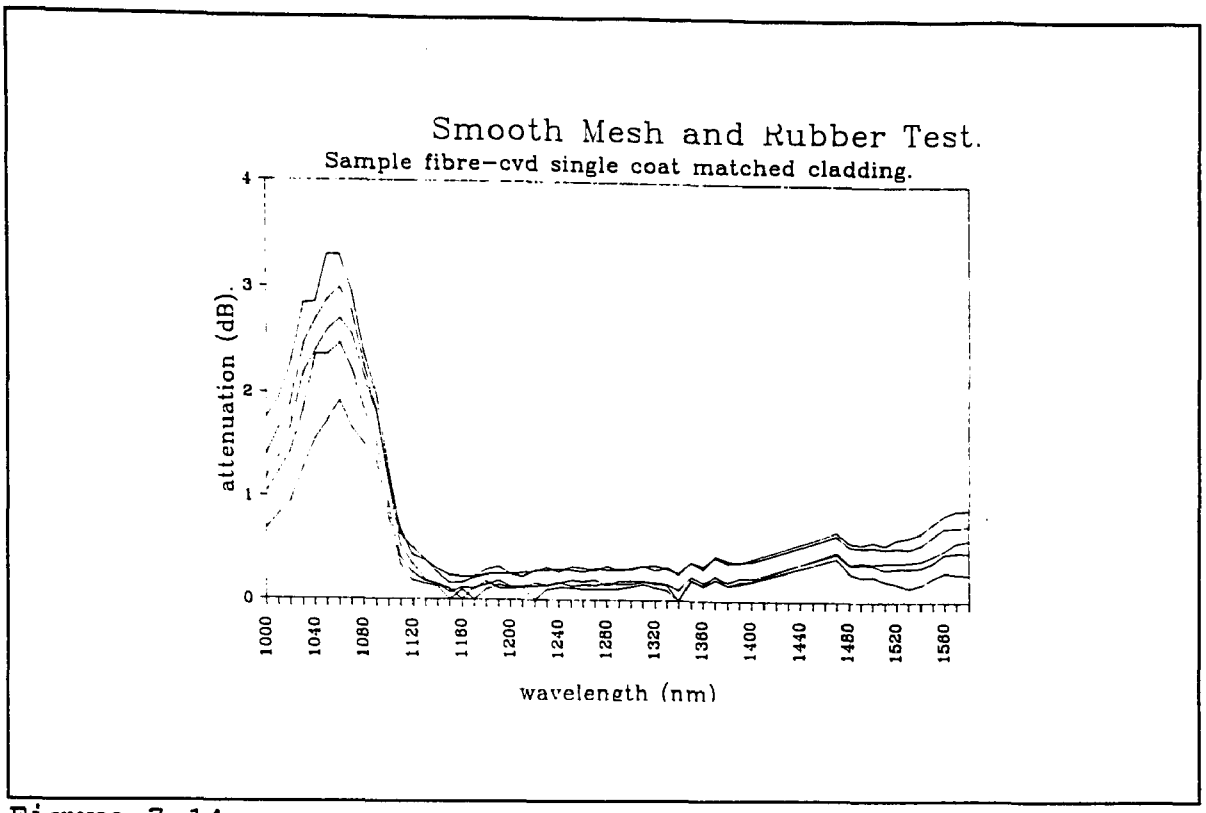

Figure 7.14

Fig 7.13 shows the rough mesh and rubber spectral attenuation trace. While the trend of the graph's lines is a smooth curve, oscillations in results are apparent. The lines, particularly those representing the attenuations from higher applied forces, show periodic raising and lowering of attenuation values. The higher forces of 60 and 70 N, show that the higher values of attenuation-those which are increased as a result of the perturbation spatial frequency in the fibre matching the beat length of the light travelling through it at that point-are interspersed with lower valued attenuations. The rough mesh induces perturbations whose spatial frequencies increment by large amounts which results in wide spaces in the higher attenuated wavelengths of light. It can be seen that the 60 and 70 N attenuation lines, appear to be a high level of attenuation interspersed with points of lower level attenuation. The majority of wavelengths are therefore highly attenuated as required. The lowest applied force, (30 N), line appears to be a set of lower level attenuations interspersed by an occasional higher level one. The significant peak on the 30 N line is the one at 1250 nm. This peak shows the level of attenuation which might have been achieved across the whole spectrum, had all wavelengths

been highly attenuated. Because neither the 40 or 50 N lines show a peak at the 1250 nm wavelength, it can be deduced firstly that the peak was not normal for the test variation or force-that is were the test carried out on other fibres, a peak would not occur at this point; and secondly the high point of the 30 N line which *crosses* the two attenuation lines above it suggests that both the 40 and 50 N lines are also at the lower attenuation level. This theory is borne out by the attenuation patterns when all three low level applied force lines appear to rise and fall together between 1340 and 1380 nm. The lines will, given proper condition perform in a similar manner. The peak at 1250 nm is clearly a rogue result since it is not reflected in any of the lines, and it is reasonable to assume that below applied forces of 60 N, the test induces attenuations of lower levels, while at 60 N and above higher levels of attenuation result.

Observations from Fig 7.13 would seem to suggest that the microbending part of the loss mechanisms present at 60 and 70 N is mainly at the higher level attenuation which, while because of the roughness of the mesh increments the spatial perturbation frequencies coarsely, covers a wide enough light spectrum. The lower applied force lines, 30, 40 and 50 N appear unaffected by the mesh, which suggests that the microbending induced is most active only at a small number of wavelengths. Those wavelengths may be the most significant ones such as when the fibre is lying parallel or at 45° to the warp and weft of the mesh. These are clearly the largest of the perturbations, with other angles producing smaller perturbations which would require more force to encourage the fibre under test to be bent by it. The lower force lines are therefore being fully perturbed only at the major spaces on the mesh, while the smaller bends were unable to perturb the fibre until higher forces were applied.

Fig 7.14 shows the spectral attenuation on the smooth mesh and rubber test. All applied force lines on the smooth mesh and rubber test were elevated to the higher level of attenuation. This was shown by the fact that interruptions in the smooth attenuation line were dips rather than rises in the smooth line height. Wavelengths of light not covered by perturbation spatial frequencies, with lowered

attenuations prove that the smooth mesh excites a broad range of frequencies at small increments to the higher level of attenuation at all applied forces.

Optimum coverage of wavelengths at the broadest wavelength window is to be obtained with the smooth mesh. An equally broad coverage but with larger gaps between raised attenuation wavelength bands is produced by the rough mesh.

7.3.3 Modes of Loss Induced by the Microbend Test.

The final test, that for the nature of the loss modes induced by the microbend test, was tested using a spectral plot.

Figs 7.13 and 7.14, show the spectral attenuations induced by the microbending test variations at each applied force. Each figure shows the results obtained from a single sample fibre with each line indicating the attenuation observed at one applied force. Again, the line representing the lowest levels of attenuation, relates the attenuation induced by an applied force of 30 N, (the lowest level of force).

The figures show representative fibre results from the rough and smooth mesh and rubber tests. It was found that the attenuations produced by the card tests both contained a high degree of macrobending as evinced by attenuations at 1550 nm greater than twice the attenuations at 1300 nm on the spectral attenuation graphs. It was deduced that the card based tests made a bad match between holding material and mesh, and that the combination caused perturbations which were too severe. The card may have been too firm to allow the fibre to retreat into it slightly, thus allowing a lessening of the effects of the mesh. For this reason the tests were found to be non-conformant of the second requirements of the tests.

For the rubber based tests, the spectral attenuation traces merited closer inspection since both tests produced graphs which showed the dominant mode of loss to be microbending. For both Figs 7.13 and 7.14, it can be seen that the attenuation at 1550 nm is less than or equal to twice the attenuation at 1300 nm.

The smooth mesh and rubber spectral attenuation graph, (Fig 7.14), shows that on this test variation, for all applied forces, the attenuation measured at 1550 nm is always twice the attenuation measured at 1300 nm. The prevailing mode of loss is clearly microbending. The rough mesh and rubber graph, (Fig 7.13), demonstrates that the selection of the rough mesh on the basis that it would produce loss modes which lay on the macro/microbending dividing line was correct. The lower applied forces of 30 and 40 N yielded attenuation plots in which the attenuation ratios suggested microbending as the dominant loss modes. The higher forces of 50, 60 and 70 N tended to suggest that the additional applied forces had increased the severity of the perturbations induced and that this change had altered the loss mode emphasis from micro to macrobending. The soft rubber which was chosen so as to mould the fibre to the mesh profile rather than constrict it on the high points of the mesh, had induced bends so severe that they became the radii which induce macrobending. The large gaps between the wire allowed the significant bends to occur, where the smooth mesh or the rough mesh with lower applied forces would have prevented it. From the point of view of microbend purity, therefore, the best option would appear to be the smooth mesh and rubber test or using low levels of applied force, the rough mesh and rubber test, using low values of applied force.

7.3.4 Interim Conclusions.

From 7.3.1., it was deduced that all variations of the microbend test were capable of yielding highly repeatable results. The opto electronic measurement equipment was found to be the limiting factor of the accuracy and hence the repeatability of the test. (Appendix J describes the monitoring

equipment used and endeavours to quantify errors and noise levels produced by it.) When choosing the most suitable test variation, the levels of attenuation and the increments in attenuation had to be checked to ensure they were not overwhelmed by background noise levels.

From 7.3.2., it could be seen that both mesh variations when used with the rubber holding material induced perturbations across a very wide range of spatial frequencies and therefore made the test a more faithful reproduction of the conditions a fibre would experience in the cable, although a rough mesh using higher applied forces was accepted as producing the best performance from the microbend test with respect to this criteria. A smooth mesh, it was decided, was capable of inducing well distributed microbends across a very wide spectrum with a high resolution of frequencies. Lower applied forces on the rough mesh and rubber test tended not to yield higher level attenuations which characterised the "preferred" microbend result.

Section 7.3.3, describes how the smooth mesh test appears to induce very pure microbends for all values of applied force. The rough mesh and rubber test displayed microbending as the dominant loss mode at the lower applied force levels, which tended slightly to macrobending at the higher levels. The card test, while not generating the very pure microbends available from the rubber based tests were nevertheless capable of testing the fibres in a useful way. While the nature of the loss modes was unknown, it was reasonable to assume that amongst modes of loss active were macro and microbending and that the test was inducing its modes of loss in a very consistent way. The card based tests therefore constituted a good method of assessing the resistance of fibres to general modes of loss and might demonstrate the performance of fibres once in the more realistic environment of the telecommunications cable.

From these results, it can be deduced that the optimum combination of materials for microbend induction is smooth mesh and rubber. The constraints imposed by the measurement equipment through

background noise, suggest that until better monitoring equipment is acquired, higher applied forces should be used to increase the attenuation levels and therefore reduce the proportional effect of the background noise.

An alternative would be to use the rough mesh and rubber test. If this were done, the level of applied force would have to be very carefully chosen. A force of 50 N would appear to be the best force for this variation, being a compromise between the macrobending evident at the higher applied forces, and the lower forces which do not tend to perturb fibres at the higher frequencies.

All test variations are useful for specific applications which can be basically subdivided according to holding material. The rubber based tests assess microbend performance, while card based tests measure general resistance to loss modes. The grade of mesh used appears to dictate the severity of the test, but does not alter the basic nature of the loss modes induced. As long as the specific features of the variations are borne in mind, all test variations can be used and may provide a useful insight into the performance of the optical fibre.

7.4 Performance of Various Sample Fibre Types on the Microbend Test.

7.4.1 Introduction.

The fibres of four manufacturers were investigated on the microbend test. The manufacturers were:

i) OFU,

ii) Corning,

iii) AT&T,

iv) Lycom.

In the technical paper shown in Appendix A, only three types of fibre were discussed. The reason for this was that only two Lycom fibres were tested during the pilot study and so were judged to be too few in number to draw any meaningful conclusions from the results. The fibres were included in this report on the pilot study however for completeness. As discussed previously, each manufacturer of fibre used a slightly different fibre/coating combination and these are discussed below.

OFU fibre was produced by the modified chemical vapour deposition, (MCVD), process and was a nominally matched cladding fibre. It had a single coating layer and the coating was designed to be, as with all fibres in the sample, mode stripping.

The Corning or Deeside fibre was produced by the outside vapour deposition, (OVD), process. It was matched cladding, double coat fibre.

The AT&T fibre, like the OFU examples was produced by the MCVD process, but had depressed cladding. The AT&T, like the Corning fibre was doubly coated.

The fourth fibre type, the Lycom fibre which was not discussed in Appendix A, was a MCVD produced fibre with matched cladding and a double layer of coating. The refractive index profiles of the first three types of fibre are discussed in Chapter 3. Lycom fibre profile was identical to the OFU shape in every respect.

For brevity, the convention for naming the fibres used in Appendix A will also be used here. Each fibre type will be described by a letter with the addition of the Lycom fibre. The naming system is therefore:

i) OFU, MCVD matched cladding, single mode fibre-Type A,

ii) AT&T, MCVD, depressed cladding, double coat fibre-Type B,

iii) Corning, OVD, matched cladding, double coat fibre-Type C,

iv) Lycom, MCVD, matched cladding double coat fibre-Type D.

The analysis of fibre performances on the microbending test was carried out using standard techniques. Five sets of data were taken for each test variation and the average at each applied force was found. The procedure was carried out on each test fibre for all test variations and both wavelengths and the results are discussed below.

Although only two Lycom fibres were tested on each variation which did not constitute a representative sample of the fibre of that manufacturer, the fibre was included in the results graphs so that the full range of the work of the pilot study could be seen.

The purpose of this section of work was to investigate the comparative performances of each of the fibre types used in the study.

7.4.2. Results

The results from the sample fibres will be viewed in light of the conclusions drawn in section 7.3. with regard to the nature and quality of loss modes induced by the microbend test.

Appendix D shows graphical results from tests carried out on individual fibres during the pilot study. All fibres tested are represented in the appendix and results are shown from all four test variations and at both 1550 and 1300 nm light wavelengths. The results graphs were produced using normal test procedure with each line representing the performance of a fibre on a particular test variation and at a particular wavelength; and with the results from each fibre being the mean taken over five

individual sets of results. The results shown in Appendix D are grouped by variation and by wavelength with the first two graphs in each category showing results from type A fibres, the third and fourth graphs in each category showing the results from type C fibres, and the fifth graph in each category showing the results obtained from types B and C fibres. On the fifth graph, the first seven results lines represent type B fibres and the last two result lines represent type D fibres. Along the right hand side of each graph are the identification numbers for each of the sample fibres with a key for point markers relating to the results lines. Each type of fibre, because it was from a different manufacturer, had a different numbering system. In the fifth graph in each category, the type B fibres can be identified from their long, three part numbers, while the type D fibres were the last two on the sheet whose identification numbers contain two hyphens.

For all test variations and for any sample fibre, the attenuation at 1550 nm was always greater than the attenuation at 1300 nm. The theoretical explanation of this effect is discussed in 7.4.1, and is verified experimentally here.

The first test variation addressed in Appendix D, is that of rough mesh and card. From 7.3, it was believed that the card tests, while not being a very pure source of microbend induction would be a rigorous test of general attenuation susceptibility and would yield highly repeatable results.

At 1550 nm, type A fibre results appeared to be more broadly scattered than any of the other types, (the scatter of type A fibre results and parameters will be dealt with fully in 7.5), although the average performances were broadly of the same order. It was seen that the average type A performance on this variation was better than the average type C performance. If the card test is taken to be a general test of attenuation susceptibility, (additional modes of loss including macrobending), then the conclusions drawn would appear to concur with those of [4.6], where it was reported that type A fibres showed a lower susceptibility to the macrobending mode of loss than equivalent fibres

of type C. The type C fibres showed less scatter between fibre results than those of type A. It appeared that the results from the type D fibres, although only two were tested and so the sample was not highly representative, showed that these fibres produced results of comparable magnitude to those produced by the type A fibres. The best performance on the test was produced by the type B fibres. Here, a high correlation between the different fibre results was observed, and the attenuations produced were all lower than those seen for all other sample fibres, except one of the type A fibres.

The results measured at 1300 nm reflected those seen at 1550 nm, and the interrelations between the different fibre types appeared to remain intact. The same type A fibre which performed well at 1550 nm, also displayed performance at 1300 nm comparable to the superior performance of the type B fibres.

The majority of results lines were straight, parallel and few cross overs between results lines occurred. This suggested that similar modes of loss were induced in all test fibres and that the variations in attenuation were due to parametric and design differences between fibre types.

The second variation of the test whose results are shown in Appendix D, is the rough mesh and rubber test. In 7.3, the rough mesh and rubber test was found to be less severe and to induce microbend loss modes which were more pure than its card based equivalent, although the macrobending evident in the card test was also present in the rubber variation at the higher applied forces.

From the results, type A fibre d9121361a3071 could again be seen to be producing very low attenuations, and consistency between corresponding fibre results from both versions of the rough mesh test was observed in fibre which yielded higher than average attenuations. The majority of type A fibres produced attenuations which were comparable to type C and D fibres. Type B fibres showed

a duality in performance. Half of the sample showed exceptional consistency and very low levels of attenuation, while the other half appeared less consistent with attenuation performances which overlapped those of types A and C.

The rubber test was capable of inducing loss modes which were more purely microbending than the card based equivalent. It would be reasonable to assume that the type B fibre had a good resistance to general modes of loss, but was comparatively less resilient to the microbending mode of loss in the particular. This hypothesis was tested when the smooth mesh and rubber test variation, (which is also capable of inducing very pure microbends), is addressed, (see Appendix A).

1300 nm results from the rough mesh and rubber variation, like those from the card based equivalent mirrored very closely, with a number of exceptions, the 1550 nm performance. The type A fibres appeared more tightly grouped and the results lines straighter and more parallel, (except for the normally highly attenuating "rogue" fibres belonging to this type), at 1300 nm than at 1550 nm.

The improved correlation between type A fibre results at 1300 nm from 1550 nm, could be due to a varying mode field diameter at these wavelengths. The MCVD process might have a greater tendency to broadening the MFD at 1550 nm than the OVD fibres. Thus, whereas at 1300 nm the MCVD and OVD fibres have a similar performance perhaps with the MCVD fibres correlating better due to smaller MFD; at 1550 nm, the type A fibre's MFD could have increased sufficiently in size to affect the resistance of the sample fibres to the microbend effect. Even a minimal change in MFD would have a noticeable effect on the performance and may be due to the MCVD manufacturing process. The MCVD fibres appear to be inherently more resistant to loss modes of this type, and the cumulative effect of varying MFD and manufacturing process is much the same in each case. The greater inclination of the MCVD MFD to broaden at 1550 nm, is possibly due to the dip at the centre of the refractive index profile characteristic of MCVD produced fibres. The reduced central refractive

index value might allow more power to spread at the higher wavelength. Were this the case, varying dip sizes between fibre samples would lead to differing performances on the microbend test thus producing the greater spread of results seen.

At 1300 nm neither type A nor type C fibres produced a low attenuation fibre whose performance was comparable with that of the bulk of type B fibres.

The fifth graph in the 1300 nm set for this test variation showed two examples of negative increments for increasing applied forces. The first was for the lowest attenuating type B fibre j3fa53605a1rw b001207 6090. For the two highest applied forces, this fibre showed an average decrement, rather than an increment with increasing force. Because of the magnitude of the attenuations involved, it could be assumed that this decrease was due to measurement error introduced by the monitoring equipment via background noise, (as discussed in 7.3). This erroneous result could therefore be discarded and the necessary conclusions drawn form the remainder of the type B fibre results. Type B fibres maintained low attenuation performances and good consistency between the results from different fibres.The decrement observed on type D fibre 919-105-445, was more difficult to explain. In the two test variations so far examined, this fibre had consistently shown high attenuation. Clearly the fibre showed an above normal susceptibility to loss modes, but this did not explain the decrement observed. The attenuations induced in the fibre were sufficiently large to remove the significance of background noise, and since no error could be found in either fibre or results, the performance had to be accepted as correct. Examination of the 1550 nm performance of the same fibre revealed that a "dip" in the performance line occurred at the same applied force as the decrement on the 1300 nm results. This discovery further added weight to the theory that the decrement was a true representation of the fibre performance, although no reason could be found.

The third variation in Appendix D is smooth mesh and card. At 1550 nm, the fibre lines appeared to be much more ordered than in either of the rough mesh tests above. The performance lines of the rogue fibres, while remaining distinct form the average group of fibres, did not demonstrate the instability or cross overs seen previously. Amongst all types of fibres, despite the apparent order in the results, there was a very much greater tendency towards scattering, which was particularly great amongst type C fibres whose spread was as broad in this variation as that of type A. The worst performing type C fibre displayed an attenuation which was greater for the first time than the worst type A fibre.

Clearly the nature of the loss modes induced by this smooth mesh test was radically different to those imposed by the rough mesh variants suggested high reproducibility of loss modes for all fibres, while the spread of attenuations hinted at high sensitivity to the changes of parametric profiles of the fibres. The highly attenuating fibres from all types had changed from those produced by the rough mesh variations, which pointed to radically different loss mode induction by this smooth mesh variant. The increments in attenuation produced by this variation showed a very great tendency to increase in magnitude with applied force. The lines of the fibres under test tended to curve so that they became steeper at higher forces to a greater degree than had been seen in either of the variations addressed above. This suggested that at the higher applied forces, spurious modes of loss such as macrobending were introduced and became gradually more significant. If the smooth mesh and card test, like the rough mesh variation was a test of general loss mode resilience in fibres, it would be expected that the non linear modes of loss such as macrobending would cause curves in the results lines such as those seen here.

On the smooth mesh and card test despite the broader spread of type C fibres, the performance of types A and C fibres appeared to be comparable at 1550 nm, and type D fibres appeared also to demonstrate similar performances. Type B fibres as had come to be expected, showed a superior

resistance to the loss modes imposed by the test variation. Although the increments were small and background noise therefore proportionally more significant, this fact appeared not to affect the quality of results. The majority of lines produced were smooth and the same type of increasing gradient characteristic of the smooth mesh and card test.

The 1300 nm results as normal showed less scatter and lower attenuations than their 1550 nm equivalents. There was less similarity between fibres which constituted the rogue groups of 1550 and 1300 nm results on the smooth mesh test than had been seen on either of the rough mesh groups. The mixed nature of the loss modes induced by the card variations of the test, suggested therefore that at 1550 nm the emphasis of the loss mode set imposed by the test had subtly changed highlighting a different set of weaknesses in the test fibres. If the card tests are an indication of resistance to general loss modes, then both 1300 and 1550 nm results are useful because of the differing weighting imposed by the wavelength.

Type A and C fibres again demonstrated comparable performances with smooth curves of gradually increasing gradient in both cases. One of the type D fibres showed a performance comparable to that of the type A and C fibres, and one showed a performance equal to that of the type B fibres which, as normal were good. In the 1550 nm results one fibre from the type B set showed non typical results. The same fibre in the 1300 nm results returned negative increments when none of its peers had. Clearly in this test this fibre was behaving non typically and was thus producing results which could not be accepted. At 1300 nm the type A and C fibres showed comparable performances although the spread of type C fibre results was smaller than that of the type A fibres. The type B fibres demonstrated their high resistance to loss modes and the spread of results from the type D fibres was wider than had previously been seen.

The last variation whose results are shown in Appendix D is smooth mesh and rubber. This was the least severe of the test variations and the very low attenuations on the y axes of the results graphs reflect this. The 1550 nm results graphs show that the type A fibres have the greatest scatter of the types tested. The same type A fibre as has been seen previously to perform well on other test variations again produced comparatively low attenuations. The rogue type A fibres were very strongly in evidence, although rather than being clearly distinct from the average groups of fibres, there appeared to be a gradual change from normal to rogue fibres which fell between the two performance groups had average attenuations and levels of instability. This imposed a different perspective upon the results. In the three previous variations, rogue fibres had been viewed as a separate performance group to the average fibres. This new development shows that the fibres lie on a spectrum of performance quality at one end of which are high performance fibres with high stability and low attenuation, and at the other end are rogue fibres with high attenuations and low stability. This demonstrates that the performance of fibres can lie anywhere on the performance spectrum,. but that the position of a particular fibre is determined by its primary parameter make up.

Type C fibres showed comparatively low scatter, and the attenuations measured in both types C and D were of comparable magnitude to those measured in the type A fibres. The varying degrees of scatter observed between different fibre types, if the above hypothesis is correct, must be due to the parameter make up of the fibres involved. If this assertion is correct, in 9.5, where fibre parameters are closely examined, type A fibres will exhibit a much wider parameter base than any of the other fibre types. The increased and more gradual scatter observed in type A fibres shows the sensitivity of the smooth mesh and rubber test which appears to be completely unhindered by background noise.

Type B fibres demonstrate the lowest levels of attenuation of any of the fibre samples. The stability of the results, even at the very low attenuations observed, shows how low the critical level is at which background noise becomes significant. Although the background noise was known to be present, at

these levels of attenuation, it was not the critical fact or determining instability. It was found that the position of the fibre on the "stability spectrum" determined both the stability and the attenuation performance of a fibre and that this position was determined by the parameters of a fibre. This hypothesis will be fully tested in 7.5 where a link between attenuations and parameter characteristics will be sought.

From the nature of the loss modes induced by the test, type B fibres was found to be highly microbend resistant. This disproves a hypothesis form the rough mesh and rubber test section, where it was deduced that the type B fibre showed a comparatively low resistance to the microbend mode of loss. Clearly the larger scatter observed previously on the rough mesh test was a product of spurious loss modes active on that test to which the type B fibres were proportionally more susceptible than had been preciously seen.

The variation shows less progressive gradient increase than was seen in the smooth mesh and card test. The changing gradient present also on this variation, suggests that rather than being caused by the various spurious loss modes, the effect was caused by the fine mesh. The holes in the mesh were small enough for the inherent stiffness in the fibres to prevent them from being forced into the mesh contours. The increasing force caused the fibre to more and more closely follow the mesh form and thus cause non linear increases in attenuation levels.

Examination of the highest attenuating type A fibres showed that they were different from those seen on the card variations. There was agreement between the worst performing fibres on both rubber tests, proving the similarity on loss modes induced by the rubber based tests. No similarity between the fibres which produced high attenuations existed on the card test variations, proving that the different meshes caused different loss modes to become dominant and therefore show deficiencies in different fibres.

The 1300 nm results from all fibres as has come to be expected, show less scatter than their 1550 nm counterparts. The widest scatter in results was again seen in type A fibres which again pointed to the broadest parameter base belonging to type A fibres. The low attenuations involved at this wavelength indicated that of all variations and wavelengths, the smooth mesh and rubber test at 1300 nm was where the background noise became a disruptive factor in results accuracy. The instability of results extended to low attenuations, suggesting that the critical level of attenuation had been reached. At the 1300 nm wavelength, no clear rogue groups of fibre existed and all groups tended to be predominantly made up of average performing fibres. The attenuations of both types A and C fibres was comparable to that of type A and type B fibres demonstrated the lowest levels of attenuation. One of the type Fibres exhibited an attenuation decrement with increasing force, but this was discarded and attributed to background noise interference.

Both smooth mesh test variations demonstrated little similarity between highly attenuating fibres at 1300 and 1550 nm wavelengths. This was seen to be due to the fact that at 1300 nm, no clear rogue fibre group existed. The 1300 nm results were viewed as being indicative of the average performance of which a fibre type was capable; while the 1550 nm wavelength assessed the resistance to loss modes induced of particular fibres.

7.4.3 Conclusions.

A range of conclusions can be drawn from this pilot study, which cover several topics. These include:

i) the characteristics of each test variation and its applications in fibre assessment,

ii) the ability of the fibre types contained in the study to resist various modes of loss,

iii) and the quality of the measurement equipment used during the test.

During earlier stages of the pilot study, there was concern regarding errors introduced in measurements by the background noise introduced by the measurement equipment. During 7.4, it became clear that background noise had very little effect on any but the smallest measured attenuations, (noticeably the smallest of those produced by the smooth mesh and rubber test at the 1300 nm wavelength), and that it was more normal for the rogue fibres which produced higher levels of attenuation to produce less stable results lines. The levels of both attenuation and instability were deduced to be directly proportional and to vary as a direct consequence of variations in fibre parameters.

The difference in the scatter of results between 1300 nm and 1550 nm on all test variations led to the conclusion that while 1300 nm results indicated the performance of a fibre type as a whole-in effect the "normal" performance which could be expected when a particular refractive index profile was combined with a coating system-the 1550 nm results more indicated the performance of individual fibres. While 1300 nm results could be used to test the comparative performances of different fibre types, the 1550 nm results could test the comparative resistance of two fibres to certain loss modes. It had been found that the 1300 nm results were less sensitive to changes in fibre primary parameters and thus produced results where any variation in results were due to basic fibre mechanics or design. At 1550 nm, the results were considerably more sensitive to small variations in parameter make up. This was evinced both by the greater number of rogue fibres at 1550 nm and by the greater scatter of the "average" group of fibre's results.

Each test variation was seen to yield a slightly different set of rogue fibres. The only exception to this was between the two rubber based tests. Microbending was known to be highly active, (to different extents), in these tests and so some similarity between the fibres identified as rogues was expected and observed. Where a link between the rogue fibres existed, it was deduced that similar modes of loss were being induced in each case, ~(as with the rubber tests). Between the rubber tests and the

card based tests, and even between the card tests themselves, little similarity in rogue fibres identified existed. The dominant loss modes amongst the general modes of loss induced by the card tests were therefore taken to be different both from each other and form the microbends induced by the rubber tests. This concurs very closely with what was predicted in 7.3.

Each of the rough mesh test variations shows high correlation between its rogue fibre results at 1300 nm and those at 1550 nm. This link was not evident in the smooth mesh and card test. It was deduced that the loss modes dominant in the rough mesh and card test were more dependent upon the mechanical performance of the coating, and the general performance of the optical package, while the smooth mesh and card test was dependent more upon the interaction of the fibre parameters and how they affected light transmission. For this reason, the results from 1300 nm light highlighted a different set of rogue fibres to those at 1550 nm. The link between the 1300 and 1550 nm results from both rubber tests again pointed to the fact that only one mode of loss was dominant in both of these tests, and that it was microbending.

It was observed from the test variations, that where in the rough mesh tests a clear division existed between rogue and average fibre performances, it was seen that on the smooth mesh tests the dividing line was less well defined. This was concluded to be a measure of the sensitivity of the test variations. While the rough mesh tests induced only a few levels of performance, the smooth mesh tests, produced results where, rather than being either rogue or non rogue, fibres could fall anywhere along a performance "spectrum" line. At one end of the spectrum were the high performance fibres with their low attenuations and high levels of stability; while at the opposite end of the spectrum lay the rogue fibres with high attenuations and low stabilities. Average fibre performances would lie between these two extremes and the breadth of possible performances could be seen from the smooth mesh results graphs. Clearly the smooth mesh tests were more sensitive to minor parametric variations which in the rough mesh tests would cause no apparent change in results. It was decided that any fibre

could lie anywhere upon the performance spectrum dependent upon two factors: its individual parametric make up; and the position of the spectrum of that fibre's normal average performance group position. The effect of parameter changes upon fibre performance will be more closely examined in section 7.5.

Throughout the study, all types of fibre except type B showed a similar average fibre performance group attenuation on all test variations. This demonstrated that for "normal" fibres the combination of fibre manufacturing process and coating package for fibre types A, C and D had a cumulative effect which offered similar protection in all cases to loss modes. Type B fibre showed a lower average group attenuation on all variations and at both wavelengths. This fibre type was seen to be the most loss resistant of all of the fibre types.

The results from type A fibre, of all fibre types tested, showed the greatest results scatter. This was attributed to a comparatively broad parametric spread for the type A fibres which, should such a spread exist, would tend to produce scattered results due to the parameter variations. The theme of parameter spread will be more closely examined in 7.5.

The results from types A, C and D fibres showed that the cumulative effect of the manufacturing processes and the coating packages used was to produce fibres with comparable loss mode resistance. The type B fibre process/coating package showed the highest resistance to loss modes of all of the fibre types tested. When high performance fibres of types A and C were tested, their attenuations were comparable to those produced by the type B fibres, although the average fibre performance always yielded higher attenuation.

Finally, it was seen that the rough mesh test's result lines tended towards straightness, while the smooth mesh tests were more inclined to produce lines which were curved. The curvature of the

smooth mesh results lines was found to be more exaggerated in the card than in the rubber variation. It was concluded that on the smooth mesh tests, the small size of the mesh holes allowed the stiffness of the fibre to resist being forced into the mesh contours. The stiffness would resist up to a certain applied force and then progressively yield to the pressure. This would produce the curves seen. The straighter lines produced by the rubber test showed the greatest suitability of rubber over card as a holding material. Because the card was stiffer than the rubber, it was less able to force the fibre into the mesh contours. The rubber, because of its greater flexibility would mould the fibre at a much lower level of applied force thus producing straighter results lines.

7.5. Modelling the Microbend Test Results Mathematically.

7.5.1 Introduction.

Examination of the results produced by the microbend test showed differing levels of attenuation being produced by different fibre samples. Because the test was known to be highly repeatable, variations in results would be concluded to have been caused by variations in the sample fibres. It could be assumed that each fibre had an individual susceptibility to the microbend effect and therefore to the effects of the microbend test. The performance and behaviour of each fibre on the test was completely individual and dependent on the characteristics of that fibre. Geometrically, all fibres were identical to very rigorous tolerances and so the critical factors dictating the fibre microbend susceptibility must have been its optical parameters.

If the assumption that fibre susceptibility to the microbend effect is dependent upon the individual parameter "signature", of that fibre is correct; the performance of a fibre on the microbend test should be predictable. The parameters, both primary and secondary of a fibre are measured and recorded throughout the production process. Given a complete knowledge of the fibre signature, and assuming

a linear relationship between the fibre performance and its parameters, it would not be unreasonable to assume that the performance of fibres on the test could be predicted from a knowledge of its parameters.

Using regression, a mathematical relationship between performance and parameters could be established and once established, this relationship could be used to predict the performance on the test of new fibres.

The theory was tried using the pilot study fibre sample. Fibre test performance on each test variation, at each light wavelength and at each applied force, were regressed against each recorded fibre parameter in turn. Parameters used included cut off wavelength, mode field diameter and a range of refractive index parameters. The results from this set of trials proved unsuccessful. While some correlation between performance and parameters was observed, the correlations were not great enough to suggest reliable prediction of performance on any of the test variations.

Inspection of the results suggested that although some agreement existed, the correlation on any one parameter was not sufficiently large for it to be adopted as being indicative of the fibre's performance on the microbend test. It became clear that while fibre performance on the microbend test was dependent upon the variations in parameters, it was not individually related to any one of the parameters. It was dependent rather upon the variation in several parameters to a greater or lesser extent. Single regression could not adequately describe a multi-faceted relationship of this kind and so was abandoned. In its place multiple regression was adopted.

Multiple regression involved the linking, via formula of the form:

$$y = a_1x_1 + a_2x_2 + a_3x_3 + \ldots\ldots + a_nx_n,$$

where y= a dependent variable.
$x_1 \ldots x_n$ = independent variables.
$a_1 \ldots a_n$ = independent variables.

The y value would be the value to be predicted, at this stage the measured attenuation on a test variation, at a particular wavelength, at an applied force; the x values are the free, (independent), variables in this case the fibre parameters; and the a values are constants added to the independent variables to make the formula equate. Computer packages available were capable of taking an independent variable and matching it to several independent variables. This type of computer produces correlation coefficients which allow assessment of the accuracy of the regression model produced.

Several multiple regressions of this kind proved to have very low values of correlation between predicted and actual results. It was realised that all of the independent variables were not contributing favourably to the accuracy of the regression model. A more intelligent modelling method was required. Methods used so far inserted all independent variables regardless of their effect on the model accuracy. A system which weighed the effect of each independent variable and inserted only those which would improve the model accuracy were required. The method finally adopted was that of stepwise multiple regression. The method involves the selective incorporation of independent variables in the regression model dependent solely upon their contribution to its accuracy. The method of multiple regression is explained fully in Appendix E.

Having established the multiple regression methodology, The dependent and independent variables were collected as a single data file. The y variables were the test results from all fibres on all test variations at both wavelengths and at all applied forces. One dependent variable column might therefore be titled 1550 nm rough mesh and rubber test at 50 N applied force.

The independent variables were simply columns of fibre parameters. Variables included at this stage were:

i) cut off wavelength,
ii) mode field diameter (1300 Gaussian),
iii) mode field diameter (1550 Gaussian),
iv) mode field diameter (1300 Petermann),
v) mode field diameter (1300 Petermann),
vi) ΔN (actual),
vii) ΔN (calculated),
viii) dip size (actual),
ix) dip size (calculated),
x) cladding depression,
xi) tan concentricity,[2]
xii) blue concentricity.

Each of the y variables then had a multiple regression carried out on it against the independent x variables.

Despite an increase in correlation coefficients, the accuracies of the models produced remained too low for predictions with reasonable confidence levels to be made using them. In 7.4, it was discovered that each fibre manufacturing type/coating package had a different "average" or normal performance range. It was decided that while parameters could be used as independent variables to completely describe the fibre itself, no quantitative information was available which could describe coating variations, the effect they had upon light transmission or the degree of protection they offered against loss mode such as microbending. Clearly no model whose independent variables inadequately described the system they were attempting to simulate, could hope to achieve high correlation levels. While the fibre coating packages remained uncategorised or quantified, a model would not be assembled which produced adequate correlation levels. The solution, it was decided , lay in separating the fibres by coating and manufacturing type. In this way it was hoped that the coating would not vary

---

[2] Concentricities refer to those of the core as described in Chapter 2. Tan and blue refer to opposite ends of the fibre preform, (MCVD process, Chapter 3). The blue end is the start end of the preform when it is on the deposition lathe, (the cooler end), the tan end is where the burner finishes its traverse run, making it hotter.

in any way within a regression sample. This approach assumed complete homogeneity throughout the coating of a manufacturer, but this was viewed as being valid on the grounds that a) coating was continuously extruded on to the fibre leading to very consistent coverage, and b) were the assumption not valid, correlations would remain low.

Stepwise multiple regression was carried out on all fibre types separately. The sample was random and so no prior knowledge of the spread of each parameter within a fibre type was available. Correlation high enough to justify a reliable model was obtained only for type A fibres. Inspection of the parameter sets of each of the fibre types revealed that in the cases of fibre types B and C, (type D was not regressed since only two examples of the fibre type had been tested), the random selection procedure had produced parameter spreads which were very narrow. The only fibre type whose parameter base was of a width which allowed successful regression was type A. Because the selection procedure was random, no conclusions could be drawn form the parameter spreads themselves, only that chance, (and possibly the larger size of the type A sample), had yielded a sample whose parameters were conducive to regression.

The remainder of 7.5, is dedicated to the analysis of results produced by stepwise multiple regression of the type A fibre test results on all variations at both wavelengths and all applied forces against their parameter set.

7.5.2 Results

Four test variations were in existence and tests were carried out at two wavelengths on all variations. 32 individual regressions were therefore carried out on the results which yielded a very large volume of data. For brevity, it was felt necessary to summarise the results obtained rather than show them

in full, although an example of a regression which works through each step and explains the salient terms and definitions is shown in Appendix E.

The purpose of the pilot study has not been to develop a regression model, but to assess the feasibility of the project and to give an indication of the required direction for the remainder of the project. The results have been directed towards this end and so are ostensibly concerned with deciding the probability of successful results being obtained form future work in this field.

Tables 7.1 - 7.4 below summarise the stepwise multiple regression results obtained from the type A pilot study fibre sample on all four test variations and at both wavelengths.

Dependent (y) Variable. Attenuation (dB/km)	Independent (x) Variable	Coeff. of Determination. (r)	Correlation Coeff. (r^2)	Signif. T	Signif. F (all vars)
1550nm,30N	1550nm Gaussian MFD constant.	0.70402	0.49565	0.000 0.000	0.000
1550nm,40N	1550nm Gaussian MFD constant.	0.79074	0.62527	0.000 0.000	0.000
1550nm,50N	1550nm Gaussian MFD constant.	0.81465	0.66366	0.000 0.000	0.000
1550nm,60N	1550nm Gaussian MFD constant.	0.80275	0.64440	0.000 0.000	0.000
1550nm,70N	1550nm Gaussian MFD constant.	0.78426	0.61506	0.000 0.000	0.000
1330nm,30N	1550nm Petermann MFD constant.	0.59924	0.359019	0.0002 0.0011	0.0002
1330nm,40N	1550nm Petermann MFD constant.	0.67836	0.46017	0.0000 0.0001	0.0000
1330nm,50N	1550nm Gaussian MFD constant.	0.70278	0.49390	0.0000 0.0000	0.0000
1330nm,60N	1550nm Gaussian MFD constant.	0.71165	0.50645	0.0000 0.0000	0.0000
1330nm,70N	1550nm Gaussian MFD constant.	0.71733	0.51457	0.0000 0.0000	0.0000

Table 7.1 Summary of Results of Stepwise Multiple Regression Carried Out on Rough Mesh and Card Type A Fibre Results.

Dependent (y) Variable. Attenuation (dB/km)	Independent (x) Variable	Coeff. of Determination. (r)	Correlation Coeff. (r^2)	Signif. T	Signif. F (all vars)
1550nm,30N	1550 nm Petermann MFD Dip Size Constant	0.45344 0.59211	0.20561 0.35059	0.0005 0.0147 0.0008	0.008 0.0015
1550nm,40N	1550 nm Petermann MFD. Dip Size Constant	0.53935 0.66449	0.29090 0.44154	0.0000 0.0079 0.0001	0.0012 0.0002
1550nm,50N	1550 nm Petermann MFD. Dip Size Constant	0.59484 0.70549	0.35383 0.49771	0.0000 0.0064 0.0000	0.0003 0.0000
1550nm,60N	1550 nm Petermann MFD. Dip Size Constant	0.63794 0.73948	0.40696 0.54684	0.0000 0.0048 0.0000	0.0001 0.0000
1550nm,70N	1550 nm Petermann MFD. Dip Size Constant	0.66585 0.75336	0.44335 0.56755	0.0000 0.0063 0.0000	0.0000 0.0000
1330nm,30N	1550 nm Petermann MFD. Dip Size Constant	0.39158 0.53805	0.15333 0.28950	0.0022 0.2290 0.0030	0.0242 0.0059
1330nm,40N	1550 nm Petermann MFD. Dip Size Constant	0.42845 0.56644	0.18357 0.32086	0.0010 0.0198 0.0015	0.0129 0.0030
1330nm,50N	1550 nm Petermann MFD. Dip Size Constant	0.48478 0.60642	0.23501 0.36775	0.0003 0.0177 0.0005	0.0042 0.0010
1330nm,60N	1550 nm Petermann MFD. Dip Size Constant	0.55871 0.65837	0.31215 0.43346	0.0000 0.0167 0.0001	0.0007 0.0002
1330nm,70N	1550 nm Petermann MFD. Dip Size Constant	0.60135 0.69102	0.36162 0.47750	0.0000 0.0150 0.0000	0.0002 0.0001

Table 7.2 Summary of Results of Stepwise Multiple Regression Carried Out on Rough Mesh and Rubber Type A Fibre Results.

Dependent (y) Variable. Attenuation (dB/km)	Independent (x) Variable	Coeff. of Determination. (r)	Correlation Coeff. (r^2)	Signif. T	Signif. F (all vars)
1550nm,30N	1550 nm Gaussian MFD. Constant	0.74275	0.55168	0.0000 0.0000	0.0000
1550nm,40N	1550 nm Gaussian MFD. Constant	0.75614	0.57174	0.0000 0.0000	0.0000
1550nm,50N	1550 nm Petermann MFD. Constant	0.77612	0.60237	0.0000 0.0000	0.0000
1550nm,60N	1550 nm Petermann MFD. Constant	0.80311	0.64499	0.0000 0.0000	0.0000
1550nm,70N	1550 nm Petermann MFD. Constant	0.80659	0.65058	0.0000 0.0000	0.0000
1330nm,30N	1550 nm Petermann MFD. Dip Size Constant	0.5622	0.31598	0.0001 0.0443 0.0002	0.0004
1330nm,40N	1550 nm Petermann MFD. Constant	0.65649	0.43097	0.0000 0.0001	0.0000
1330nm,50N	1550 nm Petermann MFD. Dip Size Constant	0.69527 0.74231	0.48340 0.55103	0.0000 0.0419 0.0000	0..0000
1330nm,60N	1550 nm Petermann MFD. ΔN Constant	0.72204 0.77514	0.52134 0.60085	0.0000 0.0206 0.0000	0.0000
1330nm,70N	1550 nm Petermann MFD. ΔN Constant	0.76624 0.81977	0.58713 0.67202	0.0000 0.0091 0.0000	0.0000

Table 7.3 Summary of Results of Stepwise Multiple Regression Carried Out on Smooth Mesh and Card Type A Fibre Results.

Dependent (y) Variable.	Independent (x) Variable	Coeff. of Determination. (r)	Correlation Coeff. (r^2)	Signif. T	Signif. F (all vars)
1550nm,30N	1300 nm Petermann MFD Dip Size Constant	0.67407 0.74042	0.45437 0.54823	0.0000 0.0183 0.0000	0.0000
1550nm,40N	1300 nm Petermann MFD Dip Size Constant	0.71413 0.78357	0.50999 0.61399	0.0000 0.0080 0.0000	0.0000
1550nm,50N	1550 nm Petermann MFD Dip Size ΔN Constant	0.70002 0.78888 0.82888	0.49003 0.62234 0.68704	0.0000 0.0002 0.0206 0.0000	0.0000
1550nm,60N	1550 nm Petermann MFD Dip Size ΔN Constant	0.72001 0.79969 0.84350	0.51842 0.63950 0.71150	0.0000 0.0001 0.0117 0.0000	0.0000
1550nm,70N	1550 nm Petermann MFD Cut Off Wavelength Dip Size Constant	0.74885 0.81247 0.85309	0.56078 0.66011 0.72776	0.0000 0.0096 0.0119 0.9402	0.0000
1330nm,30N	1550 nm Petermann MFD Dip Size Constant	0.51907 0.62115	0.26944 0.38582	0.0002 0.0236 0.00047	0.0007
1330nm,40N	1550 nm Petermann MFD Dip Size Constant	0.60985 0.70390	0.37192 0.49548	0.0000 0.0110 0.0000	0.0000
1330nm,50N	1550 nm Petermann MFD Dip Size Constant	0.67232 0.75348	0.45202 0.5677.	0.0000 0.0081 0.0000	0.0000
1330nm,60N	1550 nm Petermann MFD Dip Size Constant	0.71743 0.79202	0.51471 0.62729	0.0000 0.0053 0.0000	0.0000
1330nm,70N	1550 nm Petermann MFD Dip Size Constant	0.67796 0.75345	0.45962 0.56769	0.0000 0.0103 0.0000	0.0000

Table 7.4 Summary of Results of Stepwise Multiple Regression Carried Out on Smooth Mesh and Rubber Type A Fibre Results.

7.5.3 Conclusions

It is clear that all test variations are capable of producing regression models which have a high level of correlation with the measured values. Low levels of significant F and significant t demonstrate the improbability of the relationships which were established coming about by chance. These consistently low measures add further credibility to the models and suggest that were a more comprehensive study carried out, suitably accurate predictive models would result. It became clear that the investigation should take the type A fibres, broaden the sample, increase the sample size and carry out another series of multiple regressions.

Hypotheses stated in 7.4 which attributed the spread of type A test results to the broad base of fibre parameters contained in the sample were proven to be correct. While the random sample produced a relatively broad scatter of results lines in section 7.4, in section 7.5 it was this which allowed the regression to be carried out successfully of type A fibres. It proved that should it be required, a model could be developed for may fibre/coating combination providing that the sample used to develop the model was suitably chosen.

The type A fibres selected for the main study will be chosen so that a broad parameter base exists which will allow predictive models to be constructed. In future work where similar models are developed for other fibre types, similar precautions will be taken.

7.6 The Pilot Study-Review.

In the course of the pilot study, three basic areas were investigated;

i) The quality of the microbend test produced and the particular virtues and applications of each of its variations,

ii) A comparison of the performances of four types of fibre manufacturing type/coating combination,

iii) Examination of the feasibility of a model capable of predicting the performance of fibres on the microbend test variations.

The results and conclusions relating to these three topics have been extensively discussed and conclusions drawn in the preceding sections. The aim of section 7.6 is therefore to use the conclusions drawn throughout the pilot study to deduce the best future course of work for the main part of the project.

One of the initial intentions of the project was to develop in an assessment of the comparative performances of various fibre types. On completion of the pilot study, it was felt that this topic had been adequately addressed and that no further advantage would be gained form additional comparison of results form different fibre types. The type D fibres were not included in this statement as only two had thus far been tested, but it was felt that the test for this fibre type could be made as a separate mini project and did not constitute a section in the second part of the project.

The emphasis of the project was therefore shifted to modelling fibre performance. It has been shown above that the microbend performance of fibres may be modelled from their parametric make up. It was also seen above that the performance of fibres on the card based tests which induced general loss

modes could also be modelled in the same way. It was felt that the card based tests might assess the resistance of fibres to the multiple loss modes they would experience during the cabling process. Were this the case, it would be possible not only to model production increments and attenuations against test results, but also against the parameter sets already developed.

It was decided therefore that the second part of the project would involve the linking of the following three bodies of data:

i) data A: the attenuations measured in fibres at each stage of the production process and at both wavelengths and the increments between them,

ii) data B: the primary and secondary parameters of the fibre in the sample measured throughout its production,

iii) data C: the test results taken for all applied forces, at both wavelengths on all test variations.

Table 7.5 shows the regressions which will be carried out.

These regressions will be carried out on data sets greatly increased in size, and relations will be made thus:

i) the performance of fibres in the production process will be related to the parameters of the fibre,

ii) the performance of fibres of the test variations will be related to fibre parameters,

iii) the performance of fibres in the production process will be related to the performance of fibres on the test variations.

Dependent (y) Variable.	Independent (x) Variable(s).
A	B
C	B
A	C

Table 7.5. The Stepwise Multiple Regressions to be Carried Out During the Main Study to Link the Various Bodies of Data.

It is hoped that these relations will allow:

i) the redefinition of specifications so that, (to within set confidence limits), only fibres that will pass the end specifications for telecommunication cables will be used,

ii) graphs will be drawn which allow the prediction of finished cabled fibre attenuations given either the parametric signature of the fibre, or the results of fibre on one of the test variations.

Clearly for this type of situation to be achieved, a large body of data in which there is complete confidence must be assembled. The main study will begin by assembling a large accurate data base which will allow accurate modelling in all three cases to take place.

CHAPTER 8.0.

DEVELOPMENT OF A PREDICTIVE MODEL FOR MICROBEND AND CABLED FIBRE PERFORMANCE.

8.1 Introduction

From Chapter 7, the possibility of predicting the performance on the microbend test of the type A fibres appeared to be a real possibility. Several of the applied force values could be modelled using combinations of parameters of the sample fibres to what appeared to be high levels of confidence.

During the pilot study, only type A fibres were modelled since each manufacturer incorporated a different coating type with different characteristics. Because no qualitative values capable of describing the coating characteristics could be found steps were taken, as far as possible, to achieve homogeneity of coating across the fibre sample. This was done by using the fibre from only one manufacturer in the fibre sample and therefore only one type of coating. This approach theoretically eliminated variables due to coating variation from the model but made the assumption that all coating applied by the chosen manufacturer had identical properties. This assumption was clearly incorrect, but because of the chemical nature of the coating, the methods incorporated to apply it to a fibre and the standards to which the coating material was expected to comply: the assumption was taken to be valid to within acceptable levels of variation. Modelling within the second part of the project therefore centred upon type A fibres. It was intended that should the modelling processes be successful, the fibre/coating combinations produced by other manufacturers would be addressed, with the final intention of incorporating all models into one overall calculation which would assess levels of microbend performance in a test fibre regardless of manufacturer or coating style.

Thus far, the project had dealt only with the design and integrity of the test and with the production of the performance of fibres upon the test. The pilot study had established that the loss modes active in cables were of a complex nature and that no accurate, repeatable method could be designed which would simulate these effects. Following the success of the pilot study in modelling the behaviour of fibres on the microbend test, the researcher therefore felt justified in extending the field of interest to include fibres in cables. If it were known that no test could be made which would adequately describe the experiences of fibres in cables, re-direction of the study of the performance of cabled fibres might reveal some pattern which would allow prediction of fibre's performances.

It was realised when this approach was adopted, that the study of pure microbending had been used to its full extent and that combinations of loss modes imposed on a fibre during the cabling process. Because the study began by centring upon the microbend effect, the success of the pilot study meant that the microbend test would continue to be researched; however the scope of interest of the project had now been broadened to include the real as well as the theoretical investigation.

8.2 Methods of Analysis

As stated in 8.1, the investigation was broadened for the main study to include both the microbend test and the case of cabled fibres. In effect, the research addressed one mode of loss in its purest form as well as the multiple attenuation sources seen by optical fibres in cables. It was hoped that the methods and techniques used successfully in the pilot study to predict microbend susceptibility, could be directly transplanted to both larger samples for microbend investigation and to the real situation of multiple loss inducements as seen in cables.

Fifty seven type A fibres were chosen at random from normal cable production and three sets of data were assembled on them. The first body of data was made up of the parameters of the fibres in the

sample. The values used included both primary and secondary parameters and were intended to completely describe the silica glass of the fibres. As stated above, no account could be taken of the properties or influence of the acrylate coating on the fibre. The coating of each fibre type was however taken to be consistent-hence the use of only type A fibres in the sample. The second set of data was made up test results from the microbend test measured at both 1300 and 1550 nm and on all four test variations. The data was of the form used in the pilot study and was recorded in data spreadsheets in exactly the same way. The third set of data recorded the attenuations measured in the test fibres at each stage of the cable production process. In producing optical cables of the loose tube variety as previously discussed, construction stages are as follows:

i) stage 1: fibre imported into the factory,

ii) stage 2: fibre inserted into loose tubes,

iii) stage 3: multiple tubes and necessary fillers stranded around central strength member and interstitial filler and paper tape applied,

iv) stage 4: sheath core in metal tape and final plastic sheath.

It was felt that two effects would be significant in the process attenuations of the fibres. These were the fibre's susceptibility to the cable induced loss effects and the experiences of the fibre when inserted into a cable. It was felt that a fibre's susceptibility to loss modes would manifest itself as a high increment in attenuation between stages of the process, while the quality of the cabling process and its effects upon a fibre would be reflected in the absolute attenuations observed in fibres at various stages of the process. Therefore, in order to monitor and attempt to quantify both the susceptibility of fibres to loss modes and the variation in experiences imposed on fibres by the cabling process, both absolute and incremental attenuations at each stage of the process were recorded. The final data record of the main project sample fibres was therefore made up of the following readings:

i) 1550 nm stage 1 attenuations,
ii) 1550 nm stage 2 attenuations,
iii) 1550 nm stage 3 attenuations,
iv) 1550 nm stage 4 attenuations,
v) 1300 nm stage 1 attenuations,
vi) 1300 nm stage 2 attenuations,
vii) 1300 nm stage 3 attenuations,
viii) 1300 nm stage 4 attenuations,
ix) b-a,
x) c-a,
xi) d-a,
xii) c-b,
xiii) d-b,
xiv) d-c,
xv) f-e,
xvi) g-e,
xvii) h-e,
xviii) g-f,
xix) h-f,
xx) h-g.

Body A: absolute and incremental attenuations measured as the fibres progressed through the various stages of the production process.
Body B: fibre parameters-the primary and secondary parameters describing the silica glass fibres but omitting descriptions of the primary coating layers.
Body C: the results measured on the four variations of the microbend test at both the 1300 and 1550 nm light wavelengths.

Table 8.1 Summary of the Main Data Sets.

All possible attenuations, both incremental and absolute were included in the data file; and all measurements were carried out at both 1300 and 1550 nm. In this way, it was hoped that every

opportunity had been provided for the effects of the fibre susceptibility, or the cable quality to manifest itself in a meaningful and controlled manner.

After collection of the data therefore, three bodies of data existed:

It was proposed that an attempt be made to establish a link: firstly between the cable performances of the fibres and both the fibre parameters and the test results; and secondly to verify the results of the pilot study by attempting to link the results obtained from the microbend test to the parameters of the fibres contained in the sample. In essence therefore, attempts would be made to establish links thus:

dependent variable	independent variable set
A	B
B	C
C	B

Table 8.2 Pairs of Data Sets between which Links were Sought using Stepwise Multiple Regression.

The procedure, if successful would firstly allow the prediction of fibre susceptibility to the multiple loss modes active in the cabling process. This regression allowed for the fact that microbending was

one of many loss modes active and that to investigate the cable performance of fibres, the opportunity had to be allowed for other loss modes to be taken into account. The second regression was used in order to take into account the fact that while multiple loss modes were active in cables, microbending might have been the predominant one or the one most likely to vary with fibre parameter. Were this the case, the relationship between microbend test performance and cable performance of fibres would be very close. The first regression was a repeat of that carried out in the pilot study and sought to reproduce the results obtained and enhance the accuracy of the model. Were the regression of data sets A against C successful, this final C against B regression would finally eliminate the need to carry out the test and would allow, through prediction of microbend test results from parameters, the prediction of cable performance from microbend susceptibility. It was felt that by broadening the scope of interest in this way, all possible opportunities for the regression to establish a relationship had been given.

8.3 The Performance Data-base

It was assumed that because of the wide variation in sample parameters yielded by the fibre sample of the pilot study, the random selection of fibres for the main research would yield a parameter spread of similar breadth and range. Examination of the final parameter spread of each sample showed this to be the case. From this observation, it is clear that any low correlation results could not be attributed to a variation in the "character" of the fibre sample.

As discussed previously and in Appendix E, the regression system used was stepwise and linear. For this reason, if relationships such as x^2, or $1/x$, linked the dependent to the independent variables, the computer would fail to recognise it and successfully incorporate it into the model. It was felt that the accuracy of the pilot study model might have been improved by the introduction of the more complex relationships and it was felt that the accuracy of the model could not be jeopardised by the omission

of such data. In order to remove this possibility and improve the probability of establishing the required relationships, variations of the basic data set were inserted into the data base. Because the parameter information was used as independent variables for the regressions of both the test results and the cable performances, it was felt that variations to the basic data set should be built into the B body of data-the fibre parameters. The parameter data set for the main project therefore basically contained the following values:

i) Cut off wavelength,

ii) 1550 nm Petermann MFD,

iii) 1550 nm Gaussian MFD,

iv) 1300 nm Petermann MFD,

v) 1300 nm Gaussian MFD,

vi) delta N (actual),[1]

vii) delta N (relative),

viii) Dip size (actual),

ix) Dip size (relative),

x) Cladding depression,

xi) Tan concentricity,

xii) Blue concentricity.

Thus data set B contained twelve groups of data. This set of "normal", data was then supplemented by variations of it which were intended, as discussed above to maximise the opportunity of establishing a relationship. Additional groups of data added to the original set were:

---

1 For definitions of relative and actual parameters, see chapter 3.

i) 1/2,

ii) x^2,

iii) $1/x^2$,

iv) e^{-x},

v) e^{-2x},

This increased the number of data ranges in the data set from 12 to 72. For the main part of the regression, the base 12 variables were employed and the need for the enhanced data set would be noted.

8.4 Regression

57 fibres were tested for the main project. This large sample size meant that the 1 % significance level[2] for the correlation coefficient, r, dropped to 0.3083. Thus, in the regression, r had only to be 30% or greater for significant correlation to have been achieved.

Tables 10.3-10.5 shows the level of correlation coefficients for each regression carried out during the multiple regression.

Table 10.6 is a key to the abbreviations used in Tables 10.3-10.5.

---

2 The chance (1 %) of concluding that a correlation coefficient was significant when it was not.

Dependent Variable (A data)	Independent Variables (B data) selected			
	first B selection	correlation coefficient, r.	second B selection	correlation coefficient, r.
a1	b3	.28		
a2	b8	.31		
a3	b3	.34	b11	.48
a4				
a5	b5	.27		
a6				
a7				
a8				
a9	b11	.32		
a10	b1	.33	b11	.46
a11				
a12				
a13				
a14	b4	.34		
a15				
a16				
a17	b8	.26	b9	.41
a18				

Table 8.3 Regression carried out relating cabling performance of fibres against their parameters, (data groups A and B respectively).

Dependent Variable (C data)	Independent Variables (B data) selected					
	first B selection	correlation coefficient r.	second B selection	correlation coefficient r.	third B selection	correlation coefficient r.
c1	b1	.34				
c2	b1	.35				
c3	b1	.35				
c4	b1	.36				
c5	b1	.36				
c6	b11	.30				
c7	b3	.30				
c8	b3	.30				
c9	b3	.30				
c10	b3	.31				
c11	b5	.48				
c12	b5	.42	b11	.52		
c13	b5	.42	b11	.51	b8	.58
c14	b5	.43	b11	.51	b8	.57
c15	b5	.44	b8	.53		
c16	b11	.29				
c17	b3	.30				
c18	b3	.30				
c19	b3	.31				
c20	b3	.31				

Table 8.4 Regression carried out relating fibre test performance against fibre parameters, (data groups C and B respectively).

Dependent Variable (A data)	Independent Variables (C data) selected					
	first C selection	correlation coefficient r.	second C selection	correlation coefficient r.	third C selection	correlation coefficient r.
a1	c9	.47				
a2	c61	.56				
a3	c8	.45				
a4	c1	.54				
a5	c8	.44				
a6	c8	.38				
a7						
a8	c9	.33				
a9	c12	.37	c5	.46		
a10	c13	.30	c15	.42		
a11	c6	.30				
a12	c4	.26	c15	.36		
a13	c1	.36				
a14						
a15	c1	.32	c15	.47	c14	.57
a16						
a17	c1	.28	c15	.40	c11	.49
a18	c6	.36				

Table 8.5 Regression carried out relating cabling performance of fibres against their test performances, (data groups A and C respectively).

parameter number	Data Group A-cabling performance.	Data Group B-fibre parameters	Data Group C-fibre tests performance
1	1550 nm fibre attenuation	cut off wavelength	1550 nm rough mesh and rubber test-30 N
2	1300 nm fibre attenuation	1550 nm Petermann MFD	1550 nm rough mesh and rubber test-40 N
3	1550 nm tube attenuation	1550 nm Gaussian MFD	1550 nm rough mesh and rubber test-50 N
4	1300 nm tube attenuation	1300 nm Petermann MFD	1550 nm rough mesh and rubber test-60 N
5	1550 nm tube attenuation	1300 nm Petermann MFD	1550 nm rough mesh and rubber test-70 N
6	1300 nm tube attenuation	DN (actual)	1300 nm rough mesh and rubber test-30 N
7	1550 nm sheath attenuation	DN (relative)	1300 nm rough mesh and rubber test-40 N
8	1300 nm sheath attenuation	dip size (actual)	1300 nm rough mesh and rubber test-50 N
9	1550 nm fibre-tube attenuation	dip size (calculated)	1300 nm rough mesh and rubber test-60 N
10	1550 nm tube-sheath attenuation	cladding depression	1300 nm rough mesh and rubber test-70 N
11	1550 nm strand-sheath attenuation	tan concentricity	1550 nm smooth mesh and rubber test-30 N
12	1550 nm fibre-strand attenuation	blue concentricity	1550 nm smooth mesh and rubber test-40 N
13	1550 nm fibre-sheath attenuation		1550 nm smooth mesh and rubber test-50 N
14	1300 nm fibre-tube attenuation		1550 nm smooth mesh and rubber test-60 N
15	1300 nm tube-strand attenuation		1550 nm smooth mesh and rubber test-70 N

16	1300 nm strand-sheath attenuation		1300 nm smooth mesh and rubber test-30 N
17	1300 nm fibre-strand attenuation		1300 nm smooth mesh and rubber test-40 N
18	1300 nm fibre-sheath attenuation		1300 nm smooth mesh and rubber test-50 N
19			1300 nm smooth mesh and rubber test-60 N
20			1300 nm smooth mesh and rubber test-70 N

Table 8.6 Key to Tables 10.3-10.5, giving definitions of data codes.

8.5 Analysis

The strongest and most consistent links can be seen in the regression carried out between the microbend test and the parameters. It is clear that the conclusions of the pilot test were valid and that even at the exacting levels of significance chosen as criteria for the test, the parameters still provide an accurate model of fibre performance on the test. Each wavelength/test variation combination yielded distinct sets of results. The results could be discerned both by magnitude of r and by the independent variable chosen as being most significant. It could be deduced that each variation tested for slightly different things.

The two principle independent variables chosen were mode field diameter and cut off wavelength. The close relationship between these two variables meant that they were mutually exclusive and each test required only one or the other to describe it. Both of these variables described the width of the light beam travelling along the fibre and by implication therefore, the amount of light carried outside the fibre core most likely to "leak" from the fibre during perturbation.

The fact that different microbend tests were described by different descriptions of mode field diameter suggested that rather than being directly proportional to one another, the values of mode field diameter varied independently. They must have been determined by differently primary fibre characteristics.

The highest levels of correlation between the data sets C and B, occurred for the 1550 nm smooth mesh and rubber series. In this test, there was a significant tendency for multiple independent variables to have a direct effect upon the dependent variable. This absence of this trait amongst the other test/light wavelength combinations, suggested that the mode of light active in the smooth mesh and rubber test at 1550 nm were markedly different to those active in the other tests. This tends to suggest that the smooth mesh and rubber test at the 1550 nm wavelength was not producing microbends as pure as those in the other three cases.

Throughout the 1550 nm smooth mesh and rubber test regressions, the concentricity at the tan end of the fibre preform was constantly a significant factor. This variable was felt to be most relevant when the fibre was being compressed and lines of stress in the fibre cross section caused signal attenuation by polarising it. The reason tan end and not blue end concentricity was always chosen may have been because the majority of test fibres were coincidentally selected from the "tan" end of the fibre preform, although there was no way to verify this hypothesis. The consistent inclusion of the concentricity variable suggested compression in the 1550 nm smooth mesh and rubber test which verified the above theory that the loss modes active in this test were radically different to those in the other variations. Both the rough and smooth meshed 1300 nm tests returned concentricity as being significant at their lowest level of applied force. This was expected at these lower levels of signal, the pressure would simply compact the fibre rather than force it to follow the form of the mesh. At higher forces, the effect was no longer evident. It was concluded that the 1550 nm smooth mesh and rubber test was the least indicative of microbend susceptibility of all of the tests assessed here.

The actual dip size was seen amongst the significant independent variables in the 1300 nm smooth mesh and rubber regression. The actual dip size was simply a measure of the depth of the dip in refractive index at the centre of the core of an MCVD fibre, as distinct from the calculated dip size, which measured the area of the cone formed in the core refractive index peak by the dip. It can therefore be concluded that it is the depth of the dip, rather than any other characteristic\ of it which affects the radius of the light beam travelling along the fibre and therefore the tendency of that fibre to "leak" light.

The 1300 nm results from both the rough and the smooth mesh tests could be seen to be almost identical. They exhibited both identical correlation coefficient values at each applied force, and used the same independent variables. This suggested that both were testing for the same loss modes.

The test which provided the most accurate results was the 1550 nm smooth mesh and rubber. The inclusion, however of the concentricity in the calculation lead to the belief that compression of the test fibre played a significant part in the test. For this reason, the test was finally rejected as being suitable for the prediction of the microbend resistance of fibres.

The 1300 nm tests were consistent and only included compression as a significant loss mode at the lower values of applied force. They were therefore considered to be more accurate. These tests were felt therefore to be suitable for the assessment of microbend performance of fibres but values of performance predicted for the test using parameters were felt to be slightly unreliable.

The rough mesh and rubber test was seen not only to produce good microbend performance indications, but also to be suitable for simulation using a parameter based model. The reason for the additional predictability of the 1550 nm test might have been the increased mode field diameter of

light at this wavelength. The essentially more unstable wavelength might have accentuated any faults due to parameter make up rendering the fibre's performance more predictable.

The parameter which was most significant on the 1550 nm rough mesh and rubber test was the cut of wavelength. This was not unexpected as the parameter defined the wavelength of light at which bent fibre begins to leak light. This value would tend to indicate the ability of a fibre to constrain its light when subjected to a torturous path.

The regression of cabled fibre performance against parameters yielded the least correlated and most inconsistent results. It was felt that no conclusions could be drawn from the relationships which were established because of the large number of zero correlations evident; and that the relationships which did exist were felt to be established by chance rather than by any actual relationship. Three conclusions could be drawn from the data: either there was no link between the parameters and the performance of the fibres in cables or, the regression system had not been provided with all data necessary to establish a relationship, or the cabling induced losses included other mechanisms than microbending in a random fashion. The latter case was taken to be the case since clearly, the parameters did have an effect upon the final performance of a fibre. The magnitude of the effect of the parameters was unclear when compared to other influences and if the work was to be concluded, these factors should be examined and taken into account. Effects such as the route taken by fibres through the production system to final cable completion obviously had a relevance which was ignored during the main study. Were these effects included, the accuracy of any predictive model might be improved. It was decided that while the inclusion of more factors which might affect cabling performance might improve the accuracy of a model, the final model accuracy might never achieve levels of correlation greater that the minimum required for significant results. Random effects might predominate in cables with controllable effects and measurable parameters taking only a small part. It must be decided how much control is exercised by engineers over process variables and whether

this level allows accurate quantifiable data to be inserted into the regression package before this line of investigation can be further pursued.

The relationship between the fibre performance in cables to tests performance was very similar to its relationship to fibre parameters. while there was less evidence of "non relationships", and the correlation levels seemed higher, there was little evidence of consistency of descriptive microbend test. The gradual decrease in correlation levels as the fibres progressed through the manufacturing process suggested that additional activities introduced additional factors to the fibres, outside what was dealt with by the microbend test. It was not expected that the microbend test would indicate cabled fibre performance, however examination of the results shows that in most cases, fibre susceptibility had a significant relationship with the performance of this in cables. The only stage of production at which fibre performance was close to the line of no significance or where no relationship was found to exist was the final sheathing stage. The final production stage was concluded to introduce the highest level of extraneous effect to the cabled fires. The 1300 nm rough mesh and rubber test was used most often to product the performance of the fibres in the cab;es. It was thought that this was because this test was more general than the 1550 nm rough mesh and rubber test and so would better simulate the effects experienced by the fibres in cables. The low correlation between parameters and cable performance could be associated with this results because of the low levels of correlation experienced between the 1300 nm rough mesh and rubber test and the parameters.. The parameters could model relatively inaccurately, the performance of fibres on the 1300 nm rough mesh and rubber test. Therefore in cables, the cumulative effect of incomplete modelling of the test by the parameters equated to poor modelling of cabled performance by the parameters.

The varying tests used to model the cable performance, indicate the changing effects on the fibres of the tests at different applied forces. The high variability of correlation values for the incremental

section of the performance data, suggests that the results of subtracting two inaccurately modelled base characteristics is a lowered correlation level in the resulting value.

The actual cable performance results suggest that 1300 nm performance is more predictable than 1550 nm performance. This, as described above, may be due to the increased mode field radius at the higher wavelength leading to more loss susceptibility. It also suggests that at 1550 nm, light in fibres is more prone to change be unquantifiable cable effects.

8.6 Interim Conclusions

The research into cabled induced losses produced a test which was both highly repeatable and which indicated of the ability of fibres to resist the microbending mode of loss.

The test was adopted by British Telecommunications as a national test standard and continued promotion through such bodies as IEC, (International Electrotechnical Commission), and ETSI, (European Telecommunications Standards Institute), seeks its international recognition.

Of the tests brought forward from the pilot study, the 1550 nm rough mesh and rubber test was found to be the most indicative of microbend performance, and this test was found to be suitable for modelling using only the parameters of fibres to be tested on it.

Each of the tests considered as part of the main study was found to test slightly different aspects of the fibre ability to constrain light within it under various conditions.

Cut off wavelength and the Gaussian approximation of mode field diameter were found to be significant in determining the resistance of fibres to loss modes. The more accurate definition of mode

field diameter given by the Petermann system was not used as part of any model during the main study. It can be concluded that while the Petermann definition gives a more accurate description of the power distribution within the fibre, the Gaussian system is more useful in the analysis of the implications of mode field diameter upon the fibre's performance.

Different tests were modelled using Gaussian mode field diameters at different wavelengths, (1300 and 1550 nm). This suggested that the relationship between the spot sizes at these two wavelengths were not directly proportional, but were instead slightly mutually independent and as such representative of different aspects of the fibre character.

Of the microbend tests in the main study, the 1550 nm smooth mesh and rubber test produced the least pure microbends. The impurity of loss modes was felt to be principally due to stress in the fibres from compression of the test leading to loss due to polarisation of the signal within it. This test was also observed to be the most easily modelled using the fibre parameters.

The lowest levels of applied force on tests were observed as being the least reliable indication of microbend performance because of their inclusion of compression as a significant mode of loss.

Both the rough and the smooth mesh and rubber tests at the 1300 nm wavelength were found to be producing identical loss modes, possibly because of the relatively small spot size at this wavelength.

The 1300 nm rough mesh and rubber test modelled most closely the cabled performance of fibres. It was therefore concluded to be the most general of the tests investigated as part of the main study.

CHAPTER 9.0.

GENERAL CONCLUSIONS.

9.1 Review.

The project began with a review of the current fibre and cable production technology and of the problems and design criteria normal with both. From a basic understanding of cable induced loss modes and why they come about, the project then moved on to highlight particular areas for study and the preferred mode of research.

Targeting the microbend mode of loss for particular attention, a review of existing test technology was carried out and the shortcomings 2nd advantages of each was highlighted. The test with the most potential-the compression based test-was used as a base and then developed to improve its levels of microbend purity and repeatability.

Using results from this test, links via predictive mathematical modelling between fibre performance of the test and fibre parameters proving the hypothesis that fibre's resistance to loss modes is predetermined by their inherent parameter mix.

Using the test and the mathematical model, a technical paper was presented at the International Wire and Cable Symposium in 1989 in Atlanta Georgia. The paper was subsequently republished as an article in a trade magazine [9.1]. The test was subsequently examined by the optical cabling industry and by British Telecom, (BT), and was eventually adopted by BT as an industry wide reference test method for fibre microbend susceptibility.

The second part of the work sought to continue the development of the predictive performance model into the cabled environment. It sought to link microbend test results, fibre parameters and cabled fibre performance in the same mathematical way as before. At this stage of the work, it was found however that other variables apart from fibre parameters were present and were significant in the determination of fibre performance.

It was at this point that the work was stopped and the lessons learned reviewed. The potential of the line of research had been demonstrated and enough was learned to ensure that with minor additions to the information base, the work could be taken to a successful conclusion.

9.2 Further Work

In order to continue the analysis of loss modes in cables, additional investigation of the systematic and random effect active in cables should be carried out. It was felt that although the models produced for the cabling performance were as accurate as possible given the input data, their accuracy could be improved by more experience of the actual effects.

In addition to merely considering the parameters of input fibres, thought should be given to factors such as production route, which were clearly omitted from the analysis of the main study to date.

It is felt that while the modelling of microbend performance is now possible, work still has to be carried out if successful predictive modelling of the production process is to be accomplished. The experiences of the main study have formed an invaluable base from which this work can be continued to a further stage of refinement.

APPENDICES.

Appendix A

Microbending Technical Paper.

DEVELOPMENT OF A NON-DESTRUCTIVE TEST FOR MICROBEND LOSS MECHANISMS IN CABLED FIBRE.

P.A.Sutton, J.L.L.Roberts, A.T.Summers - STC *
A.Phoenix, D.Rees - Polytechnic of Wales **

* Cable Products Division, Newport, Gwent, UK.
** Treforest, Mid Glamorgan, UK.

ABSTRACT.

Microbending within optical fibres is a loss mechanism which is accentuated during cable manufacture. Whilst the fibres' transmission characteristics are invariably within the required specification, some deteriorate due to the cabling process. No method currently exists for identifying fibres most likely to exhibit this behaviour. This paper describes attempts to address this issue and to identify the parameters dictating microbend performance. A new microbend test is developed which is repeatable and representative, and a model is presented which enables fibre performance to be predicted.

INTRODUCTION.

Optical fibre cables have many advantages over their co-axial and copper equivalents which include light weight, small diameter and excellent transmission characteristics. However, optical waveguides are sensitive to mechanical and environmental influences and the preservation of the fibre's properties is a major challenge in cable manufacture.

Two major mechanisms of signal loss in cabled fibres have been classified as macro and microbending. While the mechanisms of macrobending are well documented and understood [1,2], those of microbending are not. Broadly, microbending is a mechanism of loss caused by perturbations along the fibre axis. The magnitude of the microbending effect in a cabled fibre is a function of both the fibre's parameters, and the way the fibre rests in the cable.

When a bobbin of fibre is tested before cabling to establish its inherent loss, the observed attenuation will not only be a function of the fibre itself, but also of the way it is wound onto the drum. A fibre within specification can appear to have an excessively high loss simply because of poor drum winding. It was for this reason that tests which deduced fibre performance from a short sample taken from a drum were developed.

The causes of microbending are diverse, with the phenomenon being unpredictable and difficult to quantify. This is reflected in the industrial tests which are currently used to measure the effects of microbending and in the general approach to the problem. Two tests for microbending currently in existence are the basket weave and the graphite paper tests [3,4]. They are examples of the traditional approach to microbending and use fibre cross overs and irregular perturbations to promote losses. These methods in general produce unrepeatable results and in the case of the graphite test, can prove destructive to the fibre sample.

Any test should not only classify the loss of a fibre compared to others, but also allow an actual prediction of cabled fibre performance. For this reason, the emphasis of this investigation compared with previous papers [5,6] (which have provided indices of relative performance for various fibre designs), has been the prediction of actual cabled fibre attenuations rather than the comparison of test performances.

A feature of the conventional approach to microbending is to assess the susceptibility of fibres to the phenomenon, without explaining the causes of that susceptibility. An aim of this investigation has therefore been to relate microbend sensitivity to fibre parameters.

From the above considerations, the requirements in analysing the microbending phenomenon were taken to be as follows:-

(i) A repeatable, representative microbend test was required which would be non destructive to the fibre samples;

(ii) The results of the microbending tests should be linked to a fibre's physical characteristics in an attempt to develop loss prediction algorithms relevant to all fibres.

These considerations were predominant in progressing the work.

TEST DEVELOPMENT AND OBJECTIVES.

In the previous section, the objectives of the work were outlined. A microbending test was required which was both repeatable and representative. Repeatability implied not only the need for consistent results across several samples of the same fibre, but also embodied the notion of total test non-destructiveness.

The test was intended to be representative in as far as the results measured could be extrapolated to predict microbend attenuations within cables. The ultimate aim was to quantify the relationship between measured test attenuations and individual fibre parameters. This would allow the test to be superseded by a performance prediction algorithm utilising fibre parameters.

In designing a new microbend test, the shortcomings of existing tests were considered and the design modified to eliminate them. Inconsistencies in results commonly arise due to problems such as:-

(i) The method of perturbation inducement is a random pattern;

(ii) The fibre is placed on the inducement differently each time the test is performed;

(iii) Inconsistent placing of the fibre causes a different length to be compressed during each test.

These shortcomings lead to inaccurate results, producing tests with limited integrity.

The rig designed for this test is shown in Figure 1. It incorporated features to specifically overcome the problems listed above. Mesh was used so that a regular rather than random perturbation pattern was imposed on the fibre; two locating pins prevented all movement between surfaces; and the fibre was laid in a loop so that the sample would experience all directions of mesh to minimise directional inconsistencies. Dimensional accuracy was ensured by marking a circle on the holding material. A slot cut at the fibre crossover prevented spurious

losses due to unwanted compression at this point. The fibre sample was arranged (in a circle of known diameter in a fixed position) on the holding material, which was attached to the top block. This ensured that every sample had an identical position on the mesh. Both the mesh and the top block were located on the pins to ensure consistency of placement.

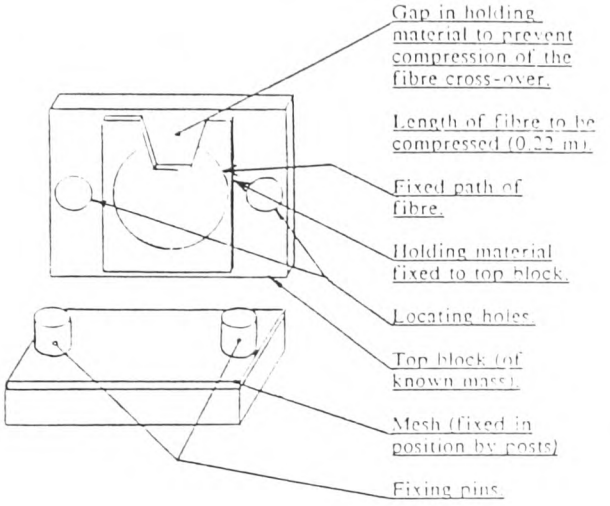

Figure 1. Microbending Test Design.

Two types of gauze, 50 (fine) mesh, and 20 (rough) mesh were used as perturbation inducements in conjunction with two kinds of holding material, neoprene rubber and card. Combinations of these materials produced four variations of the test. On all of these tests, 0.22 m of fibre was compressed by forces of 30, 40, 50, 60 and 70 N. The resulting attenuations were analysed and related to their respective fibre parameters.

The fibre samples were selected at random without regard for their parameters. For this reason, no performance related conclusions should be drawn from the parametric distributions.

CHARACTERISTICS OF CVD AND OVD FIBRE.

Three fibre types were chosen in order to evaluate the validity of the test. The designs were:-

(i) Modified Chemical Vapour Deposition (MCVD) matched cladding single coat fibre;

(ii) Modified Chemical Vapour Deposition (MCVD) depressed cladding double coat fibre;

(iii) Outside Vapour Deposition (OVD) double coated fibre.

For brevity, throughout the remainder of this paper, the aforementioned fibres will be referred to as types A, B and C respectively. The refractive index profiles of these fibres are shown in Figures 2,3,4.

For all fibres, certain parameters were measured in order to relate them to test performance. The refractive index parameters measured are shown in Table 1, along with additional derived values. Figure 2 shows the points on the profiles from which the refractive index parameters were taken.

In addition, the fibre transmission parameters shown in Table 2 were measured for each of the fibres.

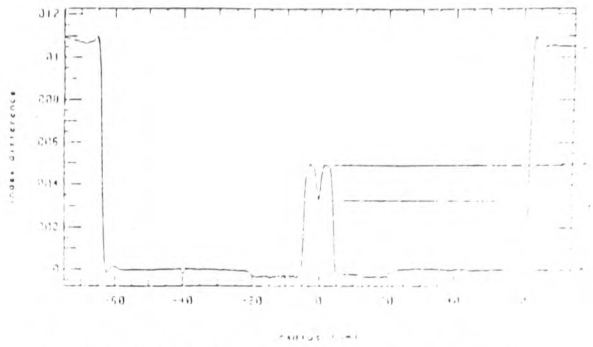

Figure 2. Refractive Index Profile of Type A Fibre.

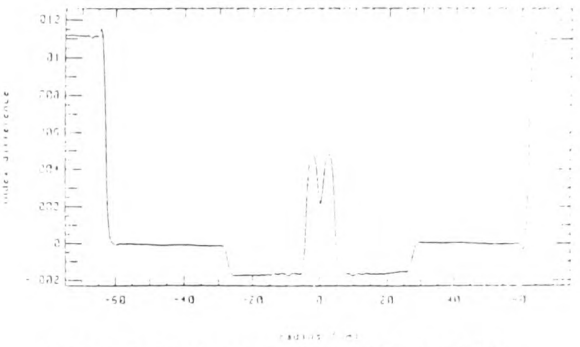

Figure 3. Refractive Index Profile of Type B Fibre.

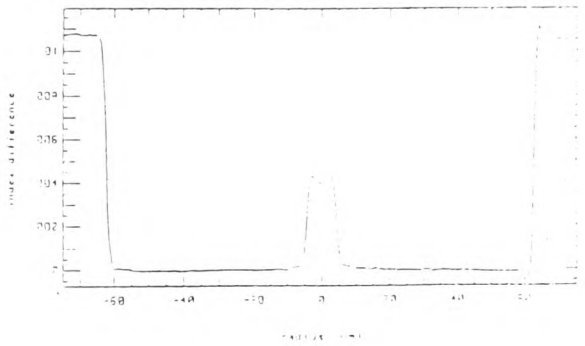

Figure 4. Refractive Index Profile of Type C Fibre.

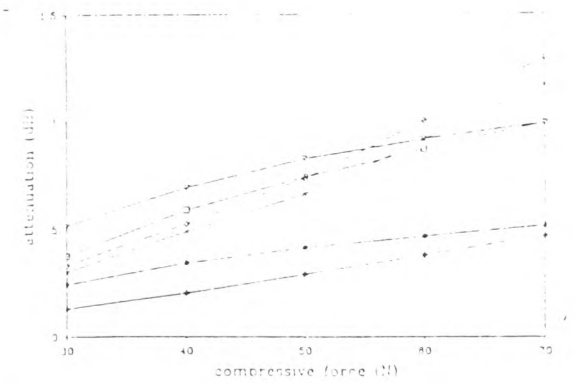

Figure 5. Absolute Attenuations from Type A Fibres on the Smooth Mesh and Rubber Test at 1550 nm.

Parameter	Symbol
dip index	n_d
peak index	n_1
cladding index	n_2
cladding depressed index	n_3
dn* $(n_1 - n_2)$	Δ_n
dip size* $(n_1 - n_d)$	Δ_p
cladding depression* $(n_3 - n_2)$	Δ_c

* derived values.

Table 1. Measured and Derived Refractive Index Parameters with Symbols.

Parameter	Symbol	Dimension
cut off wavelength	λ_c	nm
1300nm Petermann mode field diameter	ω_{p13}	μm
1300nm Gaussian mode field diameter	ω_{g13}	μm
1550nm Petermann mode field diameter	ω_{p15}	μm
1550nm Gaussian mode field diameter	ω_{g15}	μm

Table 2. Measured Fibre Transmission Characteristics, Symbols and Units.

RESULTS.

Figure 5 is an example of a plot of attenuation against applied force for the smooth mesh and rubber test. The graphs demonstrate the individual loss characteristics resulting from each of the tests. Each variant of the test induced differing levels of attenuation in the fibre sample. The rough mesh tests tended to be more severe than the smooth mesh ones, while the rubber caused higher losses than the card.

The tests were designed to induce only the microbending mode of loss. However, it was recognised that other modes of loss might exist, affecting to varying degrees the accuracy of results from the different tests. For this reason, the tests were critically assessed to identify those most likely to produce pure microbending induced attenuations.

The card tests were likely to lead to the fibre undergoing periodic constriction rather than the axial perturbations required for microbending. Therefore whilst producing consistent results, there was evidence that the test promoted modes of loss other than microbending.

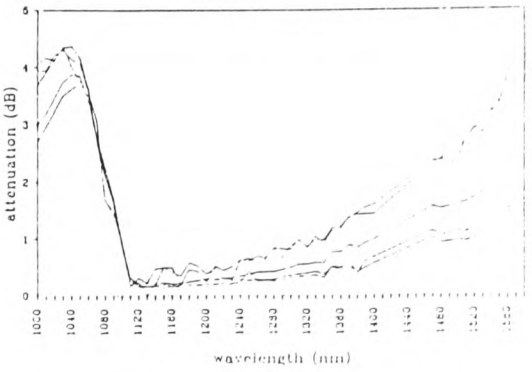

Figure 6. Absolute Spectral Attenuations for Type A Fibres on the Rough Mesh and Rubber Test for Various applied forces.

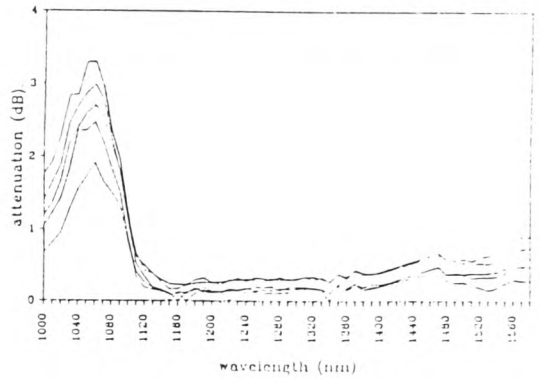

Figure 7. Absolute Spectral Attenuations for Type A Fibres on the Smooth Mesh and Rubber Test for Various applied forces.

The rubber based tests were more likely to cause pure microbending. It was however necessary to ensure that the degree of macrobending was insignificant. This was proved by examination of the information in Figures 6,7, showing spectral attenuations for the rubber tests. For both graphs, each line is a different applied force increasing at intervals of 10 N from 30 to 70 N. Macrobending is evidenced by the attenuation at 1550nm being greater than twice the attenuation at 1300nm [7]. In Figure 6 for some compressive forces, the attenuation at 1550nm met this criterion, suggesting slight macrobending had been induced. On the smooth mesh and rubber test in Figure 7 however, the 1550nm attenuation was always less than twice the 1300 nm result proving the absence of macrobending. The smooth mesh and rubber tests therefore did not produce macrobending as a major mode of loss.

The smooth mesh and rubber test could promote other undesirable modes of loss. If the mesh were too fine, the fibre

would be unable to follow its form and the test would cause mainly compression. The possibility of this effect having any significance, was eliminated by carrying out compression tests between two flat plates. The forces required to produce attenuations of the magnitude observed in the smooth mesh and rubber test, were many times greater than those used in the test itself. Another mode of loss other than compression was therefore in operation, which indicated that microbends had been induced. It was concluded that the smooth mesh and rubber test provided the desired microbending effects.

The observed increase in signal attenuation with applied force, while not being a linear relationship was characteristic for each individual fibre. This suggested that the fibre parameters dictated not only the absolute attenuation, but also the nature of the loss/force relationship.

The signal attenuations for all fibres within a test variation were of comparable magnitude. It could therefore be concluded that the combined effect of each fibre's characteristics, ie. refractive index profile, process method and coating type, lead to microbend resistance levels of a similar order.

The precautions already described for the design and construction of the smooth mesh and rubber test, contributed positively to the repeatability of the measured attenuations. The performance of a fibre was measured by taking five readings on a test and then calculating their average. The repeatability of the test is demonstrated by Figure 8 where for various forces, the distributions of a typical fibre's measured attenuations about their averages are shown. It can be seen that the measured attenuations never exceeded ± 10% of the average attenuation, giving a very high degree of repeatability.

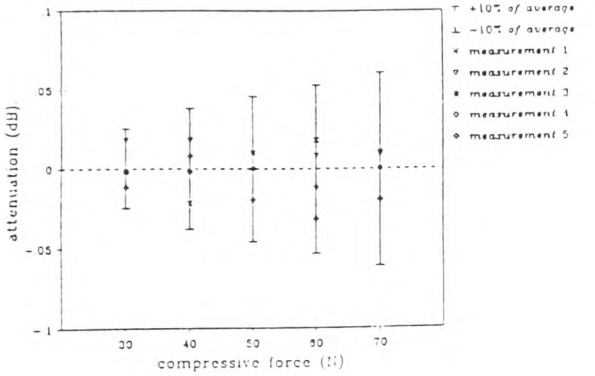

Figure 8. Error in Measured Values at Particular Applied Forces at 1550nm about their Averages.

ANALYSIS.

The consistency of the results verified that a mathematical model could be used to predict the fibre performance, obviating the need to perform the test. The first attempt to quantify the link between parameter and performance involved plotting a fibre's parameters one at a time against its attenuations at each value of applied force for each test. This method was abandoned since it was realised that not only was performance a function of multiple parameters, but the parameters themselves were interrelated. Clearly, no attenuation could be linked to a parameter in isolation, since the mechanism of loss was a function of many variables.

It was for this reason that the method of stepwise multiple regression [8,9], was used to develop the mathematical models. Stepwise multiple regression investigated each of the parameters in turn, its relationship with the fibre performance and its interrelation with other parameters. In this way, it was possible to eliminate parameters detrimental to the model, or so closely linked to other parameters that they contributed nothing to its accuracy.

It was found that the sample of type A fibres had a sufficient spread of parameters to allow the multiple regression programme to run successfully resulting in models with a high confidence limit. This unfortunately was not the case with the type B or C fibres, which had a narrower base of parameters. In these cases, the multiple regression package failed to uncover any attenuation-related parameter trends.

Having selected smooth mesh and rubber as the optimal test, the analysis enabled a mathematical relationship to be developed for the prediction of type A fibre performance. Table 3 displays some of the statistical data which shows the high degree of accuracy to which the model predicted the measured performance. The coefficient of determination, R^2 is a measure of the accuracy of the predicted figures compared with the measured ones. The significant T value is the probability that T, the ratio of each coefficient to its error, occurred as a result of random effects. F is the ability of the equation to explain the variability of the measured values. Significant F is the probability that the relationship stated in the model could have come about by chance. Therefore the combination of high values of R^2,T and F, and negligible 'significant' T and F values, demonstrated the validity of the model.

Table 4 shows the parameters used in the model and the individual coefficients of determination of each when regressed with the microbend attenuation values.

Parameter	Model value
R^2	87%
Signif T (ω_{p15}) (Δ_p) (Δ_n) (constant)	 0.0000 0.0001 0.0117 0.0000
Signif F (all variables)	 0.0000

Table 3. Statistical Parameters Showing Accuracy of Model Relating to the Smooth Mesh and Rubber Test.

Variable	Coeff. of Determination
(ω_{p15})	75%
(Δ_p)	1%
(Δ_n)	21%

Table 4. Coefficients of determination of the individual model variables.

The parameter with the greatest influence on the model's predictions was the 1550nm Petermann mode field diameter (ω_{p15}). The reason for this being that the mode field diameter (mfd) is indicative of the amount of light being carried outside the fibre core. The larger the proportion of light outside the core, the greater the possibility of light leaking out of the fibre when it encountered perturbations. The various mathematical descriptions of mfd are strongly interrelated; thus the multiple

regression programme required only one in the model. The choice of the 1550 nm Petermann representation suggested that for this test, it was the best description of the power distribution within the fibre.

Equation (1) models the 1550 nm performance of type A fibres for the smooth mesh and rubber test using an applied force of 60 N.

$$\text{predicted test attenuation (dB)} = 0.99(\omega_{p15})+245(\Delta_p)-196(\Delta_n)-9.517 \quad (1)$$

where ω_{p15},Δ_p and Δ_n have been defined in Tables 1,2.

Figure 9 shows a plot of predicted against actual attenuation on the smooth mesh and rubber test at 1550 nm using the above equation.

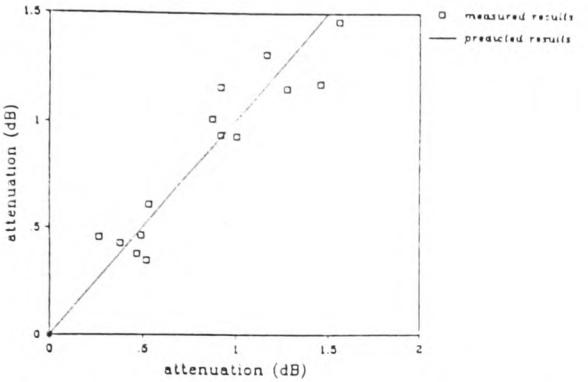

Figure 9. Absolute Attenuations Predicted by the Model for Type A Fibre on the Smooth Mesh and Rubber Test at 1550nm for an Applied Force of 60 N.

CONCLUSIONS.

A repeatable, non destructive optical fibre test was developed which induced microbending as the dominant loss mechanism.

Results using the above test on CVD matched cladding single coat fibre, have been analysed using a stepwise regression technique. This has produced a mathematical model which gives high statistical correlation with measured values, and in which the 1550nm Petermann spot size was the most significant parameter.

ACKNOWLEDGEMENTS.

The authors would like to thank the DTI/SERC, Teaching Company Directorate for their part funding of this programme of work, and STC's directors for their permission to publish this paper.

REFERENCES.

[1] Gambling W.A., Masumura H., Ragdale M.,'Curvature and Microbending Losses in Single-Mode Optical Fibres.',Optical and Quantum Electronics 11, 1979.

[2] Roberts J.L.L., Summers A.T., Barnes S.R.,'Bend Characteristics of Fibres Manufactured by CVD, OVD, and VAD Techniques.', Proc. EFOC/LAN '88, Amsterdam, June 1988.

[3] Grasso G., Meli F., SOCIETA' CAVI PIRELLI S.p.A.-Italy. ECOC '88 - Conference publication number 292 Part 1.

[4] Brambley R.J., Ashworth D.M., STL Report,'Microbending Performance of Fibre Packages.', Private Communication, June 1984.

[5] Artiglia M. et al,'Bending Loss Characterisation in Single-Mode Fibres.', Proc. 13th ECOC '87, Helsinki, Sepetmber 1987.

[6] Francois, Bayon, Alard. 'Characterisation Procedure of Fibre Packaging Relative to Microbends.', Electron. Lett. (G.B.), Vol 21 N°.11, pp 471-2, 23 May '85.

[7] Oswald T., STC Report, Private Commucication, December 1984.

[8] Bond K.M., Scott J.P., 'Essential Business Statistics: a Minitab Framework ', PWS Kent, 1988.

[9] Ryan, Joiner, Ryan, 'Minitab Handbook.', Second Edition, Duxbury Press, 1985.

AUTHORS.

Paul Sutton was born in Birmingham, England in 1966. He attained a B.Eng (Tech) Honours Degree in Mechanical Engineering from the University of Wales Institute of Science and Technology in 1988. In September of the same year, he began a two year Teaching Company Programme with STC and the Polytechnic of Wales for an M. Phil in optical fibre technology. This paper is the result of his work to date. Paul is an associate member of the I. Mech. E.

Llyr Roberts was born in Barry, S. Wales in 1964. He graduated from the Polytechnic of Wales in 1986 with a B.Sc. in Electrical and Electronic Engineering, and then in 1989 with an M. Phil in Optical Fibre Cable Technology gained via a Teaching Company programme with STC. He is currently a senior engineer with STC, where he is the industrial supervisor for this project. In addition, he is studying for a part-time MBA which he hopes to complete in 1990.

Andy Summers was born in Haverfordwest, Wales in 1961. He graduated from Aston University in 1984 with a B.Sc. in Electrical and Electronic Engineering. After this he joined STC as Measurements Engineer, to develop production and reference test methods for optical cable manufacture. In 1986, he became Quality Manager for the Optical Fibre and Cable Manufacturing Units. He transferred to the Technical Department in 1987 with responsibility for optical cable development. He is now the technical manager of STC's cable products division in Newport.

Allan Phoenix graduated in 1972 from Liverpool University with a degree in Electrical Engineering. He was appointed to British Telecom where he had responsibility for Exchange modernisation in Liverpool and later became head of Technical support in the South Wales District. In 1985 he moved to London where he had responsibility for the computerisation of B.T.'s network information. In 1987 he took a Senior lectureship in the Polytechnic of Wales where he lectures in Information Technology and related subjects.

David Rees is the Deputy head of Department of Electrical and Electronic Engineering at the Polytechnic of Wales. He gained the degree of B.Sc. in Electrical Engineering from University College Swansea in 1967, and a Ph.D in Signal Processing applied to composite frequency testing in 1976. His industrial experience includes five years with British Steel and two years with Imperial Chemical Industries. Over the past ten years he has managed a SERC/DTI teaching company between the Polytechnic of Wales and STC. He is a fellow of the IEE.

Appendix B

Procedure for the measurement, and treatment of the resulting data with the fibre loop/wire mesh microbend test.

NOTE: It is essential that repeatability is sought at all stages of testing if repeatable results and pure microbends are to be produced.

The following is for personnel about to begin measuring with the mesh microbend test, and who require a set of data comparing fibres within a sample.

Software Required:

The software used on the test will be required to calculate cumulative attenuation values from a set of incremental increases, produced by the increasing forces applied to the microbend test. The nature of the data which the test produces, and its subsequent processing requirements are described below.

The fibre attenuation is measured before any load is applied to the test.

The top block is applied and when the signal level settles, (some amplifiers use a moving window system of measurement and so a finite delay may be required before true signal level is attained), the level is again measured. The difference between the signal levels before and after the application of the force, is the incremental attenuation arising from an increase in applied force of 30N.

An additional force of 10N is now applied and the incremental increase in attenuation is again measured. The cumulative loss is the sum of the two increments measured so far, and is equal to the increase in attenuation due to an applied force of 40N. This process is repeated until the incremental increase in attenuation due to the applied force increasing from 60 to 70N has been recorded, and the cumulative total calculated. At this stage, all of the force is removed and the process begun again.

Six discrete measurements are therefore necessary in order to deduce the attenuation increments and cumulative totals due to five applied forces. The absolute (cumulative) attenuation due to an applied force, is therefore the sum of the incremental attenuations measured to that point.

Software may be required which is specifically written for the application.

Procedure:

Preparation:

Fibre:

Ensure good cleaves at both ends of the fibre sample,

Ensure the fibre sample is free from grease and that no particles which may affect results are present.

Rig:

Ensure that the rubber "holding material", is securely fixed to the base plate. Any movement of the rubber will allow the pencil fibre loop drawn on it to move relative to the reference posts. A movement of this kind might invalidate test results. If comparison data is required between current and previous fibre samples, then if no movement has occurred of the rubber relative to the reference posts, the comparison will be valid. If the rubber has moved relative to the posts, either:

i) ensure secure fixing of the holding material then calibrate the system using a test fibre, (the test procedure is described below),

ii) secure the holding material, then re-test a number of fibres from a previous sample. Matching results will prove validity of any comparisons made.

Place the wire meshes to be used during the test one at a time on the reference posts. If any "play" is apparent, the holes are too large and smaller ones should be drilled elsewhere on the mesh.

Ensure the mesh markings will facilitate consistent orientation of the meshes (there are four possible mesh positions on the posts).

Place the top block on the reference posts. Excessive play will indicate holes too large; friction preventing smooth movement of the top block along the posts due to holes too small will invalidate measurements made. If the latter condition applies, lubricant may rectify the fault, but may lead to inconsistent loading as its level will constantly vary. The force applied by the top block should be 30N.

Ensure that the holding material is clean and that the fibre circle drawn on it is both clean and sharp: a line which is thin so that no question of the correct placement of the fibre may occur is essential. No inconsistency in the placing of the fibre may be allowed if results with integrity are to be attained.

Ensure that meshes to be used during the test are flat.

Holding tape,

Pieces of tape no wider than 3mm, will be required, and no more than three pieces of tape may be used to fix any fibre sample to the pencil loop on the holding material, (see Fig B.1).

Measurement:

1) Strip and cleave a fibre as well as possible, and insert it into the measuring equipment.

2) Note the signal strength of the light travelling through the unconstrained fibre.

3) Using a maximum of three pieces of tape, (cut as described above), placed at points a,b and c of Fig 1, fix the fibre to the pencil loop. A perfect fit is required and any deviation by the fibre from any part of the pencil loop, will mean that the fibre has to be removed from the holding material, and the measurement process restarted from the start of action point 3.

4) Once fixed to the pencil loop, the signal strength passing through the fibre should be checked. Any change in signal strength will indicate, (if the fibre loop is not too small and hence inducing microbends), that either the fibre, or the holding material has foreign bodies on it capable of invalidating results. In this case, the fibre should be removed from the test rig, and the procedure should be restarted from the fibre preparation section.

5) Check the fibre follows the pencil circle on the holding material perfectly. If it does not, remove the fibre from the holding material and return to action point 3.

6) Set the wavelength of the light at which the test is to be carried out. (For the purposes of this trial, since spectral attenuations will be used, this may not be necessary.)

7) Select the required mesh, (rough or smooth), and place it on the reference posts, checking its orientation.

8) Push the mesh down until it is close to the fibre without coming into contact with it.

9) Take the signal strength reading of the fibre in its unloaded condition.

10) Add the top block, gently lowering it down the reference posts, finally allowing it to push the mesh onto the fibre. At no point should the block be allowed to fall and should be supported until it has come to rest completely.

11) Take a measurement of signal strength: the difference between this and the former reading is the incremental attenuation induced by an applied force of 30N.

12) A force of 10N should now be applied to the top block. If weights are used to do this, they should be lowered with care onto the marked centre of the top block. The signal level should again be measured. When the increment in attenuation between 30 and 40N has been calculated, it is added to the initial incremental increase. The cumulative total is the attenuation caused by an applied force of 40N. This method of measurement is valid, since none of the microbends induced have changed between the first and second levels of force being applied. The fact that two stage loading is used, is irrelevant compared to the fact that no conditions change between stages of loading.

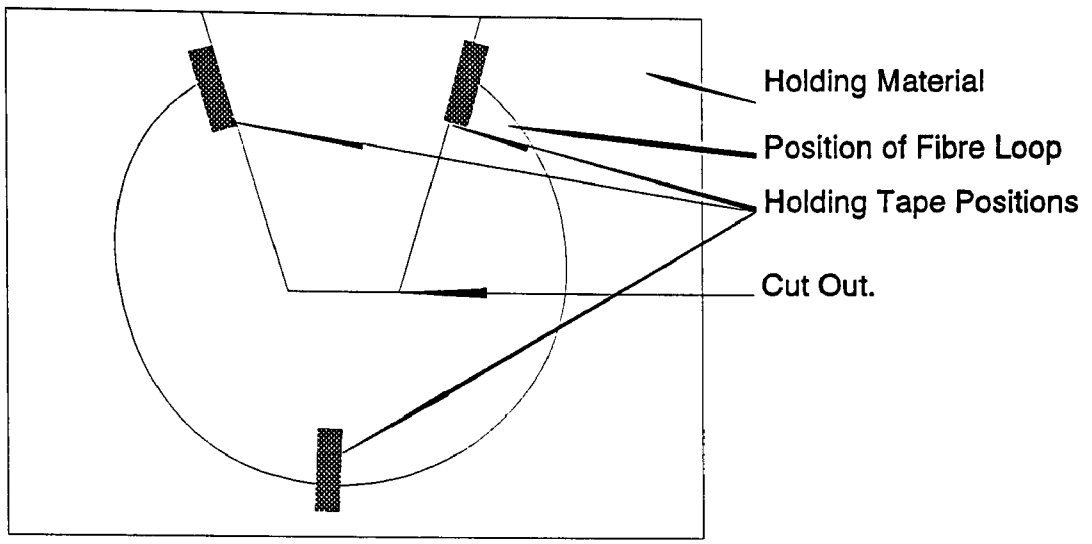

Figure B.1 Recommended Position of Holding Tape on the Fibre Loop.

Table 1 Demonstration of data handling system necessary for the mesh microbend test.

a, measured absolute attenuations.

test	load (*10 N).					
	unloaded	3	4	5	6	7
1	a	b	c	d	e	f
2	g	h	i	j	k	l
3	m	n	o	p	q	r
4	s	t	u	v	w	x
5	y	z	aa	ab	ac	ad

b, calculated incremental increases at each load.

test	load (* 10 N).					
	unloaded	3	4	5	6	7
1		b-a=ae	c-b=af	d-c=ag	e-d=ah	f-e=ai
2		h-g=aj	i-h=ak	j-i=al	k-j=am	l-k=an
3		n-m=ao	o-n=ap	p-o=aq	q-p=ar	r-q=as
4		t-s=at	u-t=au	v-u=av	w-v=aw	x-w=ax
5		z-y=ay	aa-z=az	ab-aa=ba	ac-ab=bb	ad-ac=bc

c, attenuation due to each applied force-cumulative totals.

test	load (* 10 N).					
	unloaded	3	4	5	6	7
1		ae	ae+af=bd	ag+bd=be	ah+be=bf	ai+bf=bg
2		aj	aj+ak=bh	al+bh=bi	am+bi=bj	an+bj=bk
3		ao	ao+ap=bl	aq+bl=bm	ar+bm=bn	as+bn=bo
4		at	at+au=bq	av+bq=br	aw+br=bs	ax+bs=bt
5		ay	ay+az=bu	ba+bu=bv	bb+bw=bx	bc+bx=by
total		bz	ca	cb	cc	cd

d, averages calculating correct test results.

	load (* 10 N).				
	3	4	5	6	7
average	bz/5	ca/5	cb/5	cc/5	cd/5

13) Further increases in mass of 10N, interspersed with measurements are carried out until a total mass of 70N is attained. at each stage of the loading, the incremental increase in attenuation measured is added to the cumulative total that far to deduce the running total. For five incremental increases, six measurements are thus required.

14) Remove all force (including the top block), from the rig. Remove the mesh and check that the fibre is still in place on the pencil loop. If it is not, the previous set of results is invalid and the procedure should be restarted from action point 3.

15) If the fibre remains in place, repeat steps 8-14 a further four times.

16) At the end of the result gathering period, the five sets of cumulative attenuations produced, should be compared, and the final result should be the numerical average of all five results.*

17) If necessary, re-select mesh and spot wavelength as required. There are four possible combinations of mesh and wavelength (1300 and 1550nm), and all should be included for the purposes of this trial.

18) On completion of full tests on a fibre sample, remove the fibre from the rig and test equipment, ensuring all pieces of tape are removed from the holding material.

19) If any more fibres are required, return to the start of the check procedure with the new fibre.

* Table 1 demonstrates the principle of data collection described in action points 10-16.

Appendix C

Spreadsheets Uses for Data Storage.

(1300nm Rough Mesh and Card and 1550nm Smooth

Mesh and Rubber Sheets Displayed)

rough mesh and card measured data
1300

MAKER	FIBRE ID	CUT	INDUCEMENT
ofu	b9396601a6241	1	rough mesh
ofu ap	c9311062a201		rough mesh
ofu ap	c9311112a402		rough mesh
ofu ap	c9311091a501		rough mesh
ofu ap	b9357331a203		rough mesh
ofu ap	b9357252a302		rough mesh
ofu ap	c9271382a321		rough mesh
ofu ap	c9347171a601		rough mesh
ofu ap	c9357221a121		rough mesh
ofu	b9396752a3081	1	rough mesh
ofu ap	b9357201a501		rough mesh
ofu	b9396871a5072	2	rough mesh
ofu	b9396591a8061	1	rough mesh
ofu	b9396741a1031	1	rough mesh
ofu	b9396671a6221	1	rough mesh
ofu	b9396631a1052	2	rough mesh
ofu ap	c9311091a102		rough mesh
ofu ap	c9316422a101		rough mesh
ofu ap	c9316441a301		rough mesh
ofu ap	c9311152a101		rough mesh
ofu ap	c9357271a531		rough mesh
ofu ap	c9311091a502		rough mesh
ofu	b9407371a5021	1 of 1	rough mesh
ofu	a9407361a4031	1 of 2	rough mesh
ofu	a9407251a7211	1	rough mesh
ofu	a9407361a1042	2 of 1	rough mesh
ofu	b9406081a6031	1 of 1	rough mesh
ofu	a9416271a1031	1 of 2	rough mesh
ofu	b9407741a2022	2 of 2	rough mesh
ofu	b9416331a2011	1 of 1	rough mesh
ofu	b9407341a2021	1 of 2	rough mesh
ofu	b9407371a3012	2 of 2	rough mesh
ofu	b9407251a6051	1 of 1	rough mesh
ofu ag	u6b9357252a6011	1 of 2	rough mesh
ofu ag	u6b9397721a5022	2 of 2	rough mesh
ofu ag	u6b9406021a3041	1 of 2	rough mesh
ofu ag	u6b9397641a1051	1 of 1	rough mesh
ofu	b9396811a2011	1	rough mesh
ofu ag	u6b9397871a5031	1 of 2	rough mesh
ofu ag	u6b9397641a2081	1 of 2	rough mesh
ofu ag	u6c9397011a1072	2 of 2	rough mesh
ofu ag	u6b9396491a4062	2 of 2	rough mesh
ofu ag	u7b9406061a2021	1 of 2	rough mesh
ofu ag	u7b9397431a8011	1 of 2	rough mesh
ofu ag	u7b9406021a2071	1 of 1	rough mesh
ofu ag	u7b9406021a4061	1 of 2	rough mesh
ofu ag	u7b9397641a3281	1	rough mesh
ofu ag	u7b9397871a2252	2	rough mesh
ofu ag	u7b9397431a5041	1 of 2	rough mesh
ofu ag	u2b9406071a3031	1 of 2	rough mesh
ofu ag	u2c9397011a2012	2 fo 2	rough mesh
ofu ag	u7b9397871a5032	2 of 2	rough mesh

HOLDING MATERIAL	BLOCK MASS (KG)	FIBRE LENGTH (cm)	150-T A
card	3.127	22.05	0.05
card	3.127	22.05	1.15
card	3.127	22.05	0.86
card	3.127	22.05	1.08
card	3.127	22.05	1.31
card	3.127	22.05	0.39
card	3.127	22.05	1.39
card	3.127	22.05	0.68
card	3.127	22.05	1.08
card	3.127	22.05	0.5
card	3.127	22.05	1.5
card	3.127	22.05	0.04
card	3.127	22.05	0.12
card	3.127	22.05	0.16
card	3.127	22.05	0.11
card	3.127	22.05	0.1
card	3.127	22.05	0.99
card	3.127	22.05	1.76
card	3.127	22.05	1.3
card	3.127	22.05	0.5
card	3.127	22.05	0.79
card	3.127	22.05	1.17
card	3.127	22.05	0.65
card	3.127	22.05	0.59
card	3.127	22.05	1.03
card	3.127	22.05	0.49
card	3.127	22.05	0.54
card	3.127	22.05	0.75
card	3.127	22.05	0.74
card	3.127	22.05	1.84
card	3.127	22.05	2.37
card	3.127	22.05	1.28
card	3.127	22.05	0.77
card	3.127	22.05	1.19
card	3.127	22.05	2.1
card	3.127	22.05	1.16
card	3.127	22.05	1.16
card	3.127	22.05	0.06
card	3.127	22.05	1.94
card	3.127	22.05	0.73
card	3.127	22.05	1.52
card	3.127	22.05	1.07
card	3.127	22.05	1.08
card	3.127	22.05	2.53
card	3.127	22.05	0.49
card	3.127	22.05	0.9
card	3.127	22.05	1.91
card	3.127	22.05	1
card	3.127	22.05	1.43
card	3.127	22.05	1.53
card	3.127	22.05	1.26
card	3.127	22.05	0.73

card	3.127	22.05	1.21
card	3.127	22.05	1.01
card	3.127	22.05	1.57
card	3.127	22.05	1.58
card	3.127	22.05	2.19

15T-1 A	151-2 A	152-3 A	153-4 A	150-T B	15T-1 B	151-2 B	152-3 B
0.08	0.06	0.15	-0.03	0.86	0.42	0.2	0.22
0.21	0.2	0.22	0.45	1.29	0.17	0.16	0.33
0.21	0.1	0.18	0.15	0.98	0.09	0.04	0.11
0.24	0.21	0.21	0.15	1.16	0.26	0.15	0.24
0.38	0.41	0.14	0.26	1.32	0.4	0.39	0.26
0.08	0.08	0.07	0.04	0.38	0.09	0.14	0.03
0.43	0.38	0.13	0.37	1.4	0.32	0.34	0.25
0.21	0.18	0.07	0.19	0.67	0.26	0.13	0.1
0.32	0.28	0.1	0.08	1.17	0.28	0.22	0.12
0.14	0.09	0.01	-0.01	0.47	0.08	0.06	0.04
0.36	0.38	0.21	0.29	1.55	0.25	0.44	0.32
0.04	0.09	0.11	0.09	0.07	0.01	0.08	0.1
0.13	0.13	0.18	0.09	0.18	0.09	0.14	0.15
0.02	0.03	0.09	0.09	0.11	0.15	0.01	0.11
0.04	0.11	0.07	0.12	0.2	-0.02	0.14	0.1
0.06	0.09	0.12	0.13	0.14	0.04	0.1	0.11
0.26	0.1	0.16	0.06	1	0.17	0.25	0.08
0.11	0.71	0.31	0.08	1.87	0.42	0.29	0.38
0.57	0.65	0.35	0.35	1.38	0.57	0.62	0.34
0.13	0.27	0.13	0.11	0.56	0.17	0.24	0.25
0.18	0.21	0.21	0.13	0.79	0.3	0.13	0.24
0.23	0.13	0.19	0.19	1.28	0.13	0.19	0.12
0.17	0.28	0.05	0.17	0.58	0.24	0.26	0.15
0.1	0.12	0.11	0.11	0.66	0.06	0.12	0.04
0.27	0.45	0.15	0.25	1	0.26	0.24	0.18
0.15	0.14	0.14	0.18	0.62	0.16	0.15	0.11
0.37	0.36	0.34	0.2	0.59	0.37	0.45	0.27
0.22	0.08	0.24	0.1	0.72	0.21	0.07	0.15
0.09	0.11	0.07	0.1	0.82	0.02	0.04	0.12
0.48	0.42	0.4	0.23	1.78	0.37	0.39	0.44
0.76	0.47	0.4	0.33	2.24	0.75	0.58	0.58
0.29	0.18	0.18	0.16	1.31	0.18	0.2	0.19
0.26	0.26	0.27	0.17	0.94	0.21	0.18	0.26
0.21	0.24	0.08	0.2	1.2	0.26	0.16	0.12
0.59	0.63	0.42	0.35	2	0.65	0.53	0.45
-0.02	0.04	-0.01	0.02	1.19	-0.03	-0.04	0
0.15	0.09	0.06	0.11	1.2	0.18	-0.04	0.16
0.01	0.01	0	0.04	0.05	-0.07	0.1	0.04
0.38	0.46	0.29	0.3	1.75	0.62	0.42	0.23
0.15	0.09	0.09	0.17	0.75	0.05	0.07	0.14
0.4	0.32	0.16	0.31	1.52	0.38	0.24	0.3
0.21	0.13	0.11	0.02	1.35	0.23	0.17	-0.07
0.29	0.34	0.18	0.31	1.14	0.23	0.24	0.23
0.62	0.12	0.28	0.34	2.51	0.59	0.3	0.26
0.07	0.05	0	0.08	0.52	0.09	0.04	0.05
0.37	0.29	0.27	0.32	0.82	0.39	0.27	0.27
0.56	0.67	0.36	0.3	1.95	0.52	0.51	0.41
0.22	0.25	0.23	0.19	1.12	0.28	0.19	0.29
0.58	0.36	0.33	0.2	1.48	0.53	0.4	0.35
0.38	0.08	0.19	0.09	1.63	0.19	0.17	0.13
0.05	0.05	0.13	0.23	1.14	0.12	0.01	0.07
0.31	0.25	0.19	0.21	0.73	0.27	0.18	0.17

0.07	0.02	0.11	0.13	1.36	0.04	0.03	-0.02
0.32	0.35	0.19	0.13	1.18	0.41	0.13	0.27
0.4	0.37	0.18	0.14	1.5	0.5	0.15	0.12
0.26	0.19	0.05	0.19	1.48	0.3	0.31	0.16
0.55	0.51	0.25	0.26	2.22	0.53	0.51	0.26

153-4 B	150-T C	15T-1 C	151-2 C	152-3 C	153-4 C	150-T D	15T-1 D
0.12	0.12	0.06	0.03	0.12	0.09	0.06	0.09
0.29	1.16	0.29	0.2	0.24	0.27	1.23	0.18
0.2	0.95	0.12	0.12	0.12	0.13	1.04	0.09
0.11	1.1	0.26	0.2	0.19	0.14	1.25	0.13
0.14	1.33	0.32	0.38	0.25	0.26	1.2	0.45
0.05	0.46	0.06	0.11	0.04	0.09	0.4	0.09
0.24	1.39	0.44	0.2	0.25	0.27	1.48	0.36
0.12	0.68	0.17	0.2	0.12	0.15	0.8	0.15
0.3	1	0.27	0.33	0.04	0.19	1.11	0.18
0.04	0.49	0.12	0.02	0.08	0.1	0.51	0
0.14	1.57	0.16	0.44	0.2	0.14	1.66	0.35
0.05	0.04	0.05	0.03	0.14	0.08	0.09	0.01
0.28	0.13	0.17	0.11	0.27	0.17	0.14	0.13
0.03	0.11	0	0.11	0.05	0.07	0.16	0.11
0.1	0.14	0.05	0.09	0.09	0.11	0.09	0.09
0.13	0.12	0.07	0.08	0.08	0.1	0.16	0.05
0.11	1.02	0.2	0.19	0.11	0.13	0.92	0.29
0.23	1.8	0.19	0.51	0.35	0.22	1.98	0.23
0.31	1.41	0.5	0.63	0.41	0.33	1.48	0.6
0.03	0.59	0.25	0.14	0.09	0.19	0.6	0.17
0.1	0.8	0.35	0.1	0.21	0.16	0.9	0.22
0.23	1.18	0.21	0.17	0.1	0.26	1.2	0.2
0.05	0.62	0.15	0.23	0.21	0.11	0.76	0.12
0.14	0.56	0.11	0.1	0.14	0.02	0.61	0.07
0.23	1.17	0.36	0.01	0.15	0.27	1.05	0.18
0.16	0.55	0.24	0.09	0.09	0.14	0.62	0.22
0.25	0.5	0.34	0.32	0.43	0.22	0.63	0.3
0.1	0.71	0.2	0.12	0.17	0.09	0.72	0.11
0.04	0.83	-0.01	0.08	0.06	0.06	0.85	0.01
0.18	1.71	0.42	0.39	0.35	0.33	1.65	0.39
0.2	2.42	0.67	0.43	0.55	0.38	2.31	0.62
0.16	1.38	0.25	0.27	0.14	0.2	1.44	0.34
0.13	0.85	0.31	0.23	0.14	0.26	0.92	0.15
0.16	1.21	0.11	0.23	0.14	0.22	1.15	0.19
0.29	2.06	0.61	0.6	0.39	0.35	2.08	0.6
0.03	1.13	-0.02	0.03	-0.02	0.1	1.15	0.11
0.03	1.21	0.07	0.17	0.02	0.1	1.18	0.14
-0.01	0.01	0.01	0.04	0.06	0.02	0.05	0.04
0.17	1.81	0.5	0.32	0.22	0.3	1.96	0.38
0.21	0.7	0.08	0.04	0.14	0.17	0.64	0.05
0.26	1.58	0.32	0.31	0.29	0.26	1.53	0.46
0.15	1.28	0.19	0.11	0.03	0.11	1.18	0.14
0.27	1.12	0.2	0.19	0.26	0.34	1.19	0.27
0.2	2.47	0.6	0.36	0.26	0.3	2.65	0.45
0.07	0.54	0.1	0	0.07	0.03	0.57	0.11
0.32	0.9	0.38	0.19	0.33	0.36	0.87	0.33
0.27	1.97	0.55	0.64	0.33	0.4	1.91	0.62
0.17	1.09	0.2	0.29	0.14	0.25	1.02	0.24
0.31	1.51	0.46	0.4	0.33	0.28	1.51	0.47
0.04	1.6	0.21	0.24	0.11	0.1	1.59	0.36
0.14	1.21	0.07	0.07	-0.01	0.18	1.17	0.1
0.25	0.8	0.24	0.18	0.22	0.3	0.76	0.26

0.13	1.29	-0.08	0.01	-0.03	0.1	1.03	-0.04
0.16	1.21	0.28	0.27	0.35	0.06	1.14	0.32
0.14	1.63	0.36	0.29	0.13	0.03	1.59	0.42
0.19	1.55	0.28	0.2	0.17	0.19	1.5	0.25
0.32	2.21	0.61	0.42	0.34	0.27	2.28	0.37

151-2 D	152-3 D	153-4 D	150-T E	15T-1 E	151-2 E	152-3 E	153-4 E
0.05	0.14	0.07	0.03	0.06	0.11	0.09	0.08
0.33	0.14	0.28	1.28	0.19	0.13	0.32	0.31
0.02	0.2	0.12	1.01	0.14	0.02	0.17	0.17
0.28	0.15	0.12	1.17	0.18	0.22	0.16	0.08
0.33	0.26	0.23	1.39	0.33	0.35	0.25	0.27
0.03	0.07	0.01	0.37	0.11	0.13	-0.03	0.13
0.26	0.15	0.23	1.36	0.4	0.35	0.17	0.33
0.12	0.17	0.11	0.74	0.15	0.15	0.11	0.2
0.29	0.11	0.15	1.14	0.2	0.28	0.2	0.09
0.14	0.08	0.07	0.41	0.12	0.02	-0.02	0.19
0.29	0.16	0.14	1.67	0.28	0.23	0.32	0.09
0.02	0.04	0.1	0.1	0.03	0.06	0.12	0.1
0.08	0.2	0.21	0.09	0.14	0.13	0.16	0.07
0.04	0.07	0.11	0.19	0.08	0.11	0.07	0.03
0.06	0.15	0.08	0.16	0	0.05	0.12	0.13
0.1	0.14	0.06	0.14	0.05	0.09	0.08	0.18
0.15	0.05	0.06	0.99	0.29	0.16	0.07	0.13
0.42	0.26	0.24	1.78	0.38	0.35	0.24	0.17
0.5	0.35	0.45	1.36	0.63	0.55	0.41	0.26
0.24	0.2	0.06	0.61	0.21	0.23	0.15	0.13
0.19	0.19	0.15	0.9	0.24	0.23	0.1	0.14
0.17	0.06	0.22	1.14	0.29	0.13	0.2	0.2
0.24	0.13	0.1	0.57	0.16	0.23	0.19	0.13
0.1	0.13	0.05	0.57	0.01	0.17	0.09	0.09
0.45	0.14	0.23	1.09	0.24	0.24	0.17	0.2
0.08	0.16	0.14	0.67	0.17	0.08	0.13	0.16
0.37	0.33	0.34	0.63	0.46	0.25	0.34	0.4
0.16	0.17	0.12	0.79	0.19	0.17	0.06	0.16
0.04	0.02	0.04	0.75	0.06	0.04	0.05	0.06
0.46	0.32	0.41	1.63	0.48	0.41	0.39	0.23
0.62	0.34	0.28	2.19	0.65	0.63	0.44	0.25
0.25	0.11	0.09	1.21	0.33	0.33	0.17	0.16
0.27	0.23	0.11	0.88	0.13	0.35	0.14	0.21
0.19	0.16	0.25	1.23	0.27	0.16	0.11	0.24
0.56	0.4	0.32	1.98	0.66	0.51	0.39	0.45
-0.15	0.03	0.02	1.1	0.06	-0.05	-0.08	0.04
0.09	0.13	0.07	1.2	0.18	0.13	0.05	0.07
0.05	-0.03	0.03	0.09	0.01	0.09	0.12	0.09
0.4	0.21	0.16	1.83	0.41	0.33	0.3	0.09
0.15	0.08	0.21	0.67	0.1	0.08	0.15	0.28
0.14	0.17	0.21	1.47	0.38	0.36	0.15	0.31
0.15	0.02	0.11	1.23	0.08	0.18	0.07	0.11
0.22	0.11	0.4	1.31	0.26	0.24	0.21	0.31
0.5	0.15	0.34	2.6	0.57	0.41	0.19	0.46
0.05	0.03	0.06	0.55	0.08	0.07	0.08	0.04
0.28	0.23	0.28	0.9	0.39	0.2	0.33	0.26
0.37	0.3	0.34	1.9	0.61	0.32	0.37	0.39
0.11	0.25	0.18	0.94	0.13	0.22	0.2	0.16
0.38	0.31	0.21	1.46	0.5	0.3	0.46	0.26
0.17	0.16	0.2	1.56	0.47	0.07	0.17	0.05
0.06	0.05	0.03	1.09	0.12	0.06	0.03	0.14
0.13	0.21	0.25	0.83	0.2	0.15	0.23	0.21

-0.02	0.05	0.07	0.97	0.01	0	0.01	0.12
0.22	0.35	0.09	1.19	0.3	0.24	0.2	0.11
0.22	0.23	0.19	1.59	0.42	0.24	0.1	0.11
0.19	0.19	0.2	1.52	0.31	0.13	0.1	0.26
0.45	0.3	0.3	2.09	0.56	0.4	0.26	0.22

smooth mesh and rubber measured data
1550

MAKER	FIBRE ID	CUT	INDUCEMENT
ofu	b9396601a6241	1	smooth mesh
ofu ap	c9311062a201		smooth mesh
ofu ap	c9311112a402		smooth mesh
ofu ap	c9311091a501		smooth mesh
ofu ap	b9357331a203		smooth mesh
ofu ap	b9357252a302		smooth mesh
ofu ap	c9271382a321		smooth mesh
ofu ap	c9347171a601		smooth mesh
ofu ap	c9357221a121		smooth mesh
ofu	b9396752a3081	1	smooth mesh
ofu ap	b9357201a501		smooth mesh
ofu	b9396871a5072	2	smooth mesh
ofu	b9396591a8061	1	smooth mesh
ofu	b9396741a1031	1	smooth mesh
ofu	b9396671a6221	1	smooth mesh
ofu	b9396631a1052	2	smooth mesh
ofu ap	c9311091a102		smooth mesh
ofu ap	c9316422a101		smooth mesh
ofu ap	c9316441a301		smooth mesh
ofu ap	c9311152a101		smooth mesh
ofu ap	c9357271a531		smooth mesh
ofu ap	c9311091a502		smooth mesh
ofu	b9407371a5021	1 of 1	smooth mesh
ofu	a9407361a4031	1 of 2	smooth mesh
ofu	a9407251a7211	1	smooth mesh
ofu	a9407361a1042	2 of 1	smooth mesh
ofu	b9406081a6031	1 of 1	smooth mesh
ofu	a9416271a1031	1 of 2	smooth mesh
ofu	b9407741a2022	2 of 2	smooth mesh
ofu	b9416331a2011	1 of 1	smooth mesh
ofu	b9407341a2021	1 of 2	smooth mesh
ofu	b9407371a3012	2 of 2	smooth mesh
ofu	b9407251a6051	1 of 1	smooth mesh
ofu ag	u6b9357252a6011	1 of 2	smooth mesh
ofu ag	u6b9397721a5022	2 of 2	smooth mesh
ofu ag	u6b9406021a3041	1 of 2	smooth mesh
ofu ag	u6b9397641a1051	1 of 1	smooth mesh
ofu	b9396811a2011	1	smooth mesh
ofu ag	u6b9397871a5031	1 of 2	smooth mesh
ofu ag	u6b9397641a2081	1 of 2	smooth mesh
ofu ag	u6c9397011a1072	2 of 2	smooth mesh
ofu ag	u6b9396491a4062	2 of 2	smooth mesh
ofu ag	u7b9406061a2021	1 of 2	smooth mesh
ofu ag	u7b9397431a8011	1 of 2	smooth mesh
ofu ag	u7b9406021a2071	1 of 1	smooth mesh
ofu ag	u7b9406021a4061	1 of 2	smooth mesh
ofu ag	u7b9397641a3281	1	smooth mesh
ofu ag	u7b9397871a2252	2	smooth mesh

```
ofu ag u7b9397431a5041        1 of 2   smooth mesh
ofu ag u2b9406071a3031        1 of 2   smooth mesh
ofu ag u2c9397011a2012        2 fo 2   smooth mesh
ofu ag u7b9397871a5032        2 of 2   smooth mesh
ofu ag u2b9397871a2251                 1 smooth mesh
ofu ag u2b9406021a4062        2 of 2   smooth mesh
ofu ag u2c9397011a1271                 1 smooth mesh
ofu ag u2b9397641a2282                 2 smooth mesh
ofu ag u3b9357252a6012        2 of 2   smooth mesh
```

HOLDING MATERIAL	BLOCK MASS (KG)	FIBRE LENGTH (cm)
rubber	3.127	22.05
rubber	3.127	22.05
rubber	3.127	22.05

rubber	3.127	22.05
rubber	3.127	22.05
rubber	3.127	22.05
rubber	3.127	22.05
rubber	3.127	22.05
rubber	3.127	22.05
rubber	3.127	22.05
rubber	3.127	22.05
rubber	3.127	22.05

150-T A	15T-1 A	151-2 A	152-3 A	153-4 A	150-T B
0.23	0.05	0.08	0.02	0.06	0.21
0.26	0.12	0.16	0.1	0.14	0.24
0.05	0.02	0.01	0.02	0	0.06
0.15	0.1	0.13	0.06	0.14	0.17
0.19	0.13	0.09	0.11	0.04	0.15
0.13	0.05	0.05	0.07	0.07	0.17
0.23	0.15	0.2	0.09	0.15	0.27
0.15	0.08	0.07	0.09	0.03	0.11
0.31	0.15	0.14	0.12	0.15	0.32
0.45	0.19	0.08	0.17	0.21	0.32
0.1	0.05	0.05	0.03	0.08	0.1
0.17	0.1	0.39	0.31	1.99	0.2
0.27	0.1	0.05	0.13	0.11	0.29
0.07	0.09	0.09	0.05	0.11	0.1
0.23	0.12	0.12	0.16	0.18	0.2
0.67	0.34	0.36	0.28	0.28	0.63
0.18	0.07	0.1	0.1	0.07	0.24
0.24	0.11	0.09	0.1	0.15	0.27
0.21	0.15	0.08	0.08	0.12	0.27
0.1	0.04	0.1	0.06	0.07	0.15
0.18	0.06	0.08	0.11	0.08	0.13
0.33	0.16	0.16	0.16	0.16	0.39
0.2	0.12	0.15	0.14	0.14	0.18
0.35	0.1	0.17	0.17	0.2	0.29
0.15	0.13	0.12	0.08	0.07	0.28
0.16	0.11	0.11	0.02	0.07	0.21
0.17	0.08	0.05	0.13	0.05	0.15
0.13	0.1	0.07	0.05	0.06	0.16
0.36	0.1	0.15	0.15	0.18	0.31
0.25	0.07	0.12	0.18	0.07	0.21
0.32	0.14	0.1	0.11	0.13	0.31
0.26	0.08	0.08	0.09	0.08	0.26
0.24	0.17	0.13	0.1	0.11	0.33
0.5	0.22	0.15	0.18	0.18	0.51
0.25	0.13	0.17	0.1	0.16	0.25
0.35	0.13	0.1	0.12	0.13	0.36
0.3	0.14	0.07	0.15	0.16	0.27
0.1	0.08	0	0.07	0.07	0.11
0.27	0.14	0.12	0.11	0.13	0.34
0.31	0.12	0.09	0.06	0.19	0.32
0.55	0.24	0.11	0.3	0.2	0.52
0.38	0.22	0.17	0.2	0.21	0.38
0.41	0.19	0.17	0.25	0.14	0.47
0.18	0.12	0.11	0.07	0.12	0.2
0.32	0.18	0.2	0.18	0.17	0.22
0.28	0.11	0.1	0.13	0.16	0.28
0.23	0.1	0.2	0.04	0.08	0.21
0.26	0.02	0.15	0.1	0.1	0.21

0.43	0.24	0.27	0.28	0.33	0.44
0.23	0.1	0.08	0.12	0.11	0.17
0.4	0.31	0.19	0.24	0.25	0.37
0.29	0.16	0.13	0.18	0.22	0.25
0.23	0.18	0.02	0.11	0.08	0.26
0.16	0.18	-0.04	0.13	0.07	0.19
0.26	0.11	0.07	0.1	0.13	0.25
0.51	0.19	0.21	0.26	0.3	0.53
0.28	0.1	0.14	0.12	0.08	0.3

15T-1 B	151-2 B	152-3 B	153-4 B	150-T C	15T-1 C
0.15	0.04	0.04	0.05	0.21	0.13
0.14	0.16	0.11	0.06	0.28	0.16
-0.02	0	0.03	0.05	0.03	0.03
0.15	0.04	0.1	0.13	0.18	0.13
0.11	0.1	0.12	0.1	0.22	0.08
0.02	0.07	0.1	0.05	0.2	0.07
0.08	0.15	0.12	0.11	0.31	0.13
0.08	0.09	0.06	0.1	0.17	0.06
0.18	0.19	0.13	0.18	0.32	0.16
0.26	0.2	0.1	0.16	0.45	0.18
0.09	0.05	0.03	0.04	0.15	0.05
0.09	0.1	0.09	0.05	0.26	0.03
0.08	0.14	0.18	0.15	0.11	0.34
0.05	0.07	0.1	0.08	0.1	0.11
0.17	0.18	0.14	0.22	0.22	0.17
0.24	0.3	0.27	0.3	0.72	0.27
0.04	0.14	0.02	0.13	0.18	0.05
0.09	0.09	0.09	0.14	0.3	0.05
0.1	0.08	0.07	0.09	0.24	0.06
0.04	0.05	0.07	0.06	0.11	0.08
0.12	0.07	0.11	0.06	0.14	0.06
0.14	0.18	0.15	0.14	0.38	0.16
0.14	0.05	0.15	0.14	0.18	0.1
0.22	0.19	0.18	0.14	0.2	0.23
0.11	0.06	0.11	0.07	0.21	0.12
0.02	0.06	0.1	0.05	0.21	0.12
0.07	0.07	0	0.1	0.11	0.08
0.07	0.09	0.06	0.09	0.1	0.1
0.1	0.09	0.19	0.08	0.26	0.15
0.11	0.16	0.09	0.14	0.22	0.11
0.13	0.11	0.11	0.05	0.3	0.17
0.08	0.07	0.11	0.04	0.28	0.08
0.11	0.08	0.17	0.13	0.01	0.46
0.18	0.17	0.24	0.17	0.43	0.19
0.07	0.18	0.13	0.16	0.26	0.09
0.16	0.13	0.05	0.2	0.33	0.06
0.19	0.1	0.11	0.15	0.34	0.11
-0.04	0.06	0.1	0.13	0.16	0.02
0.09	0.12	0.09	0.13	0.24	0.18
0.1	0.19	0.06	0.17	0.25	0.15
0.21	0.21	0.14	0.26	0.46	0.21
0.22	0.12	0.23	0.14	0.42	0.17
0.14	0.31	0.27	0.13	0.5	0.25
0.14	0.05	0.13	0.11	0.21	0.05
0.19	0.2	0.15	0.28	0.33	0.15
0.09	0.12	0.08	0.13	0.24	0.08
0.12	0.07	0.1	0.17	0.24	0.15
0.08	0.1	0.14	0.06	0.19	0.08

0.2	0.26	0.27	0.29	0.46	0.24
0.1	0.08	0.1	0.15	0.17	0.09
0.22	0.24	0.26	0.14	0.38	0.3
0.17	0.17	0.19	0.19	0.28	0.17
0.12	0.09	0.12	0.08	0.25	0.14
0.07	0.08	0.09	0.11	0.24	0.09
0.08	0.14	0.07	0.14	0.29	0.11
0.26	0.16	0.26	0.21	0.49	0.32
0.02	0.17	0.13	0.11	0.22	0.14

151-2 C	152-3 C	153-4 C	150-T D	15T-1 D	151-2 D
0.08	0.09	0.08	0.26	0.13	0.06
0.09	0.19	0.09	0.22	0.1	0.14
-0.04	0.07	-0.01	0.04	0.03	-0.01
0.07	0.07	0.1	0.21	0.08	0.13
0.05	0.11	0.14	0.12	0.11	0.11
0.06	0.07	0.08	0.11	0.07	0.08
0.14	0.13	0.12	0.28	0.14	0.12
0.11	0.06	0.05	0.1	0.09	0.07
0.2	0.16	0.14	0.27	0.14	0.18
0.15	0.11	0.16	0.37	0.22	0.23
0.06	0	0.08	0.1	0.05	0.12
0.07	0.1	0.05	0.24	0.52	-0.39
0.22	0.09	0.03	0.33	-0.05	0.11
0.08	0.03	0.16	0.12	0.01	0.11
0.13	0.21	0.15	0.32	0.1	0.14
0.33	0.23	0.3	0.56	0.29	0.21
0.05	0.17	0.11	0.19	0.08	0.09
0.11	0.09	0.1	0.26	0.13	0.08
0.11	0.08	0.11	0.26	0.09	0.1
0.07	0.04	0.08	0.13	0.07	0.05
0.07	0.06	0.11	0.18	0.11	0.07
0.16	0.16	0.17	0.36	0.16	0.11
0.22	0.13	0.08	0.21	0.13	0.09
0.16	0.12	0.19	0.31	0.15	0.19
0.11	0.11	0.11	0.23	0.07	0.16
0.1	0.06	0.07	0.17	0.11	0.06
0.05	0.09	0.06	0.22	0.1	0.07
0.04	0.15	0.06	0.15	0.05	0.08
0.17	0.12	0.16	0.29	0.13	0.14
0.14	0.09	0.11	0.22	0.11	0.11
0.12	0.09	0.14	0.28	0.12	0.07
0.08	0.11	0.09	0.25	0.01	0.11
0.12	0.18	0.11	0.35	0.11	0.1
0.23	0.15	0.23	0.42	0.22	0.23
0.14	0.15	0.13	0.28	0.14	0.15
0.19	0.09	0.1	0.32	0.13	0.1
0.11	0.13	0.13	0.35	0.13	0.08
0.08	-0.01	0.12	0.12	0.07	0.08
0.13	0.09	0.11	0.28	0.18	0.07
0.13	0.13	0.13	0.31	0.14	0.18
0.25	0.22	0.2	0.47	0.24	0.22
0.12	0.23	0.2	0.47	0.17	0.16
0.22	0.2	0.18	0.43	0.28	0.19
0.09	0.11	0.13	0.25	0.07	0.06
0.15	0.19	0.17	0.31	0.12	0.17
0.11	0.14	0.11	0.3	0.03	0.12
0.09	0.07	0.14	0.2	0.13	0.14
0.14	0.06	0.15	0.21	0.14	0.06

0.28	0.24	0.27	0.38	0.25	0.3
0.1	0.08	0	0.17	0.1	0.08
0.25	0.25	0.29	0.45	0.24	0.16
0.12	0.17	0.17	0.22	0.2	0.16
0.06	0.09	0.13	0.29	0.11	0.08
0.06	0.06	0.02	0.22	0.16	0.08
0.09	0.07	0.07	0.26	0.12	0.13
0.22	0.32	0.25	0.53	0.23	0.29
0.11	0.12	0.11	0.31	0.07	0.11

152-3 D	153-4 D	150-T E	15T-1 E	151-2 E	152-3 E
0.04	0.13	0.18	0.16	0.08	0.1
0.11	0.11	0.32	0.06	0.16	0.08
0.07	0	0.05	0.01	0.03	-0.02
0.04	0.09	0.13	0.09	0.14	0.08
0.13	0.11	0.25	0.02	0.12	0.09
0.07	0.06	0.13	0.06	0.13	-0.02
0.15	0.13	0.24	0.14	0.14	0.12
0.11	0.06	0.14	0.07	0.08	0.06
0.16	0.1	0.28	0.18	0.16	0.09
0.1	0.19	0.39	0.18	0.16	0.13
0	0.06	0.1	0.05	0.05	0.01
0.1	0.13	0.16	0.12	0.05	0.2
0.03	0.17	0.28	0.04	0.21	0.17
0.05	0.09	0.11	0.09	0.07	0.1
0.17	0.21	0.26	0.08	0.12	0.14
0.26	0.35	0.6	0.22	0.3	0.27
0.08	0.13	0.19	0.09	0.08	0.1
0.04	0.11	0.27	0.09	0.12	0.07
0.09	0.11	0.25	0.1	0.08	0.1
0.06	0.11	0.18	0.02	0.05	0.07
0.04	0.11	0.19	0.11	0.06	0.11
0.11	0.18	0.32	0.13	0.18	0.15
0.1	0.09	0.18	3.09	0.14	0.09
0.07	0.15	0.38	0.1	0.18	0.12
0.11	0.02	0.28	0.07	0.13	0.1
0.06	0.1	0.16	0.08	0.16	0.06
0.06	0.11	0.19	0.05	0.11	0.07
0.04	0.09	0.18	0.04	0.09	0.06
0.09	0.14	0.28	0.13	0.21	0.11
0.14	0.08	0.19	0.14	0.09	0.08
0.1	0.11	0.27	0.13	0.17	0.08
0.15	0.02	0.26	0.12	0.06	0.08
0.14	0.11	0.35	0.11	0.12	0.1
0.17	0.28	0.45	0.2	0.22	0.2
0.12	0.17	0.28	0.15	0.15	0.18
0.16	0.12	0.25	0.19	0.15	0.13
0.1	0.16	0.31	0.12	0.15	0.14
0.05	0.08	0.18	0.04	0.05	0.12
0.13	0.1	0.31	0.09	0.13	0.15
0.15	0.07	0.26	0.19	0.16	0.04
0.15	0.26	0.49	0.24	0.27	0.18
0.18	0.24	0.5	0.18	0.15	0.11
0.18	0.21	0.48	0.21	0.17	0.19
0.14	0.11	0.24	0.09	0.14	0.06
0.16	0.19	0.32	0.21	0.13	0.16
0.11	0.17	0.24	0.14	0.08	0.12
0.12	0.1	0.26	0.06	0.15	0.13
0.11	0.09	0.23	0.1	0.12	0.12

0.27	0.24	0.49	0.26	0.26	0.19
0.11	0.06	0.18	0.13	0.04	0.06
0.21	0.15	0.33	0.12	0.14	0.12
0.19	0.15	0.29	0.16	0.15	0.16
0.1	0.12	0.23	0.12	0.05	0.14
0.16	0.07	0.2	0.13	0.07	0.09
0.05	0.17	0.28	0.12	0.11	0.09
0.29	0.3	0.56	0.33	0.26	0.31
0.15	0.21	0.27	0.11	0.13	0.1

153-4 E

0.12
0.12
0
0.12
0.1
0.09
0.17
0.07
0.1
0.19
0.09
0.04
0.3
0.1
0.09
0.31
0.05
0.11
0.07
0.04
0.09
0.17
0.14
0.11
0.14
0.08
0.04
0.03
0.14
0.12
0.07
0.13
0.15
0.21
0.13
0.12
0.17
0.04
0.22
0.15
0.17
0.2
0.28
0.07
0.15
0.11
0.12
0.1

0.28
0.09
0.16
0.17
0.08
0.05
0.13
0.32
0.15

Appendix D

Results Graphs for All Fibres

Tested During the Pilot Study.

Rough Mesh and Card Test Results.

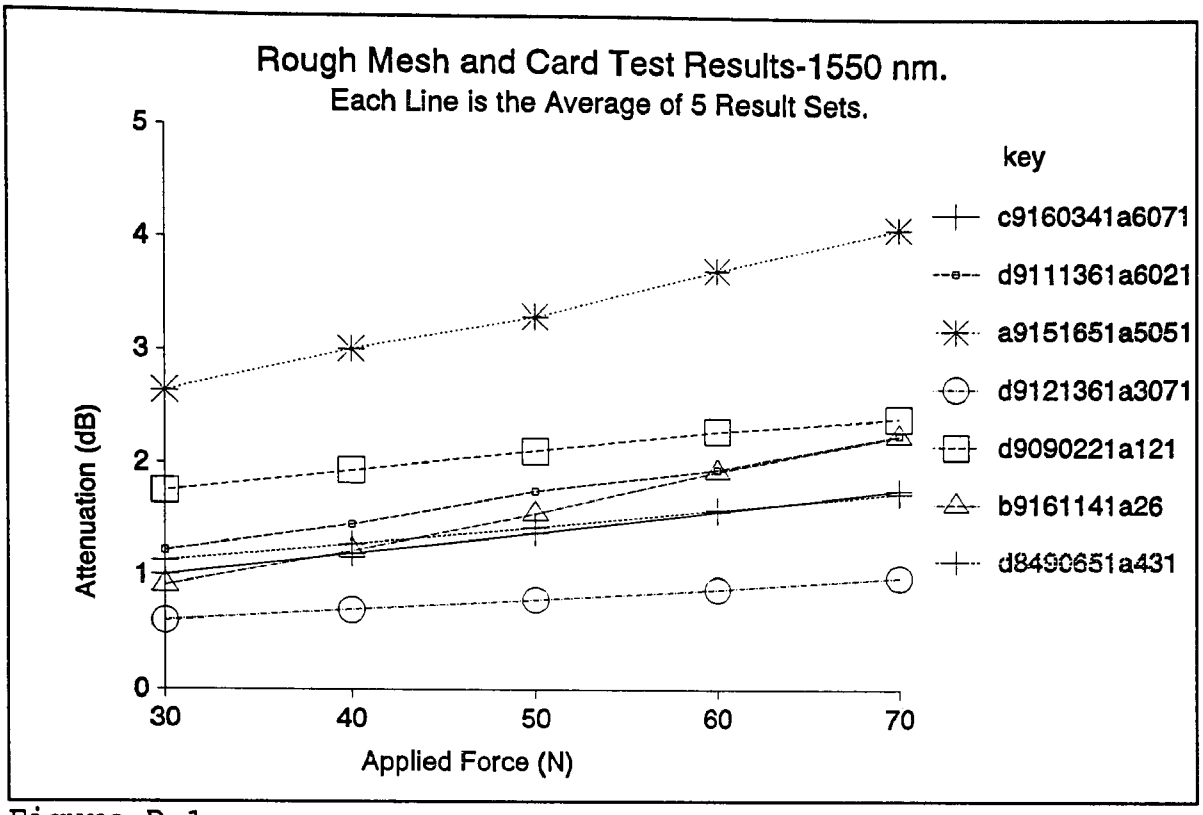
Rough Mesh and Card Test Results-1550 nm.
Each Line is the Average of 5 Result Sets.
Attenuation (dB)
0
1
2
3
4
5
30
40
50
60
70
Applied Force (N)
key
c9160341a6071
d9111361a6021
a9151651a5051
d9121361a3071
d9090221a121
b9161141a26
d8490651a431

Figure D.1

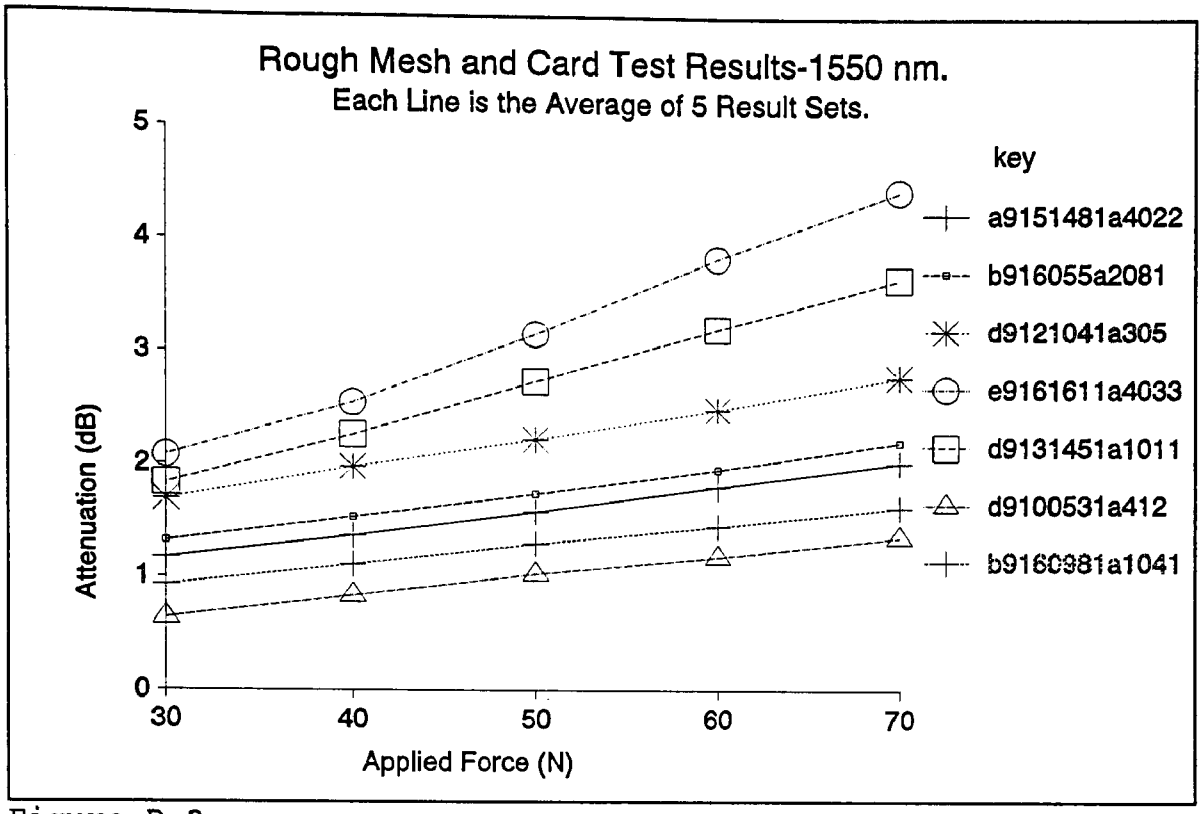
Rough Mesh and Card Test Results-1550 nm.
Each Line is the Average of 5 Result Sets.
Attenuation (dB)
0
1
2
3
4
5
30
40
50
60
70
Applied Force (N)
key
a9151481a4022
b916055a2081
d9121041a305
e9161611a4033
d9131451a1011
d9100531a412
b9160981a1041

Figure D.2

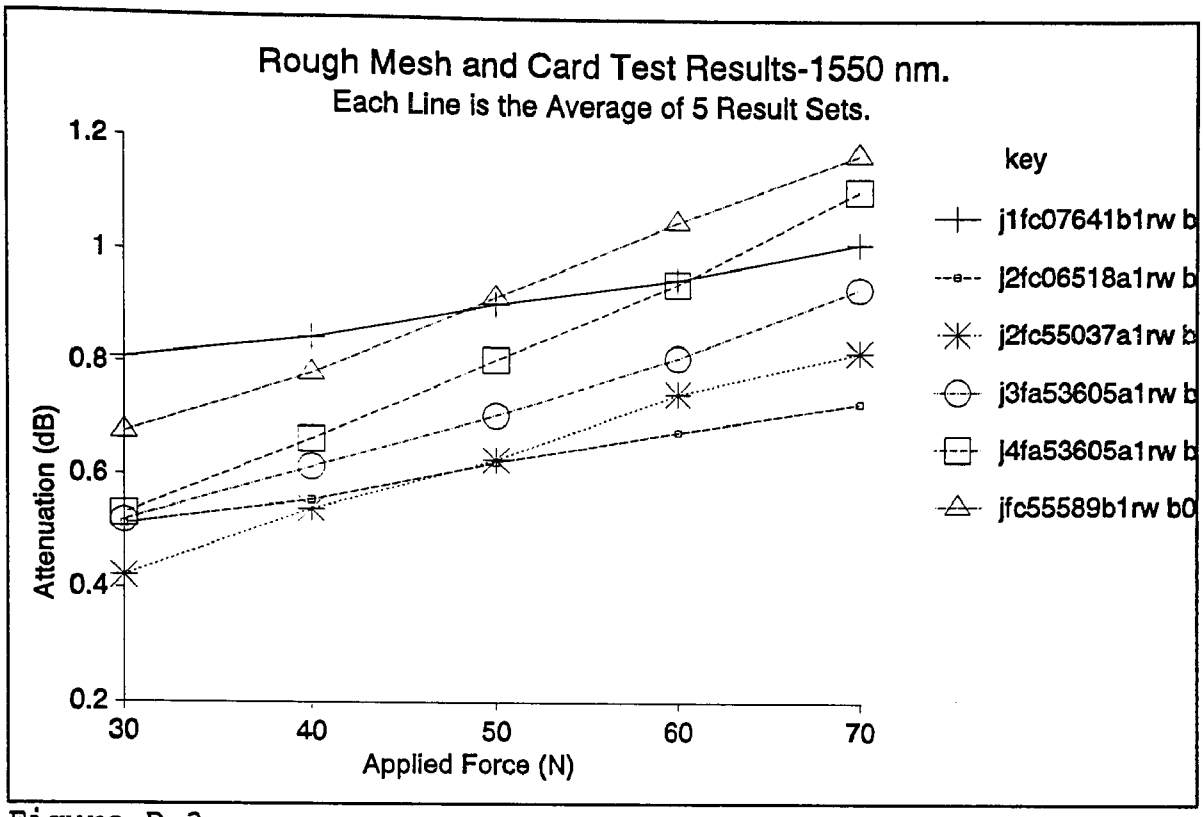
Rough Mesh and Card Test Results-1550 nm.
Each Line is the Average of 5 Result Sets.
Attenuation (dB)
1.2
1
0.8
0.6
0.4
0.2
30
40
50
60
70
Applied Force (N)
key
j1fc07641b1rw b
j2fc06518a1rw b
j2fc55037a1rw b
j3fa53605a1rw b
j4fa53605a1rw b
jfc55589b1rw b0

Figure D.3

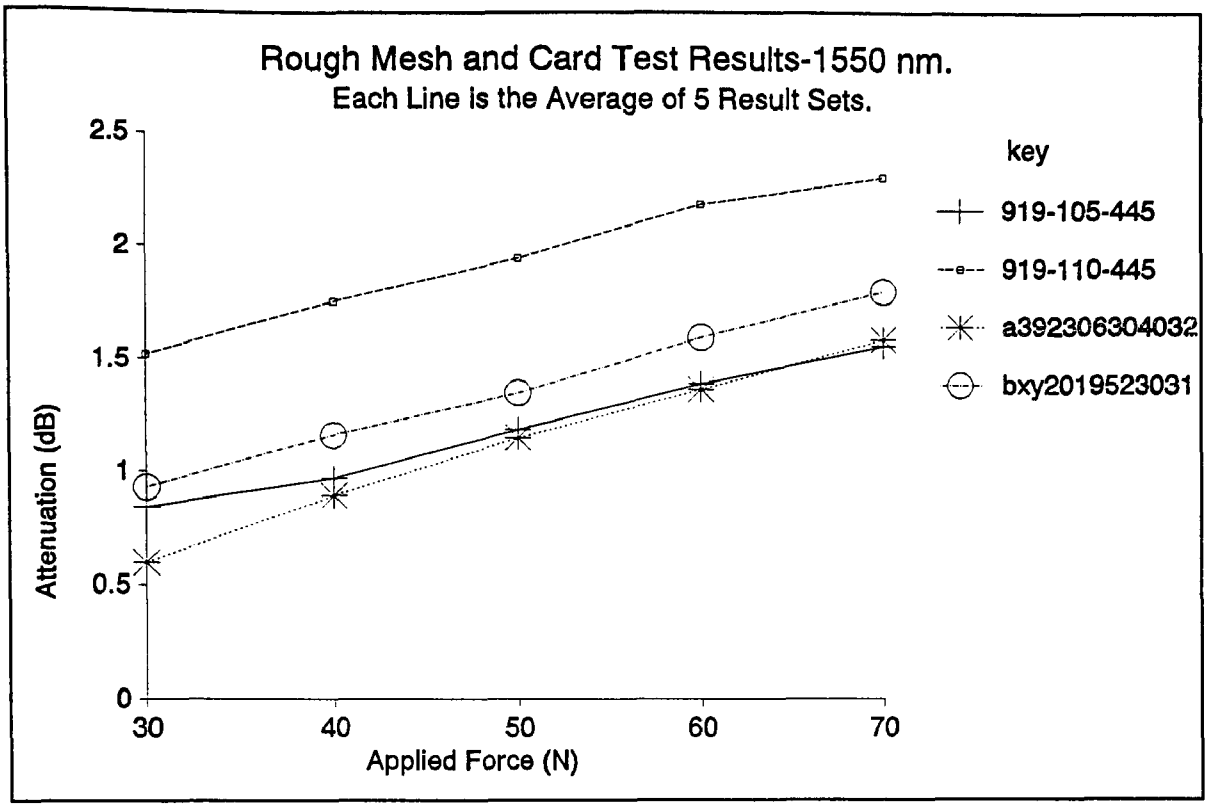
Rough Mesh and Card Test Results-1550 nm.
Each Line is the Average of 5 Result Sets.
Attenuation (dB)
2.5
2
1.5
1
0.5
0
30
40
50
60
70
Applied Force (N)
key
919-105-445
919-110-445
a392306304032
bxy2019523031

Figure D.4

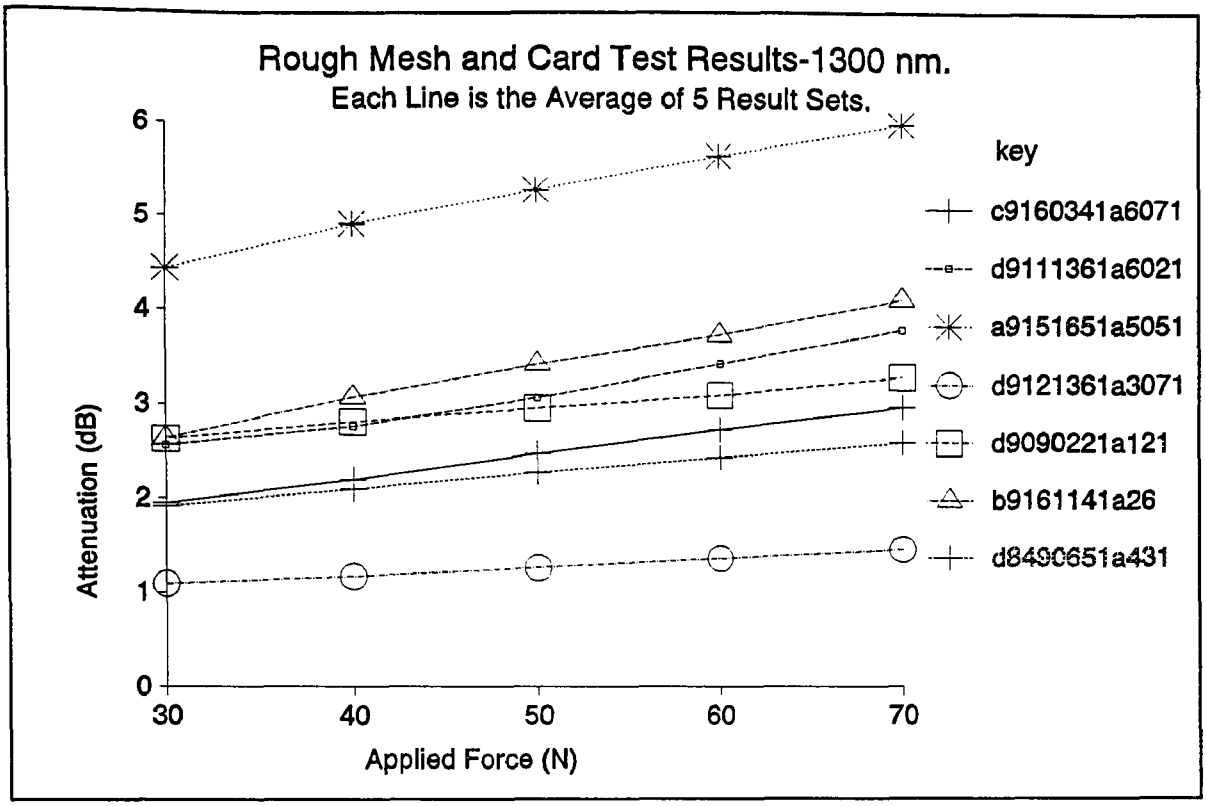
Rough Mesh and Card Test Results-1300 nm.
Each Line is the Average of 5 Result Sets.
Attenuation (dB)
Applied Force (N)
0
1
2
3
4
5
6
30
40
50
60
70
key
c9160341a6071
d9111361a6021
a9151651a5051
d9121361a3071
d9090221a121
b9161141a26
d8490651a431

Figure D.5

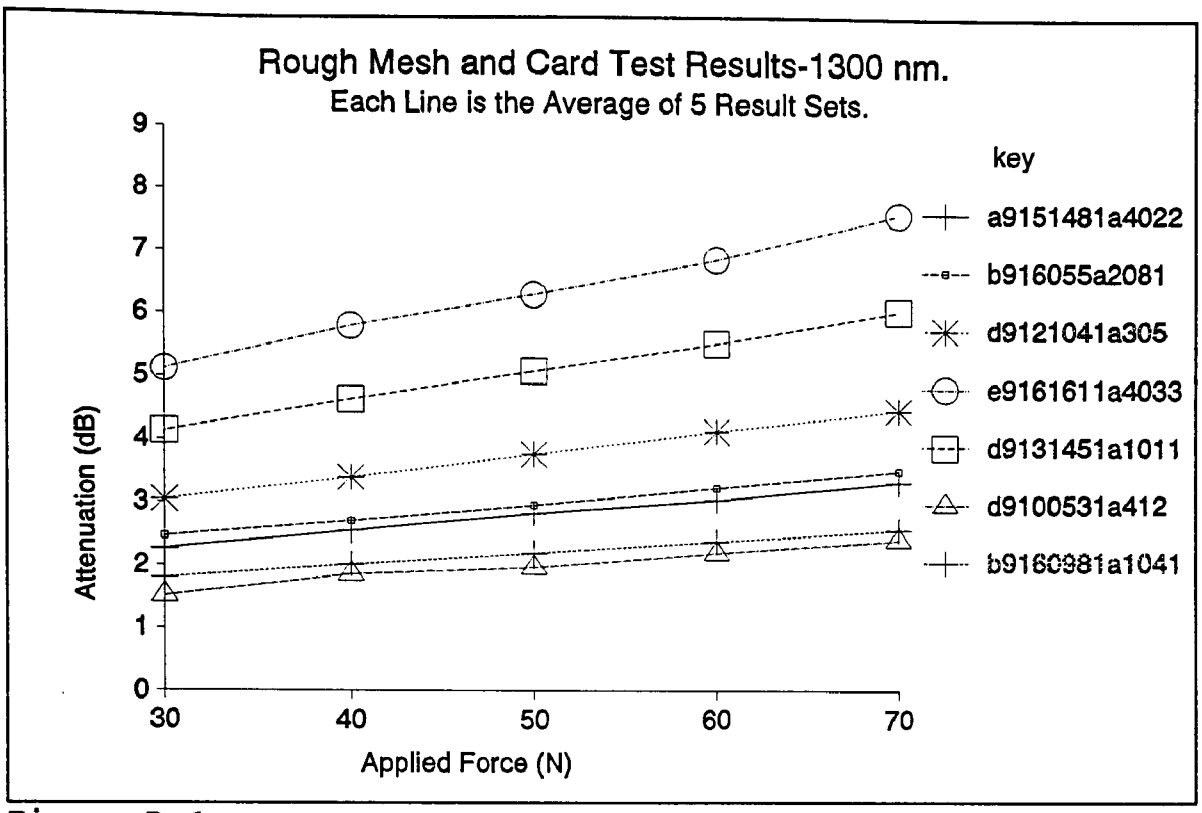
Rough Mesh and Card Test Results-1300 nm.
Each Line is the Average of 5 Result Sets.
Attenuation (dB)
Applied Force (N)
0
1
2
3
4
5
6
7
8
9
30
40
50
60
70
key
a9151481a4022
b916055a2081
d9121041a305
e9161611a4033
d9131451a1011
d9100531a412
b9160981a1041

Figure D.6

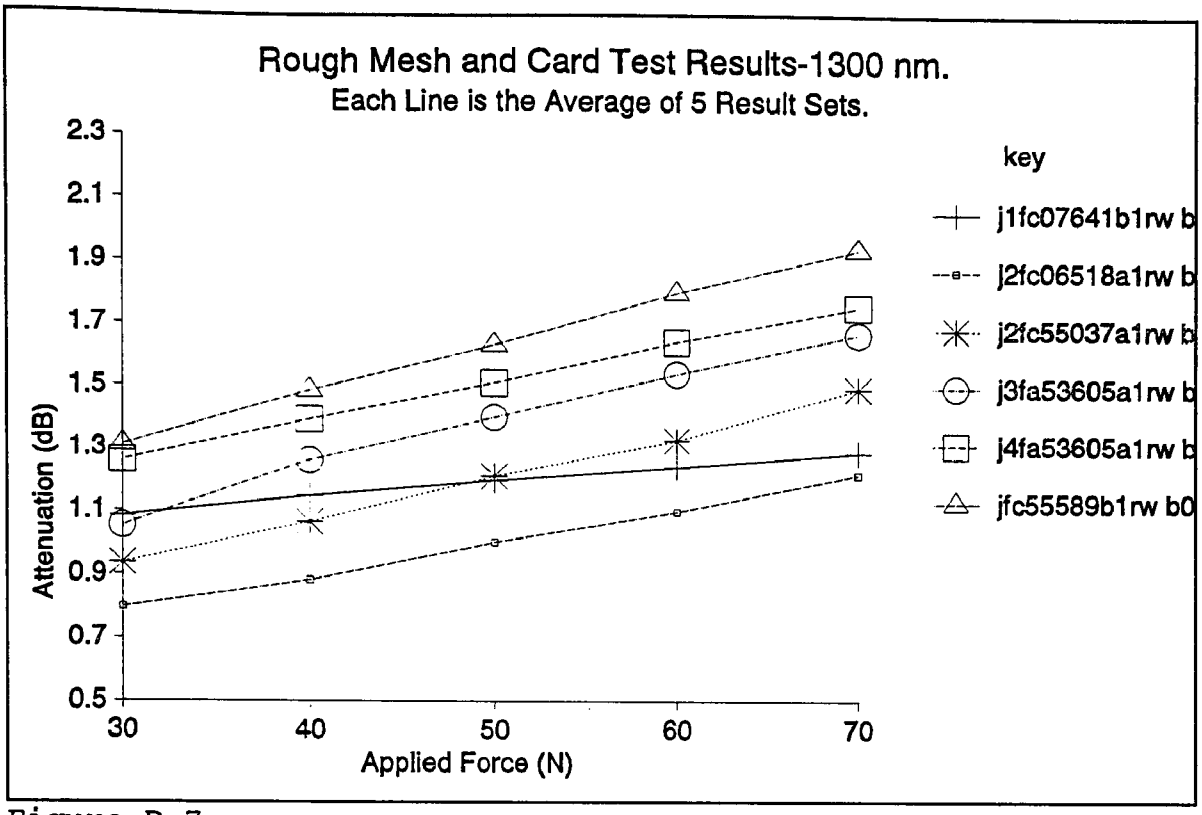
Rough Mesh and Card Test Results-1300 nm.
Each Line is the Average of 5 Result Sets.
Attenuation (dB)
2.3
2.1
1.9
1.7
1.5
1.3
1.1
0.9
0.7
0.5
30
40
50
60
70
Applied Force (N)
key
j1fc07641b1rw b
j2fc06518a1rw b
j2fc55037a1rw b
j3fa53605a1rw b
j4fa53605a1rw b
jfc55589b1rw b0

Figure D.7

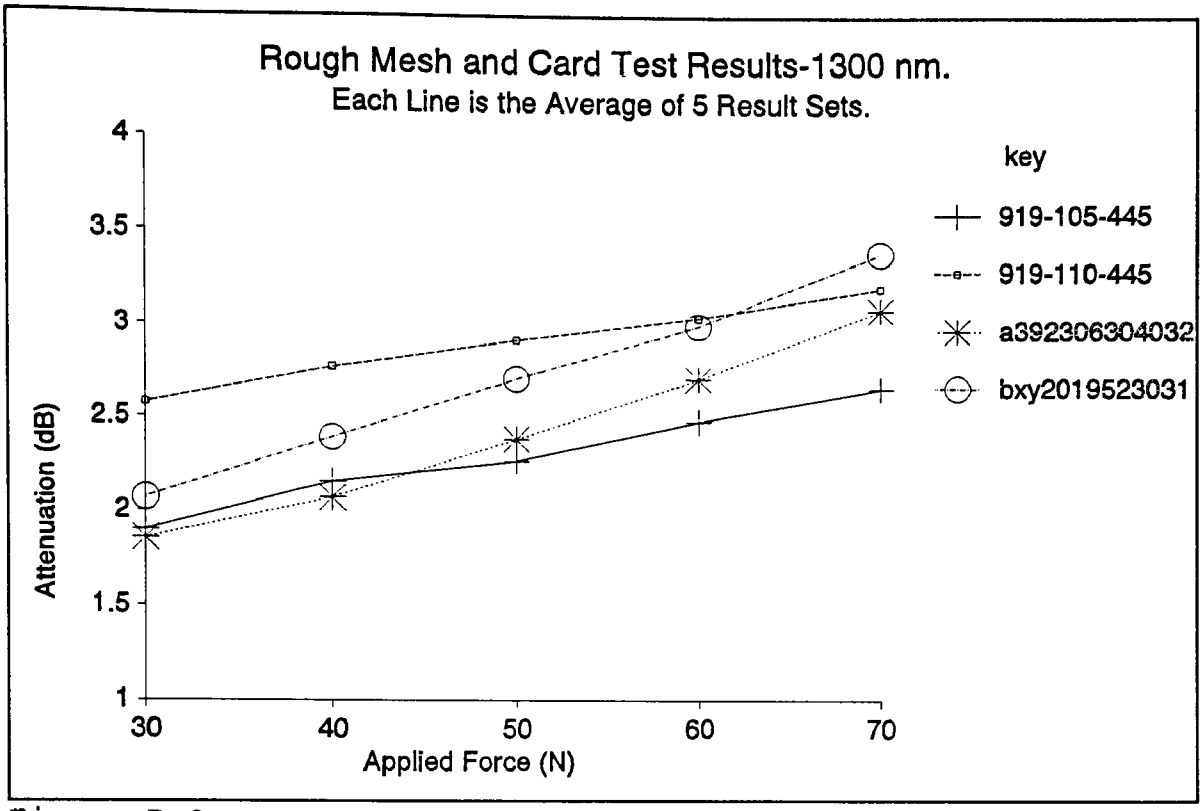
Rough Mesh and Card Test Results-1300 nm.
Each Line is the Average of 5 Result Sets.
Attenuation (dB)
4
3.5
3
2.5
2
1.5
1
30
40
50
60
70
Applied Force (N)
key
919-105-445
919-110-445
a392306304032
bxy2019523031

Figure D.8

Rough Mesh and Rubber Test Results.

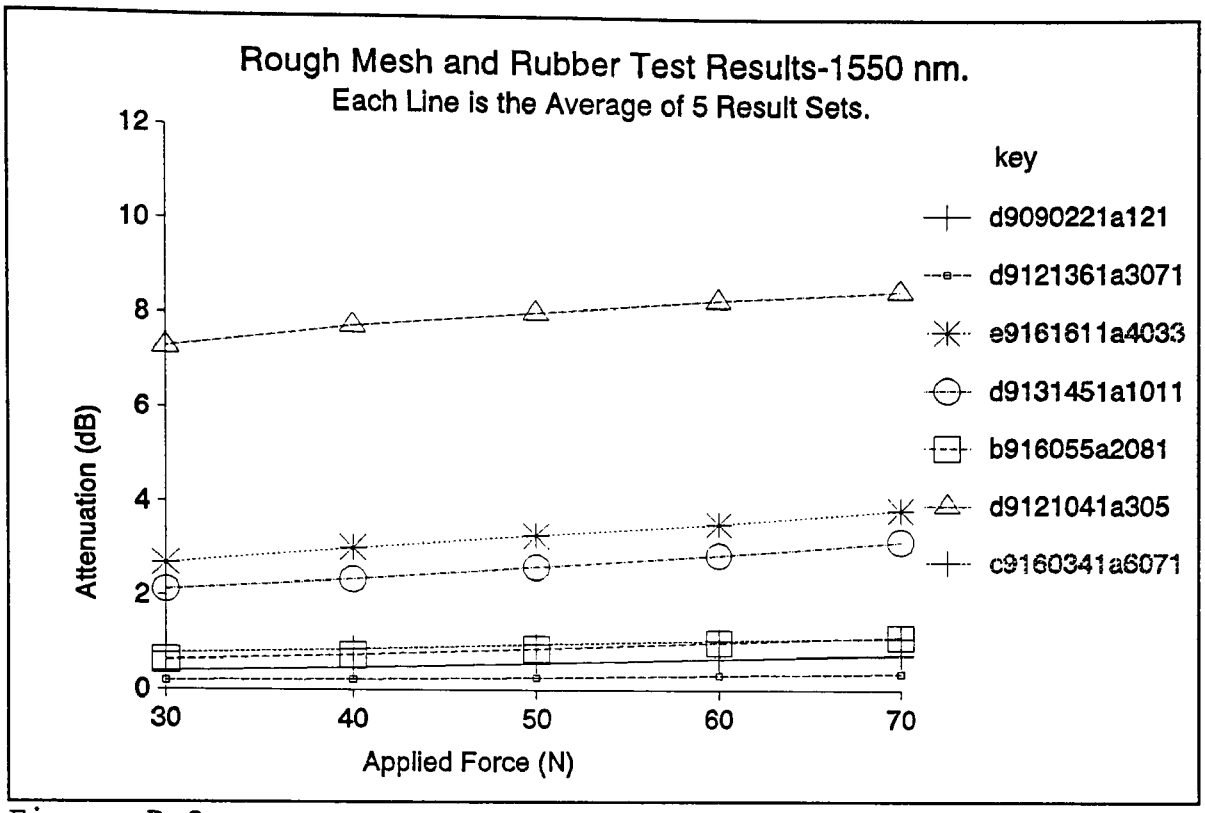

Figure D.8

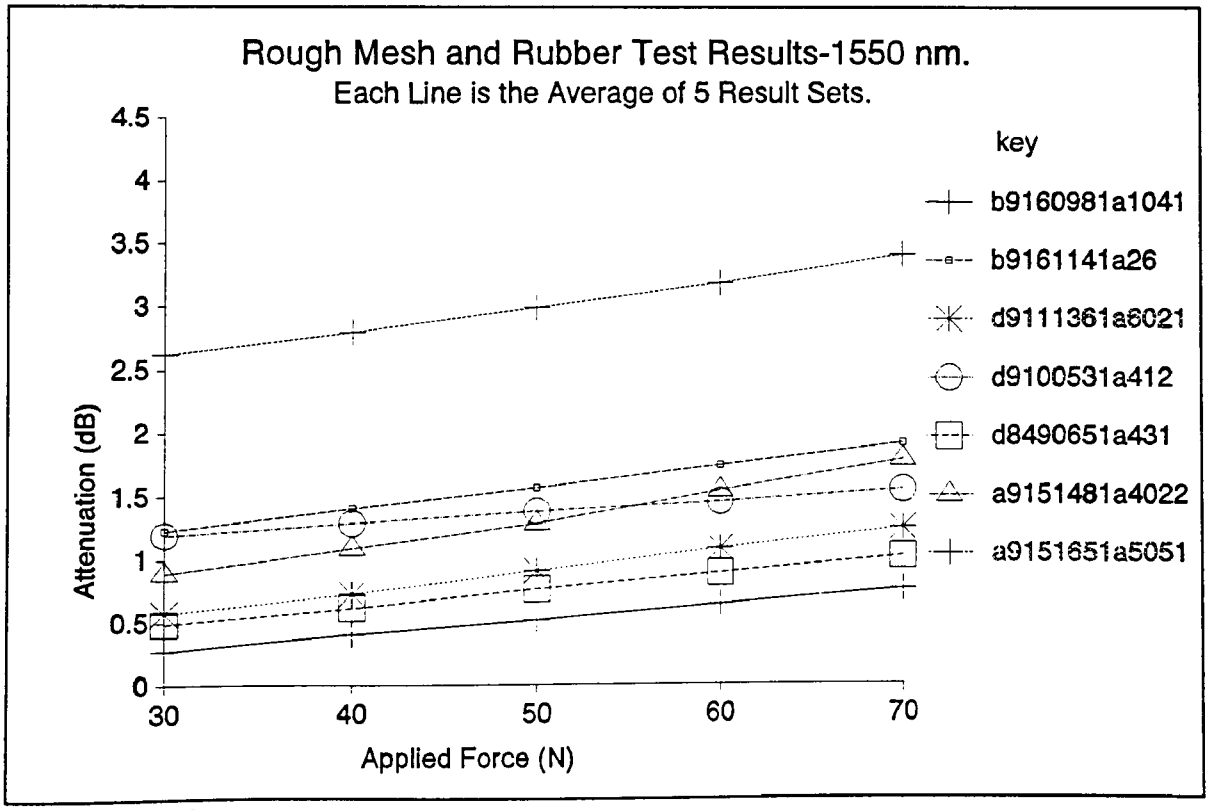

Figure D.9

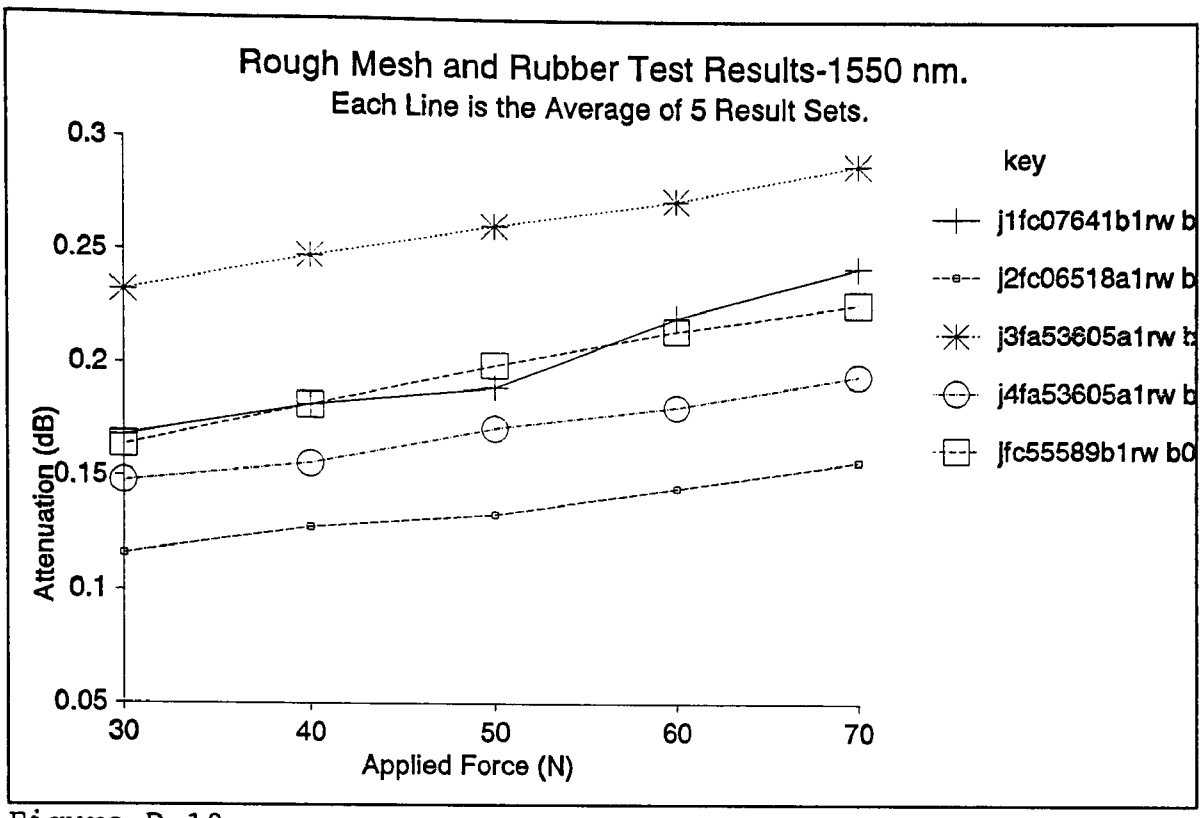
Rough Mesh and Rubber Test Results-1550 nm.
Each Line is the Average of 5 Result Sets.
Attenuation (dB)
0.3
0.25
0.2
0.15
0.1
0.05
30
40
50
60
70
Applied Force (N)
key
j1fc07641b1rw b
j2fc06518a1rw b
j3fa53605a1rw b
j4fa53605a1rw b
jfc55589b1rw b0

Figure D.10

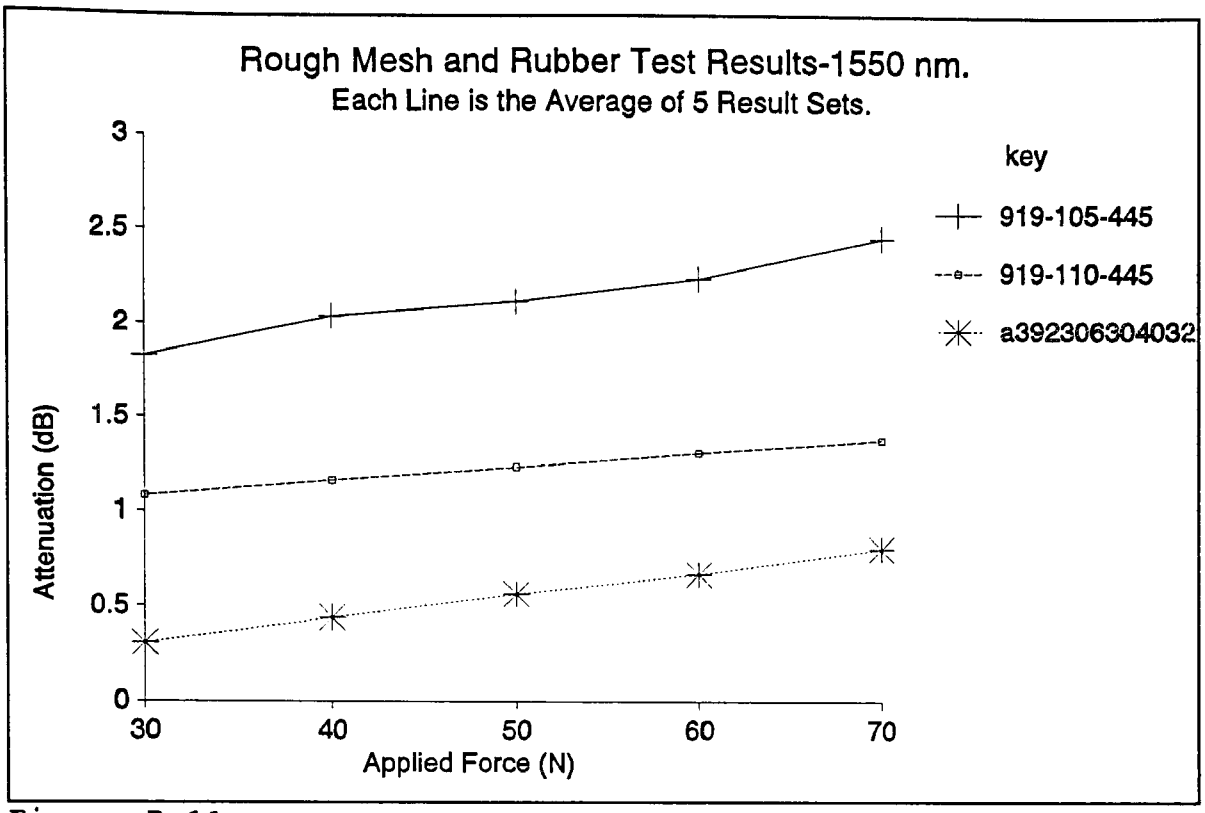

Figure D.11

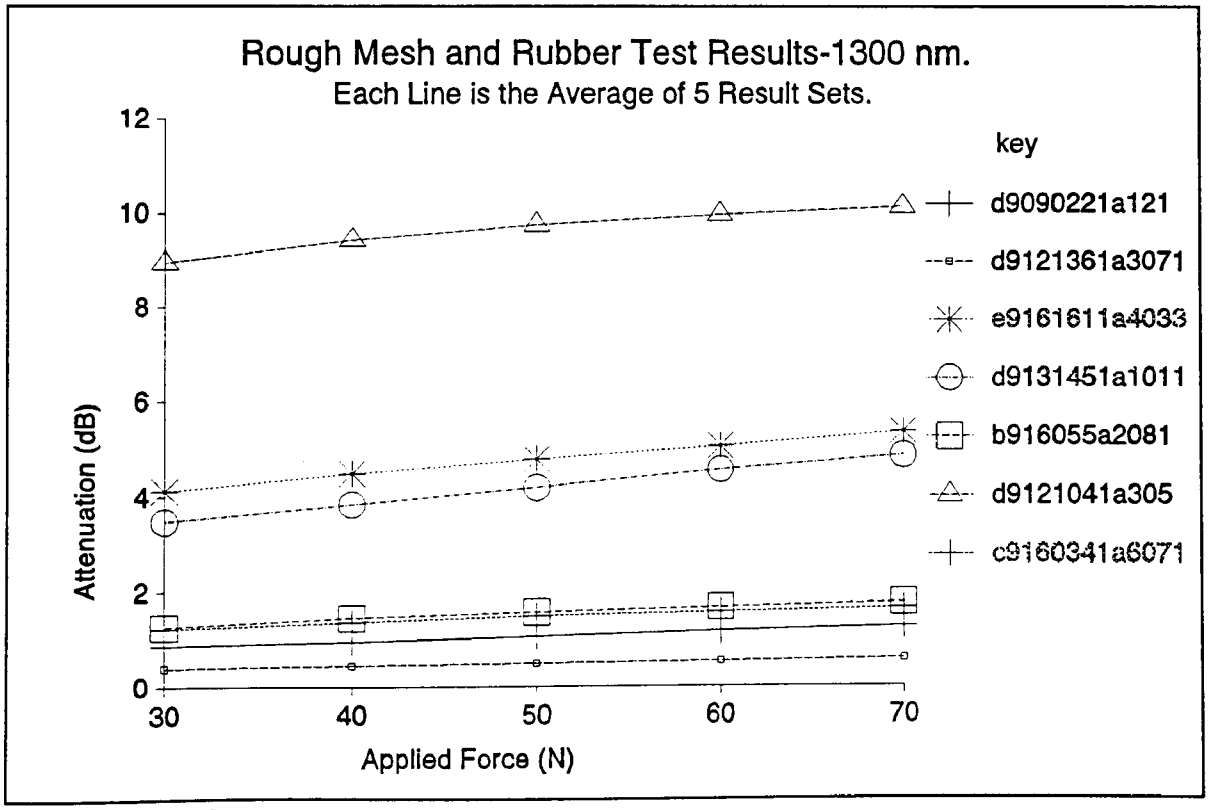

Figure D.12

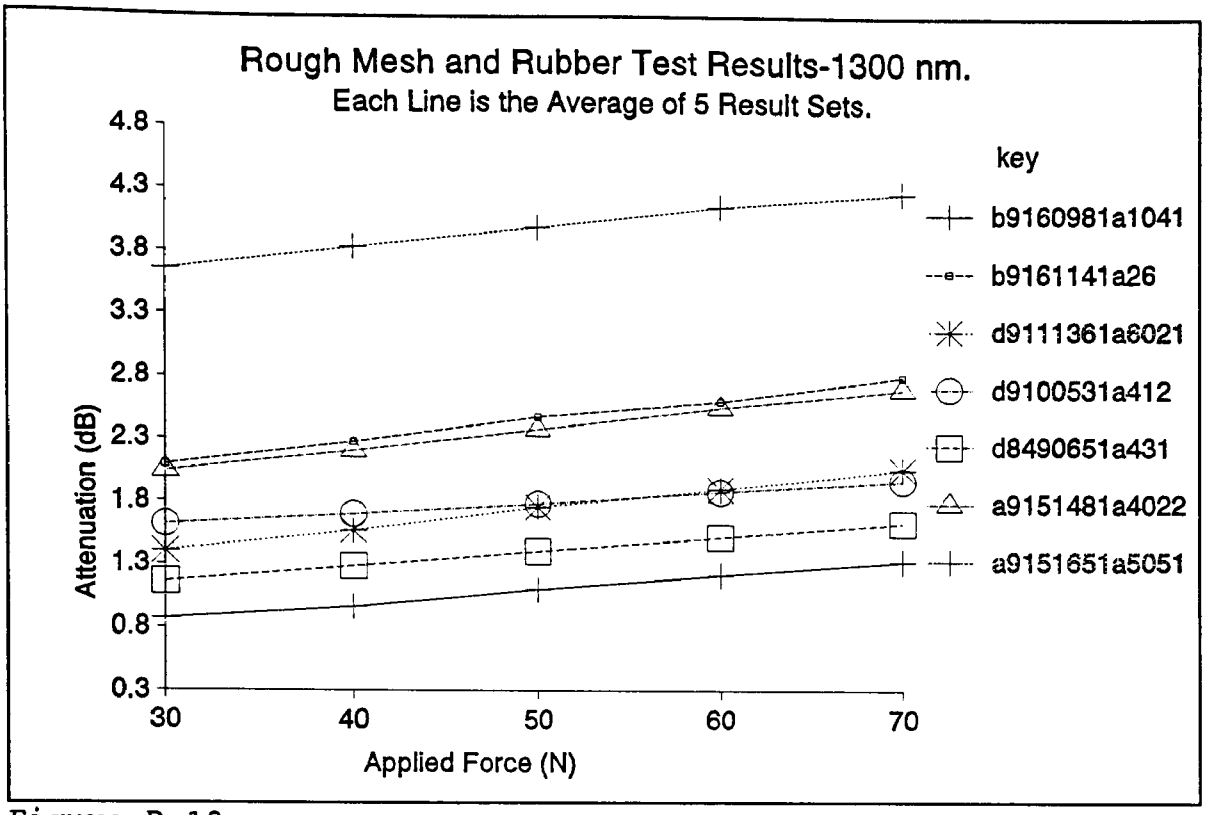

Figure D.13

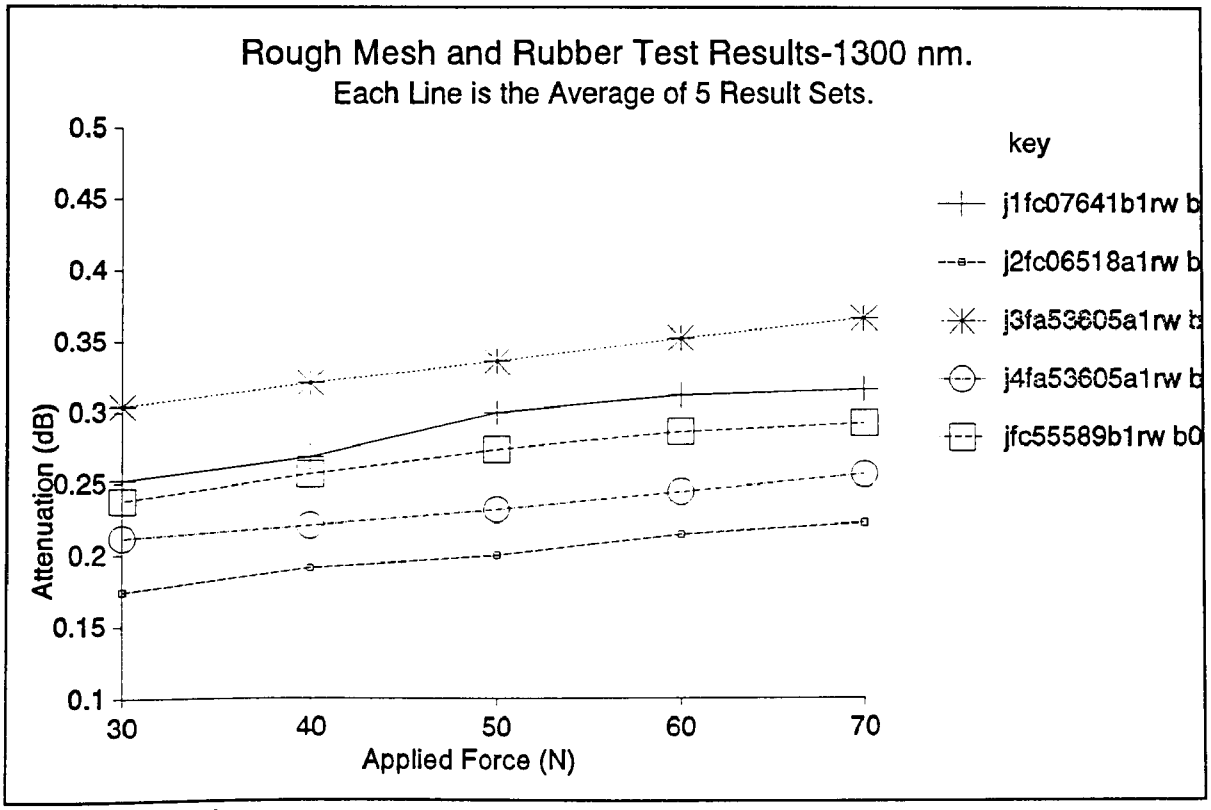

Figure D.14

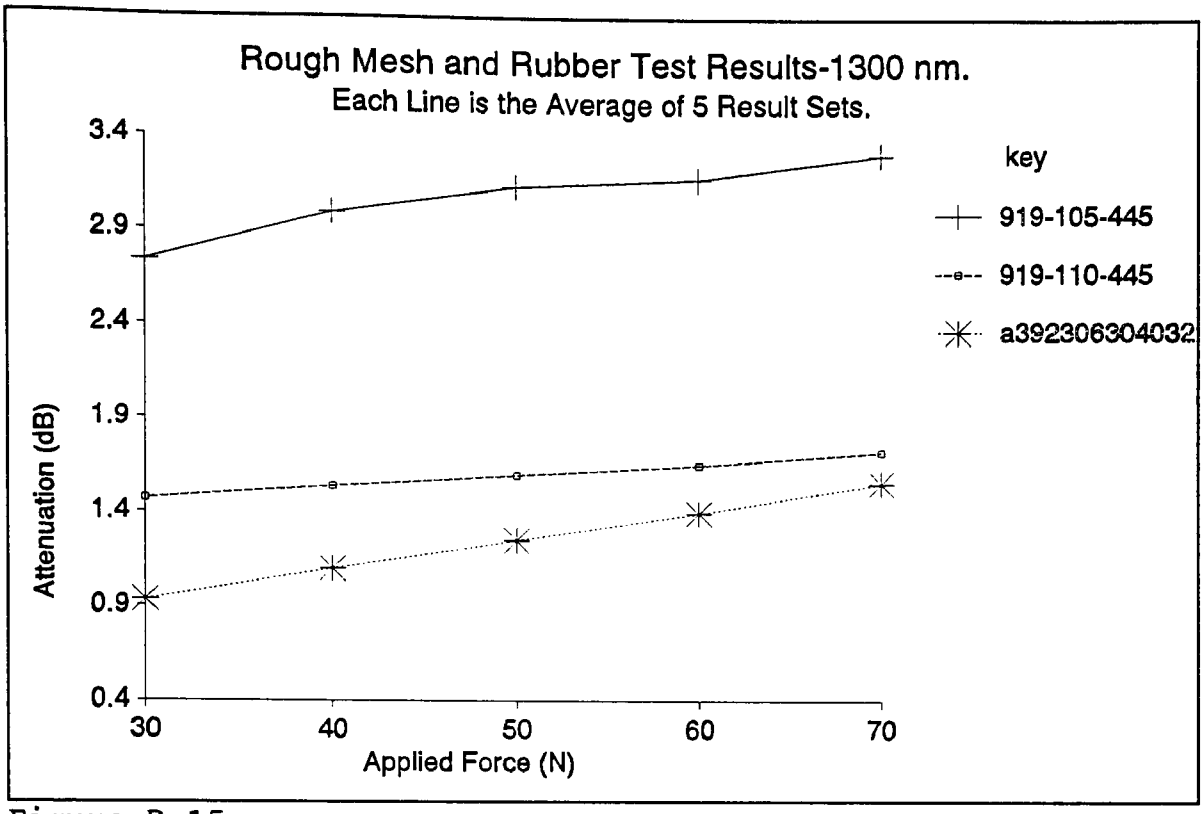
Rough Mesh and Rubber Test Results-1300 nm.
Each Line is the Average of 5 Result Sets.
Attenuation (dB)
3.4
2.9
2.4
1.9
1.4
0.9
0.4
30
40
50
60
70
Applied Force (N)
key
919-105-445
919-110-445
a392306304032

Figure D.15

Smooth Mesh and Card Test Results.

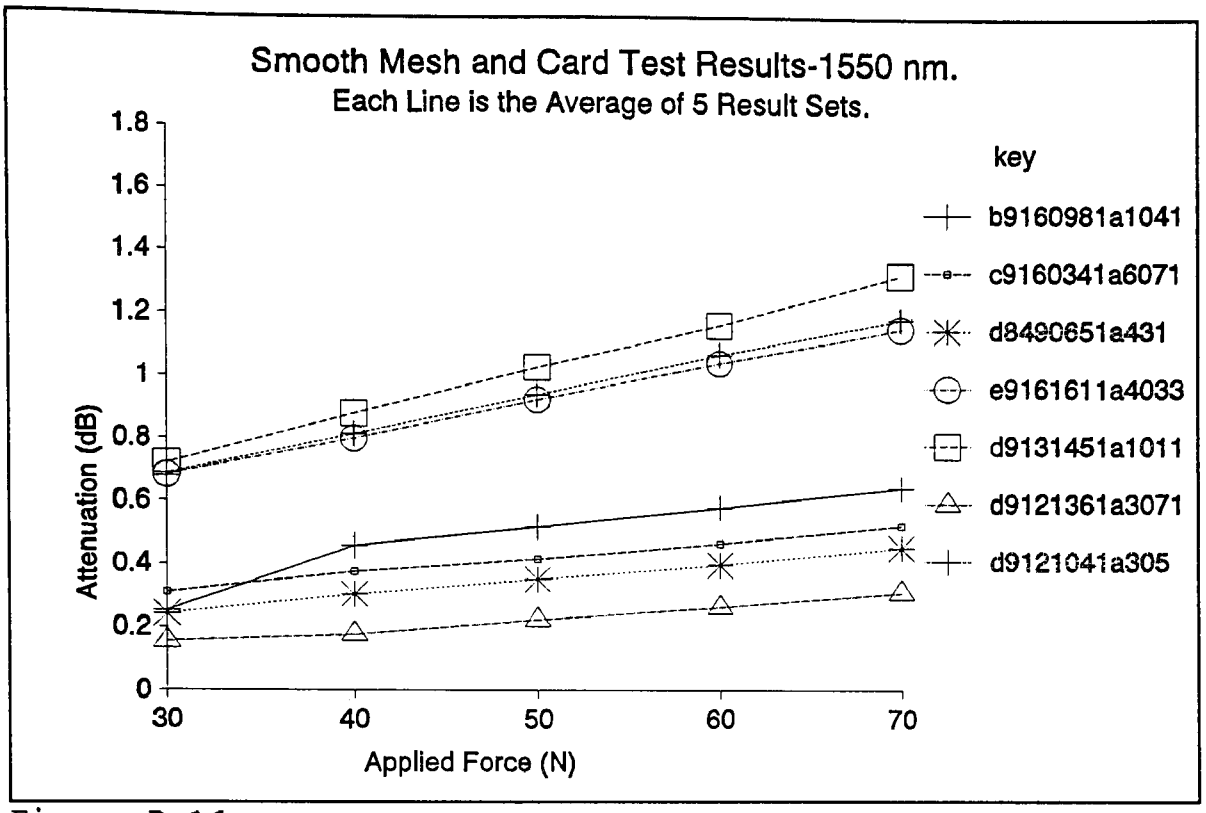

Figure D.16

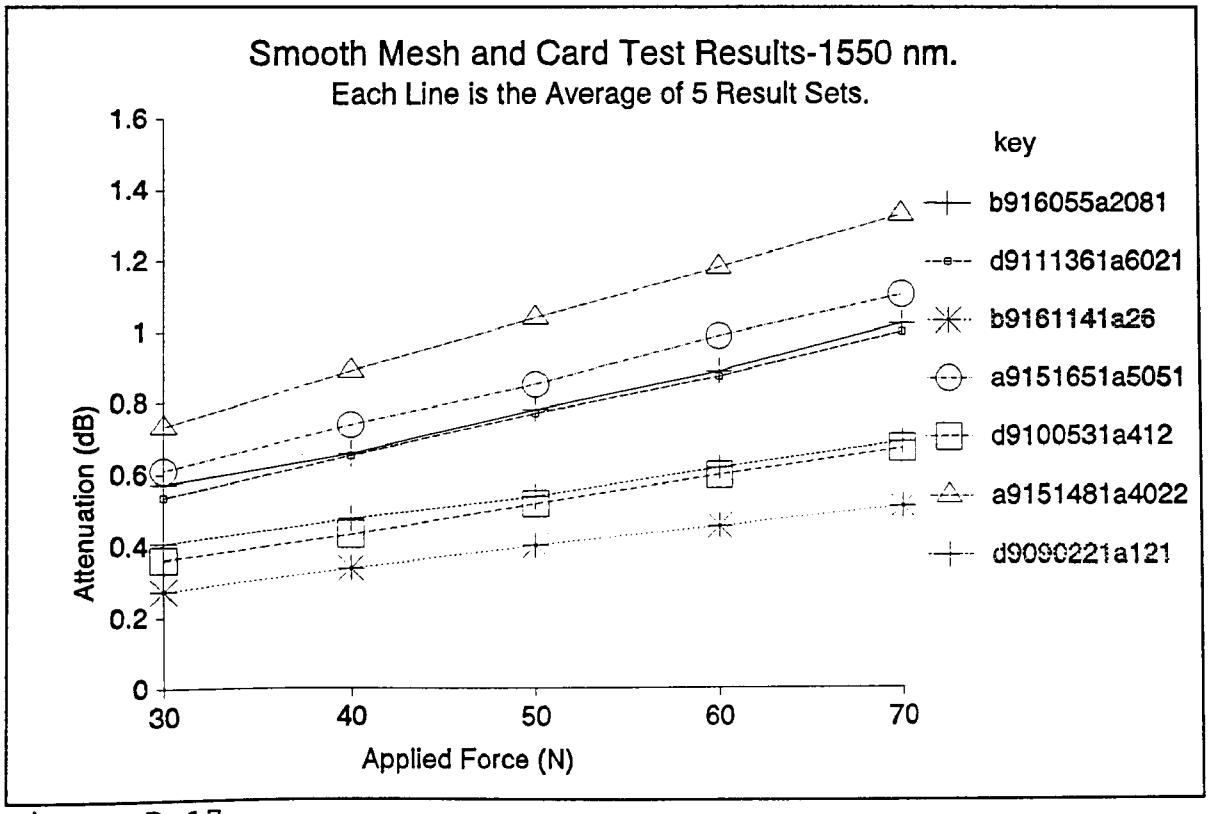

Figure D.17

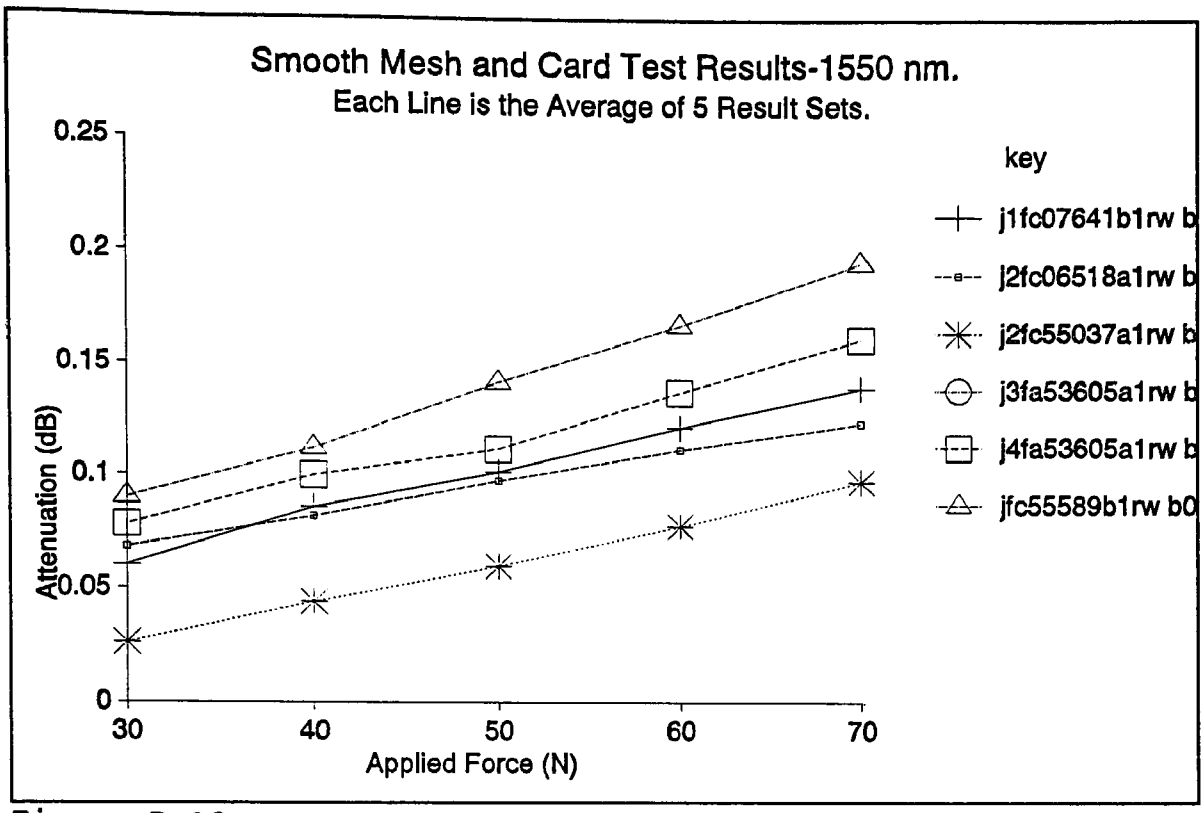

Figure D.18

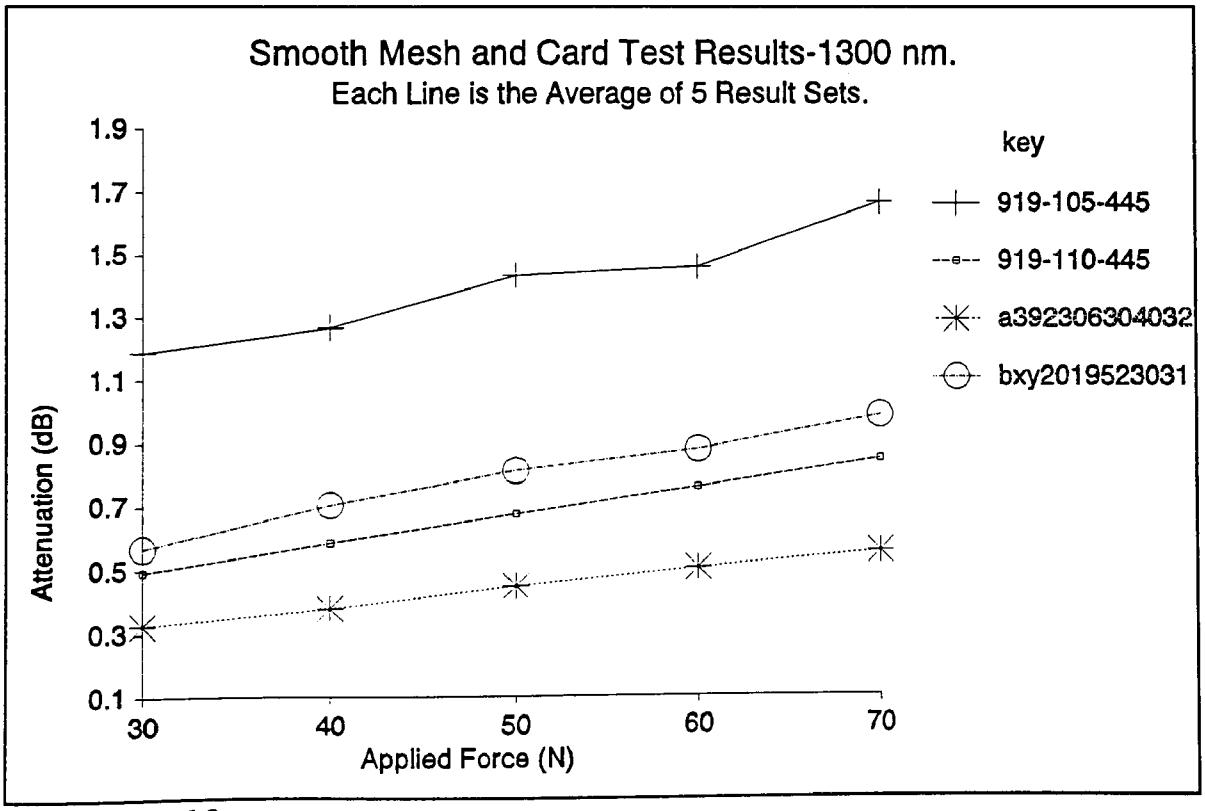

Figure D.19

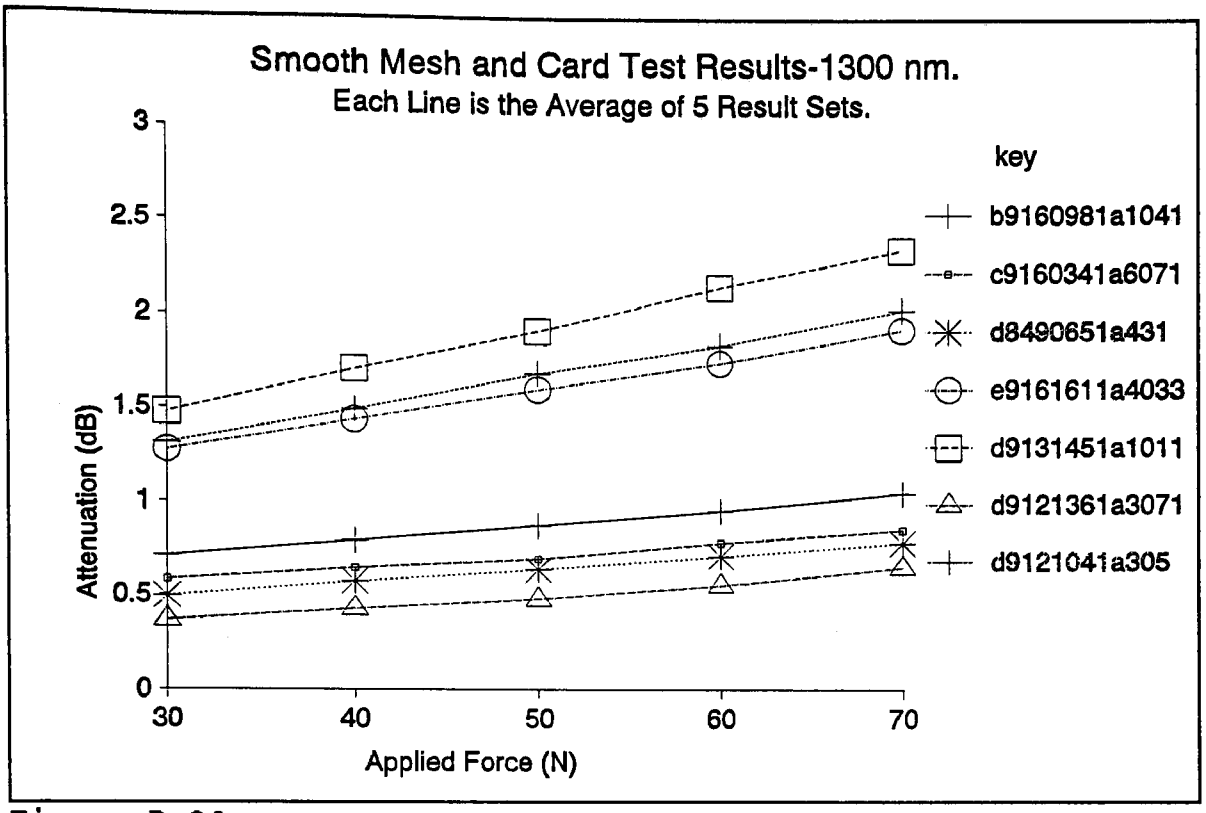

Figure D.20

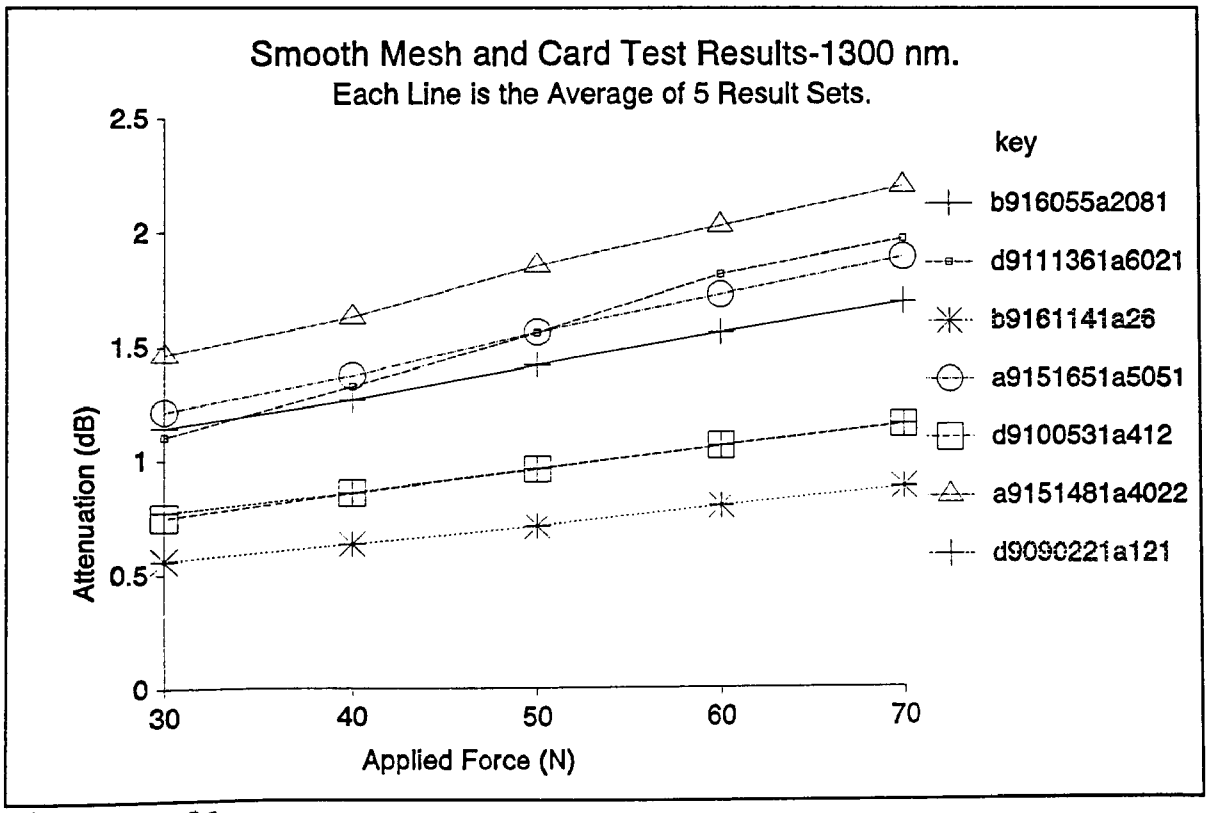

Figure D.21

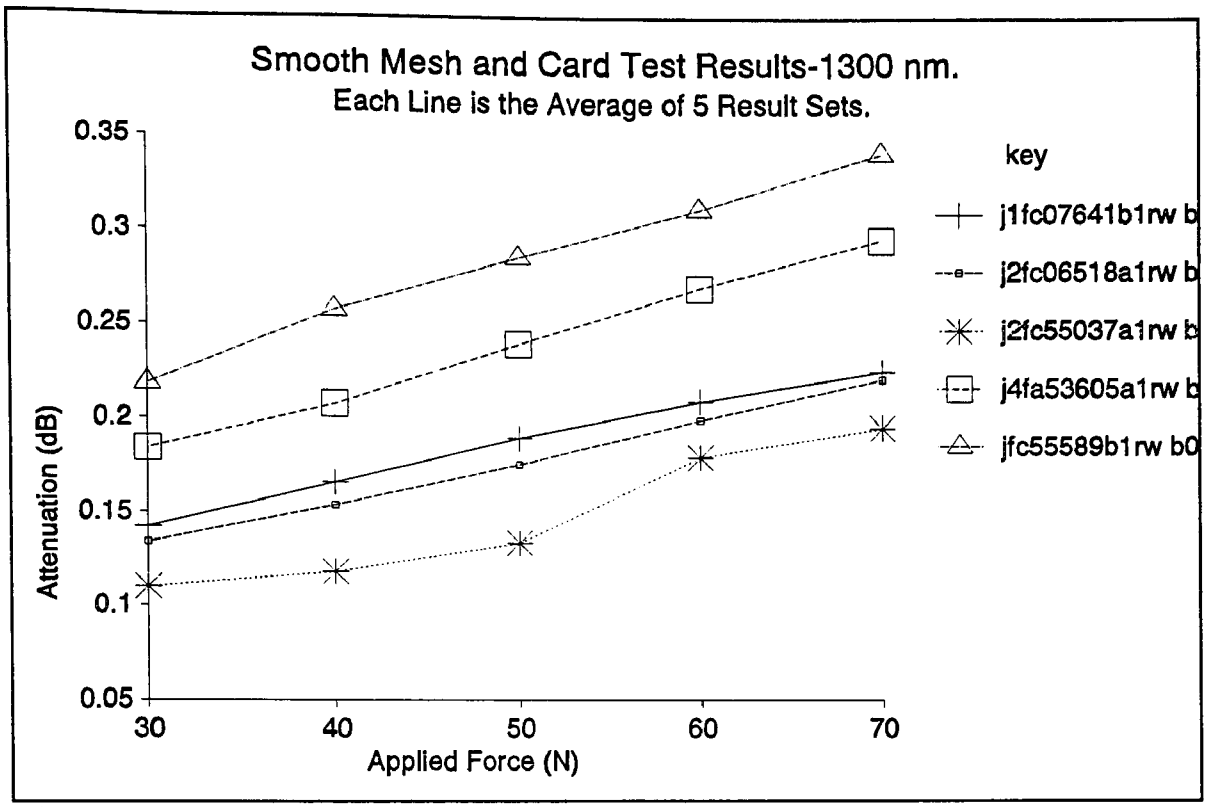
Smooth Mesh and Card Test Results-1300 nm.
Each Line is the Average of 5 Result Sets.
Attenuation (dB)
0.35
0.3
0.25
0.2
0.15
0.1
0.05
30
40
50
60
70
Applied Force (N)
key
j1fc07641b1rw b
j2fc06518a1rw b
j2fc55037a1rw b
j4fa53605a1rw b
jfc55589b1rw b0

Figure D.22

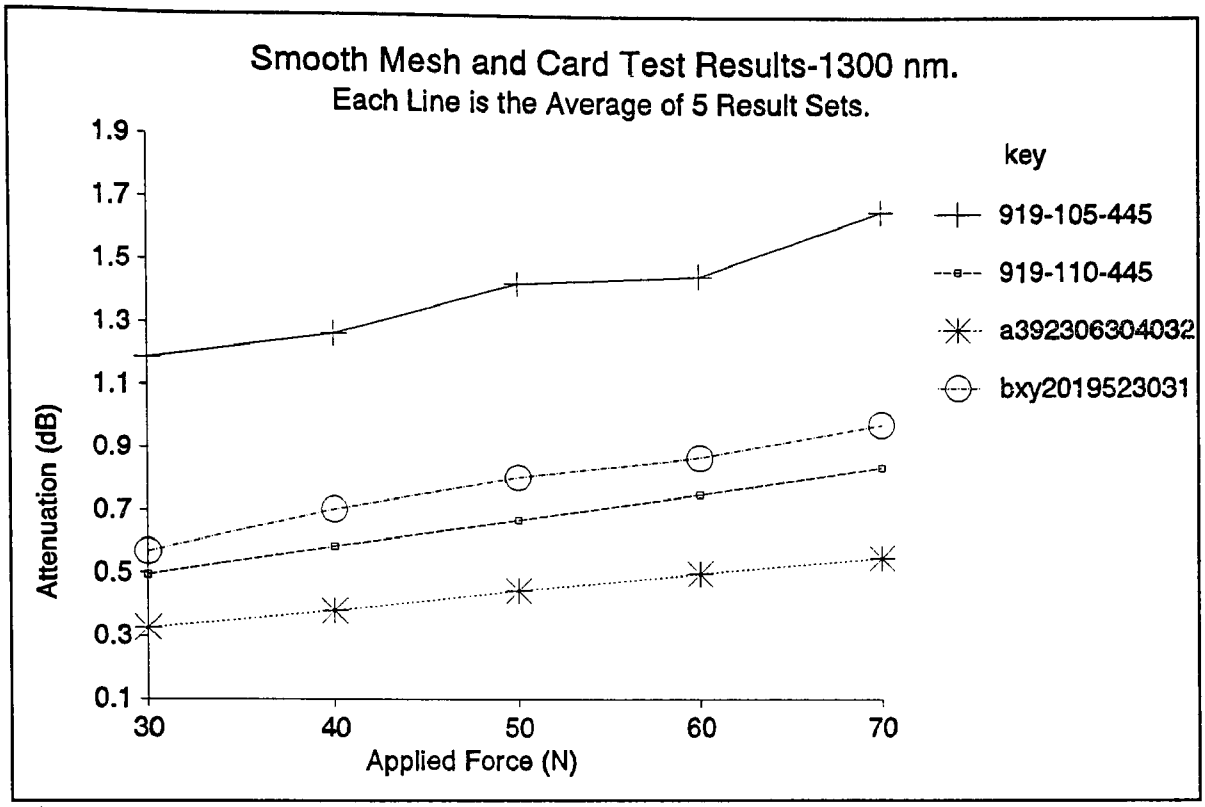
Smooth Mesh and Card Test Results-1300 nm.
Each Line is the Average of 5 Result Sets.
Attenuation (dB)
1.9
1.7
1.5
1.3
1.1
0.9
0.7
0.5
0.3
0.1
30
40
50
60
70
Applied Force (N)
key
919-105-445
919-110-445
a392306304032
bxy2019523031

Figure D.23

Smooth Mesh and Rubber Test Results.

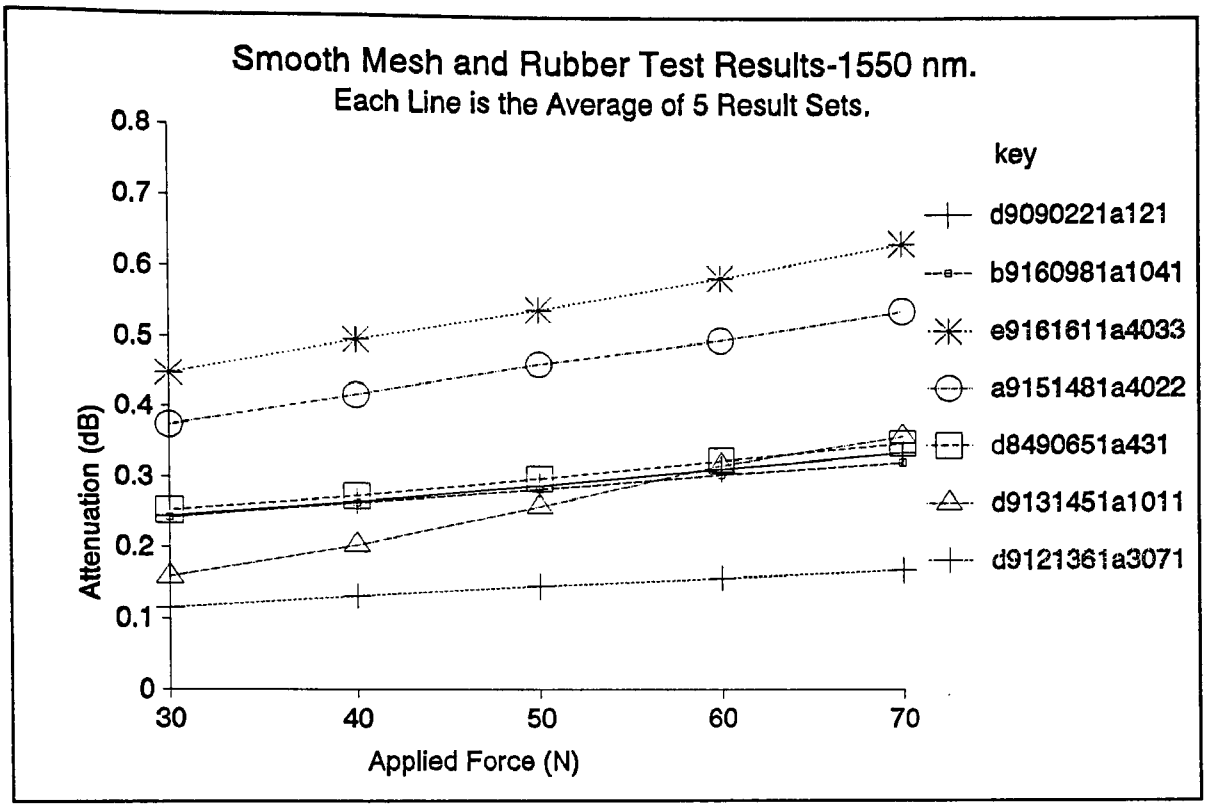

Figure D.24

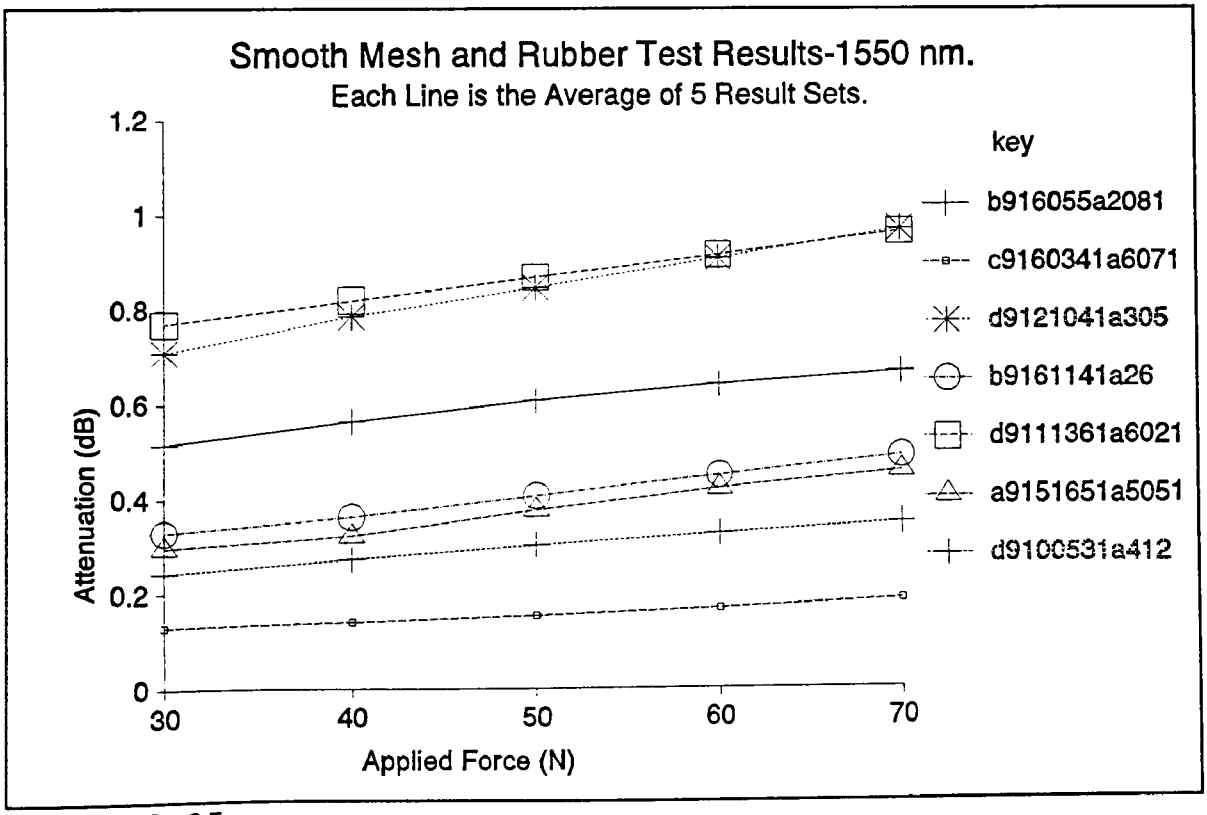

Figure D.25

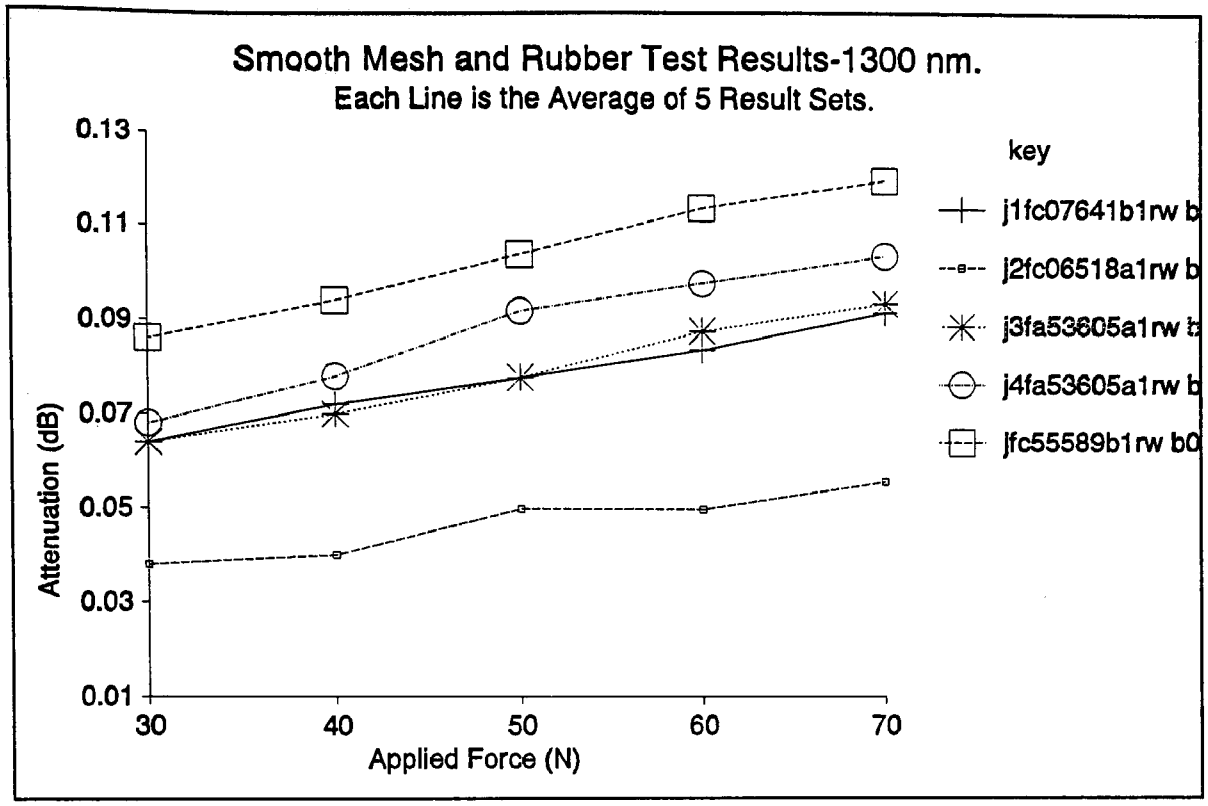

Figure D.26

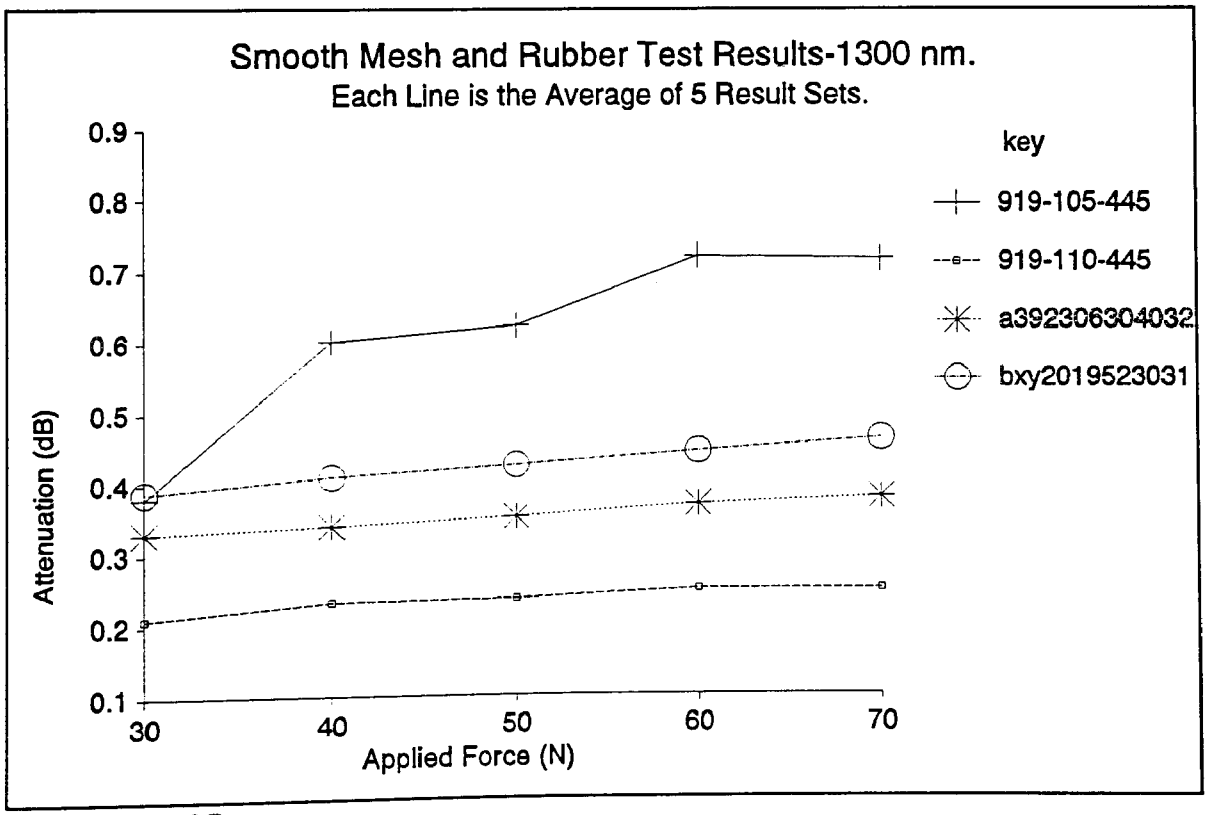

Figure D.27

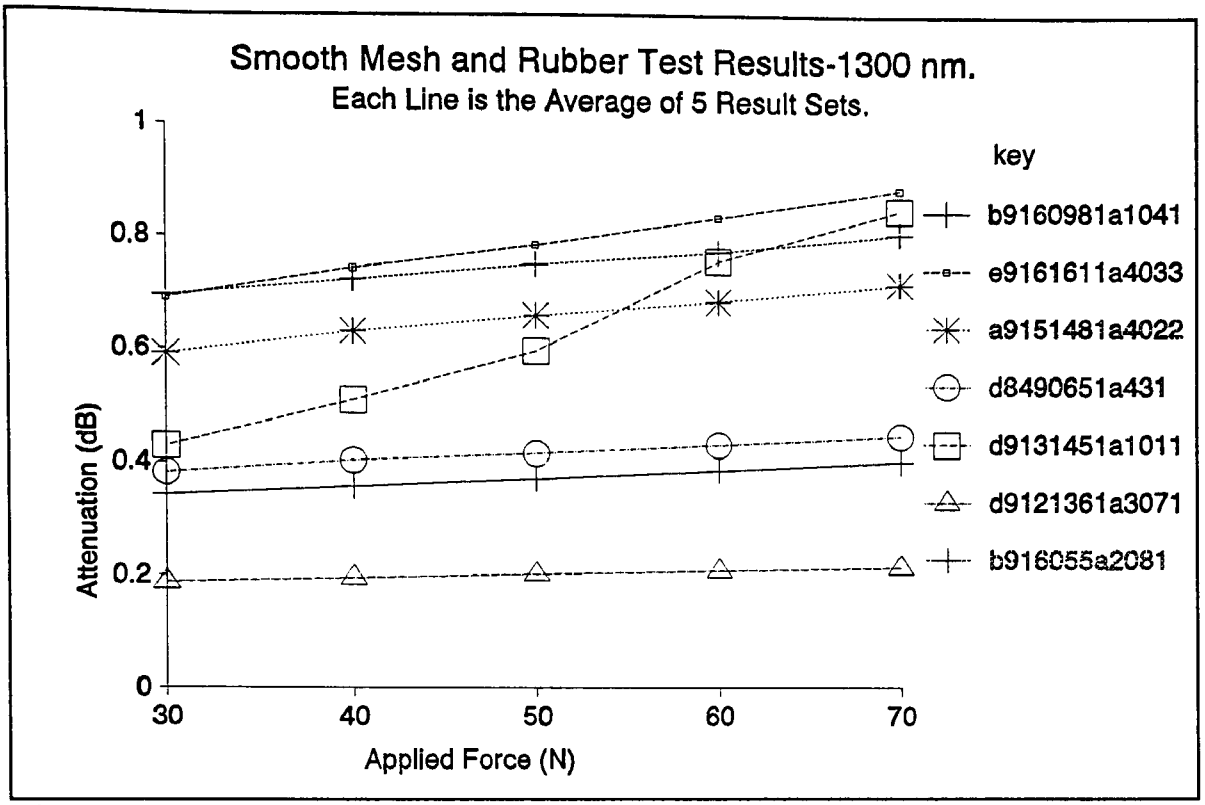

Figure D.28

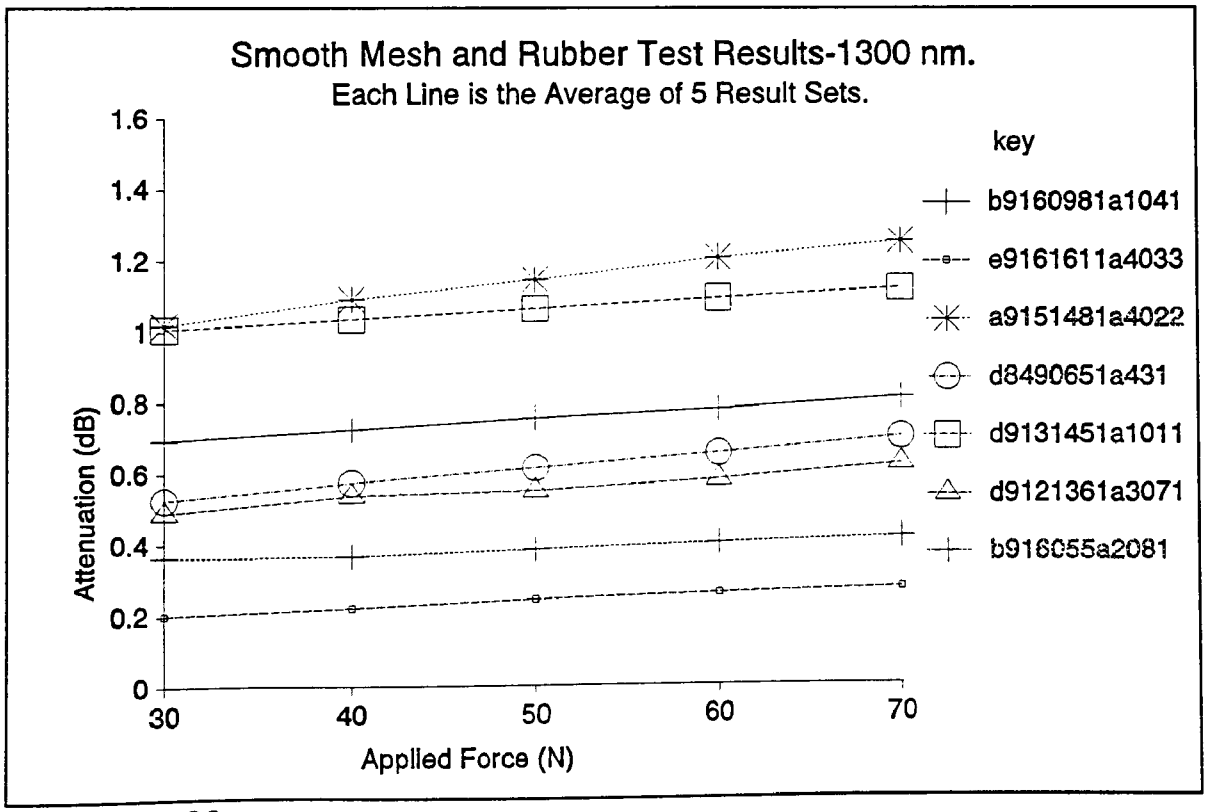

Figure D.29

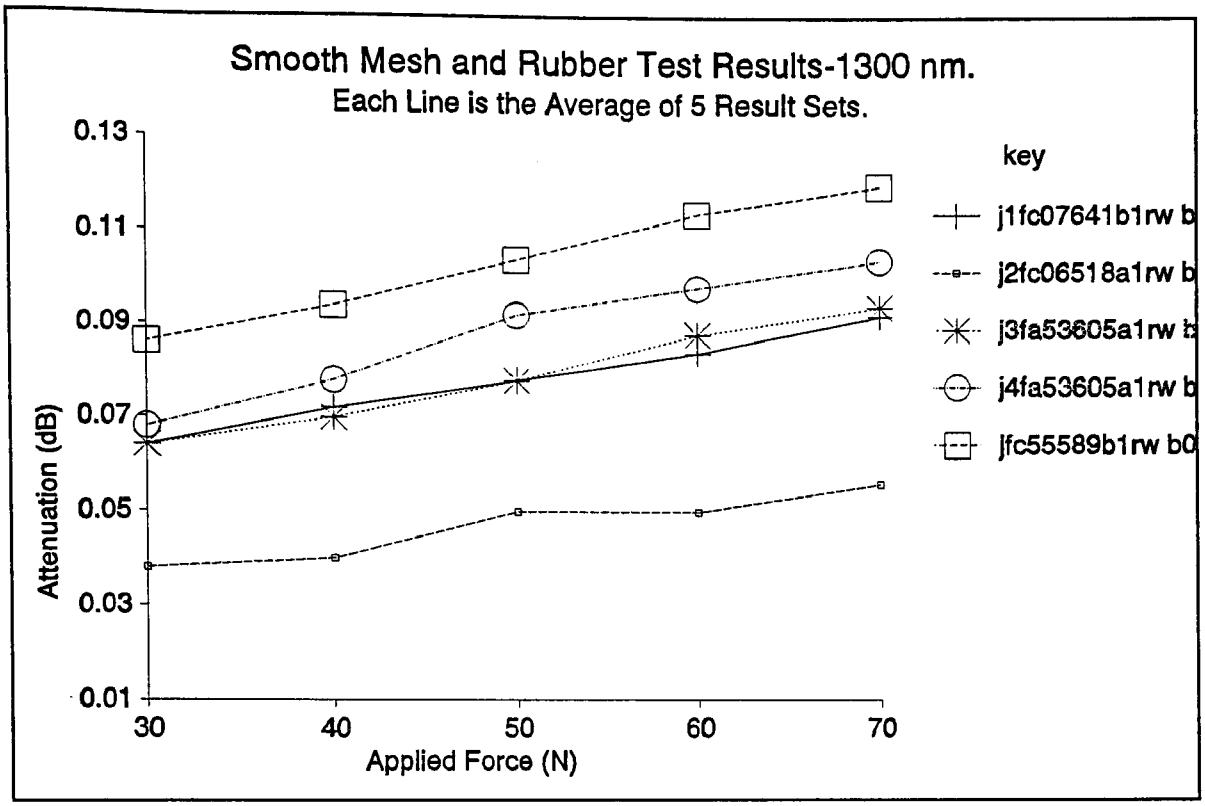

Figure D.30

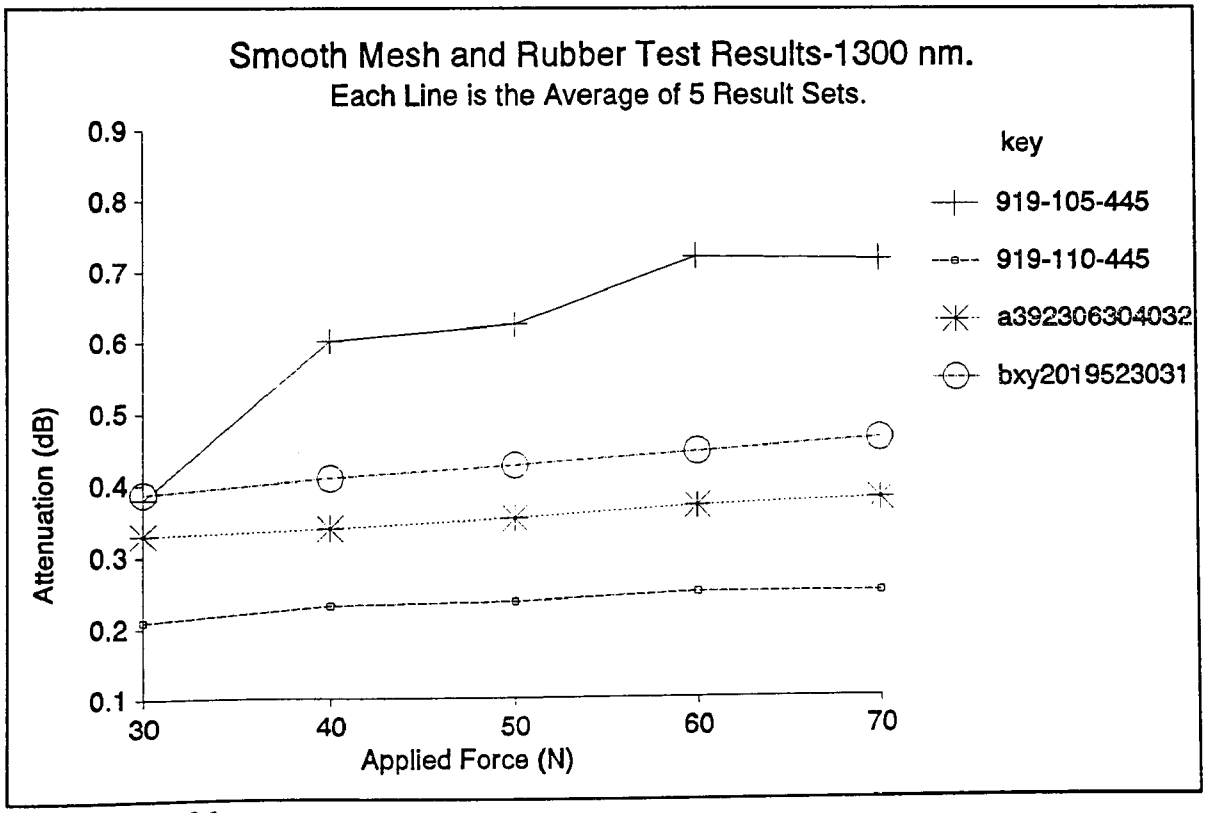

Figure D.31

Appendix E

Stepwise Multiple Regression.

Stepwise Multiple Regression.

The technique of stepwise multiple regression was chosen over standard multiple regression because it was viewed to be far superior. Multiple regression is used when a relationship of the form

$$y = a_1x_1 + a_2x_2 + ... + a_nx_n + a_{n+1}$$

has to be established. In the case of the pilot study, the y value represents one of the measured data values form the test, for example the attenuation at 50 N. compressive force, at 1550 nm., on the rough mesh and rubber test. The x_1 .... x_n values are parameters of the fibres under test and the 'a' values are the coefficients inserted in order to model the values of 'y', the independent variable. a_{n+1}, is a constant.

The problem with this type of standard multiple regression was that when x parameters were inserted, every one of them no matter how detrimental to the accuracy of the model, was inserted in it attached to a coefficient. The theory was that every x parameter named was useful to the accuracy of the model and was hence inserted. This approach was ideal for normal applications, but as has already been pointed out, all available fibre parameters were used with no account being taken of their correlation with the test data. The models resulting from this form of analysis were found to be highly inaccurate, since a large number of the parameters in the model, had no correlation with the y values. It was decided that a more selective form of model construction was required.

Stepwise multiple regression functions by checking the correlation of each available x value to the y value, and finding the most significant. When this is done, it checks through the remaining x values and finds the next most significant and removes that. It continues to repeat this process until the R^2 values of the remaining x parameters are below 0.005. When it attains this situation, it attaches

coefficients and a constant to the parameters it has extracted and thus constructs a model made up of only significant values. The suitability of this mode of regression to the study was demonstrated by the excellent correlation figures between predicted and actual performance figures shown in Appendix D..

When the pilot study was complete, it was noticed that the stepwise multiple regression which had been used, allowed only for linear relationships. If a relationship,

$y = a/x,$

or,

$y = ax^n,$

existed the model would disregard it since when viewed linearly, no relationship would exist. It was determined that in the main study, the regression package would be given the opportunity to choose form a much wider range of relationship types to allow further enhancement of model accuracy.

Appendix F

Stepwise Multiple Regression Printout and

Explanation of Terms.

The advantage of using a stepwise regression program is that within one computer run, all of the independent variables are sorted into their order of significance, and an equation is produced at each step. It is not always obvious in advance which of the variables of a complex problem will provide the best estimates of the dependent variable.

The stepwise programme allows difficulties of independent variables which are disruptive to the accuracy of the model to be omitted. The output from such a system consists of ta series of regression equations with a corresponding standard error of estimate, and a multiple correlation coefficient., One of these equations has been produced at each step. Thus, the number of independent variables per equation is successively greater as the number of steps progresses.

At each step the output includes:

Multiple regression coefficient (multiple R),

Standard error of estimate,

Analysis of variance table which includes the regression and residual,

Degrees of freedom (DF),

Sum of squares,

Mean square,

F ratio,

For the variables in the equation,

Regression coefficient,

Standard error,

F value to remove,

For the variables not in the equation,

Partial correlation coefficient,

Tolerance,

F to enter.

In addition to these output statistics, it is desirable to ensure that the following outputs are made available: means and standard deviations of each variable; correlation matrix of each variable with every other variable; list of residuals-a list showing the actual value of each value of the dependent variable given as input data, and the value calculated by using the equation derived in the final step of the regression analysis. The list then shows the difference between the actual and the computed values under the heading 'residual'.

Appendix G

Repeatability Performance of the Microbend Test-Assessment During Pilot Study.

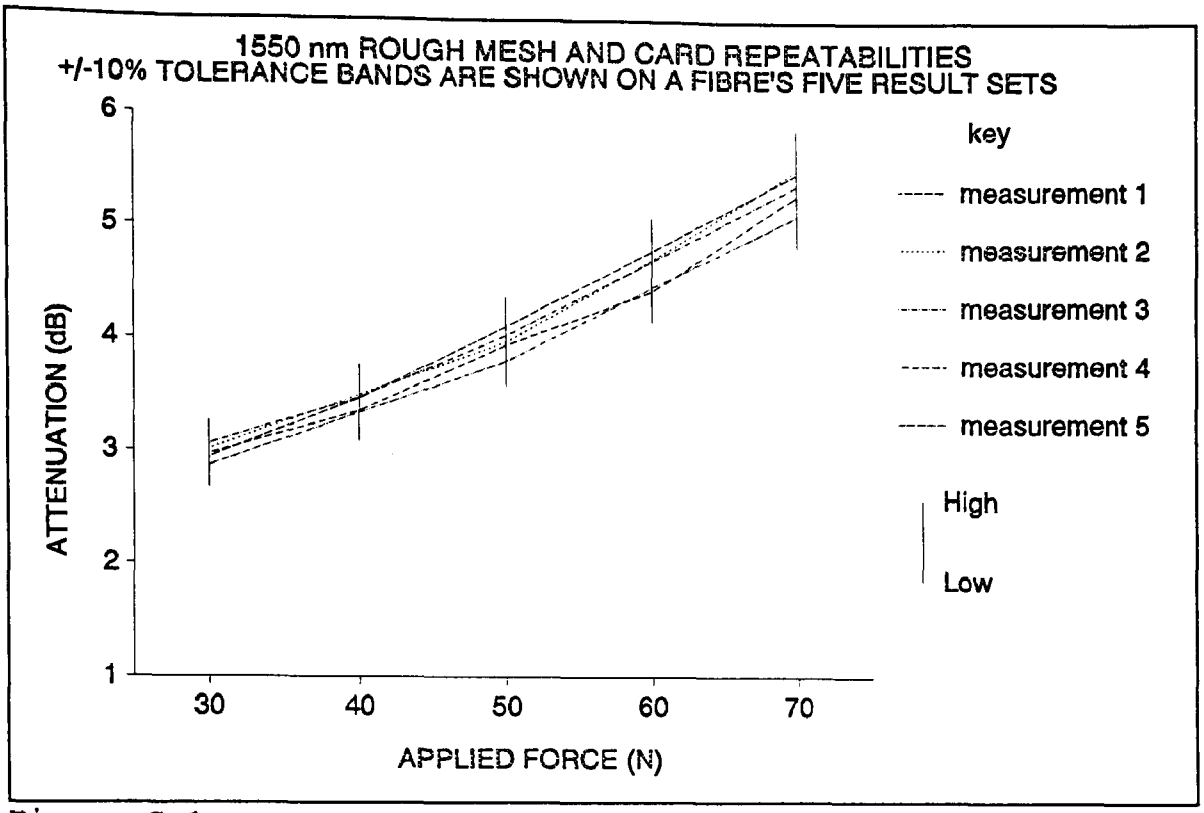

Figure G.1

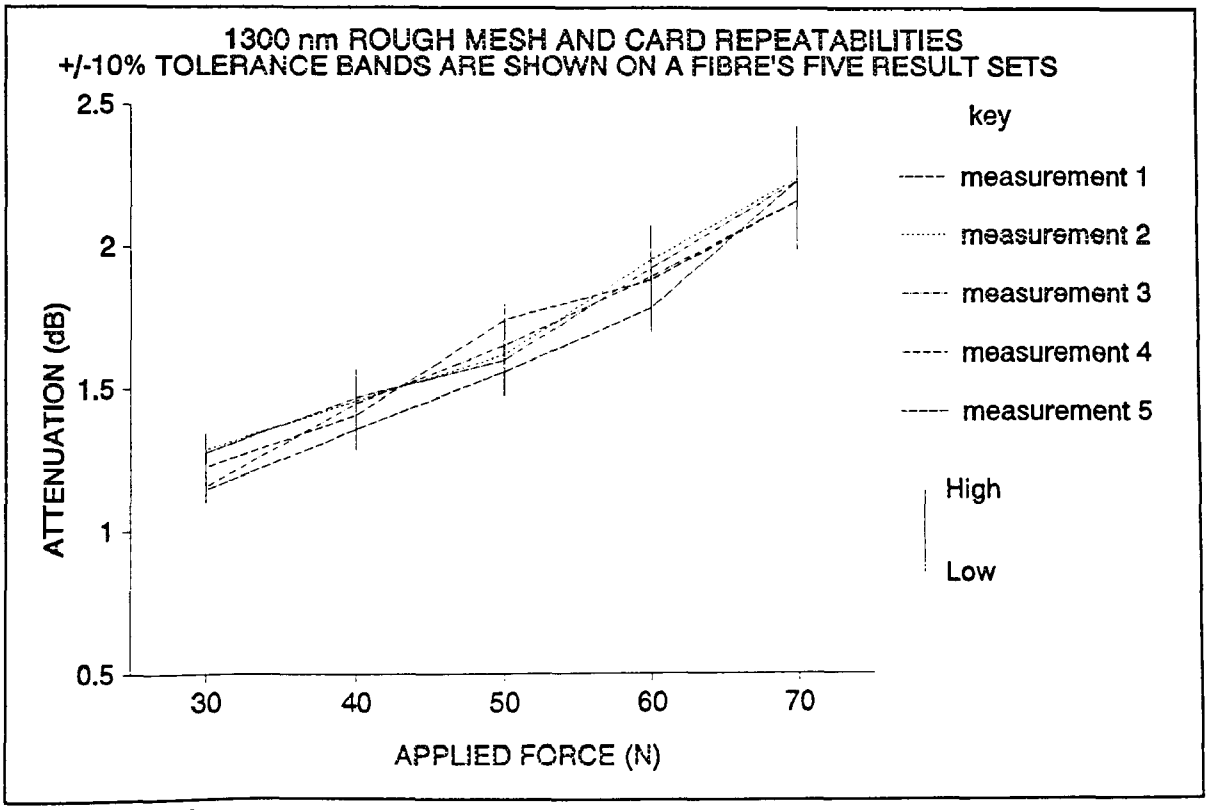

Figure G.2

Figs G.1 and G.2, show typical results from the rough mesh and card test. It was found that repeatability on this test was consistently high, with all five readings at each applied force falling well within the $\pm 10\%$limits imposed by the figures shown. Clearly the average attenuations given at all applied forces were equally representative of fibre performance. 1300nm wavelength results on the rough mesh and card test were often more highly correlated about the mean value than the 1550nm ones, suggesting that at 1550nm, slight variations in test conditions became more significant than at 1300nm. The 1300nm results were therefore more likely to give consistent results, while 1550nm results would give a greater spread while indicating more precisely the microbend susceptibility performance of fibres.

The greater susceptibility of fibres to minor variations in test conditions at 1550nm was to be expected. The mode field diameter of the light in the fibre at the higher wavelength was much greater than at 1300nm. A larger mode field diameter increases the percentage of the light signal carried outside the fibre core. If more light is carried outside the core in this way, the critical point at which light begins to escape from the fibre is more easily attained. A less severe perturbation will be capable of causing light to escape, thus rendering a fibre carrying 1550nm light more susceptible to microbending than one carrying 1300nm light.

Figs G.3 and G.4, show the repeatability performance of the rough mesh and rubber test on a representative sample of test fibres at 1550 and 1300nm. It is clear that the spread of the data is less consistent than had previously been observed with the rough mesh and card test. This suggested that the test was showing more susceptibility to minor variations in conditions which again might have pointed towards microbend modes of loss. On the rough mesh and rubber test, it was more common than on the rough mesh and card test to observe a reading which fell outside of the $\pm 10\%$ tolerances. This effect was most common amongst fibres with low attenuation values and the lower levels of applied force. This suggested that while the qualities of the mesh and holding material used affected

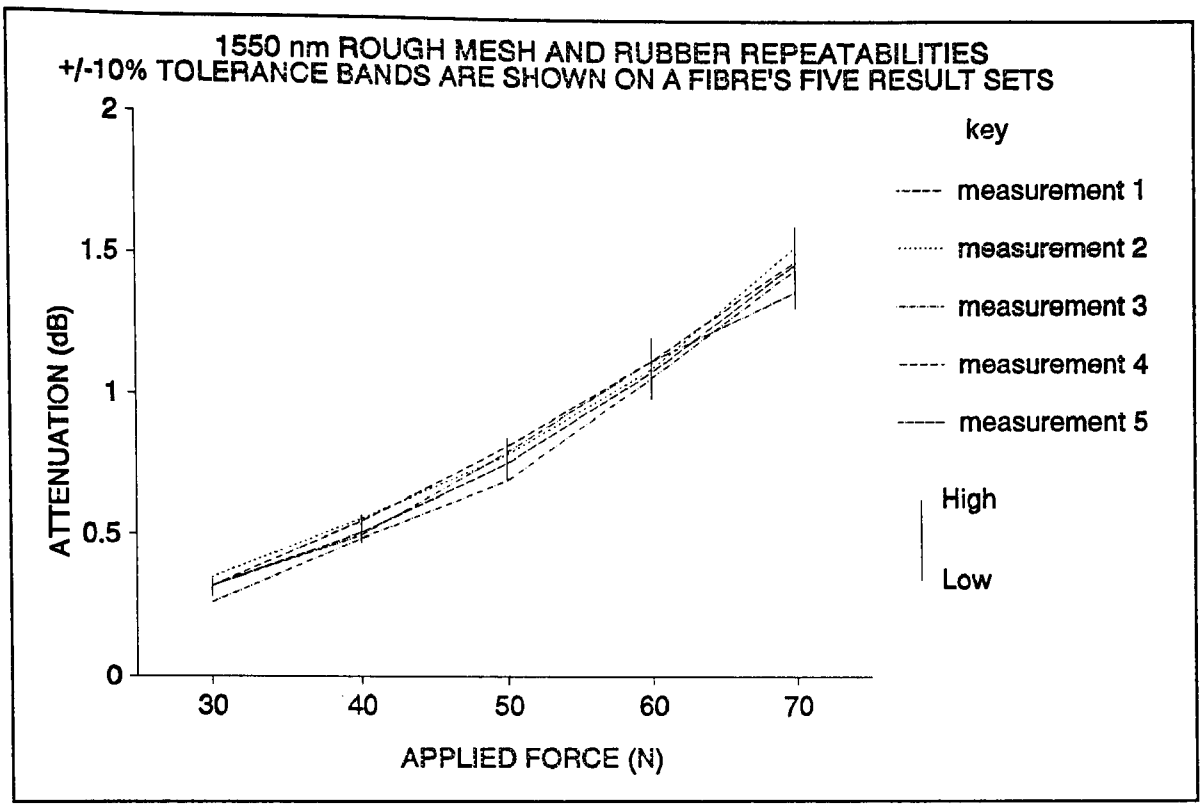

Figure G.3

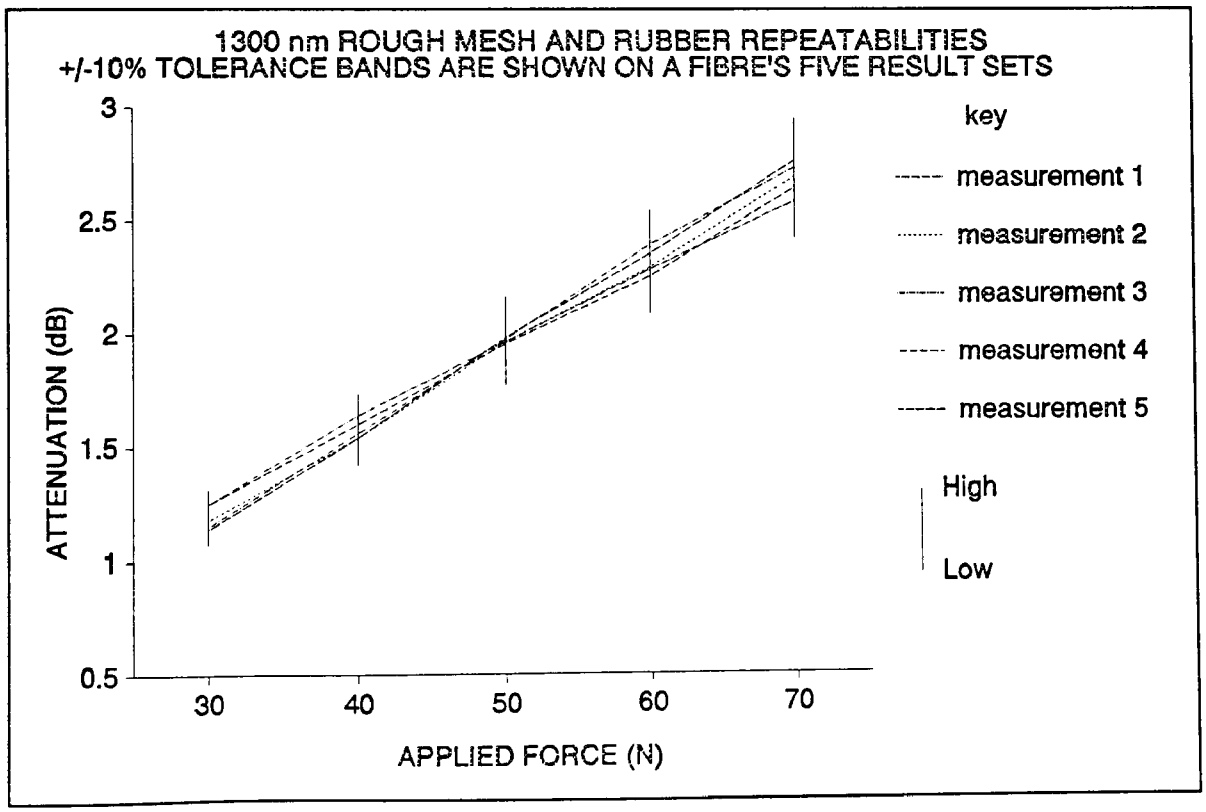

Figure G.4

both repeatability of measurements, another important factor was the level of attenuation induced. The noise induced by the equipment must have been of a level which hampered accurate measurement of induced attenuation levels. A constant level of noise would be proportionally more significant with respect to lower signal levels than to high level ones .Higher level signals would have proportionally wider tolerances with respect to noise levels reducing the significance and effects of the noise; while at low signal levels wide variations in measurement or even, no measurements at all would result.

If repeatability were the only criteria for the microbend test, the card based tests would be used in preference to the rubber based tests due to the higher levels of signal and therefore the less significant levels of noise present. The criteria however as was seen in chapter 8, were much broader than this and so while card based tests might presently be attractive, other test variations might prove to be more suitable as further analysis is carried out.

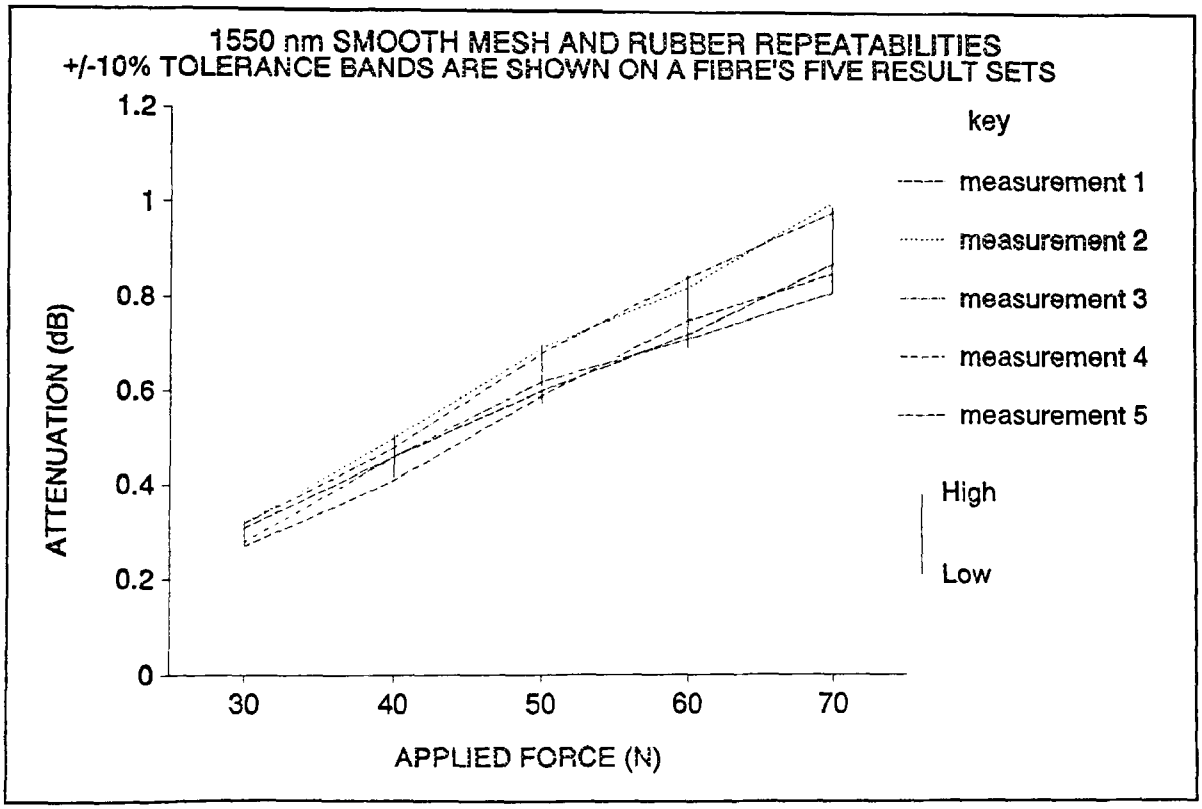

Figure G.5

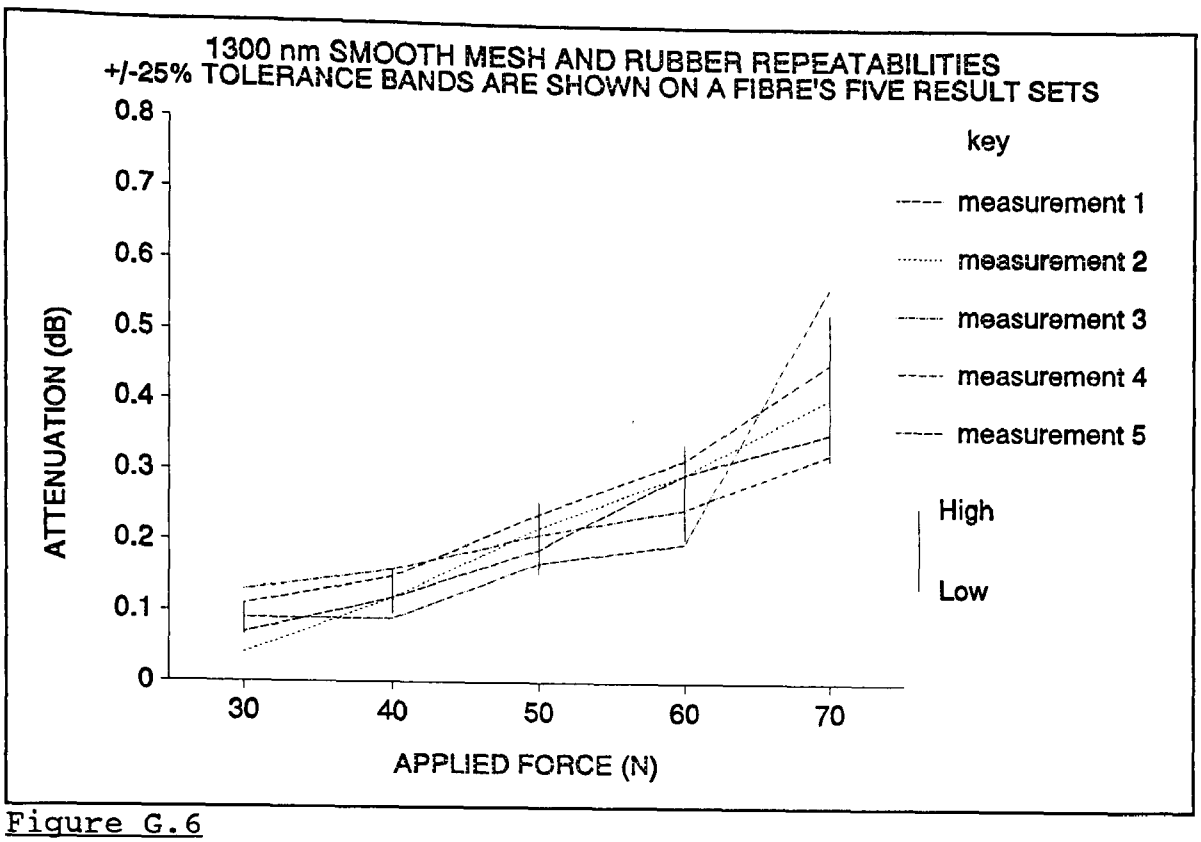

Figure G.6

The smooth mesh and rubber test repeatability graphs, (Figs G.5 and G.6), show the greater scatter common amongst test variations inducing lower values of attenuation. The smooth mesh and rubber variation shows a change from what has been said above: the 1550nm wavelength results appear to give a higher repeatability than their 1300nm counterparts. In order to show the greater spread of results produced by a lower attenuation inducing test, it was necessary to increase the tolerance limits of the figures to $\pm 25\%$. Examination of the results within the wider tolerance bands shows the effect of noise on the signal levels measured. The 25% tolerance limits appear to contain most of the measurement points at the 1550nm wavelength. At the 1300nm wavelength however, particularly the results at the lower applied force end, fall inside the base noise levels and are effectively lost. The severity of the problem is demonstrated by the fact that the higher applied forces should include a considerably larger accumulated measurement error due to the method of data handling, (explained in Appendix B), than the smaller applied forces. The lower force results, unlike the larger ones are not the sum of several results and therefore should have a smaller accumulated error. The fact that

the smaller force results show a greater degree of scatter, proves that the potential repeatability of the microbend test produced is hampered by the measurement equipment used. Were equipment of a better quality available, repeatability results could be greatly enhanced.

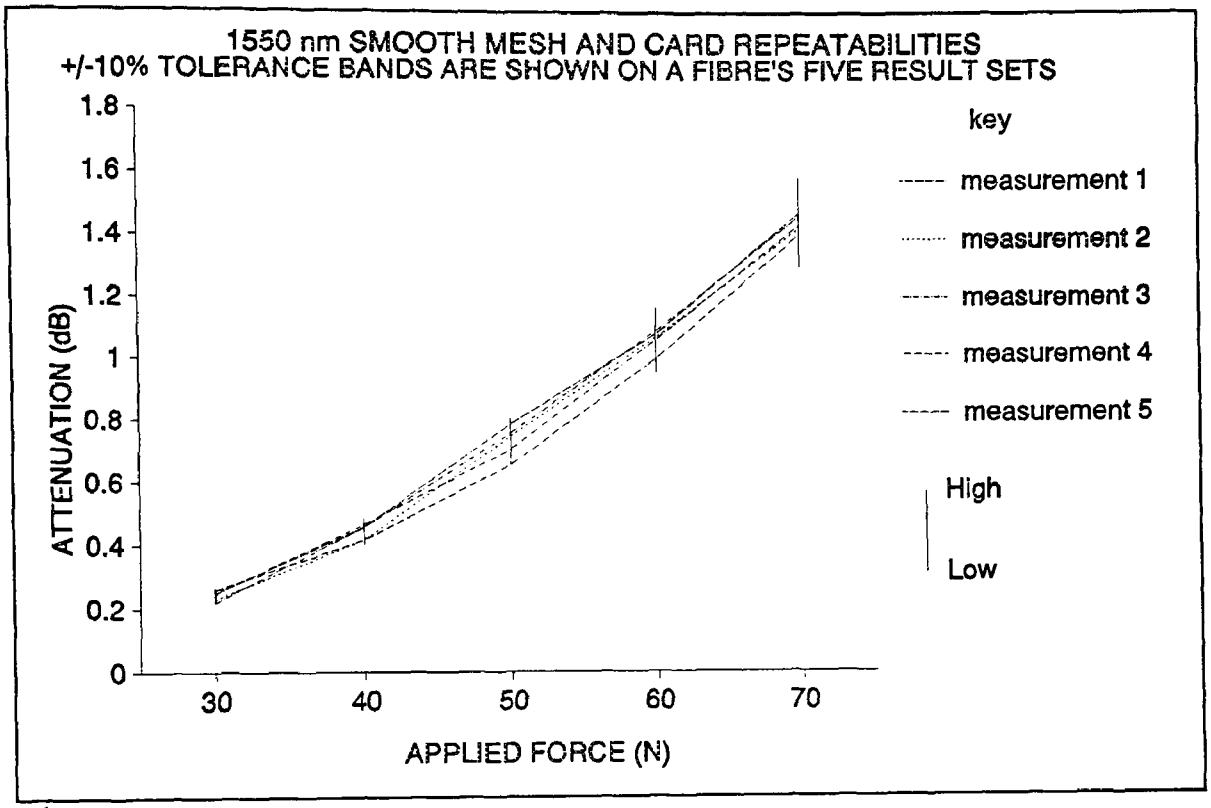

Figure G.7

Figs G.7 and G.8 show the repeatability results from the smooth mesh and card test variation. The repeatability of the 1550nm wavelength results, except at the 30 and 40N applied force levels, was high enough to allow tolerances of $\pm 10\%$ to be imposed. Clearly the card based tests yielded a high repeatability figure, which only became significant when the level of induced attenuation dropped below the level of background noise. The graphs produced from readings taken at the 1300nm wavelength were small enough to force widening of the tolerances to $\pm 25\%$.

It had become clear that the level of background noise introduced by the measurement equipment was of the order of 0.1-0.2dB. Thus any result which had an increment between adjacent readings or an absolute value of 0.2dB or less should be discarded on the grounds that measurement noise could have

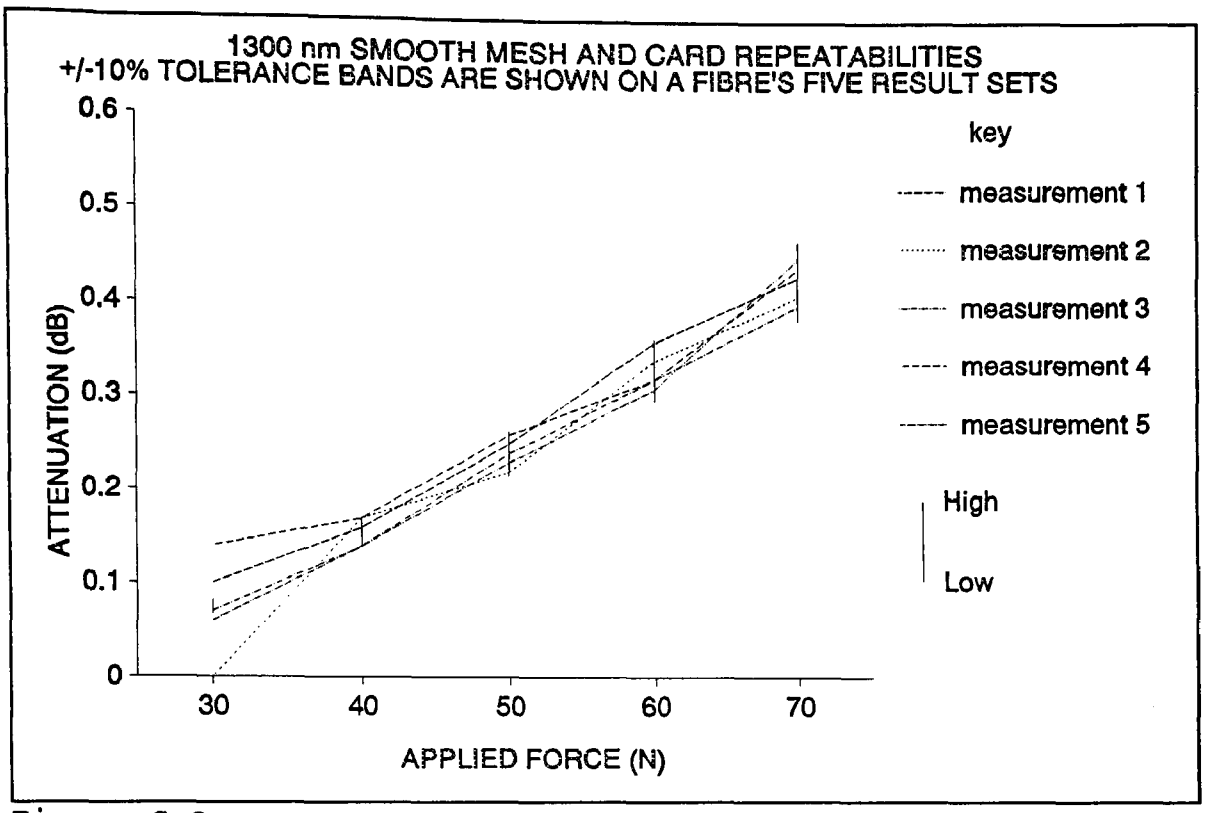

Figure G.8

induced it. This conclusion is borne out by the figures of Appendix D. The lines in each of these graphs is a plot of results taken from a single sample fibre. The lines are the average of five individual sets of results.It can be seen that the rough mesh and card results show mainly steady increases in attenuation with only occasional slight variations in line gradient.. The 1300nm wavelength average results lines showed less stability and more gradient changes than their 1550nm rough mesh and card equivalents. The absolute attenuations involved as well as the increments, were smaller than at 1550nm, and while the results could be expected to all fall within $\pm 10\%$, of the average values represented as lines here, it was clear that the 1550nm results were more stable. While the 1300nm results were known to be less susceptible to test variations than the 1550nm results, the background noise was more significant with the lower level attenuations. It can be deduced that background noise is a more significant cause of result inaccuracy and that the quality of the results produced by the test could be greatly improved with a better measurement system.

The smooth mesh and rubber test average results lines' attenuations were much lower than those seen with the rough mesh and card test. Results below the 0.1dB mark show a greater tendency towards reduced stability. It is not unusual to observe *reductions* in average attenuation levels with increasing applied force at these levels. It is very unlikely that negative increments would result from increasing applied force, suggesting strongly that these results are incorrect and are adversely affected by measurement noise. If the errors induced are due to measurement equipment shortcomings, the cut-off point below which measurements have to be discounted due to excessive background noise levels would be the same for all test variations. For this reason, it has been possible to set a minimum base and incremental induced attenuation level and thus at this stage to highlight tests most likely to be rejected because their readings consistently fall short of the criteria.

The conclusions drawn in this appendix are summarised in section 9.3.1.

Appendix H

Nature of the Loss Modes Induced by the Microbend Test-Assessment During Pilot Study.

Figs 7.13 and 7.14 show the spectral attenuations induced by the microbending test variations at each applied force. Each figure shows the results obtained from a single sample fibre with each line indicating the attenuation observed at one applied force. Clearly, the line representing the lowest levels of attenuation, demonstrates the attenuation induced by an applied force of 30N, (the lowest level of force). Similarly the line showing the highest levels of attenuation was measured with the greatest value of applied force, (70N), applied to the test. The results lines between these two extremes, represent the attenuations induced by the remaining applied forces of 40, 50 and 60N each force representing a higher level of attenuation across the light spectrum.

The figures show representative fibre results from the rough and smooth mesh and rubber tests. It was found that the attenuations produced by the tests, both contained a high degree of macrobending, as evinced by attenuations at 1550nm greater than twice the attenuations at 1300nm on the spectral attenuation graphs. It was deduced that the card based tests made a bad match between holding material and mesh, and that the combination caused perturbations which were too severe. The card may haver been too firm to allow the fibre to retreat into it slightly, thus allowing a lessening of the effects of the mesh. For this reason the tests were found to be non-conformant of the second requirements of the tests.

For the rubber based tests, the spectral attenuation traces merited closer inspection since both tests produced graphs which showed the dominant mode of loss to be microbending. For both figures, 7.13 and 7.14, it can be seen that the attenuation at 1550nm is less than or equal to twice the attenuation at 1300nm.

The smooth mesh and rubber spectral attenuation graph, (Fig 7.14), shows that on this test variation, for all applied forces, the attenuation measured at 1550nm is always twice the attenuation measured at 1300nm. The prevailing mode of loss is clearly microbending. The rough mesh and rubber graph,

(Fig 7.13), demonstrates that the rough mesh would produce loss modes which lay on the macro/microbending dividing line was correct. The lower applied forces of 30 and 40N yielded attenuation plots in which the attenuation ratios suggested microbending as the dominant loss modes. The higher forces of 50, 60 and 70N tended to suggest that the additional applied forces had increased the severity of the perturbations induced and that this change had altered the loss mode emphasis from micro to macrobending. The soft rubber which was chosen so as to mould the fibre to the mesh profile rather than constrict it on the high points of the mesh, had induced bends so severe that they became the radii which induce macrobending. The large gaps between the wire allowed the significant bends to occur, where the smooth mesh, or the rough mesh with lower applied forces would have prevented it. From the point of view of microbend purity, therefore, the best option would appear to be the smooth mesh test or the rough mesh test with low values of applied force.

Appendix I

The Ability of the Microbend Test to Induce

Perturbations across a Wide Range of Spatial Frequencies

- Assessment during Pilot Study.

The success with which the loop of fibre design on the microbend test induced perturbations which covered a wide spectrum of spatial frequencies was tested using spectral plots such as those shown in Figs 7.13 and 7.14.

Figs 7.13 and 7.14 show the spectral attenuations induced by the microbending test variations at each applied force. Each figure shows the results obtained from a single sample fibre with each line indicating the attenuation observed at one applied force. Clearly, the line representing the lowest levels of attenuation, demonstrates the attenuation induced by an applied force of 30N, (the lowest level of force). Similarly the line showing the highest levels of attenuation was measured with the greatest value of applied force, (70N), applied to the test. The results lines between these two extremes, represent the attenuations induced by the remaining applied forces of 40, 50 and 60N each force representing a higher level of attenuation across the light spectrum.

In the ideal theoretical case, the design would induce all possible frequencies of perturbation thus attenuating al light wavelengths equally. The practical case could not be expected to achieve this perfect level of performance, and so each test variation was judged on its ability to perform as close to the ideal case as possible.

Because the mesh has a finite size and therefore the number of interactions between fibre and mesh is limited, all light wavelengths cannot be attenuated equally. It would be assumed that as the fibre's angle to the mesh gradually changed, the perturbation spatial frequency would increment at each interaction. Were a more rough mesh used, the increment between adjacent perturbation spatial frequencies would be larger. Results reflecting this, would show highly attenuated light wavelengths interspersed with large gaps of wavelengths which had been less severely attenuated. A mesh which was less coarse, (more smooth), would have a smaller incremental change between adjacent perturbation spatial frequencies, effectively yielding a higher resolution when the spectral attenuation

traces were measured. The effect would be to reduce the width of the lower attenuated bands of light, theoretically giving a n attenuation curve which had a much higher percentage of higher attenuated wavelength bands. Before actual examination of the Figures, there would therefore seem to suggest that a smoother mesh would give a higher density of highly attenuated wavelengths leading to a smoother spectral attenuation curve.

Examination of Figs 7.13 and 7.14 shows that the fibre loop theory is correct. By placing a loop of fibre onto the wire mesh, the fibre interacts with the wire mesh at constantly varying wavelengths inducing perturbations covering a wide spectrum of spatial frequencies. The curves are as expected, with equal attenuation across the whole transmission window. Clearly the range of spatial perturbation frequencies is sufficiently broad. The large peak at the left hand side of bath Figs 7.13 and 7.14 is a water absorption peak which is a feature of silica optical fibres, and which was not removed from the traces by the monitoring software.

Fig 7.13 shows the rough mesh and rubber spectral attenuation trace. While the trend of the graph's lines is a smooth curve, oscillations in results are apparent. The lines, particularly those representing the attenuations from higher applied forces, show periodic raising and lowering of attenuation values. The higher forces of 60 and 70N, show that the higher values of attenuation-those which are increased as a result of the perturbation spatial frequency in the fibre matching the beat length of the light travelling through it at that point-are interspersed with lower valued attenuations. The rough mesh induces perturbations whose spatial frequencies increment by large amounts leading to the higher attenuated wavelengths of light being widely space. It can be seen that the 60 and 70N attenuation lines, appear to be a high level of attenuation interspersed with points of lower level attenuation. The majority of wavelengths are therefore highly attenuated as required. The lowest applied force, (30N), line appears to be a set of lower level attenuations interspersed by an occasional higher level one. The significant peak on the 30N line is the one at 1250nm. This peak shows the level of attenuation which

might have been achieved across the whole spectrum, had all wavelengths been highly attenuated. Because neither the 40 or 50N lines show a peak at the 1250nm wavelength, it can be deduced firstly that the peak was not normal for the test variation or force-that is were the test carried out on other fibres, a peak would not occur at this point; and secondly the high point of the 30N line suggests that both the 40 and 50N lines are also at the lower attenuation level. This theory is borne out by the attenuation patterns when all three low level applied force lines appear to rise and fall together between 1340 and 1380nm. The lines will, given proper conditions performs similarly. The peak at 1250nm is clearly a rogue result since it is not reflected in any of the lines.

Observations from Fig 7.13 would seem to suggest that the microbending part of the loss mechanisms present at 60 and 70N is mainly at the higher level attenuation which, while because of the roughness of the mesh increments the spatial perturbation frequencies coarsely, covers a wide enough light spectrum. The lower applied force lines, 30, 40 and 50N appear unaffected by the mesh, which suggests that the microbending induced is most active only at a small number of wavelengths. Those wavelengths may be the most significant ones such as when the fibre is lying parallel or at 45^0 to the warp and weft of the mesh. These are clearly the largest of the perturbations, with other angles producing smaller perturbations which would require more force to encourage the fibre under test to be perturbed by it. The lower force lines are therefore being fully perturbed only at the major spaces on the mesh, while the smaller perturbations were unable to perturb the fibre until higher forces were applied.

Fig 7.14 shows the spectral attenuation on the smooth mesh and rubber test. All applied force lines on the smooth mesh and rubber test were elevated to the higher level of attenuation. This was shown by the fact that interruptions in the smooth attenuation line were dips rather than rises in the smooth line height. Wavelengths of light not covered by perturbation spatial frequencies, with lowered

attenuations prove that the smooth mesh excites a broad range of frequencies at small increments to the higher level of attenuation at all applied forces.

Optimum coverage of wavelengths at the broadest wavelength window is to be obtained with the smooth mesh. An equally broad coverage but with larger gaps between raised attenuation wavelength bands is produced by the rough mesh.

Appendix J

Review of Attenuation Monitoring Equipment used

in Conjunction with the Microbend Test.

Fig I.1. is a schematic representation of the equipment which was used to monitor the changes in attenuation induced in fibres by the microbending test. This equipment worked in conjunction with a computer to collate data which was then processed as detailed in Appendix B.

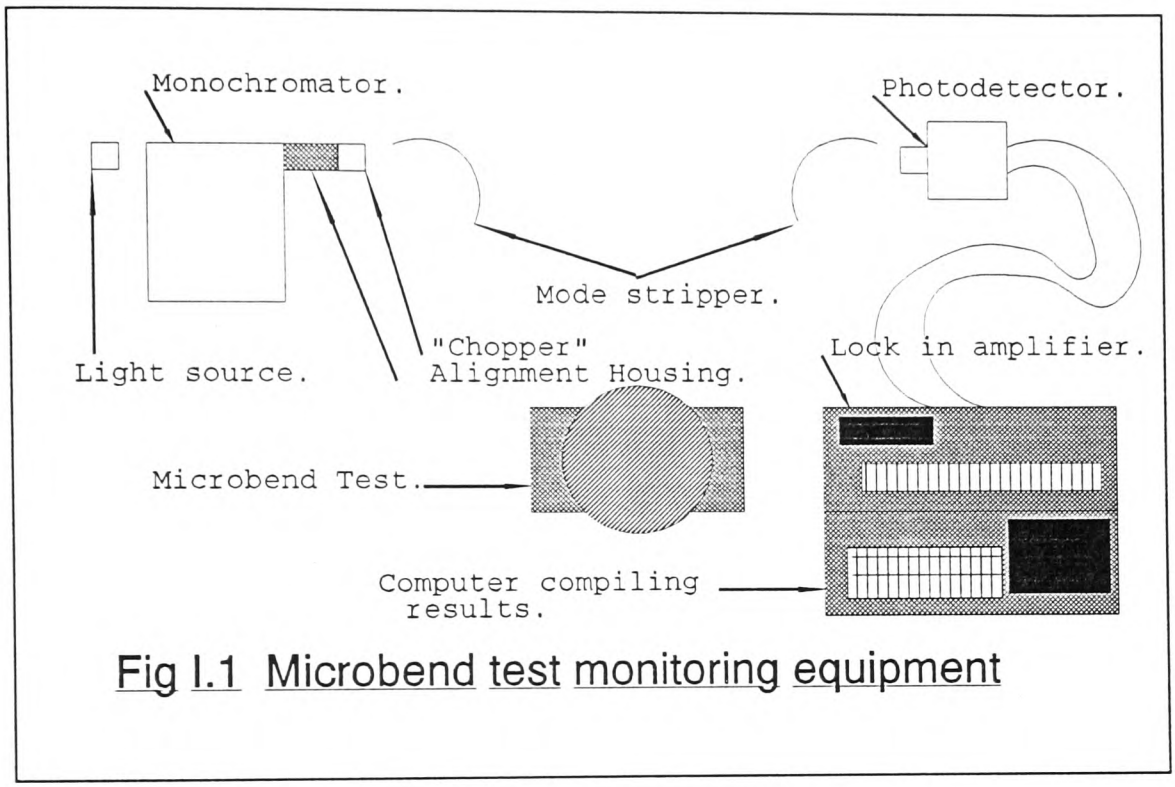

Fig I.1 Microbend test monitoring equipment

The light ray passed through the monochromator which selected the light of suitable wavelength from the input source. The "chopper" modulates the light signal to allow operation of the lock in amplifier. A mode stripper is attached which comprises a curved bath containing index matching fluid. The purpose of this equipment is to move the light power near to the fibre surface and then "pare" off any secondary modes which might be propagating. The reason for the inclusion of the stripper was to prevent any secondary modes from propagating during the test. Ordinarily the protective coating layers would be expected to strip off extra modes, but the fibre sample was sufficiently short to mean that this could not be guaranteed.

Fibre is then passed through the microbend test and a second mode stripper to a photodetector. The output of the photocell was passed to a lock in amplifier which supplied the computer with data which was processed as detailed in Appendix B.

Sources of error introduced into the data by the test equipment, (not including the microbend test), were:

Fibre cleave errors, introduced when a fibre is cleaved and passed into the photodetector housing. Each cleave will vary slightly and cleave angle and introduction of impurities to the fibre end will lead to individual modifications being made to the light signal by each of the fibres;

Monochromator movement, play in the drive mechanisms of the monochromator components and lateral movement of mirrors and lenses will mean that light wavelength and line-width will vary slightly between fibres,

Chopper instability, the chopper used was mechanical in nature and therefore capable of small frequency variations. The effect is to slightly adjust the frequencies of the modulations received by the photodetector and therefore the lock in amplifier equipment,

Detector sensitivity, the detector was sensitive to varying degrees to light of different wavelengths. For this reason the comparative power observed between the two transmission wavelengths was slightly inaccurate,

Monochromator line-width, the equipment used to produce one light wavelength had a line-width, (the wavelength width of the light omitted by the equipment), was typically +/-5 nm,

Drift in alignment housing, once the fibre had been locked into the alignment housing and the signal optimised, the fibre was not adjusted again for the remainder of the readings taken on it, (because of the cumulative nature of the results), thus an alignment drift error could be introduced,

Detector housing drift, as above, some drift error could be introduced by the detector housing.

The cumulative effects of the errors introduced by the system of measurement are summarised below, (Table I.1).

Wavelength (nm)	Attenuation Measurement Error.
1300 nm	0.02 dB/km
1550 nm	0.04 dB/km

Table I.1 Sum of errors introduced to the measured attenuation signal by the measuring equipment.

The levels of error were taken as the noise level below which signal readings were taken to be zero.